NOTICE

The quality of this microform is heavily dependent upon the quality of the original thesis submitted for microfilming. Every effort has been made to ensure the highest quality of reproduction possible.

If pages are missing, contact the university which granted the degree.

Some pages may have indistinct print especially if the original pages were typed with a poor typewriter ribbon or if the university sent us an inferior photocopy.

Reproduction in full or in part of this microform is governed by the Canadian Copyright Act, R.S.C. 1970, c. C-30, and subsequent amendments.

AVIS

La qualité de cette microforme dépend grandement de la qualité de la thèse soumise au microfilmage. Nous avons tout fait pour assurer une qualité supérieure de reproduction.

S'il manque des pages, veuillez communiquer avec l'université qui a conféré le grade.

La qualité d'impression de certaines pages peut laisser à désirer, surtout si les pages originales ont été dactylographiées à l'aide d'un ruban usé ou si l'université nous a fait parvenir une photocopie de qualité inférieure.

La reproduction, même partielle, de cette microforme est soumise à la Loi canadienne sur le droit d'auteur, SRC 1970, c. C-30, et ses amendements subséquents.

Canada

UNIVERSITY OF ALBERTA

MOBILITY CONTROL: THEORY AND EXPERIMENTAL VERIFICATION

BY

HASSAN JASPER ABDUL

Ⓒ

A THESIS
SUBMITTED TO THE FACULTY OF GRADUATE STUDIES AND RESEARCH IN
PARTIAL FULFILLMENT OF THE REQUIREMENTS FOR THE DEGREE
OF MASTER OF SCIENCE
IN
PETROLEUM ENGINEERING

DEPARTMENT OF MINING, METALLURGICAL AND PETROLEUM
ENGINEERING

EDMONTON, ALBERTA

FALL, 1994

The author has granted an irrevocable non-exclusive licence allowing the National Library of Canada to reproduce, loan, distribute or sell copies of his/her thesis by any means and in any form or format, making this thesis available to interested persons.

L'auteur a accordé une licence irrévocable et non exclusive permettant à la Bibliothèque nationale du Canada de reproduire, prêter, distribuer ou vendre des copies de sa thèse de quelque manière et sous quelque forme que ce soit pour mettre des exemplaires de cette thèse à la disposition des personnes intéressées.

The author retains ownership of the copyright in his/her thesis. Neither the thesis nor substantial extracts from it may be printed or otherwise reproduced without his/her permission.

L'auteur conserve la propriété du droit d'auteur qui protège sa thèse. Ni la thèse ni des extraits substantiels de celle-ci ne doivent être imprimés ou autrement reproduits sans son autorisation.

ISBN   0-315-94995-3

Canadä

UNIVERSITY OF ALBERTA

RELEASE FORM
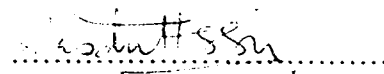
NAME OF AUTHOR: Hassan Jasper Abdul

TITLLE OF THESIS: Mobility Control: Theory and Experimental Verification

DEGREE FOR WHICH THESIS WAS PRESENTED: MASTER OF SCIENCE

YEAR THE DEGREE WAS GRANTED: FALL, 1994
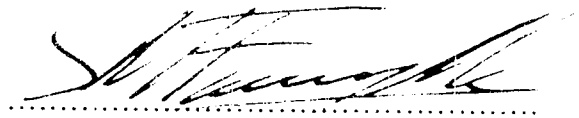
PERMANENT ADDRESS:
P. BOX 19
Bonyere
Western Region
Ghana

DATED :Aug. 31. 1994
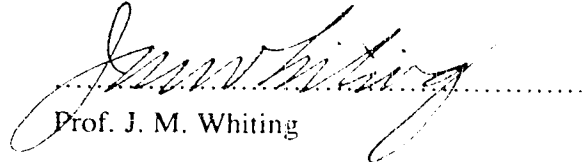
UNIVERSITY OF ALBERTA

FACULTY OF GRADUATE STUDIES AND RESEARCH
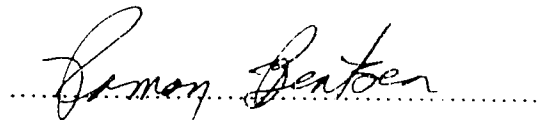
The undersigned certify that they have read, and recommend to the Faculty of Graduate Studies and Research for acceptance, a thesis entitled MOBILITY CONTROL: THEORY AND EXPERIMENTAL VERIFICATION submitted by HASSAN JASPER ABDUL in partial fulfilment of the requirements for the degree of MASTER OF SCIENCE in PETROLEUM ENGINEERING.

Prof. S. M. Farouq Ali (Supervisor)

Prof. J. M. Whiting

Prof. R. G. Bentsen

Prof. N. Rajaratnam (External Examiner)

DATED: Aug 31, 79

To

My wife, Hawa and my kids, Afiba and Hassan Jr. for their patience, understanding and support.

ABSTRACT

When stratified or bottom-water reservoirs are considered for waterflooding, channeling of the injected fluid into the high permeability zone, or in the case of bottom-water, channeling through the bottom-water zone, is of major concern. In Alberta and Saskatchewan many light and moderately heavy oil reservoirs contain a high water saturation zone underlying, and in communication with, the oil zone. Waterflooding such reservoirs may still be an economically viable process. This research addresses the problem of waterflooding such reservoirs.

Different strategies were investigated to reduce the water mobility in the bottom-water zone, while waterflooding the oil zone, to enhance oil displacement. Polymer solution with a concentration of 500 ppm was used as a blocking agent while waterflooding the oil zone to improve vertical sweep efficiency. Different surfactant concentrations were used to prepare 10% quality oil-in-water stable emulsions as blocking agents in the bottom-water zone while polymer was used as the mobility control agent in the oil zo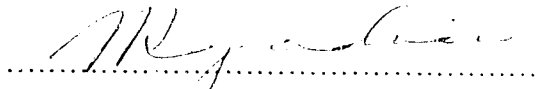ne. Horizontal wells were used for waterflooding in the presence of bottom-water. They were also used in conjunction with polymer and emulsions to flood the model.

A new mathematical equation was developed to predict accurately the volume of injected fluid channeling into the bottom-water layer during a waterflood. The mathematical model accounts for crossflow while waterflooding a reservoir underlain with bottom-water. A calculation procedure for oil recovery performance using the crossflow equations was developed. It is shown that using polymer as the mobility control agent in the oil zone and emulsion as the blocking agent in the water zone minimizes crossflow. The model was also used to predict oil recovery performance observed by previous investigators[42,43,55], with an error of 8% or less. The experiments conducted in this study showed that using blocking agents (viz. polymer or emulsion) when waterflooding reservoirs with bottom-water improved oil recovery over that obtained using a conventional waterflood. The use of a horizontal injector and producer pair in waterflooding prevented formation of an oil bank in the water zone, but it was no better than a vertical injector-vertical producer combination as far as oil recovery is concerned.

v

ACKNOWLEDGEMENTS

TABLE OF CONTENTS

viii

LIST OF TABLES

LIST OF FIGURES

NOMENCLATURE

Symbols

A	cross-sectional area of the model, m^2
A_o	cross-sectional area in the oil zone, m^2
A_w	cross-sectional area in the bottom-water zone, m^2
d_d	drop diameter, m
d_p	pore-throat diameter, m
f	value of function $f(x_1, x_2)$ at point of interest
h	height of the model, m
HCPV	hydrocarbon pore volume (øSoil Voil), fraction
h_o	height of the oil zone, m
h_w	height of the bottom-water zone, m
IOIP	initial oil-in-place, m^3
k_{abs}	absolute permeability, m^2
k_{owr}	effective permeability to oil at irreducible water saturation, m^2
k_w	absolute permeability of the bottom-water zone, m^2
k_{wor}	effective permeability to water at residual oil saturation, m^2
L	length of the model, m
M	mobility ratio, fraction
M_{ab}	ratio of fluid mobility in zone a to fluid mobility in zone b, fraction
M_{ac}	ratio of fluid mobility in zone a to fluid mobility in zone c, fraction
M_{ba}	ratio of fluid mobility in zone b to fluid mobility in zone a, fraction
M_{bd}	ratio of fluid mobility in zone b to fluid mobility in zone d, fraction
M_{cd}	ratio of fluid mobility in zone c to fluid mobility in zone d, fraction
M_{ce}	ratio of fluid mobility in zone c to fluid mobility in zone e, fraction
M_{df}	ratio of fluid mobility in zone d to fluid mobility in zone f, fraction

M_{ef}	ratio of fluid mobility in zone e to fluid mobility in zone f, fraction
p	pressure, Pa
PV	pore volume, fraction
PV_{bw}	pore volume of the bottom-water zone, fraction
PV_{oil}	pore volume of the oil zone, fraction
Q	total volume flow rate in the oil and the bottom-water zones, m^3/s
q_a	volumetric flow rate in the oil zone, m^3/s
q_b	volumetric flow rate in the bottom-water zone, m^3/s
q_c	volumetric crossflow rate between layers, m^3/s
q_{c1}	volumetric crossflow rate in Section [1], m^3/s
q_{c2}	volumetric crossflow rate in Section [2], m^3/s
q_{c3}	volumetric crossflow rate in Section [3], m^3/s
q_o	volumetric flow rate in the oil zone, m^3/s
q_w	volumetric flow rate in the water zone, m^3/s
R	resistance factor
t	time, s
x_f	flood front distance from the injection end, fraction
x_{f1}	flood front distance from the injection end in the oil zone, fraction
x_{f2}	flood front distance from the injection end in the bottom-water zone, fraction
w	width of the model, m

Subscripts

a	oil zone
b	bottom-water zone
bw	bottom-water
c	crossflow

e	emulsion
o	oil
p	polymer
w	water

Greek Symbols

α_1	term defined by Eq. (4.3)
α_2	term defined by Eq. (4.4)
α_3	term defined by Eq. (4.5)
α_4	term defined by Eq. (4.6)
α_5	term defined by Eq. (4.7)
α_6	term defined by Eq. (4.8)
Δ	difference
λ	mobility, fraction
μ	viscosity, Pa.s
$\emptyset$	porosity, fraction

Chapter 1

INTRODUCTION

In Alberta and Saskatchewan many light and moderately heavy oil reservoirs contain a high water saturation zone underlying, and in communication with, the oil zone. Waterflooding such reservoirs may still be an economically viable process. However, conventional waterflood has not lived up to expectations. When stratified or bottom-water reservoirs are considered for waterflood, channeling of the injected fluid into the high permeability zone, or in the case of bottom-water, channeling through the bottom-water zone, is of major concern. Waterflood performance can be improved if effective techniques can be developed to partially plug the bottom-water zone. However, there is relatively little systematic investigation of flow mechanics in bottom-water models to be found within the petroleum literature.

In view of the foregoing, this study is an effort to add to the understanding of the flow behaviour in bottom-water formations. It especially examines experimental recovery performance under such conditions. To achieve this, a new crossflow equation has been developed to accurately predict the volume of the injected fluid channeling into the bottom-water layer as well as the ultimate oil recovery. Effective techniques have also been devised to waterflood bottom-water reservoirs using polymer and emulsion as mobility control and/or blocking agents.

Chapter 2

LITERATURE REVIEW

Waterflooding was practiced as an art for years before a scientific basis for waterflood design was developed. An understanding of waterflooding evolved primarily in the late forties from extensive research and development efforts by companies and universities combined with field experience in the seventies. The practice of waterflooding apparently began accidentally. Waterflooding, called secondary recovery, because the process yields a second batch of oil after a field is depleted by primary production, extended slowly throughout the oil-producing areas of the United States in the late forties.

2.1 Conventional Waterflood

Waterflooding is a relatively inexpensive secondary recovery method that is being used widely in the petroleum industry. However, many reservoirs still show poor performance under a conventional waterflood, especially if a high water saturation zone is present. The major reason for this is insufficient and incomplete sweep of the reservoir by the injected water, which tends to move to the producing wells through the more permeable portions of the reservoir, thus, giving a low recovery.

2.2 Waterflooding Layered Reservoirs

Several laboratory model studies have been undertaken to investigate the effect of various parameters on oil recovery in layered reservoirs. Documented evidence reveals that such reservoirs often perform poorly under conventional waterflooding. The presence of bottom-water, as is the case in this study, aggravates the problem. In view of this, as early as the sixties, many techniques were tried to improve the waterflood performance in stratified reservoirs underlain by, and in communication with, bottom-water.

2.2.1 No Crossflow

The behaviour of stratified systems is usually predicted by the Stiles[1] and Dykstra-Parsons[2] methods or some modification of these. In these two methods, the reservoir is divided into discrete homogeneous layers with no crossflow between layers. The mobility ratio is assumed to be unity in the Stiles[1] method while in the Dykstra and Parsons[2] method it is allowed to vary. In Dykstra and Parsons'[2] work, initial oil saturation was the most

important governing variable as far as oil recovery is concerned. Since crossflow was not considered in their model, Dykstra and Parsons[2] developed mathematical equations to compute the velocity of the interface in each layer, considering a two layer model.

2.2.2 Crossflow

For reservoirs in which vertical communication exists between layers of differing permeability, the problem of waterflooding is less severe, according to Jordan[3]. Evidence has been obtained from laboratory experiments (Jordan et al.[4]) that demonstrates quantitatively the effects of capillarity and the importance of flooding stratified reservoirs at such rates that beneficial effects of imbibition are realized. Henley et al.[5] studied the effects of well spacing, fluid mobilities, rates of production, capillary and gravity forces, well penetration and the well completion technique on oil recovery performance in a scaled model of a bottom-water drive. Through displacement tests they showed how well-spacing to the oil-zone-thickness ratios affected recovery for a certain producing water-oil ratio. In layered reservoirs channeling is observed to be more severe because the injected water channels into the high permeability zones (Robertson and Oefelein[6]). Fitch and Griffith[7] conducted an experimental and mathematical investigation of some factors that control miscible flood performance. They noticed that alternate gas-water injection behind a miscible front significantly enhanced miscible flood performance, both within a single layer and in a multi-layer. It was concluded that injection of a small volume of water ahead of the solvent could improve the dispersion of solvent in a layered system.

Khan[8] used a scaled layered model to study water coning. He designed his model using graded sand consolidated with epoxy resin as the oil zone, and unconsolidated sands of different mesh sizes as the water zone. He concluded that the mobility ratio had a significant effect on the water cut and the degree of water coning for a given production rate.

Mungan[9] used a cylindrical stratified model to investigate the effect of coning. He injected his fluids from the bottom. It was observed that the tighter layers appeared to have higher saturation at the time of breakthrough.

2.2.2.1 Analytical and Laboratory Studies

In view of the complexities associated with crossflow behaviour, most analytical solutions have been limited to two-layered models within specified conditions, while multi-layer model studies are restricted to numerical solutions only.

Katz and Tek[10] studied the flow of fluids in stratified porous systems with crossflow between layers. They investigated mathematically the unsteady-state flow of slightly compressible fluids during depletion of bounded stratified porous systems. Their study was also restricted to a single-phase flow system. It was reported that the performance of stratified systems, in terms of cumulative flux as a function of time, lay at all times between bounds established from single-layer theory. That is, the upper bound was given by treating the system as a single layer with arithmetically averaged physical properties. The corresponding lower bound was the summation of the fluxes from each layer treated individually. They pointed out that the variation in performance of stratified systems between the upper and lower bounds was determined by the extent to which crossflow occurred in the system. It was concluded that the early depletion performance of a stratified system lay near the lower bound, and this tended toward the upper bound as time and the radius of drainage increased.

Russell and Prats[11] investigated mathematically, the performance of a well in a bounded, layered reservoir with inter-layer crossflow. The system was composed of a centrally located well in a bounded cylindrical reservoir consisting of two layers of contrasting physical properties. The reservoir contained a single fluid. They concluded that, except for early time, in most practical cases the performance of a two-layer reservoir ccould be represented by that of a single-layer reservoir. The mathematical model they developed demonstrated that, except for early times, the behaviour of a two layered reservoir with crossflow could be duplicated by that of an equivalent single layered reservoir, with the same pore volume and the same drainage and well bore radii, as well as a flow capacity equal to the sum of the flow capacities of the layers in the crossflow system.

Lambeth and Dawe[12] conducted experimental and theoretical studies of displacements in heterogeneous porous media. Their experiments were carried out with layered systems and the displacement fluids had variations in viscosity ratio to study the effect of viscous crossflow. They observed that crossflow could improve recovery efficiency if properly accounted for and could lower recovery efficiency if neglected. In their mathematical

derivation they neglected the pressure distribution in the lower layer. This appears to be an over-simplification of the problem.

Wright et al.[13] studied slug size and mobility requirements for chemically enhanced oil recovery in heterogeneous reservoirs. They made changes in the analytical solution developed by Lambeth and Dawe[12] and added that chemical slug disintegration caused by the effect of crossflow was more severe than previously considered for heterogeneous reservoirs. It was observed that a high mobility slug would preferentially sweep the higher conductance layers, but a low-mobility slug (such as polymer) would tend to some extent to be pushed by crossflow into the lower-conductance media. For low mobility slugs, they suggested that the above mechanism must be considered before they are used for waterflood conformance improvement.

Wright and Dawe[14] studied the influence of mobility ratio on displacement efficiency for layered porous media. The serious problems that heterogeneous reservoirs pose in chemical enhanced oil recovery were pointed out in their studies. They reported the lack of systematic investigation of flow mechanics in heterogeneous reservoirs in the petroleum literature. Wright and Dawe[14] observed that crossflow was greatest where the composition changed most rapidly; that is, at the displacement fronts or transition zones between displaced and displacing fluids. It was pointed out that crossflow of incompressible fluids originated from three sources: 1) gravity; when fluids have different densities, 2) capillary pressure; when interfacial tension was large, and 3) viscous forces; when fluids have differing mobilities. It was concluded that fluid displacements within heterogeneous porous media involving negligible gravitational, capillary pressure and fluid mixing influences were very sensitive to mobility ratio, and that viscous crossflow effects played a large part in the flow mechanics, and must be quantified if predictions of displacement efficiency were to be made.

2.2.2.2 Numerical Studies

For multi-layer reservoirs only numerical solutions have been attempted to examine the effect of crossflow.

Warren and Cosgrove[15] developed a general model that approximates the effect of crossflow by making a modification in Dietz's theory to account for the variations in permeability and hydrocarbon pore volume. It was observed that not accounting for all available permeability data could lead to erroneous predictions in stratified reservoir performance. By comparing their method of predicting the behaviour of a stratified system

with the Dykstra and Parsons[2] method, they observed that their method gave lower vertical sweep for unfavourable mobility ratio and higher values for favourable mobility ratios. This was attributed to the crossflow effect. They reported that considering a stratified reservoir for waterflooding, without accounting for crossflow led to large errors in oil recovery predictions. When reservoirs are underlain with bottom-water the problem is further aggravated, especially when the water phase is mobile.

Root and Skiba[16] investigated the crossflow effects during a waterflood in a stratified reservoir for one incompressible fluid displacing another incompressible fluid of the same density and viscosity. They concluded that the early breakthrough of displacing fluid could not be stopped effectively by blocking access to it in the production and injection wells unless the high permeability zone was completely isolated. When the adjacent strata were in communication, the single-zone, production-njection method lost much of its effectiveness.

Goddin et al.[17] discussed a numerical study of waterflood performance in a stratified system with crossflow. In this study, viscous and capillary crossflow were examined in a field scale model of a two-layer, water-wet sandstone reservoir. It was reported that maximum crossflow occurred in the vicinity of the flood front in the more permeable layer just as observed in Barnes'[18] visual model. They concluded that viscous crossflow was a function of mobility ratio.

Silva and Farouq Ali[19] developed a two-phase three-dimensional simulator to investigate the effect of selective formation plugging in waterflooding a layered model. They designed a simulator using the Strongly Implicit Procedure (SIP) and this was tested under a variety of conditions. They observed from their study that partial plugging of high permeability layers was ineffective if the layers were in communication. They concluded that reservoirs consisting of a bottom water zone may be susceptible to efficient waterflooding.

El-Khatib[20] developed a mathematical model for waterflood simulation in linear stratified non-communicating layers with no crossflow, and for communicating layers with complete crossflow (that is, lower and upper bounds in the Katz and Tek[10] study). The study revealed that the effect of crossflow between layers increased the oil recovery at favourable mobility ratios and decreased it at unfavourable mobility ratios in waterflood performance predictions.

Wright et al.[21] investigated the basic flow mechanisms and dispersion of an injected chemical in layered reservoirs. They controlled the layer permeability, fluid viscosity and flow rate and observed that crossflow increased the dispersion effect.

Ahmed et al.[22] conducted experiments to study waterflooding in a two-dimensional, layered sand model that allowed visual observation. It was reported that intermediate oil recovery during a waterflood in a stratified reservoir with vertical communication was sensitive to flow rate, oil viscosity and interfacial tension (IFT). Ahmed et al.[22] pointed out that oil recovery increased when flow rate was reduced. It was concluded that oil recovery increased considerably when the oil viscosity was decreased.

2.3 Waterflooding in the Presence of Bottom-Water

Efficient and economic recovery of oil in a shallow bottom-water oil reservoir is recognized as a formidable task. High water cuts and rapidly decreasing oil rates early in the production life of such reservoirs have in many instances prompted their suspension or abandonment at very low levels of recovery[23]. Reservoir fluid characteristics required for a prediction of reservoir performance consist primarily of oil and water viscosities at reservoir temperature and pressure. Rock and fluid properties combine to yield the single most important characteristic of a waterflood: the mobility ratio. Controlling this ratio is the next topic of discussion, especially for reservoirs underlain with bottom-water.

2.3.1 Mobility Control

Mobility ratio is perhaps the single most important parameter in waterflooding bottom-water reservoirs. A number of fluids have been used to control the mobility ratio. These include thickened water, polymer and emulsions.

2.3.1.1 Mobility Control with Thickened Water

A large number of reservoirs have been partially or completely invaded by bottom water. An attempt to waterflood such reservoirs can be inefficient if the oil has a high viscosity because the injected water under-runs the oil and emerges at the producing wells without having displaced much of the oil. Barnes[18] recognized this problem in the early sixties. To improve sweep efficiency he suggested that the waterflood should be preceded by a slug of water that has been thickened with a chemical additive. A scaled laboratory model was constructed to investigate the feasibility of injecting viscous water slugs followed by water to improve recovery, while reducing the producing water-oil ratios. It was pointed out that the injection of a viscous slug in bottom-water reservoirs would: (1) reduce the duration

of the flood, (2) reduce the cost of lifting the oil and (3) increase the ultimate recovery. He observed also that injecting a large quantity of a viscous slug into such a system increased the crossflow of oil ahead of the displacing front and this lowered the water-oil-ratio (WOR) during the displacement period. The visual model showed that crossflow was most severe immediately ahead of the front and almost vanished completely at the producing well. The observed crossflow was not quantified. The study was basically directed towards increasing the viscosity of water; hence, he did not verify the effect of other chemicals on the relative permeability to water.

2.3.1.2 Mobility Control with Polymers

One of the oldest techniques to control mobility of water in waterflooding is the use of polymers. This control agent was shown to be effective in the early sixties by Pye[24]. He performed numerous field and laboratory studies of polymer flooding using polyacrylamide solutions. It was observed experimentally that the viscosity of the water-soluble polymer solutions measured in the formation sample departed markedly from those obtained using a viscometer. He quantified the unusual departure of the measured values from the expected response as the resistance factor, R, and defined it as:

$$R = (k_w/\mu_w)/(k_p/\mu_p) = \lambda_w/\lambda_p \tag{2.1}$$

where μ_p is the apparent viscosity of the polymer solution in the core. It was assumed that the permeability was constant. Pye[24] pointed out that at constant flow the injection pressure rises, and this effect was not a core plugging problem because the system reached equilibrium after some time. It was also observed that the extent of departure from the measured viscosity value was most pronounced at low concentrations. At higher concentrations the effect was approximately proportional to the solution viscosity. It was suggested that this unusual behaviour was a property of only selected water-soluble polymers, among which were the extensive family of acrylamide polymers and copolymers. It was recommended that rapid laboratory flood rates should be avoided in order to keep the resistance factor constant.

Candiford[25] reported that a polymer flood increased oil recovery by improving sweep efficiency, including microscopic displacement efficiency. He noticed a 15-20 percent recovery increase for polymer floods over conventional waterfloods, at a water-oil ratio of 10. Another interesting observation made was that a polymer flood led to a significant increase in oil recovery for linear sand packs that contained layers of different permeability. Many field examples were cited where the injection of polyacrylamide solution improved oil recovery.

Mungan et al.[26] investigated the nature of polymer floods in porous media by consecutive flow tests with brine, filtered polymer solution and brine at the same flow rate. It was observed that a change in pressure indicated a change in mobility. Another observation made was that the shear dependency and apparent viscosity increased with concentration and molecular weight of the polymer.

Dauben and Menzie[27] used polyethylene oxides and reported a dilatant rather than pseudo-plastic flow behaviour. Contrary to previous researchers, they observed a rather high flow resistance that was a function of flow rate, pore size, molecular weight of polymer and polymer concentration. It was shown that the apparent viscosity of a polymer solution approached the solution viscosity at very low flow rates and increased as the flow rate increased. This was attributed to the high flow resistance of polyethylene oxide solutions due to the effects of viscoelasticity.

Sherborne et al.[28] observed that polymer solution was a more effective flooding agent than other viscous fluids due to its "abnormal flow resistance." It was reported that the presence of interstitial water aided the displacement efficiency by a waterflood as it established the water flow channels rather uniformly.

Sarem[29] pointed out that certain polymeric waterflood additives, such as partially hydrolyzed polyacrylamides, imparted a useful but seemingly "abnormal" resistance to flow of flood water through porous rock. This "abnormal" resistance has resulted in a substantial increase in waterflood oil recovery beyond what could normally be expected from the viscosity increase that the polymer caused in the flood water. A theory was developed and qualitatively tested on laboratory data to explain the beneficial abnormal property in terms of interaction between molecular Coulomb and ionic forces. The theory was to demonstrate how the polymer could reduce the mobility of water but not that of oil.

Zaidel[30] used thickened solution (polymer) for formations underlain by bottom-water. In his analytical model, he assumed an instantaneous gravitational phase segregation along the vertical. This meant that the polymer solution entered the region with the residual oil saturation in a given section only after it had filled the zone containing zero oil saturation or the zone without any oil at all. He indicated that a polymer with a mobility lower than that of water, represented as

$$R = \lambda_w/\lambda_p > 1, \qquad\qquad (2.2)$$

where R is the resistance factor, improved oil recovery by increasing the flow resistance in the bottom-water zone, resulting in a good sweep efficiency in the oil zone. It was further pointed out that if the polymer mobility was lowered to a certain value ($R \geq 4$), the increase in resistance was primarily due to the oil bank formed in the bottom-water zone during the displacement. It was reported that polymer flooding of a formation underlain by bottom-water could have both favourable and unfavourable consequences: in the favourable case, an increase in the rate of oil displacement would be realized; in the unfavourable case, a certain amount of the oil would be lost or would flow off into the bottom-water zone if the polymer mobility was too low. It was, therefore, suggested that polymers with moderate mobility (R= 2 to 3) should be considered for displacement in bottom-water formations, in order to increase the oil rate during the displacement while minimizing loss of oil to the water zone.

2.3.1.3 Mobility Control with Emulsions

An emulsion is the aqueous solution formed when two immiscible fluids are mixed together, one dispersed as droplets in the other, and stabilized by an emulsifying agent (Bansbach[31]). The use of stable emulsions to control mobility and improve oil recovery in waterfloods was first initiated by McAuliffe[32]. The mechanism of mobility control and/or blocking will be discussed in the sections that follow.

2.4 Flow Mechanism of Polymers in Porous Media

The mechanism of polymer flow through porous media is discussed in the sections below.

2.4.1 Laboratory and Field Studies

Burcik[33] found that at high flow rates dilute solutions of partially hydrolyzed polyacrylamides were pseudo-dilatant. This meant that the solution viscosity increased with increase in flow rate as flow occurred in the porous media containing adsorbed polymers. This effect resulted in a more even flood-out from stratified beds with different permeabilites. Burcik[33] explained the pseudo-dilatancy of the polymer by the uncoiling of molecules retained in the flow channels under a velocity gradient. He emphasized that polymer molecules have diameters twenty times smaller than a typical pore size, and could lower the water permeability and in addition cause pseudo-dilatant flow due to the formation of a microgel.

Smith[34] studied the effects of molecular weight of polymer, rock and fluid properties, flow rate and temperature on polymer solution properties. It was reported that a permanent reduction in permeability was observed even after the core had been flushed with many pore volumes. In polymer flooding, the reduction in permeability was observed to be less in polymers with lower molecular weight and at low flow rates. Smith[34] demonstrated that the dilatant nature (increased apparent viscosity with increasing flow rate) of the polymer manifested itself at flow rates greater than 3.5 ml/day. It was shown that the pseudo-plastic nature of the polymer appeared at lower flow rates and higher concentrations.

Szabo[35,36] conducted experiments to determine an optimal concentration for polymer flooding in a porous medium. This study showed the effect of salinity and polymer performance in stratified reservoir models using radioactive tracers to measure the concentrations of the polymers . It was observed that increasing the polymer concentration and decreasing the salinity enhanced the recovery for small volumes of fluid injected. Szabo[35,36] proposed that the amount of oil recovered was less when polymer was injected at a later stage in the course of the experiment than when it was injected at irreducible water saturation. A higher recovery was observed when a stratified reservoir model was used as compared to that obtained from theoretical considerations. This was attributed to crossflow between the layers. It was demonstrated experimentally that mechanical entrapment played a more important role in low-permeability formations than in medium and high permeability formations.

Duda et al.[37] studied the combined effects of adsorption, mechanical entrapment, shear rate and inaccessible pore volume on effective and residual permeabilities. It was pointed out that the residual permeability was only a weak function of the flow rate of the polymer solution, demonstrating that the amount of polymer retained in the porous medium was a strong function of the polymer rate. It was suggested that mechanical entrapment was the major reason for permeability reduction with polyacrylamide, while an adsorbed layer of polymer molecules was the major reason for permeability reduction in polysaccharides.

Baijal and Dey [38] defined polymer flooding as the method of oil recovery resulting from the addition of water-soluble polymers to flood water. They suggested that the high molecular weight polyacrylamides appeared to be the most effective among polymers used for recovery of oil by polymer flooding. It was observed through laboratory studies that the reduction of residual oil saturation improved macroscopic sweep efficiency. To achieve a good mobility control in a flood, it was suggested that the displacing phase should have a mobility equal to or lower than the mobility of the oil. In their experiments it was observed that higher polymer concentrations improved oil recovery, and this was attributed to more favourable mobility ratios. It was reported that mobility reduction was mainly due to permeability reduction of the sand pack by polymer retention and interaction with solid surface, and that viscosity effects did not contribute much towards mobility control. It was finally concluded that polymer retention increased proportionately with polymer concentration of the injected solution.

Omar[39] pointed out that the control of polymer loss was one of the single most important factors in determining the success or failure of a polymer flooding process. He concluded that polymer adsorption in a formation was a function of the surface area in contact with the flooding fluid. The greater the surface area per unit of bulk volume of the flooded sand, the greater the polymer loss. Thus, fine grained sands adsorbed much more polymer per unit of bulk volume than did large grained sands. It was observed that polymer loss eventually resulted in a water-bank ahead of the polymer solution and this greatly reduced the effectiveness of the polymer in waterflooding.

Dietzel[40] studied the stability of polymer slugs under dynamic conditions. He observed that the action of a polymer slug was based on the adjustment of the mobility between the displaced phase and the displacing flood water, pointing out that two transition zones characterized the mechanism of slug flooding: (1) the transition from displaced phase to the polymer slug and; (2) the transition from the polymer slug to the displacing flood

water. A criterion for judging the dynamic stability of a polymer slug was provided by the maximal value of the concentration or viscosity in the transition zone between the displaced phase and the polymer solution. It was concluded that the viscosity profiles in the elute of flood tests offered a useful method of assessing the dynamic stability of polymer slugs.

Needham and Doe[41] asserted that, depending on the type of polymer used, the effective permeability to water could be reduced in the swept zone. It was reported that polymer flooding did not reduce the residual oil saturation (ROS), but was a way to reach the ROS more quickly or to allow it to be reached economically. Three potential ways in which a polymer flood could make the oil recovery process more efficient were pointed out: (1) through the effects of polymer on fractional flow, (2) by decreasing the water/oil mobility ratio and (3) by diverting injected water from zones that have been swept. It was noticed that the average polymer flood recovery from case histories was 8 % of the original oil in place (IOIP). It was concluded that secondary floods recover substantially more oil for less polymer than tertiary floods.

Islam[42] and Islam and Farouq Ali[43] undertook an extensive experimental study on using various chemical slugs in waterfloods for reservoirs underlain by bottom-water. They used chemical slugs such as polymer, emulsion, biopolymer gel, air, foam and carbon dioxide-activated silica gel. The parameters examined included: permeability contrast, oil viscosity, injection rate of the mobility control agent, slug size and water-oil layer thickness ratio. It was reported that polymer and emulsion performed better than the other chemicals used. A polymer slug was compared with a glycerin slug of the same viscosity and it was found that the polymer slug improved oil recovery more than the glycerin slug. It was concluded that the reduction in effective permeability by polymer was caused by mechanical entrapment and adsorption and this improved recovery by about 27% of IOIP.

Hodaie and Igci[44] conducted experiments to investigate the selection of the right type of polymer to be used to augment waterflood in reservoirs underlain by bottom-water. The effect of vertical and horizontal production wells on oil recovery was also studied. It was observed that a slightly better recovery was achieved, when a horizontal producer was used as compared to a vertical producer, for a continuous waterflood. The reverse was, however, seen when a polymer augmented waterflood was conducted.

2.4.2 Numerical Studies

Masuda et al.[45] developed a simple simulation model to predict the performance of a one-dimensional polymer flood. In their model, they assumed the two phases, oil and polymer, to be immiscible with each other. The Buckley-Leverett equation was modified and a new approach was used to calculate the fractional-flow curves. The rheological behaviour of the displacing fluid, that is, polymer, was modeled using Ellis and viscoelastic type models. Two experiments were conducted to verify the model results, using unconsolidated cores packed with glass beads of 70-100 mesh size. The polymer flood was conducted after waterflooding the model. The calculated polymer flood performance was compared with the experimental data and it was observed that the Ellis model predicted earlier breakthrough of polymer solution and lower oil recoveries than was observed experimentally. The viscoelastic model, however, predicted fractional-flow curves, oil recovery performances and breakthrough times that were very close to the experimental data. It was concluded that the viscoelastic effect of the polymer solution played a very important role in the enhancement of oil recovery .

2.5 Flow Mechanism of Emulsions in Porous Media

The mechanism of flow of emulsions in porous media are reviewed in the sections that follow.

2.5.1 Laboratory and Field Stu...es

The flow behaviour of emulsions in tubes and unconsolidated synthetic porous media was studied by Uzoigwe and Marsden[46]. It was noticed that emulsion had a Newtonian behaviour even after the dispersed-phase concentration reached 50% (volume). The emulsion, however, exhibited non-Newtonian behaviour after this concentration. The emulsion was treated as a homogeneous liquid, and no permeability reduction was observed as a result of the flow.

McAuliffe[32] used stable emulsions, that is, oil-in-water, as mobility control agents to improve oil recovery in waterfloods. To obtain an oil-in water emulsion, asphaltic crude oil was added to dilute sodium hydroxide. Emulsions with different drop sizes were injected into a consolidated sandstone under a constant pressure. It was reported that, for the emulsion to be an effective mobility control agent, the oil droplets in the emulsion should be slightly larger than the pore-throat constrictions in the porous medium. In the laboratory work, it was observed that emulsions tended to have the viscosity of the continuous phase; thus, oil-in-water emulsions tended to have the viscosity of water. It was noticed that there was a

permeability reduction even with small-droplet-diameter emulsions. This was not, however, significant, especially if the core had a fairly high permeability. It was reported that as the oil-in-water emulsion was injected, a greater amount of the emulsion entered the more permeable zones; consequently, flow became more restricted and the water began to flow into the less permeable zones, resulting in greater vertical sweep efficiency. In order to observe the effect of emulsion flow, the emulsion was diluted to 0.5 percent oil. It was observed that the average diameter of the oil droplets dictated whether the emulsion flow would substantially decrease the water permeability of the core or whether it would not. The permeability reduction caused by injecting emulsion was retained even when the emulsion was followed by many pore volumes of water. It was concluded that flow of oil-in-water emulsions through porous media was pseudo non-Newtonian regardless of how much oil the emulsion contained.

McAuliffe[47] reported a field test of an oil-in-water emulsion flood. Three percent pore volume of emulsion containing 14 percent oil was injected into the formation. Increased oil production and lower WOR's were observed from the wells surrounding the emulsion-treated injectors, compared with little or no increase in oil production and increasing water-oil-ratio for wells surrounding the water injectors. It was concluded that the emulsions decreased the channeling of the injected water, which increased the volumetric sweep efficiency, viz., 55,000 bbl of additional oil were produced with 33,000 bbl of crude oil that were emulsified and injected.

Cooke et al.[48] attributed the permeability reduction by the formation of water-in-oil emulsions to the high viscosity of these emulsions or to the formation of an oil film (lamella) across the pore throat. It was pointed out that the lamellae formed in the pore spaces effectively blocked many of the flow paths that were formerly available for the flow of water. It was reported that the resistance to flow of the lamellae and the plugging of the pores by the lamellae caused the large increase in pressure gradient that was observed immediately behind a displacement front. It was argued that the low mobility of the fluid in the region where lamellae existed and the small amount of oil within the lamellae caused the sharp gradient in oil saturation that was noticed at the displacement front.

Johnson[49] reviewed the status of caustic and emulsion flooding. The salient features of emulsions in recovering viscous oils or oils in heterogeneous reservoirs where sweep efficiency was poor was reported. It was suggested that emulsion flooding was a natural extension of the caustic flooding emulsification and entrapment mechanism. It was, however, pointed out that although the potential of emulsions for improving oil recovery was well in place, the cost of oil for emulsification and injection was a serious hindrance to wider field use.

Soo and Radke[50] pointed out that another mechanism for permeability reduction was emulsion. It was argued that when emulsions were injected into a porous medium, droplets not only blocked pores of the throat sizes smaller than their own, but they were also captured on pore walls and crevices. It was suggested that in the flow of dilute and relatively unstable emulsions two regimes of oil flow existed in the porous medium: a regime which consisted of oil droplets dispersed in water and a regime which consisted of continuous oil that had coalesced and which was transported according to its relative permeability. It was reported that two factors determined the overall permeability reduction: the volume of drops retained and how effective these drops were in restricting the flow. It was maintained that as the drop size of the emulsion increased, the drop retention increased as well. It was, however, pointed out that, at identical volume retention, smaller sized drops were more effective in restricting flow. For systems of smaller drop-size emulsions (that is, for $d_d/d_p < 0.2$ in their work), the effect of drop size on retention dominated and an increase in the drop size resulted in increased permeability reduction. On the other hand, for systems of larger drop-size emulsions, the effect of drop size on the restriction effectiveness dominated, and increasing the drop size resulted in less transient permeability reduction. They concluded that the viscosity of the oil has little effect on both the effluent concentration and transient permeability histories.

Schimdt et al.[51] proposed the use of dilute, stable emulsions to improve mobility control in enhanced oil recovery processes. It was pointed out that an oil-in-water emulsion provided microscopic mobility control through entrapment or local permeability reduction and not through viscosity ratio improvement. It was concluded that mobility ratio improvement was achievable due to the small oil droplets that were irreversibly captured in the porous medium as a result of straining and interception, and this lowered the local permeability to water.

French et al.[52] studied the use of emulsions to control mobility in steamflooding. It was observed that a reduction in permeability from emulsion plugging might not necessitate that the median droplet size was equal to or larger than the median pore throat diameter, and that competition from an ensemble of smaller droplets "crowding" a single pore would have the same effect in blocking a pore throat. It was reported that the injection of a small slug of oil-in-water emulsion prepared from oil and water available in a specific field caused a significant reduction in the permeability of the core from that field.

Islam and Farouq Ali[53] studied the blocking mechanism of emulsions and their effectiveness in controlling mobility, while waterflooding an oil reservoir, both with and without a bottom-water zone. It was reported that the reservoir and fluid properties such as oil-to-water zone thickness, oil-to-water permeability ratio, oil viscosity and emulsion slug size, affected the blocking ability of emulsions as well as their oil content in a reservoir underlain by bottom-water. The investigation showed that the smaller the oil-to-water zone thickness, the lower the ultimate oil recovery for low to moderate oil-to-water permeability ratios. Oil recovery was, however, found to increase slightly for high oil-to-water permeability ratios as the thickness of the bottom-water zone increased. A significant improvement in recovery for high viscosity oils was observed, when emulsion was used in the flood, as compared to that obtained in conventional waterflood. It was concluded that a minimum of one pore volume (bottom-water zone) of emulsion slug was required for successful blockage with emulsion, while the optimum slug size was 2.5 pore volumes.

Farouq Ali et al.[54] studied the flow of emulsions through porous media at high temperatures. In their work, they studied thermal stability of emulsions in order to appraise the flow behaviour at elevated temperatures. Experiments were conducted using surfactants emulsions, carbon dioxide/water emulsions, sodium hydroxide emulsions, acid emulsions and distilled water emulsions through porous media to investigate the changes in characteristics. The study showed that the flow of emulsions through porous media was a function of the drop-size distribution of the emulsion to pore-size distribution of the porous medium ratio. It was concluded that, for both oil-in-water and water-in-oil emulsions, the rheology of emulsions in the porous media was comparable to the rheology in a viscometer. It was reported that emulsion mobility was governed by the flow velocity, an increase in which could cause the shearing of the larger drops into smaller ones.

Yeung[55] and Yeung and Farouq Ali[56] introduced three different displacement techniques, the Emulsion Slug Process (ESP), the Alternating Water Emulsion Process (AWE) and the Dynamic Blocking Process (DBP) to improve the vertical sweep efficiency while waterflooding bottom-water formations. For emulsions with low surfactant concentrations (0.016 to 0.04 %), the DBP and the AWE processes were found to give higher oil recoveries than the ESP process under bottom-water conditions. For emulsions with higher surfactant concentrations (0.4 %), the reverse was true. Crossflow was very prominent ahead the flood front for high viscosity fluids, according to Yeung and Farouq Ali[56]. It was concluded that a high surfactant concentration did not necessarily give a higher oil recovery for both homogeneous and bottom-water reservoirs.

Mendoza et al.[57] observed that oil recovery was sensitive to injection rate for both oil-in-water and water-in-oil emulsion floods. It was demonstrated that the flood rate determined the extent of mobility ratio variation, and this in turn depended on the drop size, type and the rheological behaviour of the emulsion. Oil recovery, as a function of flood advance rate, showed a minimum rate of about 10 m/day. The type of emulsion slug (oil-in-water or water-in-oil) determined whether recovery increased or decreased with an increase in slug size. It was concluded that water-driven emulsion slugs may give a viable alternative to thermal recovery of moderately viscous oils.

Fiori and Farouq Ali[58] suggested the use of solvents in adjusting the emulsion characteristics to increase oil displacement efficiency. Incremental recoveries of up to 70% were observed when emulsion slugs were injected into partially waterflooded cores. It was concluded from their studies that carefully designed crude oil emulsions (water-in-oil) could be used as oil recovery agents for heavy oil reservoirs with low primary conductivity, poor response to waterflood and low potential for thermal recovery applications.

2.5.2 Numerical Studies

With the growing importance of emulsion as mobility control agent in flow through porous media, it is important to have a numerical model to predict accurately pressure drops and frontal movements during emulsion floods.

Devereux[59] proposed the droplet retardation model, which was based on the mechanism originally delineated by McAuliffe[46]. The model described the flow of stable oil-in-water emulsions in porous media with capillary effects, but neglected gravitation and compression effects. In this model, the transient permeability behaviour was modeled based on oil droplets passing through pores of throat size smaller than their own diameters resulting in the oil droplets having to squeeze through the pore constrictions. To pass through the tortuous paths in the porous medium, the droplets had to overcome capillary resistance in each pore throat and this retarded the emulsion flow.

Alvarado and Marsden[60] developed the bulk viscosity model in which they described emulsion as a single phase and a homogeneous fluid. In this model, emulsion was considered as a non-Newtonian fluid that did not follow Darcy's law, as a result of the change in bulk viscosity due to shear rate. Although their model had a limitation as far as prediction of transient permeability is concerned, it was useful for emulsion computations, especially for high-concentration emulsions with small drop-size to pore-size ratios.

Soo and Radke[61] proposed a filtration model for the flow of dilute, stable emulsions in porous media. For the type of emulsion flow considered in their model, it was reported that the drop size was of the order of pore size, hence drops were captured both by the straining and the interception mechanisms with the possibility of straining being the dominant mechanism. It was suggested that emulsion droplets were not only retarded when they flow through porous media as suggested by Devereux[59]; they were actually captured. The filtration model predicted transient and steady state permeability reduction caused by an emulsion. Soo and Radke[61] reported that transient flow behaviour was characterized by three parameters: a filter coefficient, a flow-redistribution parameter and a flow restriction parameter. The filter coefficient controlled the emulsions front sharpness, while the flow redistribution parameter dictated the steady state retention in addition to the flow redistribution phenomenon. Finally, the flow-restriction parameter described the effectiveness of the retained drops in permeability reduction.

Abou-Kassem and Farouq Ali[62,63] modified the bulk viscosity model, and made it more practical for both Newtonian and non-Newtonian emulsions to be handled easily in numerical studies. For non-Newtonian emulsions, the correlation was presented in the form of a modified Darcy law and tested using Alvarado and Marsden's[60] experimental data. The correlation demonstrated a quantitative description of the effect of pore size distribution and tortuousity of porous media on flow. Pressure drop predictions were also possible with this model within 2.4 % of the average absolute relative deviation based on the Alvarado and Marsden's[60] experimental data.

Khambharatana[64] undertook extensive experimental work to observe the physical mechanism that occurs when a stable emulsion flows in a porous medium. Emulsion rheology and droplet capture were investigated for different kinds of emulsion flow in two types of porous media. It was observed that the change in emulsion rheology in a porous medium had an overall trend similar to that in a viscometer for the shear rates considered. It was reported that emulsion droplets were captured according to a filtration process. A one-dimensional, three-phase (oleic, aqueous, and emulsion) model that accounted for the interactions of a surfactant, oil, water and the rock matrix was developed. This model was used to simulate linear core floods of stable emulsions and the experimental production history was compared with the simulated results. It was noticed that a multiphase, non-Newtonian rheological model of an emulsion with interfacial tension-dependent relative permeabilites and time-dependent capture showed the best predictions of the experimental core floods.

2.6 Application of Horizontal Wells in Enhanced Recovery

The use of horizontal wells has been increasing very rapidly throughout the oil industry as advances in drilling techniques continue. However, inspite of a large increase in literature references, little has been published on horizontal well applications for enhanced oil recovery (EOR) methods. The interest in horizontal-well waterflooding is very recent with most reports or publications appearing in the last half of 1991. Water coning phenomena is usually observed in oil reservoirs with a strong water drive or bottom-water. In a strong water drive reservoir a steady state flow condition prevails in the course of most of the life of the oil producing wells. The water coning problem is, therefore, dealt with in a steady state context, so that a constant production rate causes a constant pressure drawdown at every point within the constant potential boundaries in the reservoir.

2.6.1 Advantages of Horizontal Wells

The most important advantages horizontal wells have over vertical wells include: increased productivity index, near elimination of coning problems for strong water drive reservoirs, suppression of the oil bank in the case of reservoirs underlain by bottom-water and finally a higher probability of intersecting systems of vertical and horizontal fractures in reservoirs. A brief discussion of these advantages is given below.

2.6.1.1 Increase in Productivity Index

Horizontal wells provide a bigger and more effective contact area between the well and the reservoir; consequently, they can improve the fluid production rate and efficiency of the recovery process. Conventional vertical wells act as a point sink and as fluids flow radially from different regions of the reservoir towards the vertical production well the area for flow decreases, the flow velocity increases and the pressure gradient rises rapidly near the vertical well. Vertical wells have only a small part of their total length open for flow of reservoir fluids. Most of the pressure drop occurs in the vicinity of the wellbore. Horizontal wells, provide a much larger area for inflow of reservoir fluids. In view of this, the pressure drop decreases, resulting in a more even, uniform flow distribution and less oil trapping behind[65].

Borisov[66] investigated the idea of oilfield production using horizontal and highly deviated wells. An approximate equation for oil flow toward an isolated well located in the centre of a homogeneous and isotropic bed was developed to calculate the oil production rate based on the total flow resistance that was made up of two components: external resistance to inflow, and internal resistance due to flow inside the well. The analysis was conducted using horizontal wells in reservoirs bounded by a gas cap and a water leg. It was concluded that the flow of a unit length of a selectively perforated vertical well was much higher than that of a unit of length of a horizontal well. The above conclusion meant that horizontal wells were not as productive as vertical wells when water influx or gas cap expansion was the driving force.

Giger[67] showed that the productivity of a horizontal well was less sensitive to unfavourable heterogeneities in its vicinity than it was for a vertical well. It was pointed out that the pressure drop in flow toward a horizontal well was the sum of two components: the first component accounted for the partial penetration of the drainage area, and the second component represented the pressure drop due to the convergence of fluid streamlines.

Joshi[68] derived an equation to compute the steady-state oil production rate for horizontal wells draining an elliptical drainage area. With this equation parameters like reservoir anisotropy, thickness, well drainage area and eccentricities (well location other than the reservoir center) on horizontal well productivity were investigated. He examined gas and water coning tendencies as well. It was concluded that horizontal well productivity improvements depended on reservoir thickness, well length and location and reservoir anisotropy.

Ozkan and Raghavan[69] conducted a study on the performance of horizontal wells in bottom-water drive reservoirs. An analytical solution was developed to investigate the pressure distribution in these reservoirs. In the development of the equations, the wellbore was treated as a line source with an infinite conductivity or a uniform flux boundary condition. It was concluded that productivity of horizontal wells was less influenced by reservoir anisotropy as compared to the productivity of vertical wells.

Dikken[70] investigated the pressure drop in horizontal wells and its effect on production performance. It was pointed out that the commonly used assumption of laminar flow in horizontal wells was not necessarily true for most practical situations, and this was demonstrated using calculated examples. A second order differential equation was developed coupling single-phase turbulent well flow with stabilized reservoir flow and solved numerically for various boundary conditions. It was observed that turbulent well flow in the horizontal section of a horizontal well brought about an appreciable reduction of drawdown at various positions away from the lifting end of the section, and that the total production levelled off and became almost constant when the well length exceeded a certain critical value.

The use of horizontal injection wells could improve injectivity and reduce polymer degradation during polymer floods. As a result of the viscous nature of polymer solutions, injectivity in unfractured wells could be substantially less during a polymer flood than in a waterflood[71]. The higher injectivities allowed by horizontal wells could help to alleviate this problem. For a given injection pressure, the fluid velocity at the wellbore sand face could be significantly less in horizontal wells than in vertical wells. Injection and production rates could be increased by as much as ten times (without an increase in pressure) by using combinations of horizontal injection and production wells in thin formations and at wide well spacings.

2.6.1.2 Suppression of Oil Bank Formation

Chaperon[72] conducted studies to investigate the critical production rate of horizontal wells in anisotropic formations. This study assumed steady-state or pseudo-steady state flow conditions. The approach was identical to that of Muskat[73]; thus, only static stable cones were considered. Only flow in the plane perpendicular to the horizontal axis was examined. It was reported that the requirements for static and dynamic equilibrium were used to develop a simple equation to calculate the critical fluid production rate per unit length of a horizontal well in anisotropic and isotropic reservoirs. The critical rates for vertical and horizontal wells were then compared. It was observed that the critical cones came closer to the horizontal wells than to the vertical wells. The critical production rate per unit length of a horizontal well was noticed to be a function of the transmissibility of the oil layer, initial oil column thickness and the distance between the well and the lateral boundary. It was concluded that the critical production rate for horizontal wells was not as sensitive to vertical permeability variation as that for vertical wells.

Papatzacos et al.[74] derived a semi-analytical equation to calculate the cone breakthrough time for horizontal wells. In their analysis, they considered the oil-water contact and the gas-oil contact as moving boundaries. In view of this assumption, the position, shape and the size of the cones become functions of time. With these moving boundary conditions, the Laplacian potential flow equation was transformed into dimensionless form, and solved numerically. Three different cases were studied: a two-cone case with simultaneous gas and water coning, single-phase gas coning and single-phase water coning. To simulate the cone breakthrough time, they used different water viscosities, gas viscosities and anisotropic ratios. The simultated results compared favourably with actual data for the Helder field in the North Sea.

Chapter 3

STATEMENT OF THE PROBLEM

The main objectives of this study were to examine ways of efficiently waterflooding oil reservoirs (oil viscosity 1 to 200 mPa.s) underlain by bottom-water and to develop analytical expressions for crossflow. These objectives were achieved using theoretical and experimental methods, which are outlined below:

3.1 Theoretical Objectives

1. Development of modified mathematical equations for crossflow that occurs in waterflooding oil reservoirs with bottom-water

2. Development of a semi-analytical model using computer programs to make predictions

3. Utilization of these equations to calculate volume of injected fluid channeling into the bottom-water layer and investigation of the effect of frontal locations on the crossflow behaviour

4. Prediction of oil recovery utilizing the semi-analytical model

3.2 Experimental Objectives

1. Conduct waterflood experiments in a two-dimensional model using polymer and emulsion as mobility control and/or blocking agents in different injection techniques

2. Examine the effect of horizontal injection/production well combinations on recovery when utilized to waterflood oil reservoirs with bottom-water.

Chapter 4

4. MODIFICATION OF THE PREVIOUSLY DERIVED CROSSFLOW EQUATION

4.1 Introduction

Several previous studies employed idealized dual-layer porous medium models to represent the displacement flow problems of layered reservoirs[10-16]. Such models constitute a logical starting point for a systematic investigation. Fluid properties and flow conditions need to be defined for this purpose. The interpretation of previous work is often rendered difficult by the simultaneous inclusion of several factors such as capillary pressure, relative permeabilities, fluid viscosities, dispersion and gravity effects[14]. In order to make useful quantitative conclusions it is desirable to be able to investigate each factor independently of the rest.

Among the previous investigations very few are analytical solutions to layered reservoirs problems. Katz and Tek[10] and Russell and Prats[11] developed analytical solutions for two-layered reservoirs. They, however, considered only single phase compressible fluid flow. El-Khatib[20] developed a mathematical model for a linear stratified system for the cases of non-communicating and communicating layers with complete crossflow. It was said that the model could predict fractional oil recovery, water cut, total volume injected and the change in the total pressure, or the change in injection rate, at water breakthrough in successive layers. The mathematical development, however, assumed that the crossflow between the different layers was instantaneous such that there was no vertical pressure drop. That implied that there was a high vertical flow conductivity due to the large lateral area for crossflow. This assumption, however, is not valid for reservoirs underlain with bottom-water, since the vertical pressure drop is the driving force behind crossflow. Lambeth and Dawe[12] developed an analytical solution for one fluid displacing another in a two-layer reservoir. They assumed that the pressure in the lower permeability layer of their model was not affected by crossflow. This assumption can be justified only when the permeability contrast of the two layers is quite large. Such an assumption is not applicable to reservoirs underlain by bottom-water, where permeabilities of the layers are more or less the same. The next section shows a new derivation of the crossflow equation[55] without assuming a linear pressure distribution with respect to distance in either layer.

4.2 Derivation of the Modified Crossflow Equation

An expression for crossflow occurring in the course of waterflooding a two-layered reservoir model, the lower layer being a water zone, was developed by Yeung[55]. In this thesis an attempt is made to modify the crossflow equation so as to be able to handle the channeling of any injected fluid and to calculate the frontal movements of x_{f1} and x_{f2} during the flood as well as investigate the effect of frontal locations on the crossflow behaviour which was not possible in the previous work[55].

Consider a two-layer porous medium, where the upper layer is the oil zone with a permeability to oil, k_{owr}, and the lower layer is the water zone with an absolute permeability k_w. Fluid is being injected at a total rate, Q, of which q_a enters the oil zone and q_b enters the bottom zone. The following assumptions are made:

1) flow is steady state;

2) crossflow is vertical;

3) crossflow does not alter the mobility in either layer;

4) fluids are incompressible;

5) displacement is piston-like;

6) only oil is flowing ahead of the flood front in the oil zone;

7) only water is flowing behind the flood front; and

8) capillary and gravity forces are negligible.
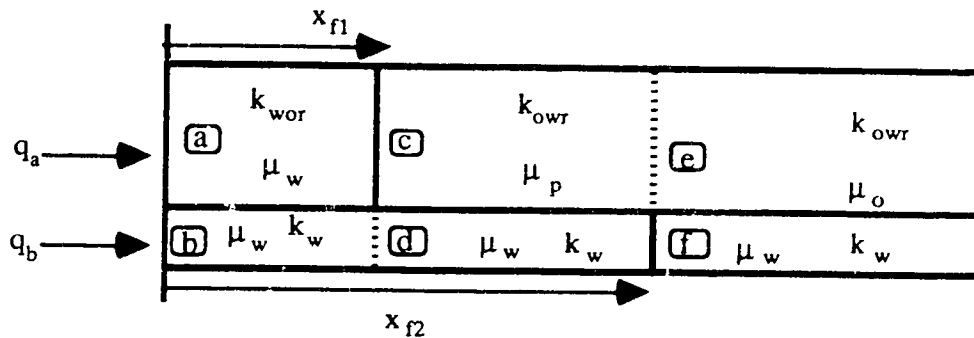
Consider a vertical section of thickness Δx and width w behind the flood front as shown below:
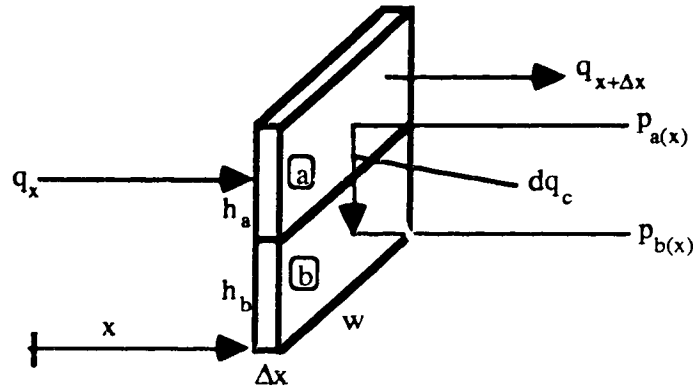
where q_x is the flow rate in Section **a** at a distance x from the injection end, $q_{x+\Delta x}$ is the flow rate in Section **a** at a distance $x+\Delta x$ from the injection end and dq_c is the vertical crossflow over the interlayer boundary. Note that crossflow is positive from **a** to **b**. Applying a mass balance to the fluid Section **a** above gives

$$q_x - \left(q_{x+\Delta x} + dq_c\right) = 0 \qquad (4.1)$$

Using Darcy's equation and rearranging one obtains

$$\left.\frac{A_a k_a}{\mu_a}\frac{\partial p_a}{\partial x}\right|_{x+\Delta x} - \left.\frac{A_a k_a}{\mu_a}\frac{\partial p_a}{\partial x}\right|_{x} = \frac{2w\Delta x}{\frac{\mu_a h_a}{k_a} + \frac{\mu_b h_b}{k_b}}\cdot\left(p_a - p_b\right) \qquad (4.2)$$

where p_a and p_b are the average pressures of the corresponding sections taken from the centre of each section. (Note that the subscripts a, b, c, d, e, f are used for simplicity.) Taking the limit as Δx approaches zero, the following differential form of Equation (4.2) results:

$$\frac{\partial^2 p_a}{\partial x^2} = \alpha_1\left(p_a - p_b\right) \qquad (4.3)$$

where $\alpha_1 = \dfrac{2}{h_a^2 + M_{ab}h_a h_b}$, and $M_{ab} = \dfrac{k_a/\mu_a}{k_b/\mu_b}$ is the mobility of the fluid in Section a to that in Section b. Carrying out similar procedures for the other sections one arrives at the following equations:

$$\frac{\partial^2 p_b}{\partial x^2} = \alpha_2 (p_b - p_a),$$

(4.4)

$$\frac{\partial^2 p_c}{\partial x^2} = \alpha_3 (p_c - p_d),$$

(4.5)

$$\frac{\partial^2 p_d}{\partial x^2} = \alpha_4 (p_d - p_c),$$

(4.6)

$$\frac{\partial^2 p_e}{\partial x^2} = \alpha_5 (p_e - p_f),$$

(4.7)

and

$$\frac{\partial^2 p_f}{\partial x^2} = \alpha_6 (p_f - p_e),$$

(4.8)

where $\alpha_2 = \dfrac{2}{h_b^2 + M_{ba}h_b h_a}$, $\alpha_3 = \dfrac{2}{h_c^2 + M_{cd}h_c h_d}$, $\alpha_4 = \dfrac{2}{h_d^2 + M_{dc}h_d h_c}$, $\alpha_5 = \dfrac{2}{h_e^2 + M_{ef}h_e h_f}$,

and $\alpha_6 = \dfrac{2}{h_f^2 + M_{fe}h_f h_e}$ and where the M's are the mobility ratios for the corresponding

sections. Solving Equations (4.3) and (4.4), (4.5) and (4.6), and finally (4.7) and (4.8) simultaneously, the following pressure equations are obtained:

$$p_a(x) = c_1 + c_2 x + c_3 \left(\frac{\alpha_1}{m_1} \right) \cdot \sinh\left(x\sqrt{m_1} + c_4\right),$$

(4.9)

$$p_b(x) = c_1 + c_2 x - c_3 \left(\frac{\alpha_2}{m_1} \right) \cdot \sinh\left(x\sqrt{m_1} + c_4\right),$$

(4.10)

$$p_c(x) = c_1' + c_2' x + c_3' \left(\frac{\alpha_3}{m_2} \right) \cdot \sinh\left(x\sqrt{m_2} + c_4'\right),$$

(4.11)

$$p_d(x) = c_1' + c_2' x - c_3' \left(\frac{\alpha_4}{m_2} \right) \cdot \sinh\left(x\sqrt{m_2} + c_4'\right),$$

(4.12)

$$p_e(x) = c_1'' + c_2'' x + c_3'' \left(\frac{\alpha_5}{m_3}\right) \cdot \sinh\left(x\sqrt{m_3} + c_4''\right),$$ (4.13)

and

$$p_f(x) = c_1'' + c_2'' x - c_3'' \left(\frac{\alpha_6}{m_3}\right) \cdot \sinh\left(x\sqrt{m_3} + c_4''\right)$$ (4.14)

where $m_1 = \alpha_1 + \alpha_2$, $m_2 = \alpha_3 + \alpha_4$ and $m_3 = \alpha_5 + \alpha_6$. The following twelve boundary conditions are used to obtain the twelve constants in the above equations.

(i) $q = q_a$ at $x=0$;

(ii) $q = q_b$ at $x=0$;

(iii) $p_a = 0$ at $x=L$;

(iv) $p_b = 0$ at $x=L$;

(v) $p_c = 0$ at $x=L$;

(vi) $p_d = 0$ at $x=L$;

(vii) $p_e = 0$ at $x=L$;

(viii) $p_f = 0$ at $x=L$;

(ix) $p_a = p_c$ at the flood front x_{f1};

(x) $p_b = p_d$ at the flood front x_{f1};

(xi) $p_c = p_e$ at the flood front x_{f2}; and

(xii) $p_d = p_f$ at the flood front x_{f2}.

The inflow of fluids into the oil and water zones is allowed to be arbitrary. In other words the rates, q_a and q_b are independent variables. Applying the above conditions, the constants are obtained as follows:

$$c_1 = \frac{\mu_a q_a L}{k_a A_a} \frac{\alpha_2}{m_1} \left(M_{ab} \frac{\alpha_1}{\alpha_2} \frac{h_a}{h_b} \frac{q_b}{q_a} + 1\right);$$

$$c_2 = -\frac{\mu_a q_a}{k_a A_a} \frac{\alpha_2}{m_1} \left(M_{ab} \frac{\alpha_1}{\alpha_2} \frac{h_a}{h_b} \frac{q_b}{q_a} + 1\right);$$

$$c_3 = -\frac{\mu_a}{k_a A_a} \left(q_a - M_{ab} \frac{h_a}{h_b} q_b\right) \frac{1}{\sqrt{m_1} \cosh\left(L\sqrt{m_1}\right)};$$

$$c_4 = -L\sqrt{m_1};$$

$$c_1' = -c_2' L;$$

$$c_2' = -\frac{\mu_s q_s}{k_s A_s} \frac{\alpha_2}{m_1} \left\{ 1 + M_{sb} \frac{\alpha_1}{\alpha_2} \frac{h_s}{h_b} \frac{q_b}{q_s} + \left(1 - M_{sb} \frac{h_s}{h_b} \frac{q_b}{q_s}\right) \left(\frac{\alpha_1}{\alpha_2} - \frac{\alpha_3}{\alpha_2} \frac{m_1}{m_2}\right) \frac{\sinh\left[\sqrt{m_1}(L - X_{f1})\right]}{\sqrt{m_1}(L - X_{f1})\cosh\left(L\sqrt{m_1}\right)} \right\}$$

$$c_3' = c_3 \cdot \frac{\sinh\left[\sqrt{m_1}(L - X_{f1})\right]}{\sinh\left[\sqrt{m_2}(L - X_{f1})\right]},$$

$$c_4' = -L\sqrt{m_2};$$

$$c_1'' = -c_2'' L;$$

$$c_2'' = c_2 + c_3 \cdot \frac{\sinh\left[\sqrt{m_1}(L - X_{f1})\right]}{(L - X_{f1})} \cdot \left\{ \frac{\alpha_1}{m_1} - \frac{\alpha_3}{m_2} + \left(\frac{\alpha_3}{m_2} - \frac{\alpha_5}{m_3}\right)\left(\frac{L - X_{f1}}{L - X_{f2}}\right) \frac{\sinh\left[\sqrt{m_2}(L - X_{f1})\right]}{\sinh\left[\sqrt{m_2}(L - X_{f2})\right]} \right\}$$

$$c_3'' = c_3' \cdot \frac{\sinh\left[\sqrt{m_2}(L - X_{f2})\right]}{\sinh\left[\sqrt{m_3}(L - X_{f2})\right]}, \text{ and}$$

$$c_4'' = -L\sqrt{m_3}.$$

The diagram below illustrates how the crossflow occurs and from this visualization, the crossflow equations are obtained. It is explicitly assumed here that $x_{f2} > x_{f1}$.
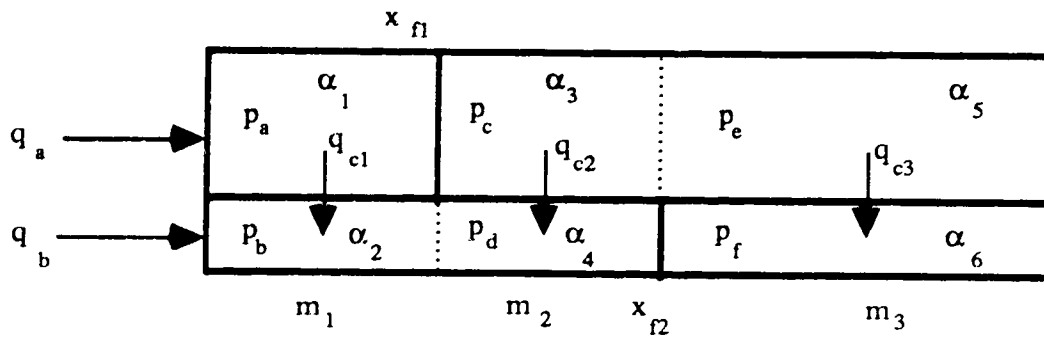
The crossflow streams represented by the vertical arrows are from the fluids in the upper layer to the lower layer. Using Darcy's equation for fluid flow, the crossflow equations are obtained as follows:

$$dq_{c1} = \frac{2wdx}{\frac{\mu_a h_a}{k_a} + \frac{\mu_b h_b}{k_b}} \cdot [p_a(x) - p_b(x)]$$

(4.15)

and

$$q_{c1} = \int_0^{x_{f1}} dq_{c1} = \frac{k_a A_a}{\mu_a} \cdot \alpha_1 \cdot c_3 \int_0^{x_{f1}} \sinh\left[\sqrt{m_1}(x - L)\right] dx$$

(4.16)

Integrating the above equation one obtains

$$q_{c1} = \frac{k_a A_a}{\mu_a} \cdot \alpha_1 \cdot c_3 \cdot \left\{ \frac{\cosh\left[\sqrt{m_1}(x_{f1} - L)\right] - \cosh\left(L\sqrt{m_1}\right)}{\sqrt{m_1}} \right\}$$

(4.17)

For crossflow in the middle section, the crossflow is visualized to be ahead of the flood front in the oil zone and behind the flood front in the bottom-water zone. The integration is, therefore, from x_{f1} to x_{f2}, and this leads to the equations below

$$dq_{c2} = \frac{2wdx}{\dfrac{\mu_c h_c}{k_c} + \dfrac{\mu_d h_d}{k_d}} \cdot [p_c(x) - p_d(x)]$$ (4.18)

and

$$q_{c2} = \int_{x_{f1}}^{x_{f2}} dq_{c2} = \frac{k_c A_c}{\mu_c} \cdot \alpha_3 \cdot c_3' \int_{x_{f1}}^{x_{f2}} \sinh[\sqrt{m_2}(x - L)] dx$$ (4.19)

Integrating the above equation we get

$$q_{c2} = \frac{k_c A_c}{\mu_c} \cdot \alpha_3 \cdot c_3' \left\{ \frac{\cosh[\sqrt{m_2}(x_{f2} - L)] - \cosh[\sqrt{m_2}(x_{f1} - L)]}{\sqrt{m_2}} \right\}$$ (4.20)

The crossflow in the last section is the crossflow ahead of the front, x_{f2} and that is obtained as

$$dq_{c3} = \frac{2wdx}{\dfrac{\mu_e h_e}{k_e} + \dfrac{\mu_f h_f}{k_f}} [p_e(x) - p_f(x)]$$ (4.21)

and

$$q_{c3} = \int_{x_{f2}}^{L} dq_{c3} = \frac{k_e A_e}{k_e} \cdot \alpha_5 \cdot c_3'' \int_{x_{f2}}^{L} \sinh[\sqrt{m_3}(x - L)] dx$$ (4.22)

Integrating the above from x_{f2} to L one gets

$$q_{c3} = \frac{k_e A_e}{\mu_e} \cdot \alpha_5 \cdot c_3'' \left\{ \frac{1 - \cosh[\sqrt{m_3}(X_{f2} - L)]}{\sqrt{m_3}} \right\}$$ (4.23)

Chapter 5

EXPERIMENTAL APPARATUS AND PROCEDURE

5.1 Description of the Experimental Apparatus

The experimental apparatus consisted of two constant-rate pumps and a specially designed aluminum core holder with a rectangular cross-section. The setup is shown in Figure 5.1. Two constant rate pumps, an ISCO pump and a Jefri pump, were used for fluid injection. Almost all the experiments required simultaneous injection of fluids; hence, the ISCO and Jefri pumps were used concurrently. For the few experiments that did not require two pumps, only the Jefri pump was used. The pump was connected to two cylinders containing floating pistons. This allowed the use of two different fluids without contaminating one with the other, at a maximum cylinder volume of 1000 ml. The maximum injection rate of the Jefri pump was 1200 ml/hr at a maximum pressure of 7000 kPa. The Jefri pump was monitored and controlled by an IBM PC and the flow rate could be adjusted with a precision of 0.1 ml/hr. The ISCO pump had a maximum capacity of 500 ml and a maximum flow rate of 400 ml/hr. A Validyne transducer was used to measure the injection pressure. The diaphragm used in this transducer could withstand a maximum pressure of 483 kPa (70 psi). The rectangular core holder was fabricated from tubular aluminum block. The inside dimensions of the core holder were 5.08 cm (2 in) width , 7.62 cm (3 in) depth and 122 cm (4 ft) length. The greater depth was chosen to allow for the packing of two or more layers. The core holder was constructed to withstand a maximum pressure of 2100 kPa when properly sealed. It had one inlet well and one outlet well at the centre of the inlet and outlet faces, respectively. These were used for the packing of the model and the measurement of absolute and effective permeabilities. The injection well was specially designed to allow the simultaneous injection of two different fluids. It consisted of two concentric lengths of tubing: the inside tubing delivered the fluid to the bottom-water layer, while the annulus was used to deliver the other fluid into the oil zone. The injection points were located at the middle of each layer (points A and B in Figure 5.1). The production well had a similar configuration as the injection well. The wells were located at 4 cm from each end of the core holder. They were made of 0.635 cm diameter tubing and fitted with porous metal-mesh caps to prevent the flow of glass beads into the production well. The core holder, hereafter referred to as the model, had a lid along the bottom side. This enabled the packing of one or more layers in the lateral direction.
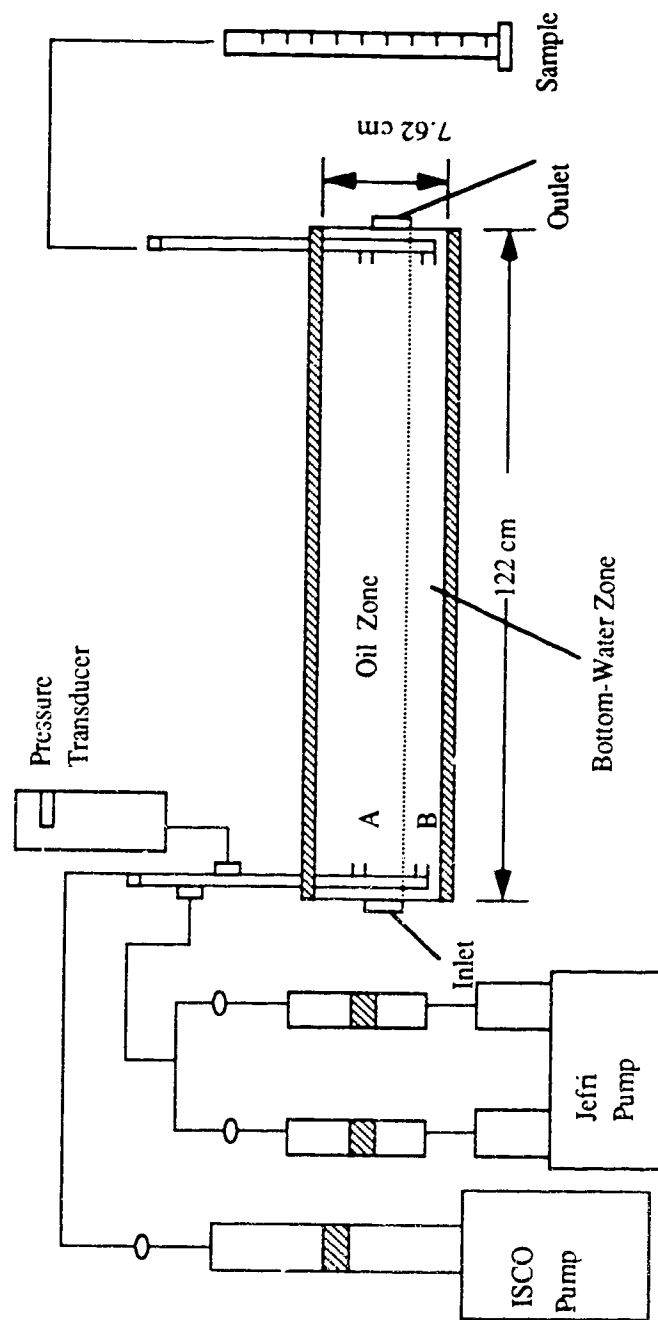
Figure 5.1 : Schematic of the Experimental Apparatus.

5.2 Procedure for Packing the Model

It took about four working days to perform a typical experiment. Most of this time was devoted to model preparation. The actual bottom-water experiments lasted normally about six hours.

To start the packing process, the core holder was mounted vertically, with the production end pointing downwards and the open (injection) end pointing upwards. Water was poured into the core holder until it was completely full. The volume of water used was noted down as the bulk volume of the core holder. The water was then allowed to drain out. Packing of the glass beads was done by the wet packing method. In this method, water and glass beads are alternately poured into the core holder. The water was allowed to drain slowly from the core holder from the outlet end. The water level was always maintained about 5 cm above the glass-beads column. This was continued until the glass beads reached the desired height inside the core holder. The glass beads used were of 70-100 mesh size (210-149 microns) with an average density of 2.5 g/ml. During the packing process, the core holder was tamped with a rubber hammer and this in combination with the slow continuous withdrawal of water by gravity from the pack ensured a uniform packing. Once the model was packed, high-pressure air was passed through the bead pack for 12-18 hours to remove all the water from the pack. Then the model was evacuated with a vacuum pump for about 18 hours to completely dry the glass beads as well as prepare the model for saturation. At the end of this period there was a vacuum created inside the core holder, and de-ionized water was allowed to imbibe into the model from the bottom end. The model was then connected to the Jefri pump from the bottom end and more de-ionized water was pumped through it until no air bubbles were observed from the water that was produced at the outlet end. A material balance was performed to determine the pore volume of the bead pack and the porosity of the porous pack was obtained by dividing the pore volume by the bulk volume.

The absolute permeability of the porous glass beads pack was then determined. At this stage the pack was fully saturated with water, and the pressure inside the core holder was atmospheric. The core holder was then rotated 90^0 and placed in the horizontal position. A pressure differential of known magnitude was applied to the core holder by introducing a stream of water under pressure into the inlet end of the model. Water was allowed to discharge at the outlet end and, when the pressure stabilized, the flow rate as well as the applied pressure was recorded. This procedure was repeated several times at different pressure settings corresponding to different flow rates. Darcy's linear flow equation was

rearranged and applied to compute the absolute permeability of the porous pack for each pressure set; that is,

$$k = \frac{q\mu L}{A\Delta p}.$$

Given that

L = 1.22 m

μ = 1.0 mPa.s (viscosity of water at normal conditions)

A = 0.003871 m^2 (cross-sectional area of the model)

then

$$k = \frac{0.31517q}{\Delta p}, \text{ where q is in m}^3/\text{sec, } \Delta p \text{ in Pa, and k in m}^2.$$

The average absolute permeability of the porous pack was obtained from plots of Δp versus q in the above equation. At the end of this process the porous pack was still completely saturated with water, but the pressure inside the core holder was no longer atmospheric. The pressure was therefore close to the last fluid pressure applied to the porous pack. Before conducting any experiment, the initial oil saturation as well as the irreducible water saturation must be known. To do this the core holder was moved to the vertical position again. MCT-10 oil was pumped into the porous pack from the top of the vertical core holder, and water was produced through the bottom (outlet). This was to guarantee a uniform displacement front and inhibit the formation of viscous fingers. Oil was injected until no more water was produced at the outlet end. Usually about two to two and a half pore volumes ensured that the water was at irreducible saturation. The difference between the volume of water imbibed into the model initially and the volume of water displaced by oil, when divided by the pore volume gave the irreducible water saturation. At this point the model was set or placed in the horizontal position in order to measure the relative permeability to oil at the irreducible water saturation. Once this was obtained using Darcy's law at different flow rates, the model, which was still in the horizontal position, was flipped upside down for the bottom-water layer packing. The model was opened by taking off the lid. The top part of the sand was scraped off using a specially designed scraper that ensured that the desired height was attained. Meanwhile, the same glass beads, some of which were used to pack the oil zone, were soaked in de-ionized water and made ready for packing. The bottom-water layer was packed manually. As glass beads are easily compacted (uniform size), the absolute permeability of the bottom-water layer was assumed to be the same as that of the previously packed glass beads. Once the water-saturated layer (bottom-water) was in place, the lid was put back on, and the model was rotated 180^0 axially to bring the oil zone on top and the bottom-water zone at the bottom.

The initial oil-in-place (IOIP) was calculated using the IOIP of the homogeneous pack multiplied by the ratio of the height of the oil zone thickness to the model thickness. Obtaining the IOIP of the bottom-water layer this way was found to be quite accurate, with less than (3-4 %) error compared to weighing the scraped-off layer to obtain the exact amount of oil removed. Five checks were performed to verify this. Consequently, all the IOIP of the bottom-water experiments were obtained in this manner.

5.3   Materials and Fluid Systems

The size of glass beads used for packing both the oil zone and the bottom-water layer was 70-100 mesh size (210-149 microns) . MCT-10 oil, supplied by Imperial Oil Ltd., was used as the oil phase and de-ionized water was used as the water phase. Oil-846, also supplied by Imperial Oil Ltd., was used as well when the MCT-10 was used up. Table 5.1 shows the properties of the oil and water phases.

Table 5.1 : Properties of Fluids Used at 22^0 C

Fluids	Viscosity (mPa.s)	Density (g/cm^3)	Interfacial-Tension (mN/m)
MCT-10	63.0	0.8770	Oil-Water 33.5
Oil-846	57.0	0.8681	Oil-Water 29.4
Distilled Water	1.0	0.9978	N/A
Polymer (500 ppm)	N/A	0.9790	Oil-848-Polymer 30.9

Flopaam 3430S, a partially hydrolyzed polyacrylamide powder, supplied by Pfizer Inc. was used in the polymer displacement experiments. For most of the experiments conducted, a 500 ppm solution was prepared with distilled water. A 700 ppm polymer solution was used as well. The stress-strain behaviour of the 500 ppm polymer solution deviated from that of a Newtonian fluid. The viscosity-shear rate plot shows a reduction in viscosity as the shear rate increases. Figures 5.2 and 5.3 show these plots.
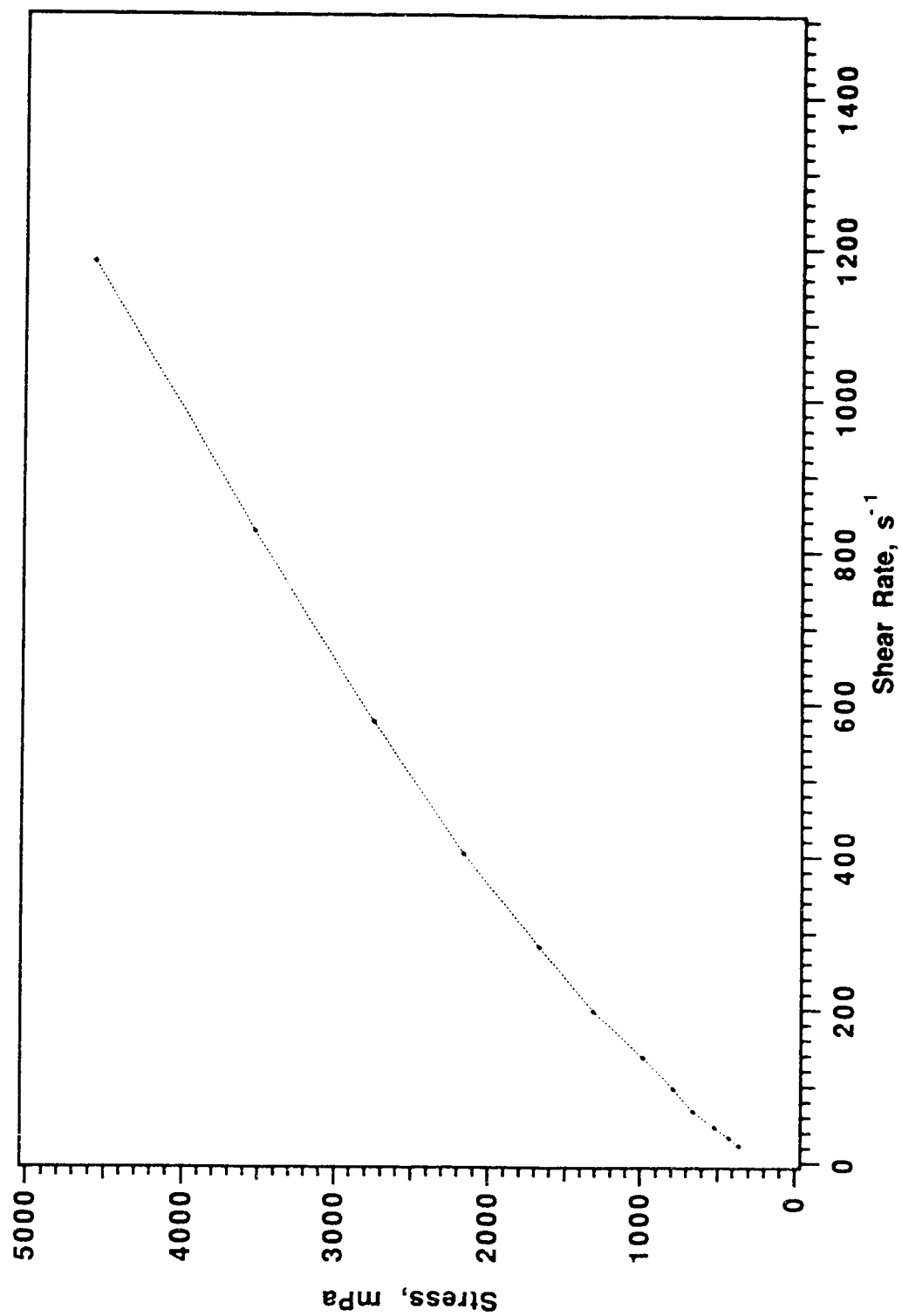
Fig. 5.2: Stress versus Shear Rate Behaviour for a 500 ppm Polymer.

Shear Rate, s^{-1}

Apparent Viscosity, mPa.s
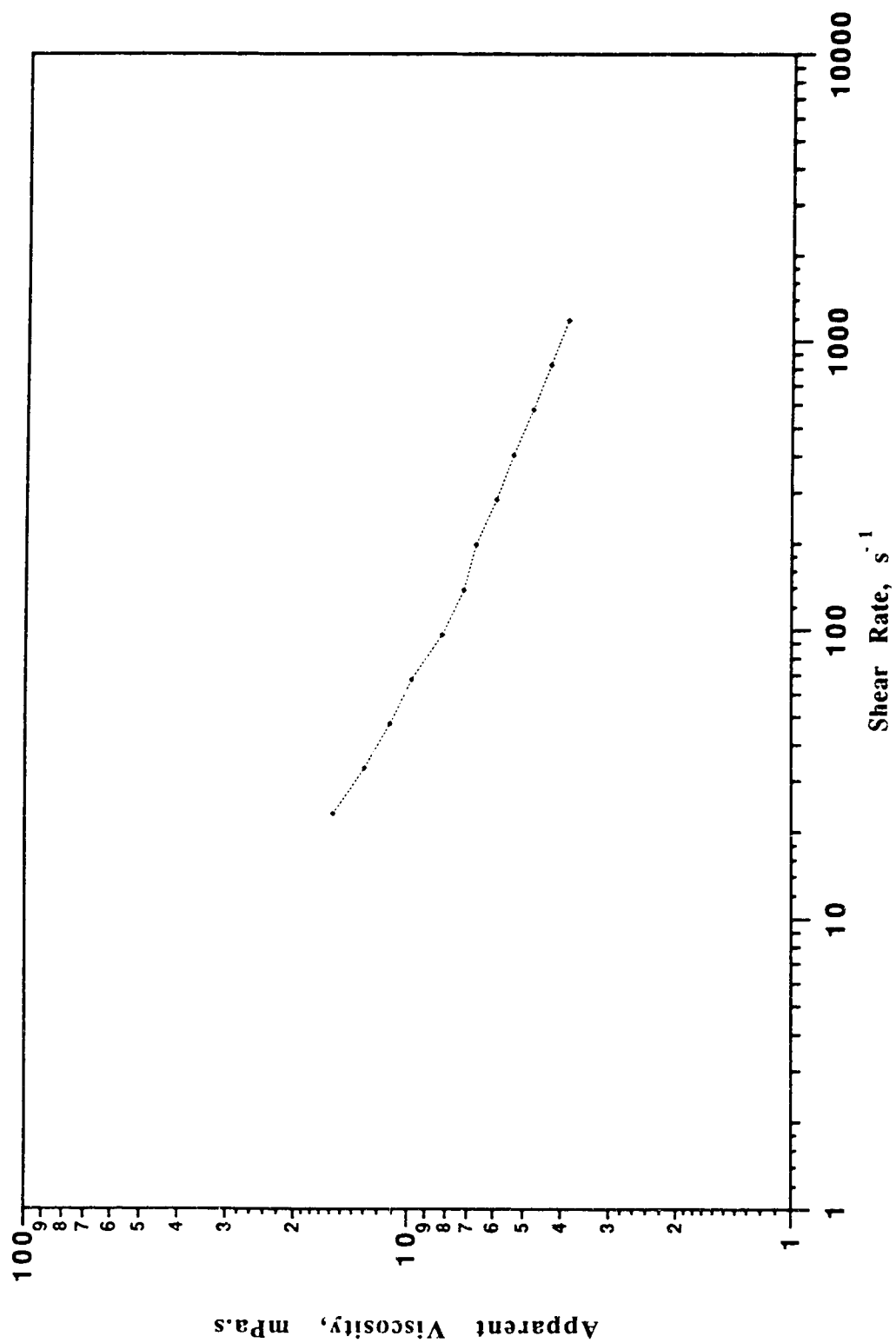
Fig. 5.3: Apparent Viscosity vs. Shear Rate for a 500 ppm Polymer.

Two different oil-in-water emulsions, with a 10% volume dispersed MCT-10 and later Oil-846, were used in the experiments as blocking agents. This amount of the dispersed phase was found to be sufficient in an earlier study[43]. The surfactant concentration (Stepanform HP-95, supplied by the Stepan Company) was varied to attain different emulsions (0.04% and 0.016% of the total volume). The stability of the emulsions was verified by visual observation. The two emulsions were found to be stable over a 24-hour time period; that is, the emulsion exhibited a single phase after a 24-hour period, with no apparent change in viscosity versus shear rate characteristics. The stress-strain behaviour of the emulsion deviated slightly from a Newtonian fluid. The viscosity-shear rate behaviour showed a constant viscosity after a shear rate of 100 reciprocalseconds. The viscosity, however, varies at lower shear rates. These plots are shown in Figures 5.4 and 5.5.
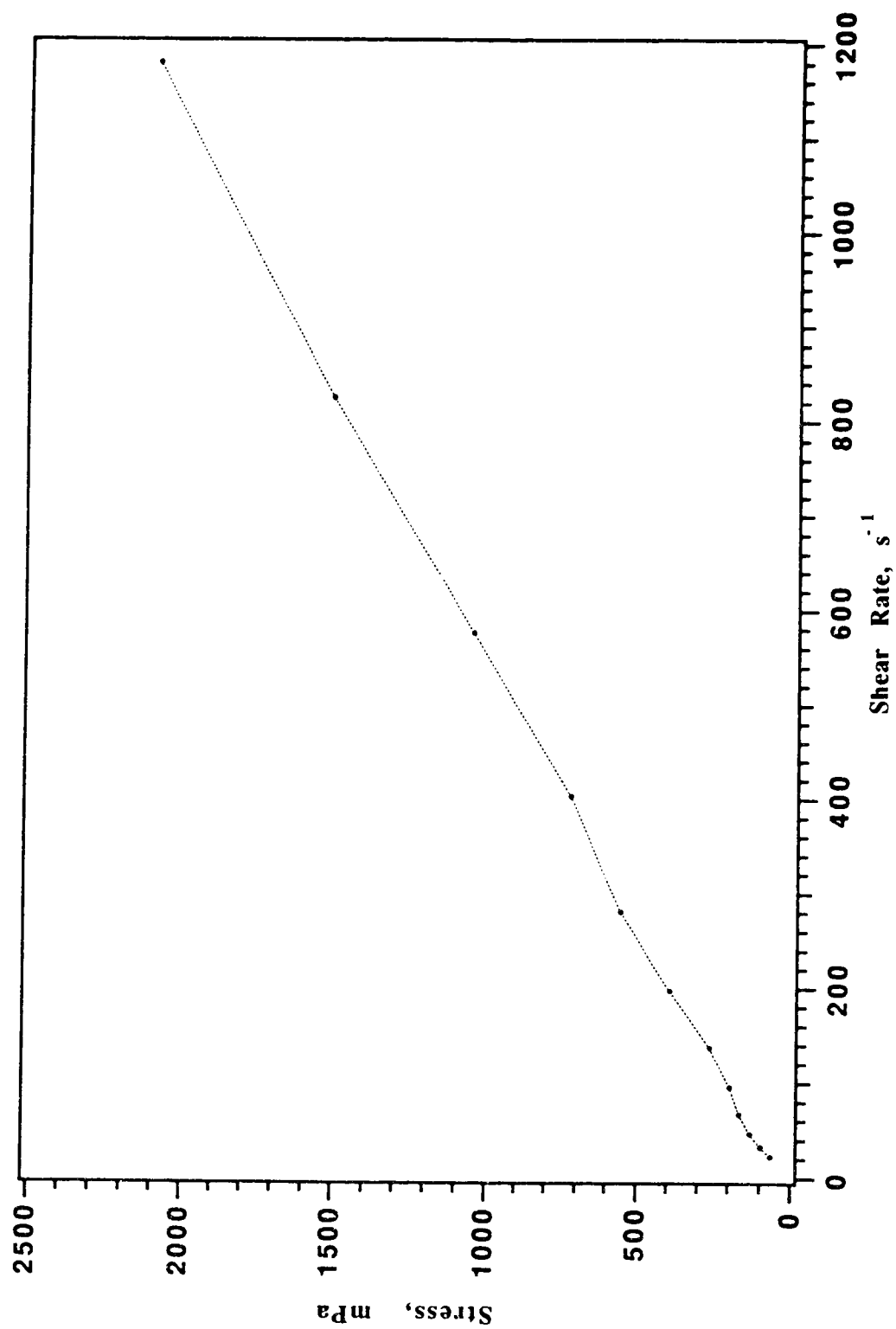
Fig. 5.4: Stress versus Shear Rate Behaviour for a 0.016% Surfactant in Emulsion.
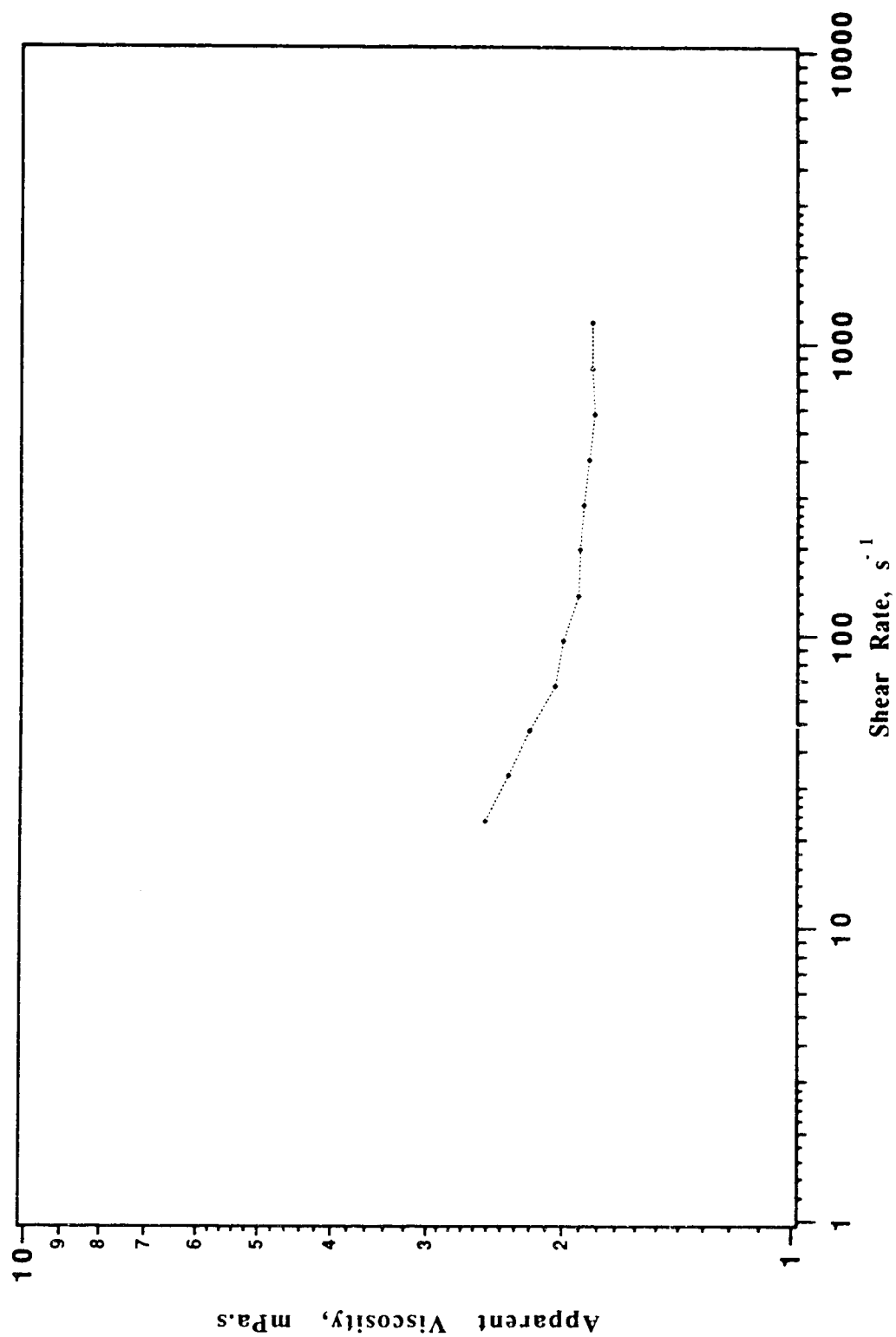
Fig. 5.5: Apparent Viscosity versus Shear Rate for a 0.016% Surfactant in Emulsion.

Chapter 6

EVALUATION OF WATERFLOOD PERFORMANCE UNDER
BOTTOM-WATER CONDITIONS

6.1   Introduction

In this research, waterflood performance was evaluated using polymer and/or emulsion as a control and/or blocking agent to improve the recovery of light and moderately viscous oils underlain by water. Basically, when an attempt is made to waterflood reservoirs with bottom-water, the injected water by passes much of the oil zone thereby resulting in low vertical sweep efficiency.

In the sections that follow, an attempt is made to mathematically elucidate the mechanism that prevails when waterflooding an oil reservoir that is underlain by bottom-water. The various techniques that are used in blocking the bottom-water zone as well as to control the relative movement of water in the oil zone for better recovery are discussed.

6.2 The Problem

The major issue that is involved in waterflooding bottom-water reservoirs is crossflow. With respect to the crossflow, q_{c1}, the following deductions can be made based on the equation. (Note that in Equation (4.17), $0 \le x_{f1} \le L$)

$$f(x_{f1}) = \cosh\left[\sqrt{m_1}(x_{f1} - L)\right] - \cosh\left(L\sqrt{m_1}\right) \le 0,$$

therefore $q_{c1} > 0$, if $c_3 < 0$. Crossflow occurs from Zone **a** to **b**, if $c_3 < 0$. There is no crossflow if $c_3 = 0$ and crossflow reverses direction, that is from **b** to **a**, if $c_3 > 0$. Therefore, as long as c_3 is not equal to zero, crossflow will exist. If the crossflow will not enhance oil recovery, then a strategy is needed to reduce c_3.

The crossflow occurring in the middle section, q_{c2}, controls the formation of the oil bank. Let us examine the equation that is obtained once again. Consider the function, $f(x_{f1},x_{f2})$, which occurs in Equation (4.20).

$$f(x_{f1},x_{f2}) = \cosh\left[\sqrt{m_2}(x_{f2} - L)\right] - \cosh\left[\sqrt{m_2}(x_{f1} - L)\right].$$

Thus, $f(x_{f1}, x_{f2}) < 0$, if $x_{f1} < x_{f2}$; also $f(x_{f1}, x_{f2}) = 0$, if $x_{f1} = x_{f2}$, and finally $f(x_{f1}, x_{f2}) > 0$ if $x_{f1} > x_{f2}$.

From the derived equations, $c_3' = c_3 \dfrac{\sinh\left[\sqrt{m_1}\left(L - x_{f1}\right)\right]}{\sinh\left[\sqrt{m_2}\left(L - x_{f1}\right)\right]}$. Then c_3' has the same sign as c_3.

From this, the following can be deduced. If $c_3 < 0$ and $x_{f1} < x_{f2}$, then the crossflow in Zones **a, b, c** and **d** is from **a** to **b** and from **c** to **d**. This can be shown as follows:
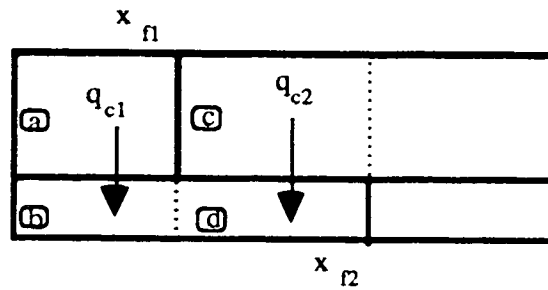
If $x_{f1} > x_{f2}$ the crossflow from **a** to **b** maintains its direction but that occurring from **c** to **d** reverses direction, (The effect on oil recovery will be shown later) as shown below.
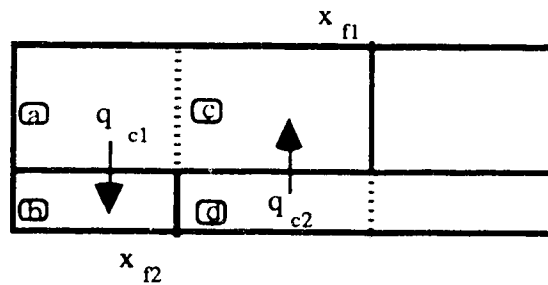
If $c_3>0$ and $x_{f1}<x_{f2}$, the direction of crossflow from Zone **a** to Zone **b** is reversed and that from Zone **c** to Zone **d** is also reversed. That is, crossflow occurs from **b** to **a** and from **d** to **c**. This is shown below:

x_{f1}

a	**c**

q_{c1} q_{c2}

b	**d**

x_{f2}
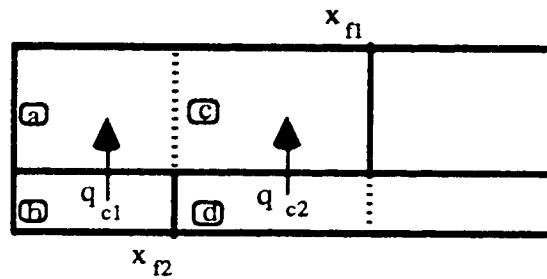
V"ile c_3 is still positive, if $x_{f1}>x_{f2}$, the direction of crossflow will be maintained in Zones **a** and **b** as mentioned above but that in Zones **c** and **d** will be reversed. In other words crossflow will occur from **b** to **a** and from **c** to **d**, as shown below:

x_{f1}

a	**c**	q_{c2}

b	**d**

q_{c1}

x_{f2}
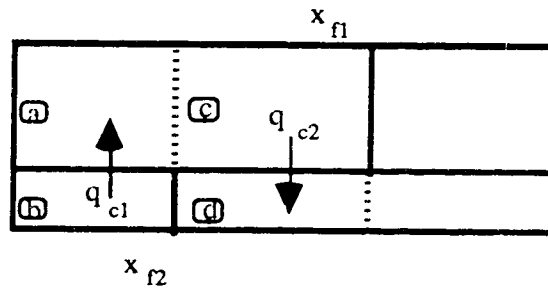
From a consideration of $f(x_{f1},x_{f2})$, it can be shown that the magnitude of the function $f=|f(x_{f1}, x_{f2})|$ becomes large, as the magnitude of the frontal separation, $|x_{f1}-x_{f2}|$ becomes large. This determines the volume of the oil bank.

The crossflow occurring in the last section is designated q_{c3}. Recall that the constant c_3'' is given by: $c_3'' = c_3' \dfrac{\sinh\left[\sqrt{m_2}(L - x_{f2})\right]}{\sinh\left[\sqrt{m_3}(L - x_{f2})\right]}$, and hence c_3'' has the same sign as c_3' and c_3. If $c_3'' > 0$, then $q_{c3} < 0$ and crossflow occurs from f to e, which is the same direction as in Zones a and b. If $c_3'' < 0$, then $q_{c3} > 0$ and crossflow reverses direction exactly as it does in the first Section. It can be inferred, then, that crossflow occurs in the same direction in the first and last Sections, whilst it reverses direction in the middle Section depending on the position of x_{f1} in relation to x_{f2}. The four possible crossflow scenarios are represented diagramatically below:
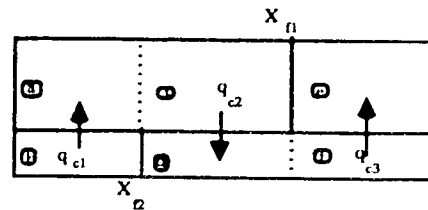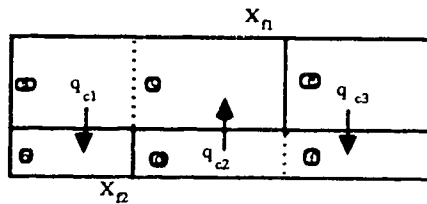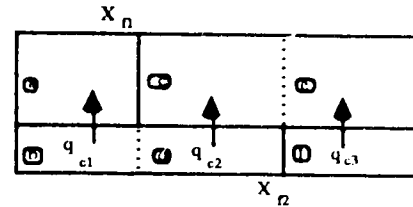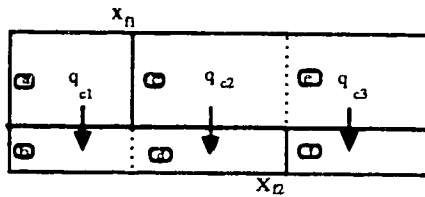
6.3 Polymer as Mobility Control Agent and Emulsion as Blocking Agent

The problem is to waterflood an oil reservoir that is underlain with bottom-water. This results in high mobility cf water in the bottom-water zone compared with that in the oil zone. To correct this problem, a viscous water slug was used as a control agent in the sixties by Barnes[18] to lower the produced WOR. Islam[42] conducted extensive experiments to select the most appropriate blocking and/or mobility control agents for bottom-water reservoirs, concluding that polymer and emulsions were the best candidates for the control of bottom-water production. Based on this study, Yeung[55] selected emulsions for this purpose. The channeling was not completely eliminated, but it was reduced considerably. To improve further on what has been achieved, polymer and emulsion have been selected to control the relative movement of water in the oil zone and to block the injected water from channeling into the bottom-water zone, respectively, in this work. A diagram illustrating this is shown below:

Blocking Agent (Emulsion)
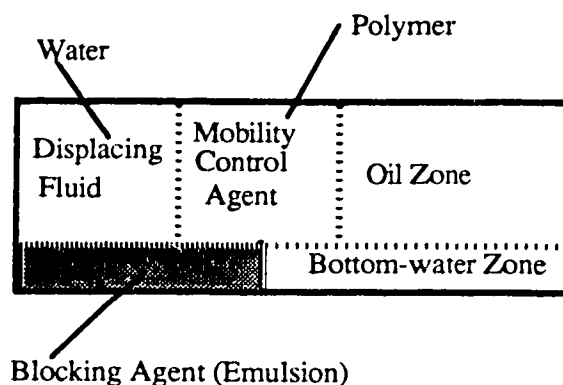
The above processes were developed to select between polymer and emulsion the one that is an effective blocking agent and the one which is an effective control agent. The Dynamic-Blocking Procedure (DBP)[55] was selected since it has been proven to be the best among the three techniques. Before that, however, experiments were conducted to check their effectiveness. In this procedure, emulsion slug was injected into the bottom-water zone which was equivalent to the pore volume of the bottom-water zone. While the emulsion was being injected, polymer was injected at the same time into the oil zone. To avoid enhancing polymer crossflow into the bottom-water zone, the same pore volume was used as in the case of emulsion. The emulsion and polymer were injected simultaneously into the bottom-water and oil zone, respectively. After injecting one pore volume of polymer, water injection followed. The experiment was continued until the water-oil-ratio (WOR) was 20.

6.4 Emulsion as Mobility Control Agent and Polymer as Blocking Agent

The purpose of using emulsion as the mobility control agent and polymer as the blocking agent was to determine which would be a better agent as far as mobility control and blocking are concerned. The same process was used as has been described above. Thus polymer and emulsion were injected simultaneously into the bottom-water region and the oil section, respectively. A diagram illustrating this is shown below:

Blocking Agent (Polymer)
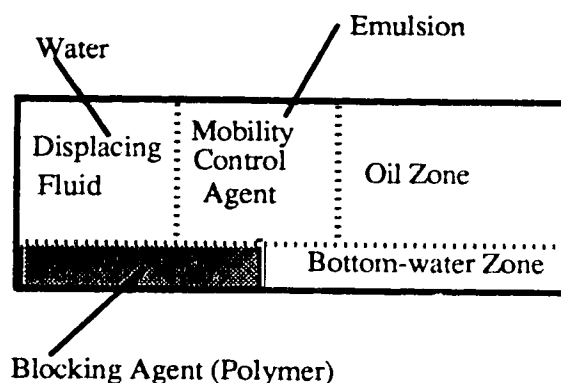
While the polymer was being injected, emulsion was injected at the same time into the oil zone. To avoid enhancing emulsion crossflow into the bottom-water zone, the same pore volume was used as in the case of polymer. The polymer and emulsion were injected simultaneously into the bottom-water and oil zone, respectively. After injecting one pore volume of emulsion, water injection followed. The experiment was continued until the water-oil-ratio (WOR) was 20.

6.5 Use of Horizontal Wells under Bottom-Water Conditions

The use of horizontal wells in reservoirs underlain by bottom-water is very limited in the literature as well as in the field. The purpose of these experiments was to study the use of horizontal wells to improve recovery as well as to try to reduce if not eliminate the oil bank that was observed when vertical wells were used in reservoirs with bottom-water. Hodaie and Bagci[44] studied the effect of vertical wells and horizontal production wells on oil recovery. They observed that for a continuous waterflood, horizontal producers show a better recovery than vertical producers.

In this study, horizontal injectors and vertical producers as well as horizontal injectors and horizontal producers were used to investigate oil recovery enhancement. More detailed discussions are found in the experimental presentation.

Chapter 7

7.1 EXPERIMENTAL DATA PRESENTATION

Thirty-two displacement tests were conducted to investigate waterflooding bottom-water reservoirs using various injection techniques by the application of polymers and emulsions. Out of the thirty-two runs conducted, twenty-seven were successful, two were repeat runs and three were failed runs. The experiments are presented in a chronological order. Figure 7.1 shows a summary of the different experiments performed. Table 7.1 gives a listing of the runs. At first, waterfloods were conducted in the absence of any bottom-water layer. Subsequently, three experiments were performed, viz., waterflood, polymer flood and emulsion flood with bottom-water zones. These six experiments serve as the base runs for the subsequent experiments. Following these, various runs were conducted with a bottom-water zone. Each of the runs that follows will be discussed according to the strategy adopted. The data for each experiment is presented in Appendix A.

Runs 1, 2 and 3: Base Runs; Homogeneous Pack

Runs 1, 2 and 3 were carried out at the same injection rate (400 ml/hr) in a homogeneous pack (that is, no bottom-water layer). This was undertaken to investigate the waterflood performance in the absence of a bottom-water layer as well as to estimate the effective permeability to water, k_{wor}, at residual oil saturation for subsequent analysis.

Run 1 was a waterflood of a homogeneous pack. Water breakthrough occurred after 0.3069 HCPV of fluid had been produced. As expected, the oil cut started at 100% and dropped sharply to 33.7% after 0.37 of HCPV of fluid had been produced. The oil recovery was 62.70% of IOIP. Figure 7.2 shows the production history for this experiment.

Run 2 was conducted using a 500 ppm polymer as the injection fluid. This was necessary because polymer was used as a mobility control and/or blocking agent and its performance in a homogeneous pack for comparison was required. Water breakthrough occurred after 0.741 HCPV of fluid had been produced. It should be noted that this experiment was conducted using a smaller cylindrical core holder (2 feet length by 2 inches diameter) . The oil recovery was 85.0 % of IOIP. The production history for this run is shown in Figure 7.3.
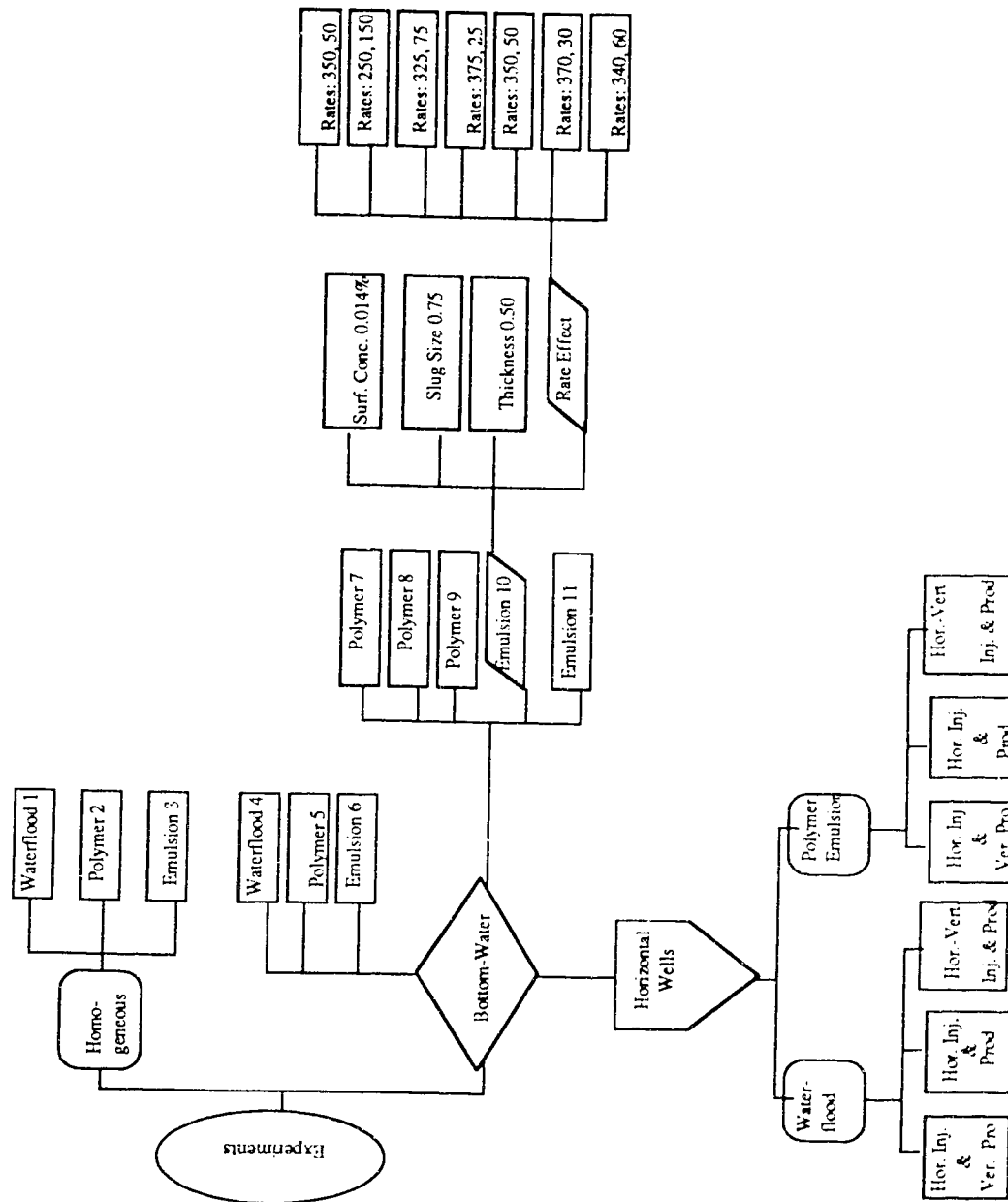
Figure 7.1: Plan of Experiments Conducted.

TABLE 7.1: Summary of the Experimental Results.

Run No.	Process	Mobility Control Agent	Blocking Agent	Slug Size PV bw	ho/hbw	kwor μm2	ko μm2	Porosity φ	Soi	IOIP ml	% Recovery @ 20 WOR
1	Base	N/A	N/A	N/A	N/A	16.3	19.8	0.376	0.923	1616	62.7
2	Base	N/A	N/A	N/A	N/A	16.5	18.5	0.17	0.967	406	85
3	Base	N/A	N/A	N/A	N/A	16.5	18.7	0.369	0.923	1527	70.5
4	WF	N/A	N/A	N/A	3	18.3	21.8	0.362	0.937	1229	57
5	PF	N/A	N/A	N/A	3	15.9	18.5	0.36	0.925	1212	55.3
6	EF	N/A	N/A	N/A	3	15.7	18.5	0.36	0.928	1233	35.5
7	DBP	N/A	Polymer	1	3	17.2	19.3	0.35	0.933	1185	64
8	P/W	N/A	Polymer	1	3	15.8	18.8	0.352	0.935	1133	54
9	P/W	N/A	Polymer	1	3	16	18.5	0.362	0.94	1136	56.6
10	DBP	Polymer	Emulsion	1	3	17	19.3	0.358	0.923	1212	69.5
11	DBP	Emulsion	Polymer	1	3	18.3	23	0.369	0.923	1286	61.8
12	DBP	Polymer	Emulsion	1	3	16	20.1	0.353	0.925	1300	43
13	DBP	Polymer	Emulsion	0.75	3	15.8	18.5	0.352	0.934	1304	51.8
14	DBP	Polymer	Emulsion	1	1	15	17	0.353	0.92	804	51.6
15	DBP	Polymer	Emulsion	1	3	17.4	22.6	0.36	0.92	1196	57.8
16	DBP	Polymer	Emulsion	1	3	15.1	18.1	0.36	0.92	1296	45.4
17	DBP	Polymer	Emulsion	1	3	15	17.3	0.359	0.93	1220	50
18	DBP	Polymer	Emulsion	1	3	15.7	18	0.357	0.938	1209	52.2
19	DBP	Polymer	Emulsion	1	3	15.3	17.3	0.354	0.938	1235	52.3
20	DBP	Polymer	Emulsion	1	3	15.3	17.3	0.355	0.933	1295	49.3
21	DBP	Polymer	Emulsion	1	3	16.3	18.5	0.376	0.923	1303	50.8
22	WF	N/A	N/A	N/A	3	16	18	0.358	0.933	1212	20.3
23	DBP	Polymer	Emulsion	1	3	15	17	0.356	0.92	1243	52.6
24	WF	N/A	N/A	N/A	3	16.2	18.5	0.376	0.94	1275	45.2
25	DBP	Polymer	Emulsion	1	3	15.1	17.8	0.376	0.92	1253	57.2
26	WF	N/A	N/A	N/A	3	15	17	0.376	0.922	1258	35.4
27	DBP	Polymer	Emulsion	1	3	15.5	17.2	0.376	0.922	1256	55.2
28	DBP	Polymer	Emulsion	1	3	16.1	18.5	0.357	0.948	1245	67.2
29	DBP	Emulsion	Polymer	1	3	16.4	18.6	0.355	0.943	1238	50.9

Base- Base Run
WF-Waterflood
PF-Polymer Flood
EF-Emulsion Flood
DBP-Dynamic-Blocking Procedure 55
N/A-Not Applicable
P/W-Polymer Injected into the Water Zone and Waterflooding the Oil Zone

For all experiments:
Polymer .500 ppm except for Run 19 which was 700 ppm

Surfactant Concentration in Emulsion = 0.016% (volume) except for Run 12 which was 0.04% (volume)
Injection Rate = 400 ml/hr except for Runs 15 to 21 which had different rates.
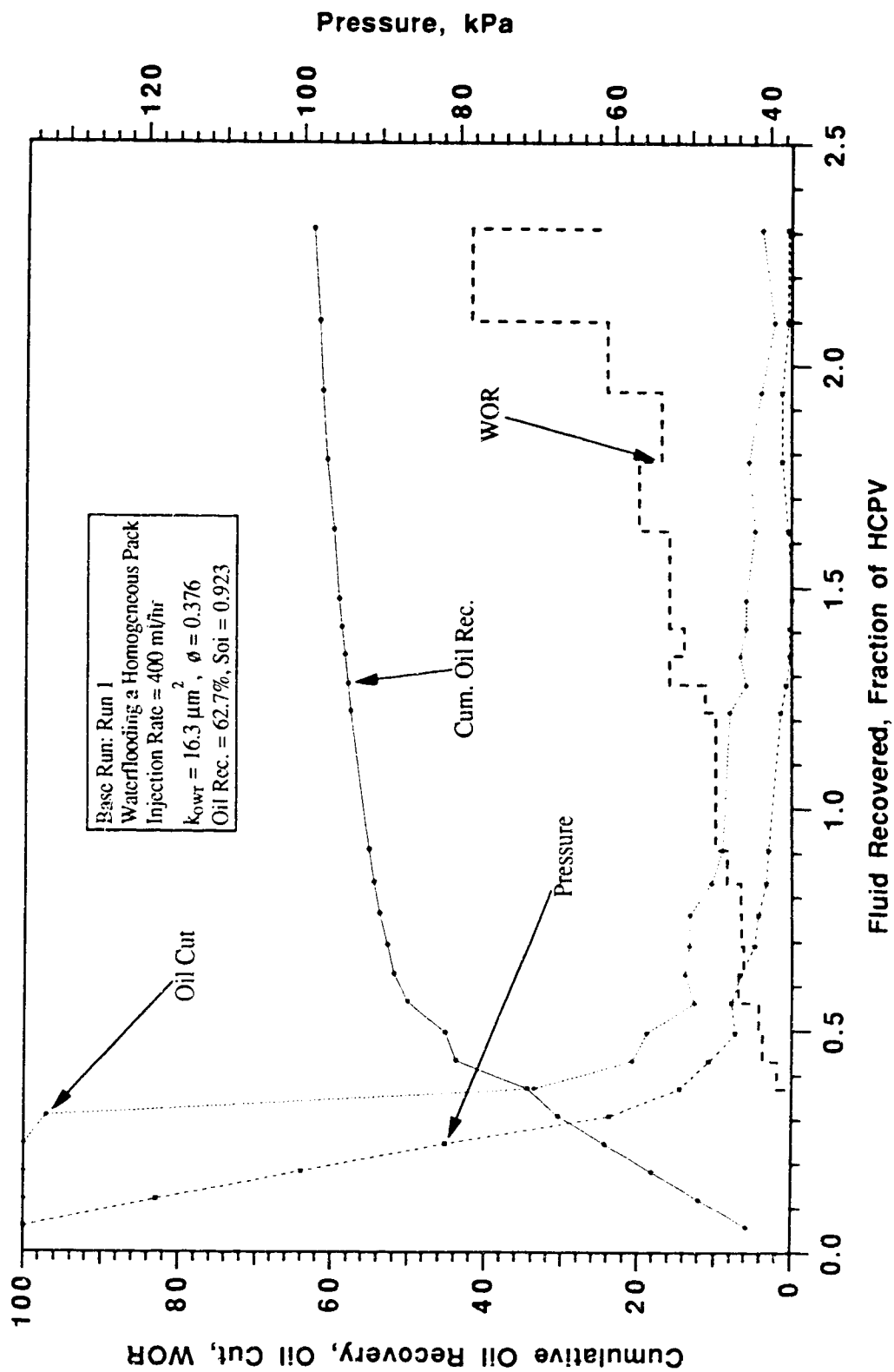
Fig. 7.2: Production History for Run 1. Waterflooding a Homogeneous Pack.
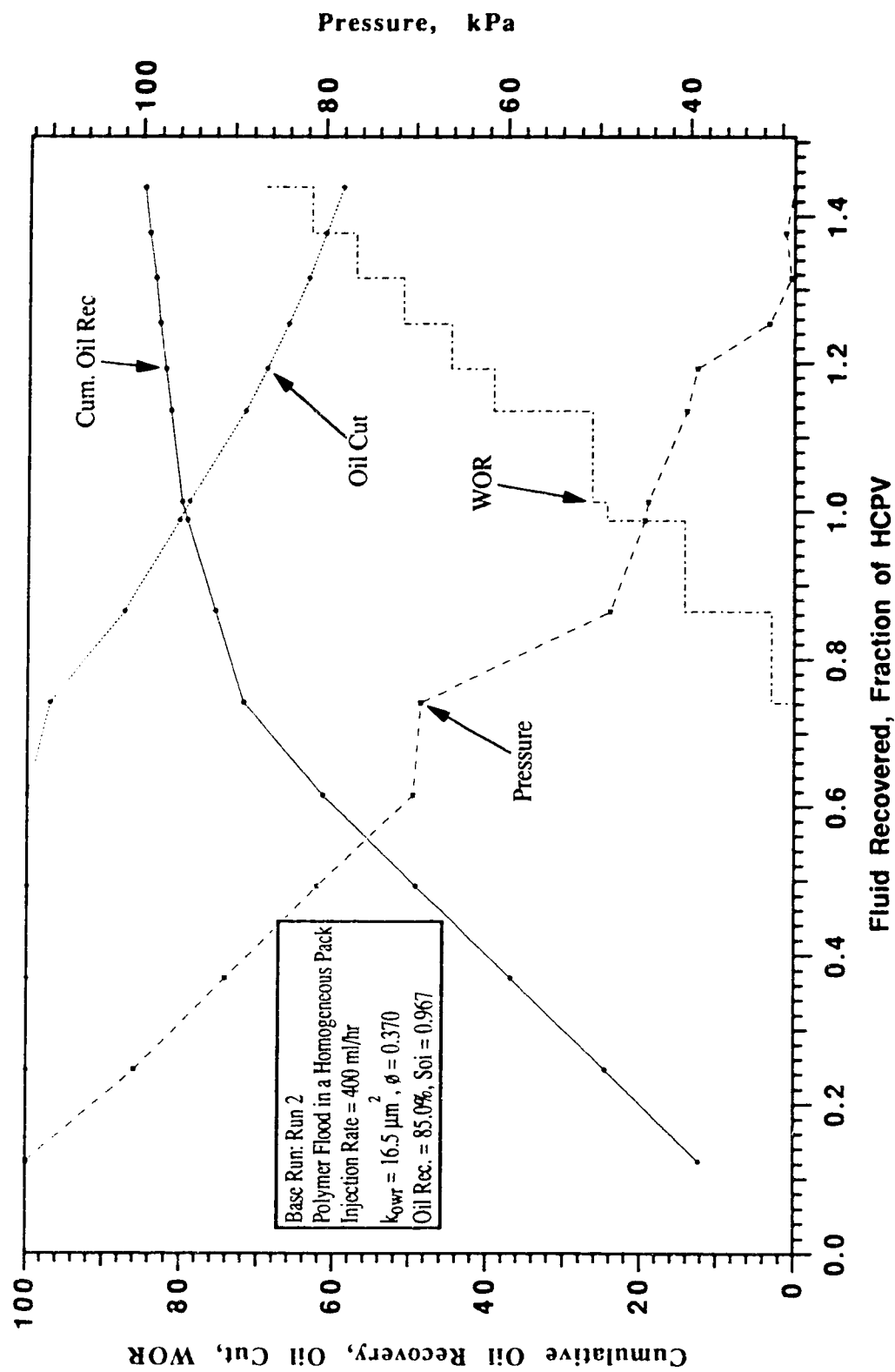
Fig. 7.3: Production History for Run 2. Polymer Flood in a Homogeneous Pack.

Run 3 was carried out by injecting a 10 percent oil-in water emulsion into a homogeneous pack. Water breakthrough occurred after 0.325 HCPV of fluid had been produced. The oil cut started at 100% and declined to 84% when water started to be produced. The oil recovery was 70.5% of IOIP. Figure 7.4 illustrates the production history for this run. These experiments, as well as the three that follow, serve as the base runs for comparison. In all these runs, the rate used was 400 ml/hr. This in terms of velocity was 2.48 m/day.

Runs 4, 5 and 6: Base Runs; Bottom-Water Layer, $h_o/h_w = 3$, $k_o/k_{bw} = 1$.

Runs 4, 5 and 6 were conducted at the same injection rate, 400 ml/hr, in a bottom-water layer with oil zone thickness three times that of the water zone ($h_o/h_w = 3$), to study the performance of waterflood, polymer flood and emulsion flood under identical conditions. The absolute permeabilities of both zones were equal ($k_o/k_{bw} = 1$). Both the injection and production wells were located at a depth of 50% of the oil zone. These tests serve as base runs since, from here on, various strategies were adopted to improve recovery.

In Run 4, water was injected into the oil zone. Water breakthrough occurred after 0.0415 HCPV of fluid had been produced. The oil cut dropped sharply to a minimum of 16% before rising. The water-oil-ratio (WOR) at the minimum oil cut was 5.4. This value dropped to 0.92 when the oil cut attained a maximum value of 52% and this occurred after 0.574 HCPV of fluid has been produced. The WOR increased gradually as the oil cut declined. The oil recovery was 57.0% of IOIP This compares favourably with the oil recovery of 50.1% obtained in previous work[55]. The test was concluded when the WOR was 20. Figure 7.5 shows the production history for this experiment.

In Run 5 all the parameters are the same as Run 4. The only difference was the injection fluid which was polymer and this was injected into the oil zone. Water breakthrough occurred after 0.0413 HCPV of fluid had been produced. The oil cut dropped gradually and rose to a maximum of 78%. The oil recovery was 55.3% of IOIP. Figure 7.6 shows the production history for this experiment.

Run 6 was conducted by injecting emulsion into the oil zone of a bottom-water pack. All the parameters were the same as in Run 5, except that the injection fluid was emulsion. Water breakthrough occurred after 0.0414 HCPV of fluid had been produced. The oil cut dropped sharply to a minimum of 11.5% before rising. The water-oil-ratio (WOR) at the minimum oil production rate was 7.7. The WOR declined again to 1.43 when the oil cut attained a maximum value of 41.2%. The oil recovery was 35.5% of IOIP. Figure 7.7 illustrates the production history for this experiment.

55
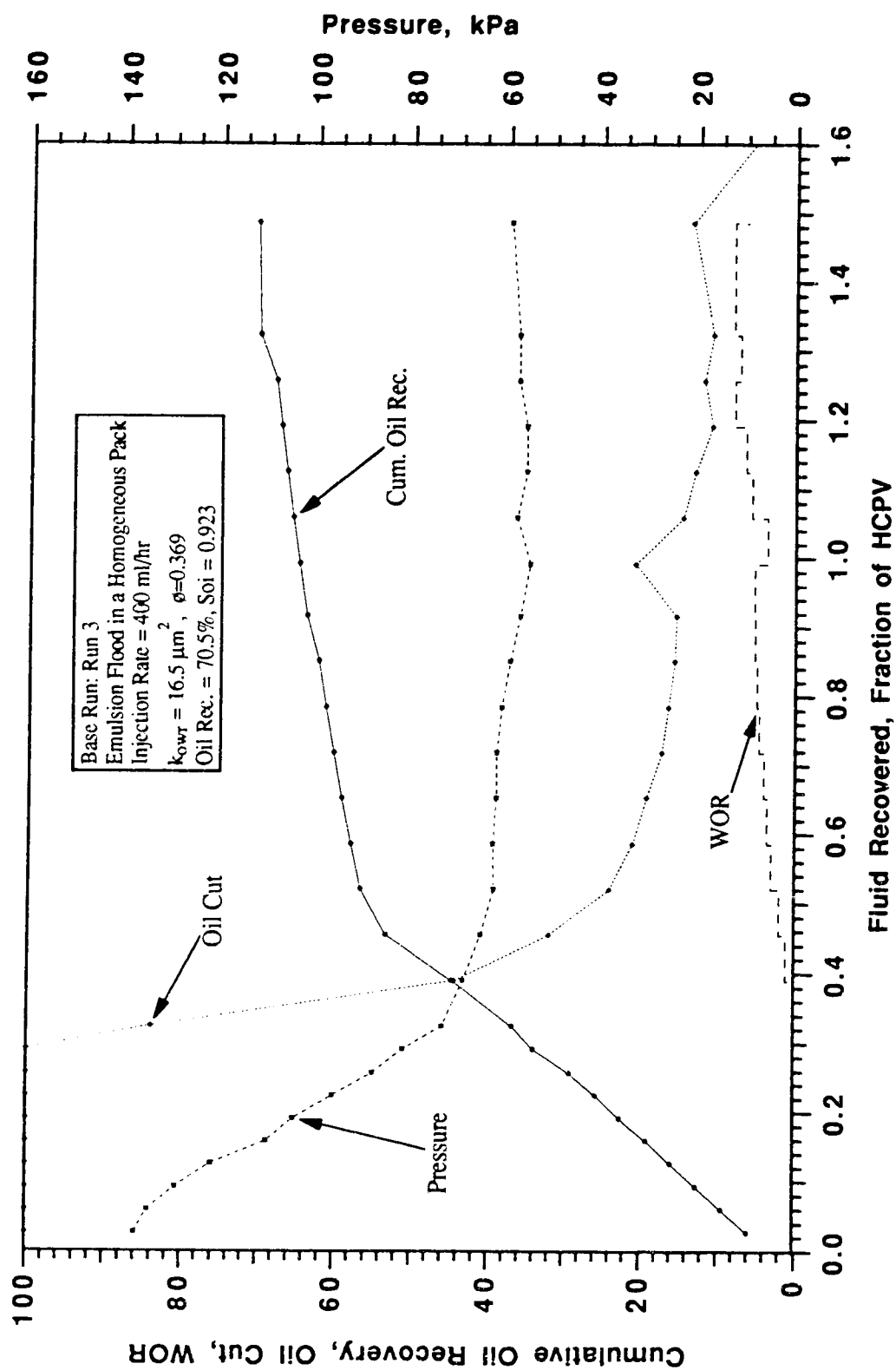
Fig. 7.4: Production History for Run 3. Emulsion Flood in a Homogeneous Pack.

Base Run: Run 3
Emulsion Flood in a Homogeneous Pack
Injection Rate = 400 ml/hr
$k_{owr} = 16.5\ \mu m^2$, $\phi = 0.369$
Oil Rec. = 70.5%, Soi = 0.923
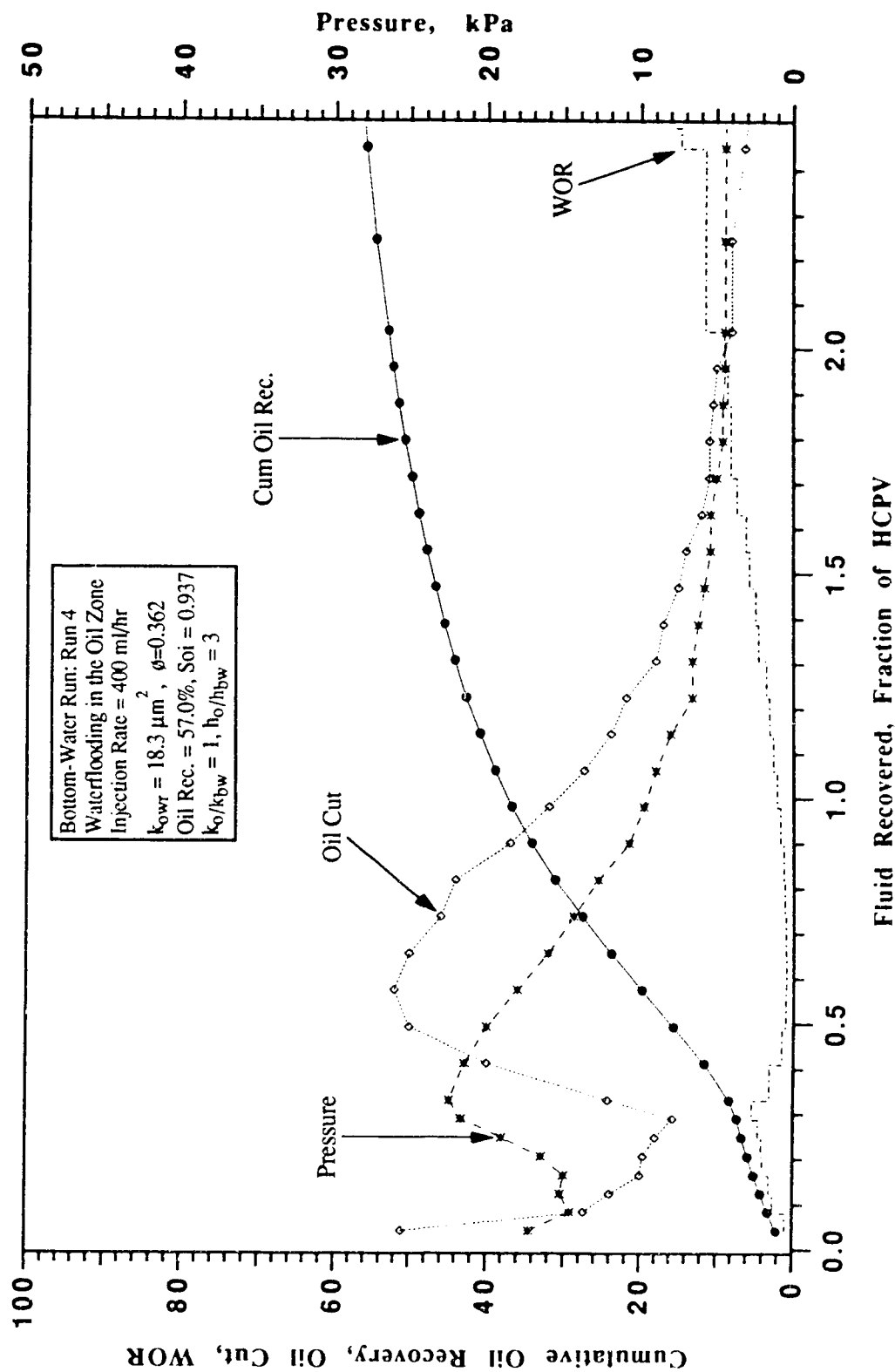
Fig. 7.5: Production History for Run 4. Waterflooding a Bottom-Water Reservoir.

56

Pressure, kPa

Bottom-Water Run: Run 5
Polymer Flood in the Oil Zone
$k_{owr} = 15.9 \ \mu m^2$, $\emptyset = 0.360$
Oil Rec. = 55.3%, Soi = 0.925
$k_o/k_{bw} = 1$, $h_o/h_{bw} = 3$

Cum. Oil Rec.

WOR

Oil Cut

Pressure

Fluid Recovered, Fraction of HCPV

Cumulative Oil Recovery, Oil Cut, WOR
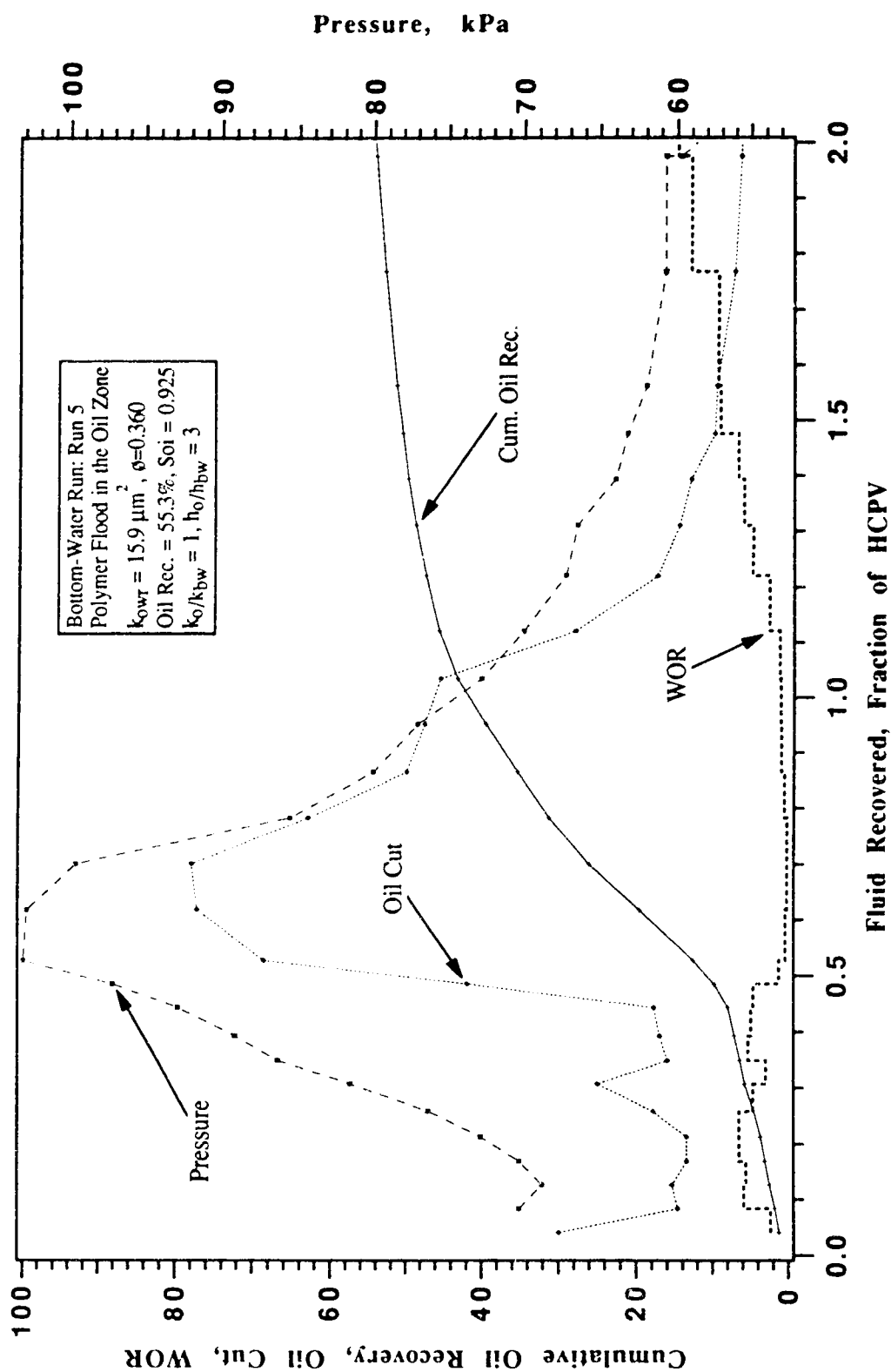
Fig. 7.6: Production History for Run 5. Polymer Flood in a Bottom-Water Reservoir.

Pressure, kPa

Bottom-Water Run: Run 6
Emulsion Flood in the Oil Zone
Injection Rate = 400 ml/hr
$k_{owr} = 15.7\ \mu m^2$, $\phi = 0.360$
Oil Rec. = 35.5%, Soi = 0.928
$k_o/k_{bw} = 1$, $h_o/h_{bw} = 3$

Cum. Oil Rec.

Oil Cut

WOR

Pressure

Fluid Recovered, Fraction of HCPV

Cumulative Oil Recovery, Oil Cut, WOR
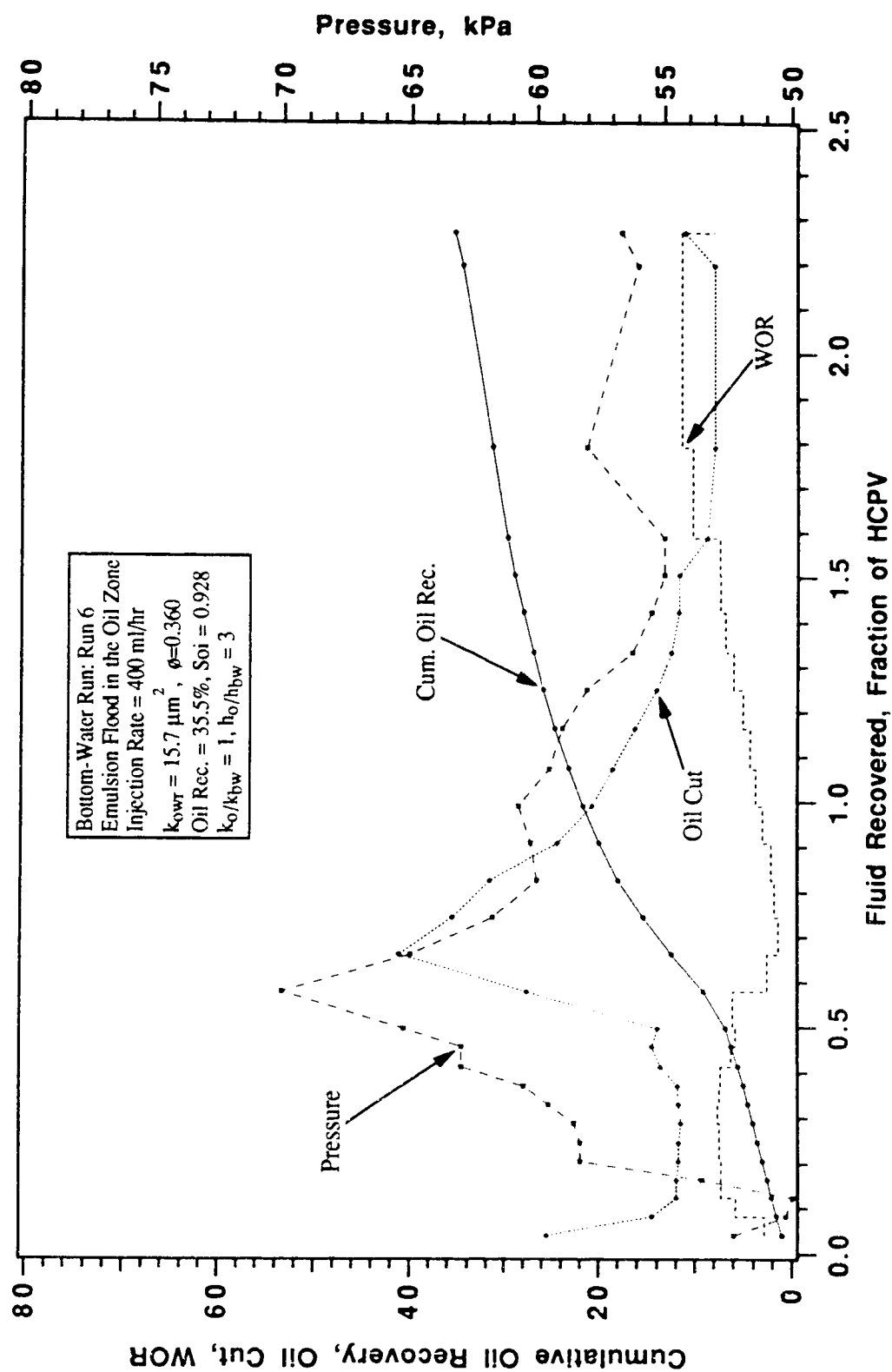
Fig. 7.7: Production History for Run 6. Emulsion Flood in a Bottom-Water Reservoir.

Run 7: Bottom-Water Run, Polymer Injected into the Bottom-Water and Water Injected into the Oil Zone, $h_o/h_w = 3$, $k_o/k_{bw} = 1$, Polymer Slug Size = 1.0 PV_{bw}, Polymer : 500 ppm.

Run 7 was performed by injecting 1.0 PV_{bw} of polymer into the bottom-water layer and water was injected into the oil zone. These injections were done simultaneously. The injection rate used was 400 ml /hr. Water breakthrough occurred after 0.04304 HCPV of fluid had been produced. Two peaks on the oil-cut curve were observed. The maximum oil cut was 49%. The oil recovery was 64.0 % of IOIP. Figure 7.8 shows the production history for this experiment.

Run 8: Bottom-Water Run, Polymer was first Injected into the Bottom-Water Zone, after which Water was Injected into the Oil Zone. $h_o/h_w = 3$, $k_o/k_{bw} = 1$, Polymer Slug Size = 1.0 PV_{bw} Polymer : 500 ppm.

Run 8 was conducted to study the injection strategy. One pore volume of polymer (1.0 PV_{bw}) was first injected into the bottom-water layer. This was followed by water injection into the oil zone. The injections were performed one after the other, unlike Run 7 where the processes were concurrent. Water breakthrough occurred after 0.0446 HCPV of fluid had been produced. The oil cut declined to 15.7% and increased to a maximum of 83.5% and dropped rapidly. The oil recovery was 54.0% of IOIP. This technique yielded a high oil production rate, but the oil recovery was lower than that of Run 7. Figure 7.9 depicts the production history for the experiment.

Run 9: Bottom-Water Run, Polymer Alternating with Water, $h_o/h_w = 3$, $k_o/k_{bw} = 1$, Polymer Slug Size = 1.0 PV_{bw}, Polymer : 500 ppm.

In this experiment one pore volume of polymer (1.0 PV_{bw}) was divided into four batches of 0.25 and injected into the bottom-water zone. This was alternated with water of equal amount (0.25 PV_{oil}) injected into the oil zone. The oil cut fluctuated and attained a peak of 70 % after 0.40 HCPV of fluid had been recovered. The oil recovery at WOR of 20 was 56.6 % of IOIP. In this run, the oil cut was better than that of Run 7 but the ultimate oil recovery was lower. The production history is shown in Figure 7.10.

Pressure, kPa

50 40 30 20 10 0

Fluid Recovered, Fraction of HCPV

3.0 2.5 2.0 1.5 1.0 0.5 0.0

Pressure

Cum. Oil Rec.

WOR

Oil Cut

Bottom-Water Run: Run 7
Polymer : 500 ppm
Inj. Rate in the Oil Zone = 300 ml/hr
Inj. Rate in the Water Zone = 100 ml/hr
$k_{owr} = 17.2 \, \mu m^2$, $\phi = 0.350$
Oil Rec. = 64.0%, Soi = 0.933
$k_o/k_{bw} = 1$, $h_o/h_{bw} = 3$
Polymer Slug Size = 1.00 PV_{bw}

100 80 60 40 20 0

Cumulative Oil Recovery, Oil Cut, WOR
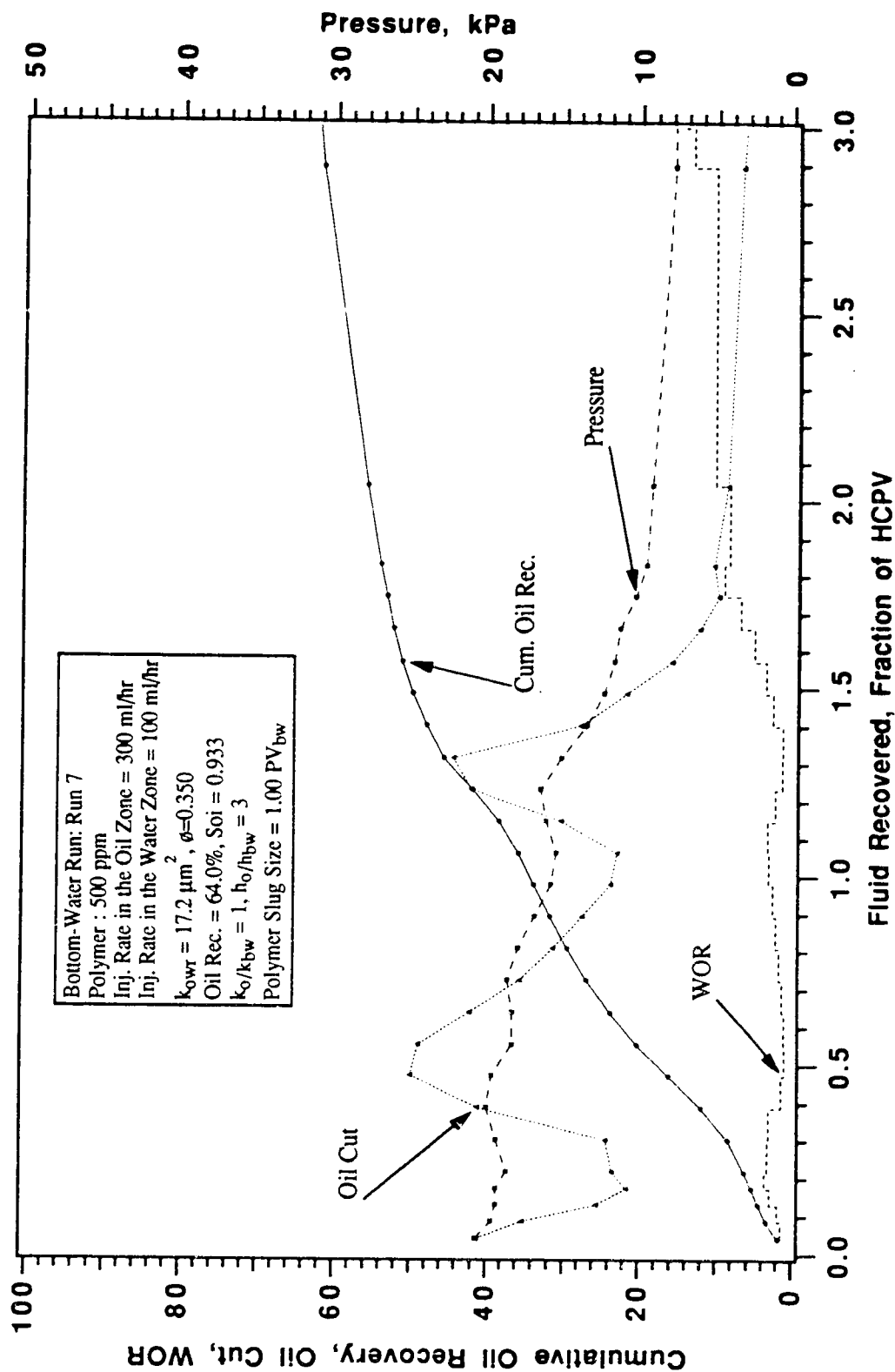
Fig. 7.8: Production History for Run 7. Polymer Used as Blocking Agent and Waterflooding the Oil Zone.
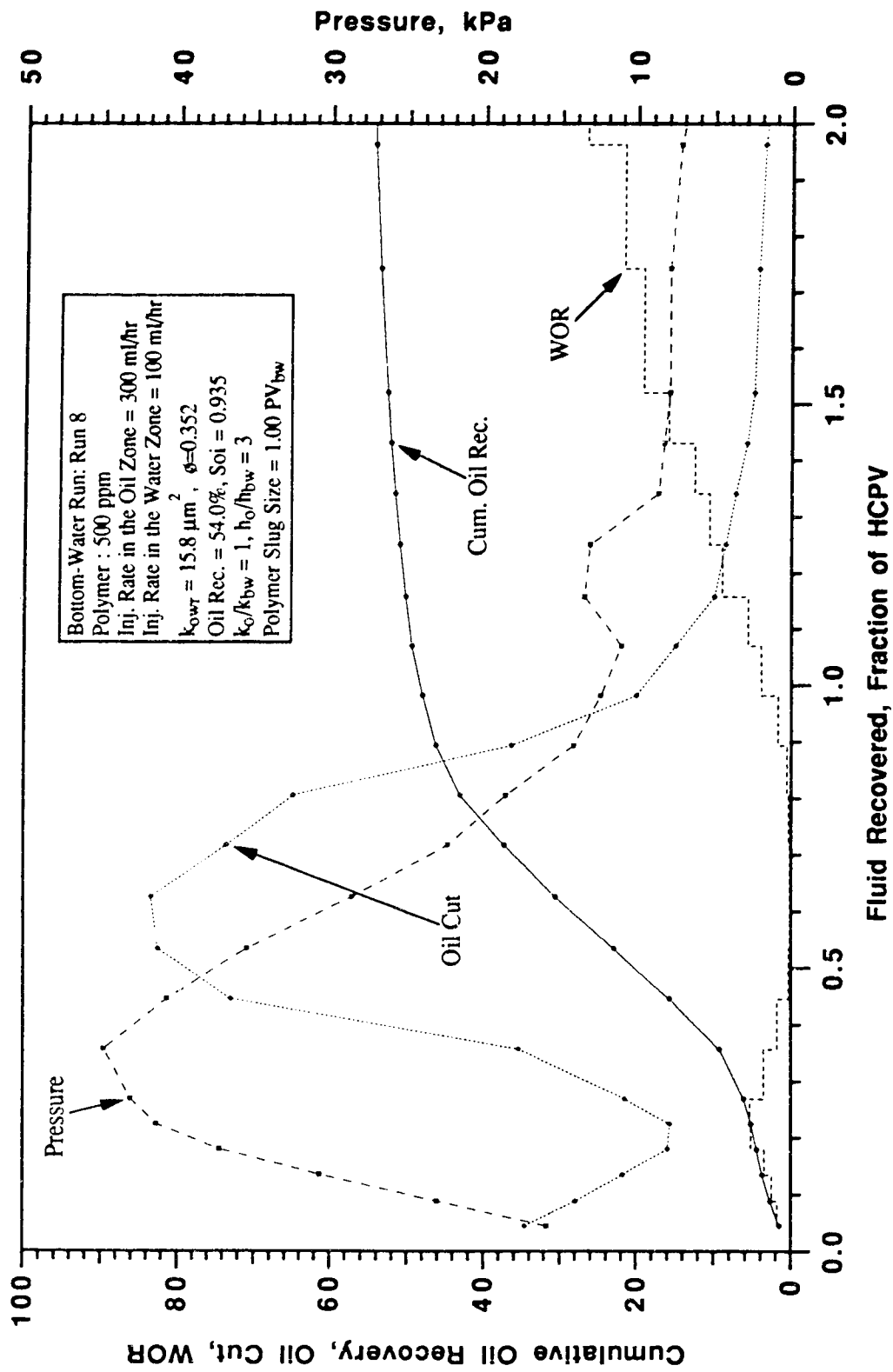
Fig. 7.9: Production History for Run 8. Polymer Used as Blocking Agent and Waterflooding the Oil Zone.
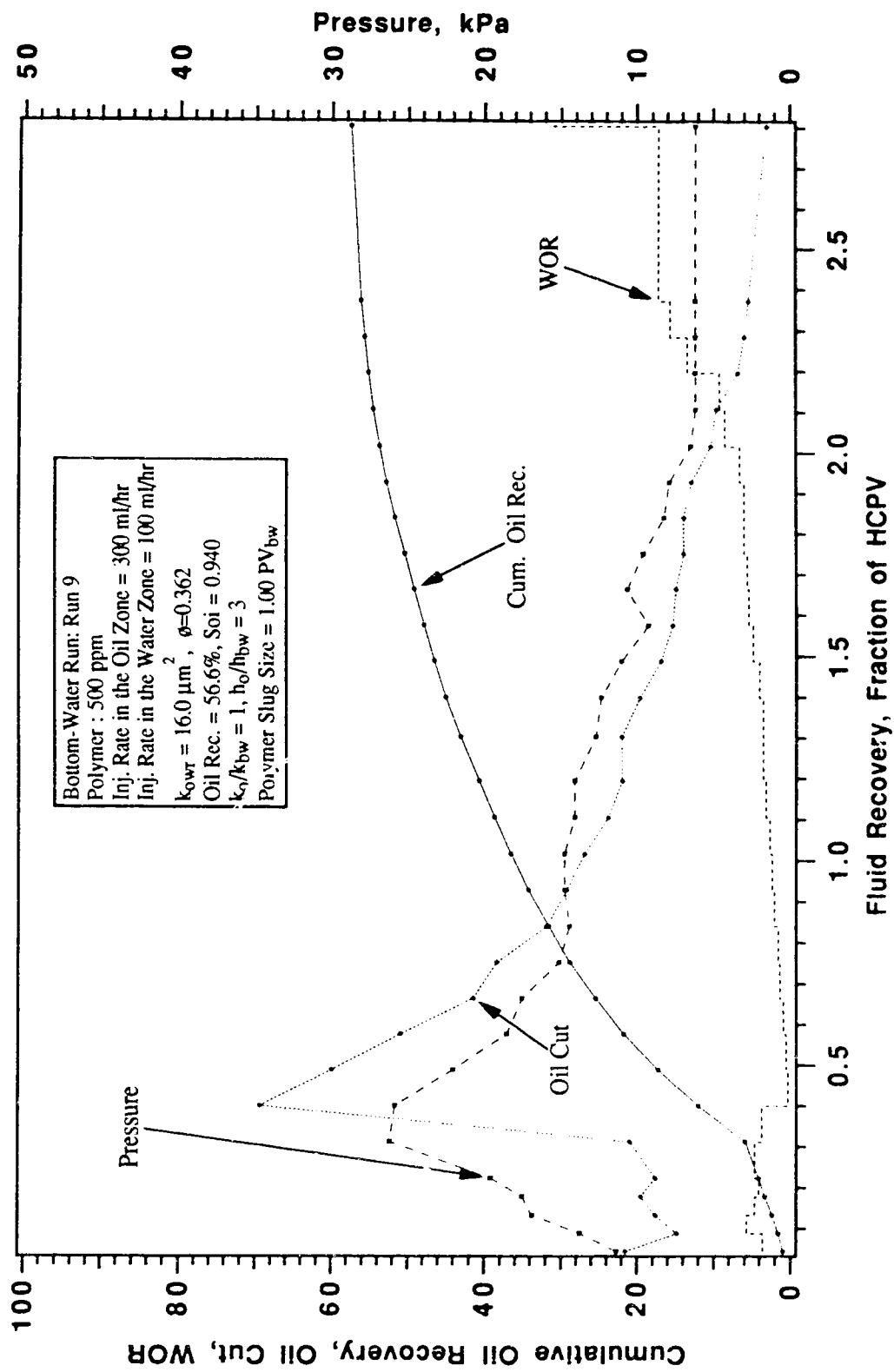
Fig. 7.10: Production History for Run 9. Polymer Used as Blocking Agent and Waterflooding the Oil Zone.

Pressure, kPa

Cumulative Oil Recovery, Oil Cut, WOR

Fluid Recovery, Fraction of HCPV

WOR

Cum. Oil Rec.

Oil Cut

Pressure

Bottom-Water Run: Run 9
Polymer : 500 ppm
Inj. Rate in the Oil Zone = 300 ml/hr
Inj. Rate in the Water Zone = 100 ml/hr
$k_{owr} = 16.0 \ \mu m^2$, $\phi=0.362$
Oil Rec. = 56.6%, S_{oi} = 0.940
k_o/k_{bw} = 1, h_o/h_{bw} = 3
Polymer Slug Size = 1.00 PV_{bw}

Run 10 : Bottom-Water Run, Emulsion Injected into Bottom-Water and Polymer Injected into the Oil Zone, Surfactant Concentration in Emulsion = 0.016%, Polymer : 500 ppm, h_o/h_w = 3, k_o/k_{bw} = 1, Slug Size = 1.0 PVbw.

In this run, one pore volume of polymer (1.0 PV_{bw}) was injected into the oil zone and an equal amount (1.0 PV_{bw}) of emulsion was injected into the bottom-water zone simultaneously. The polymer injection was followed by water injection. There was a slow decline in oil cut until it bottomed at 24% after 0.166 HCPV of fluid had been recovered. It then increased rapidly to a maximum of 75 % and decreased slowly again. The oil recovery at WOR of 20 was 69.5 % of IOIP. This technique demonstrated a higher oil production rate as well as higher ultimate oil recovery. Figure 7.11 shows the production history for this experiment.

Run 11: Bottom-Water Run, Emulsion Injected Into the Oil Zone and Polymer Injected into the Bottom-Water Zone, Surfactant Concentration in Emulsion = 0.016%, Polymer : 500 ppm, h_o/h_w = 3, k_o/k_{bw} =1, Slug Size = 1.0 PV_{bw}.

In this run, one pore volume of emulsion and one pore volume of polymer were injected simultaneously into the oil zone and bottom-water zone respectively. Notice that the polymer and emulsion injection intervals have been switched to investigate what effect that will have on recovery. The emulsion injection was followed by water injection. Water breakthrough occurred after 0.0404 HCPV of fluid had been recovered. The oil cut decreased gradually until it reached a minimum of 14%, then increased gradually to a peak of 75 % and finally decreased again. The ultimate oil recovery at WOR of 20, the termination point of the experiment, was 61.8 %. In Runs 10 and 11, all parameters were the same except the injection positions of polymer and emulsion. The production history for Run 11 is shown in Figure 7.12.

From the above experiments, it was observed that the strategy whereby polymer was injected in the oil zone followed by water, and the injection of emulsion into the bottom-water, simultaneously, was more efficient. From here on, therefore, all experiments were conducted in a similar fashion. The conditions under which the experiments were conducted will be discussed.
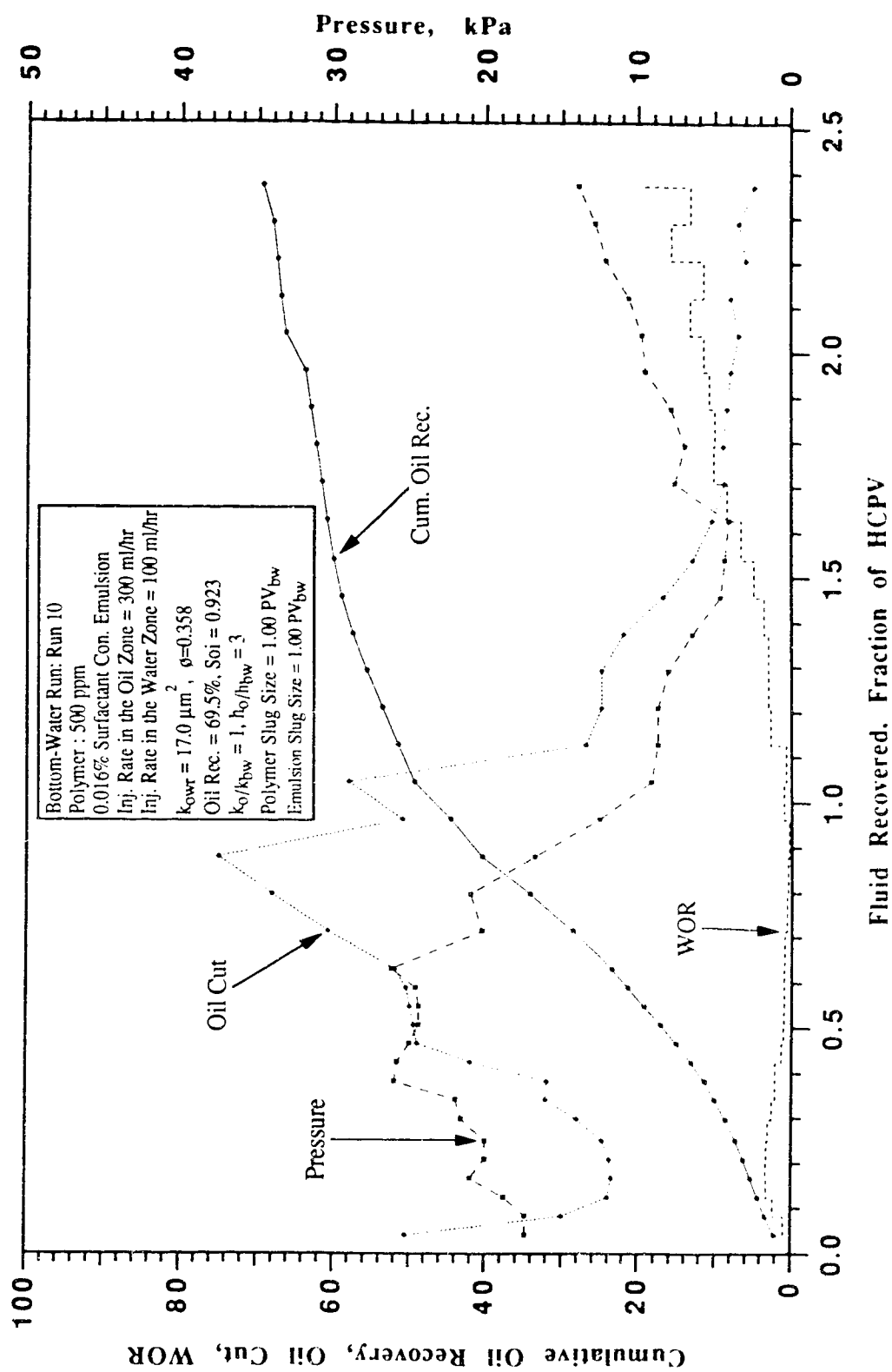
Fig. 7.11: Production History for Run 10. Emulsion Used as Blocking Agent and Polymer Used as Mobility Control Agent.
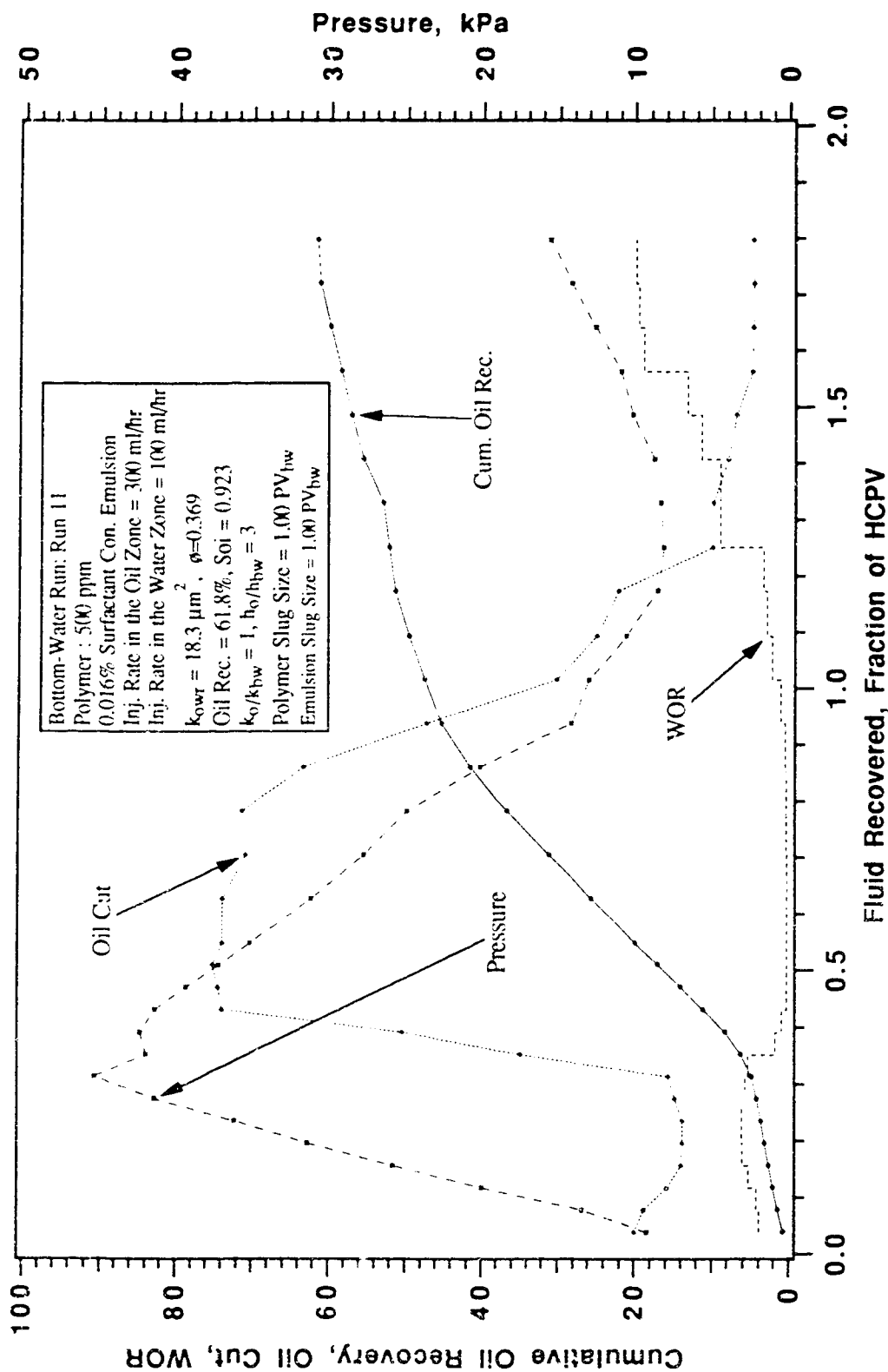
Fig. 7.12: Production History for Run 11.
Polymer Used as Blocking Agent and Emulsion Used as Mobility Control Agent.

Run 12: Bottom-Water Run with Polymer and Emulsion Injections, Surfactant Concentration in Emulsion = 0.04%, Polymer : 500 ppm, h_o/h_w = 3, k_o/k_{bw} = 1, Slug Size = 1.0 PV_{bw}.

This run was conducted to see the effect of surfactant concentration on recovery. All the parameters as well as the injection strategy are the same as that of Run 10. The only change in this test was the surfactant concentration for the emulsion. Water breakthrough occurred after 0.0392 HCPV of fluid had been produced. The oil cut decreased sharply and leveled from 11.2% to 11.8%, before increasing to a maximum of 66% and then decreasing to a lower value. The oil recovery was 43.0 % of the IOIP, after 2.325 HCPV had been recovered. Figure 7.13 shows the production history for this test.

Run 13: Bottom-Water Run with Polymer and Emulsion Injections, Surfactant Concentration in Emulsion = 0.016%, Polymer : 500 ppm, h_o/h_w = 3, k_o/k_{bw} = 1, Slug Size = 0.75 PV_{bw}.

This run was conducted to investigate the effect of slug size when simultaneously injecting polymer and emulsion into the oil zone and the bottom-water zone, respectively. The emulsion injected into the bottom-water zone was 0.75 PV_{bw} and an equal volume of polymer was injected into the oil zone that was followed by water injection. Water breakthrough occurred after 0.0513 HCPV of fluid had been recovered. The maximum oil rate was 63.7% and the oil recovery was 51.84% of the IOIP. The production history is given in Figure 7.14.

Run 14: Bottom-Water Run with Polymer and Emulsion Injections, Surfactant Concentration in Emulsion = 0.016%, Polymer : 500 ppm, h_o/h_w = 1, k_o/k_{bw} = 1, Slug Size = 1.0 PV_{bw}.

This run was conducted to study the effect of bottom-water thickness on recovery. The oil zone thickness was equal to the bottom-water zone. The water breakthrough occurred after 0.0621 HCPV of fluid had been recovered. The instantaneous oil production was almost constant until 1.204 HCPV of fluid had been produced before rising gradually to a maximum of 40% then it declined to a minimum value. The oil recovery was 51.6% of IOIP. The production history of this test is given in Figure 7.15.
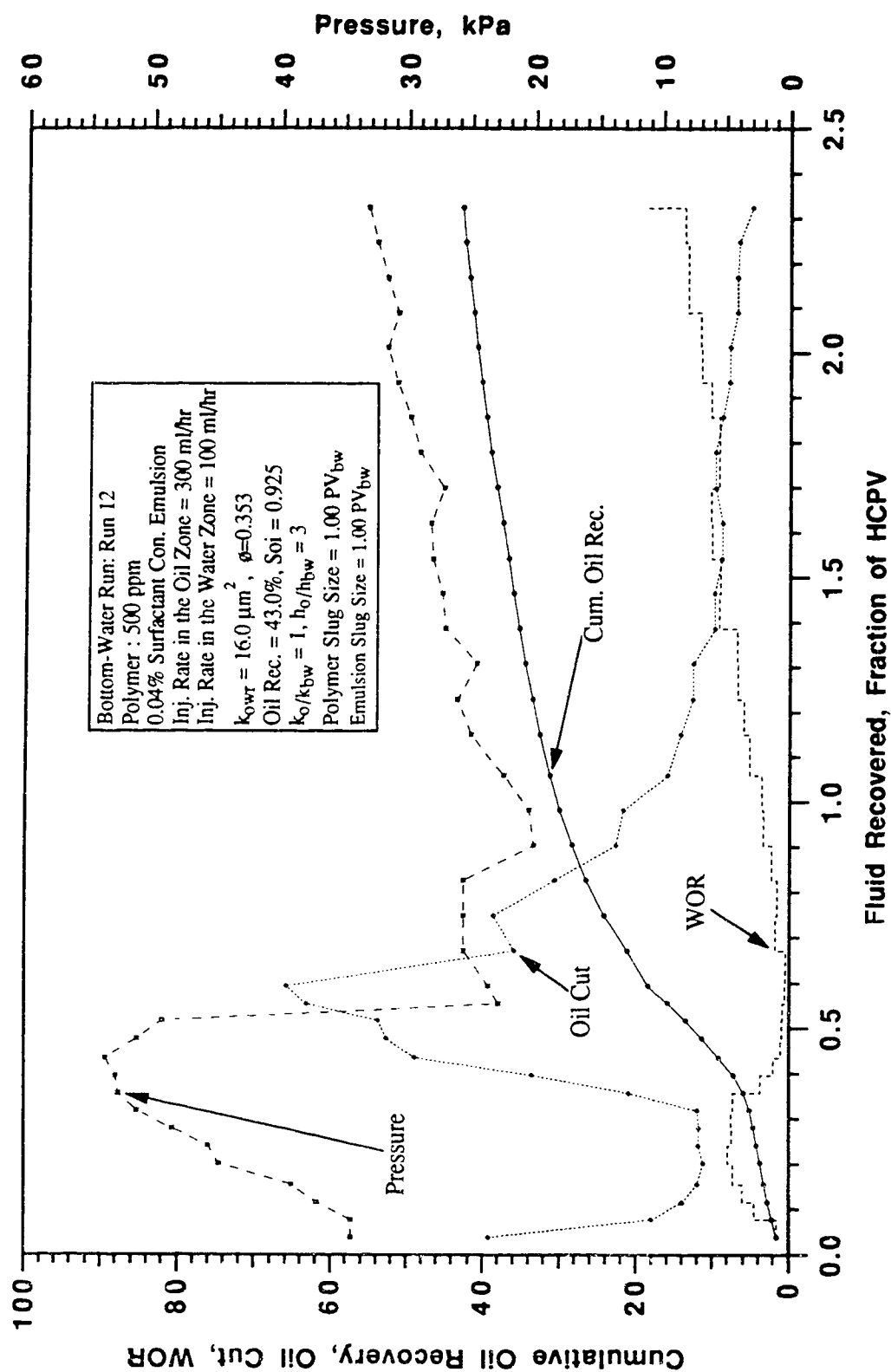
Fig. 7.13: Production History for Run 12. Effect of Surfactant Concentration on Oil Recovery.
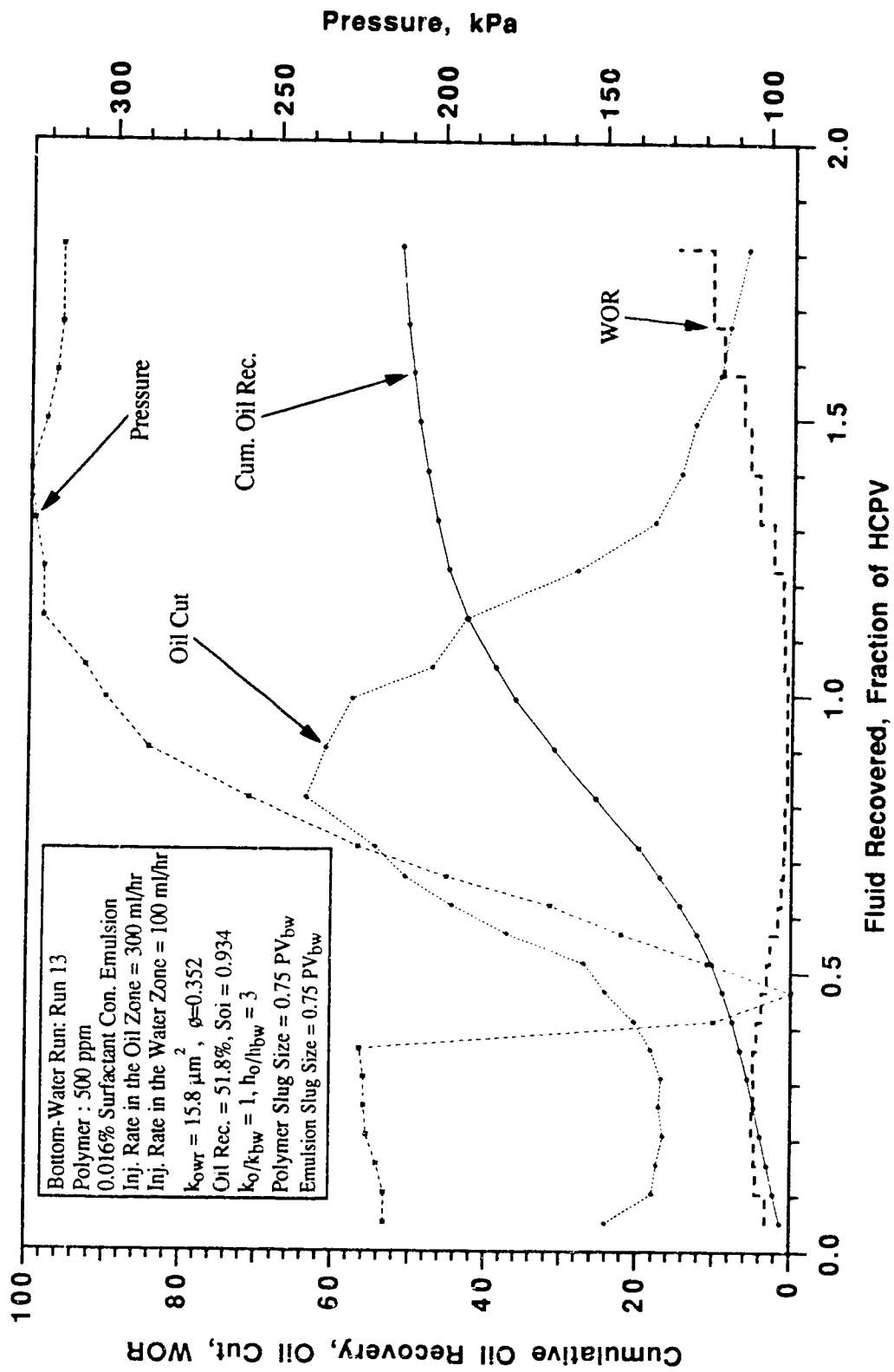
Fig. 7.14: Production History for Run 13. Effect of Slug Size on Oil Recovery for Bottom-Water Reservoirs.
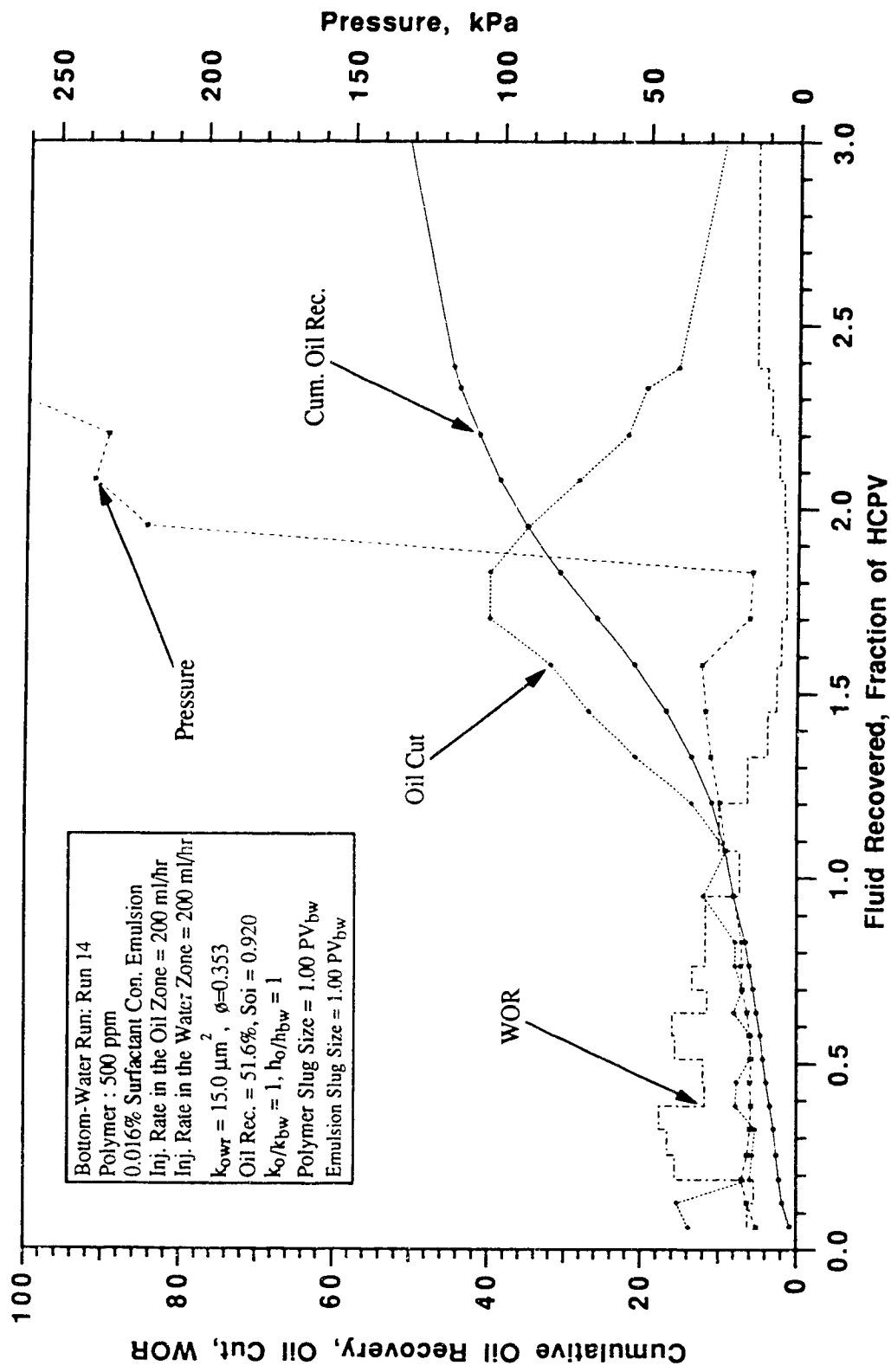
Fig. 7.15: Production History for Run 14. Effect of Bottom-Water Thickness on Oil Recovery.

A series of experiments was conducted to investigate how the rates in the oil zone and the bottom-water zone affect the instantaneous oil production and the ultimate oil recovery. Note that the rate in each zone was selected in proportion to the cross-sectional area of the zone to simulate a vertical fluid front movement.

Run 15: Bottom-Water Run with Polymer and Emulsion Injections, Surfactant Concentration in Emulsion = 0.016%, Polymer : 500 ppm, h_o/h_w = 3, k_o/k_{bw} = 1, Slug Size = 1.0 PV_{bw}, Rate (oil zone) = 350 ml/hr, Rate (bottom-water zone) = 50 ml/hr.

The total rate for both zones was 400 ml/hr. This rate was divided between the two zones according to the their cross-sectional areas. This was done in order to simulate a vertical front advance for each zone. In this experiment, all parameters were the same as those in Run 10 except that the rates in the oil and bottom-water zones were varied. Water breakthrough in this test occurred after 0.0386 HCPV of fluid had been produced. The oil cut dropped sharply to a value of 16%, then increased gradually to a maximum of 76% before decreasing again. The oil recovery was 57.8% of IOIP. The production history for this test is depicted in Figure 7.16.

Run 16: Bottom-Water Run with Polymer and Emulsion Injections, Surfactant Concentration in Emulsion = 0.016%, Polymer : 500 ppm, h_o/h_w = 3, k_o/k_{bw} = 1, Slug Size = 1.0 PV_{bw}, Rate (oil zone) = 250 ml/hr, Rate (bottom-water zone) = 150 ml/hr.

In this run, all parameters were the same as that in Run 15, except the rate in the oil zone was now changed to 250 ml/hr and the rate in the bottom-water zone was changed to 150 ml/hr. Water breakthrough occurred after 0.0394 HCPV of fluid had been recovered. The instantaneous oil production increased gradually to a maximum of 64%. The oil recovery was 45.4 % of IOIP. The production history for this experiment is shown in Figure 7.17.

Run 17 : Bottom-Water Run with Polymer and Emulsion Injections, Surfactant Concentration in Emulsion = 0.016%, Polymer : 500 ppm, h_o/h_w = 3, k_o/k_{bw} = 1, Slug Size = 1.0 PV_{bw}, Rate (oil zone) = 325 ml/hr, Rate (bottom-water zone) = 75 ml/hr.

In this run, the rate in the oil zone was 325 ml/hr and the rate in the bottom-water zone was 75 ml/hr. Water breakthrough occurred after 0.0442 HCPV of fluid had been produced. The instantaneous oil production decreased gradually to a value of 13.3 % and increased rapidly to maximum of 76.4%. The oil recovery was 46.6% of IOIP. Figure 7.18 shows the production history of the experiment.

Presuure, kPa

Cum. Oil Rec

Pressure

WOR

Oil Cut

Bottom-Water Run: Run 15
Polymer : 500 ppm
0.016% Surfactant Con. Emulsion
Inj. Rate in the Oil Zone = 350 ml/hr
Inj. Rate in the Water Zone = 50 ml/hr
$k_{owr} = 17.4 \ \mu m^2$, $\phi = 0.360$
Oil Rec. = 57.8%, Soi = 0.920
$k_o/k_{bw} = 1$, $h_o/h_{bw} = 3$
Polymer Slug Size = 1.00 PV_{bw}
Emulsion Slug Size = 1.00 PV_{bw}

Fluid Recovered, Fraction of HCPV
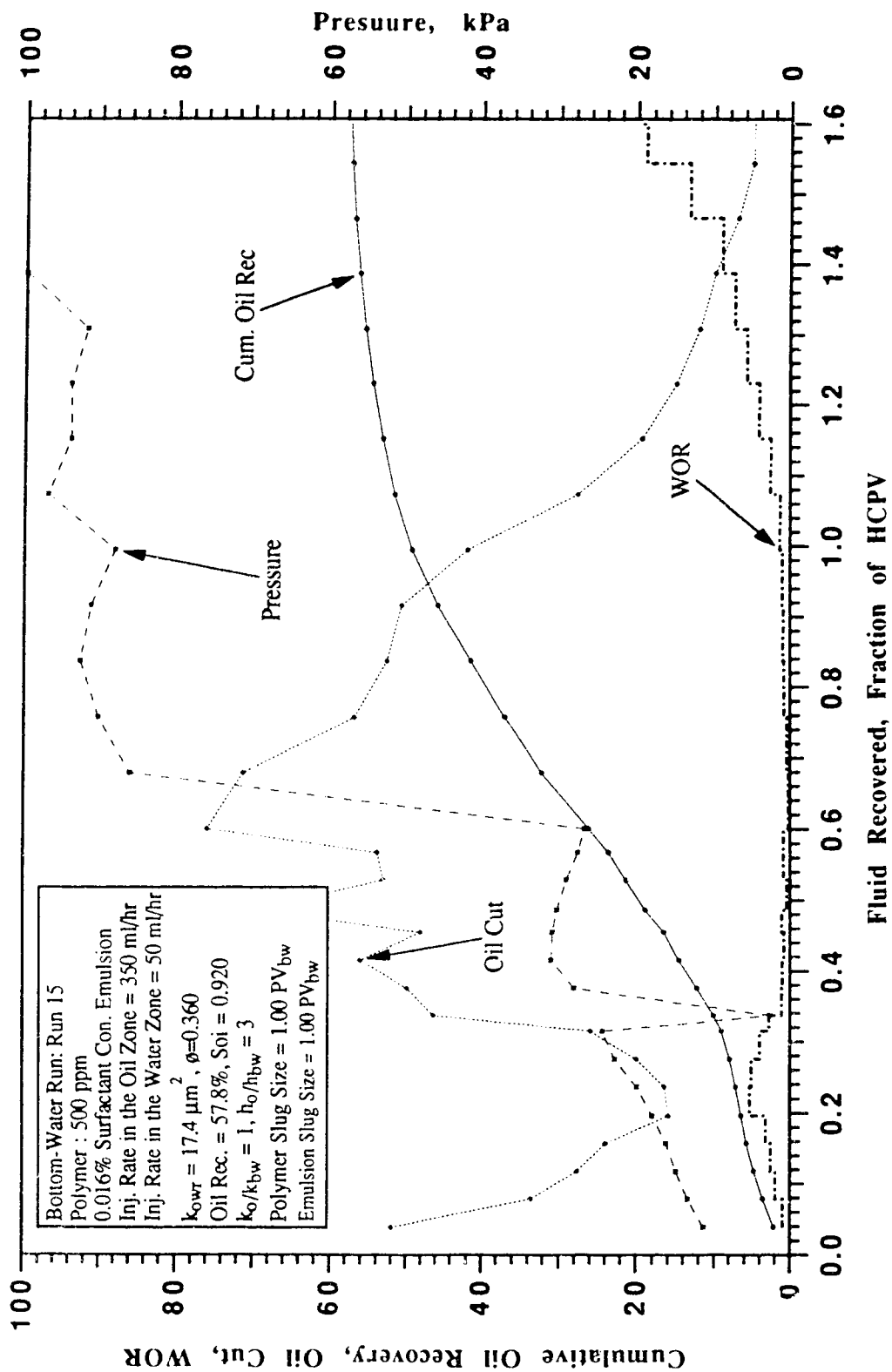
Fig. 7.16: Production History for Run 15.
Effect of Rate on Oil Recovery for Bottom-Water Reservoirs.

Cumulative Oil Recovery, Oil Cut, WOR

Pressure, kPa
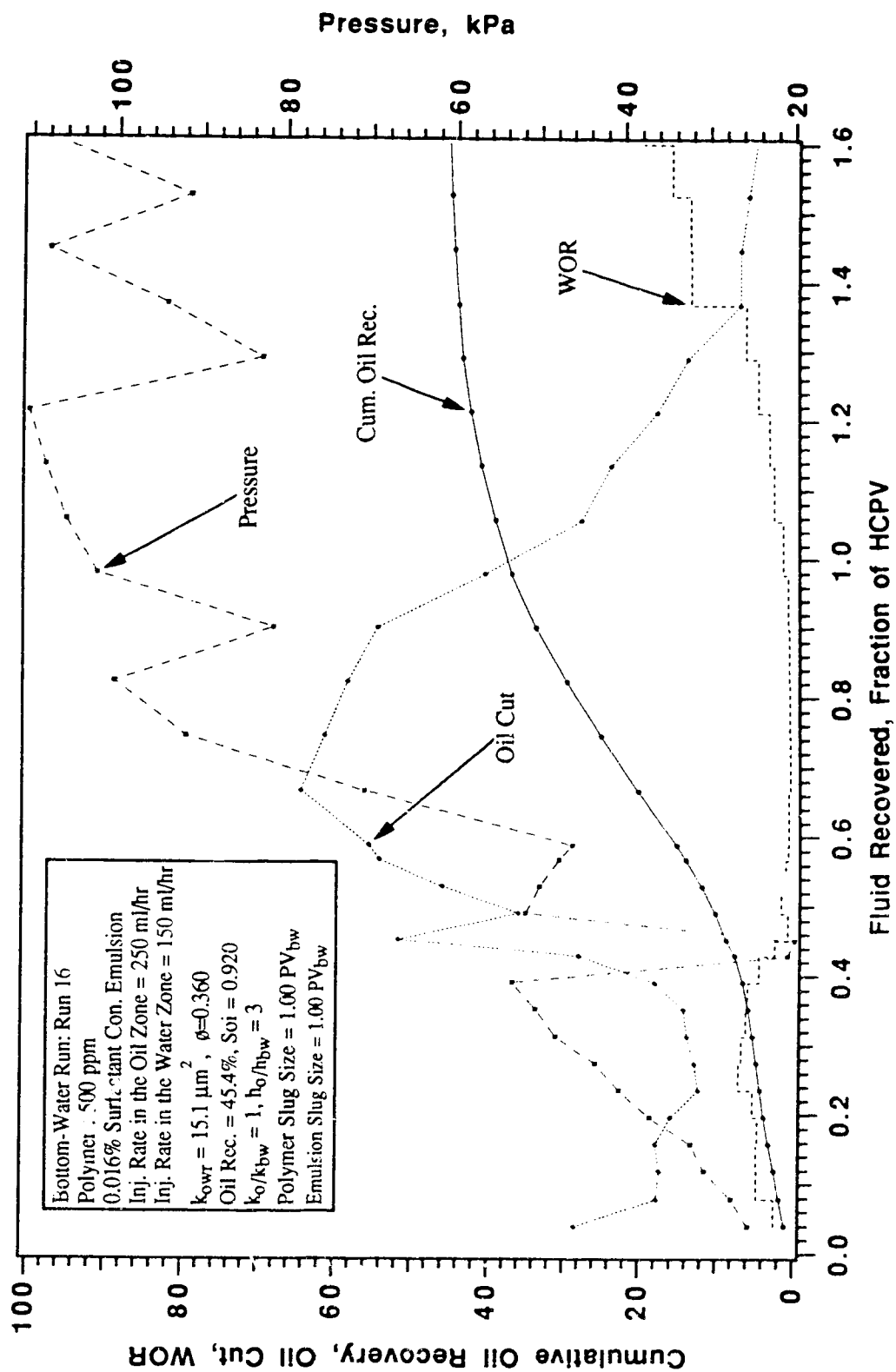
Fig. 7.17: Production History for Run 16.
Effect of Rate on Oil Recovery for Bottom-Water Reservoirs.

Fluid Recovered, Fraction of HCPV

Cumulative Oil Recovery, Oil Cut, WOR

Bottom-Water Run: Run 16
Polymer : 500 ppm
0.016% Surfactant Con. Emulsion
Inj. Rate in the Oil Zone = 250 ml/hr
Inj. Rate in the Water Zone = 150 ml/hr
$k_{owr} = 15.1 \, \mu m^2$, $\phi = 0.360$
Oil Rec. = 45.4%, Soi = 0.920
$k_o/k_{bw} = 1$, $h_o/h_{bw} = 3$
Polymer Slug Size = 1.00 PV_{bw}
Emulsion Slug Size = 1.00 PV_{bw}

WOR

Cum. Oil Rec.

Pressure

Oil Cut

Pressure, kPa

120 100 80 60 40 20 0

Cum. Oil Rec.

Pressure

WOR

Oil Cut

Bottom-Water Run: Run 17
Polymer : 500 ppm
0.016% Surfactant Con. Emulsion
Inj. Rate in the Oil Zone = 325 ml/hr
Inj. Rate in the Water Zone = 75 ml/hr

$k_{owr} = 15.0 \ \mu m^2$, $\phi = 0.359$
Oil Rec. = 50.0%, S_{oi} = 0.930
$k_o/k_{bw} = 1$, $h_o/h_{bw} = 3$
Polymer Slug Size = 1.00 PV_{bw}
Emulsion Slug Size = 1.00 PV_{bw}

Fluid Recovered, Fraction of HCPV

0.0 0.2 0.4 0.6 0.8 1.0 1.2 1.4 1.6

Cumulative Oil Recovery, Oil Cut, WOR

0 20 40 60 80 100

Fig. 7.18: Production History for Run 17.
Effect of Rate on Oil Recovery for Bottom-Water Reservoirs.

Run 18: Bottom-Water Run with Polymer and Emulsion Injections, Surfactant Concentration in Emulsion = 0.016%, Polymer : 500 ppm, h_o/h_w = 3, k_o/k_{bw} = 1, Slug Size = 1.0 PV_{bw}, Rate (oil zone) = 375 ml/hr, Rate (bottom-water zone) = 25 ml/hr.

In this run, the oil zone rate was changed to 375 ml/hr and the rate in the bottom-water zone was changed to 25 ml/hr. Water breakthrough was observed after 0.0416 of HCPV had been recovered. The oil cut decreased slowly until a minimum value of 20% and then increased rapidly to a maximum value of 73 %. The oil recovery was 52.2% of IOIP. Figure 7.19 shows the production history of this run.

Run 19: Bottom-Water Run with Polymer and Emulsion Injections, Surfactant Concentration in Emulsion = 0.016%, Polymer : 700 ppm, h_o/h_w = 3, k_o/k_{bw} = 1, Slug Size = 1.0 PV_{bw}, Rate (oil zone) = 350 ml/hr, Rate (bottom-water zone) = 50 ml/hr .

The effect of polymer concentration was examined in this test. All the parameters were the same as that of Run 15, except that the polymer concentration was changed from 500 ppm to 700 ppm to see how it affects recovery. Water breakthrough was observed after 0.0413 HCPV of fluid had been recovered. The oil cut fluctuated for a while before rising to a maximum of 84% and then declined to very low value. The oil recovery was 52.3 % of IOIP. The production history for this experiment is shown in Figure 7.20.

Run 20: Bottom-Water Run with Polymer and Emulsion Injections, Surfactant Concentration in Emulsion = 0.016%, Polymer : 500 ppm, h_o/h_w = 3, k_o/k_{bw} = 1, Slug Size = 1.0 PV_{bw}, Rate (oil zone) = 370 ml/hr, Rate (bottom-water zone) = 30 ml/hr .

In this run, the oil zone rate was changed to 370 ml/hr and the rate in the bottom-water zone was changed to 30 ml/hr. Water breakthrough occurred after 0.0386 HCPV of fluid had been recovered. The oil cut declined gradually and then rose to a maximum of 80% before decreasing again. The oil recovery was 49.3% of IOIP. Figure 7.21 shows the production history for this experiment.
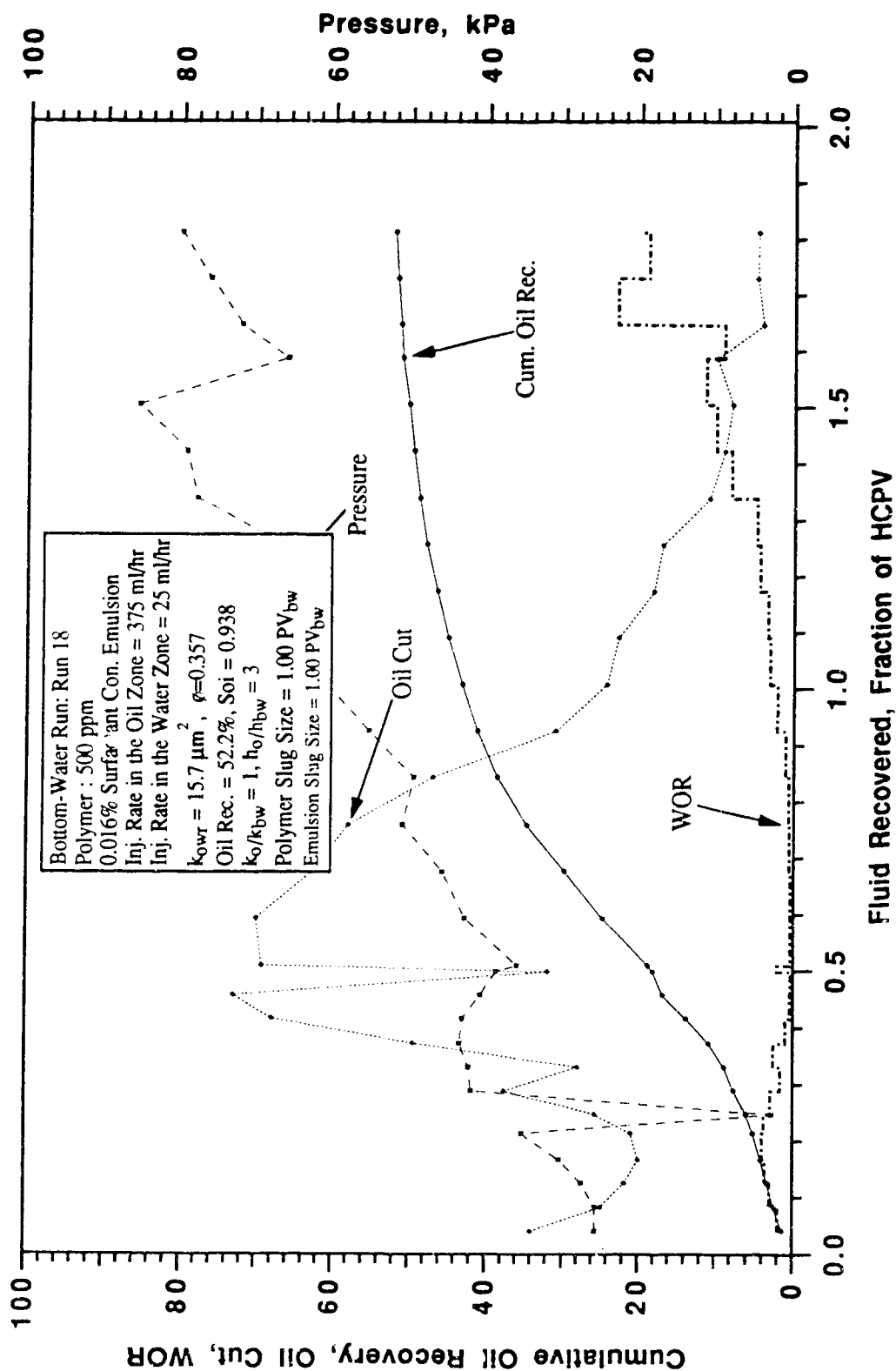
Fig. 7.19: Prodution History for Run 18.
Effect of Rate on Oil Recovery for Bottom-Water Reservoirs.
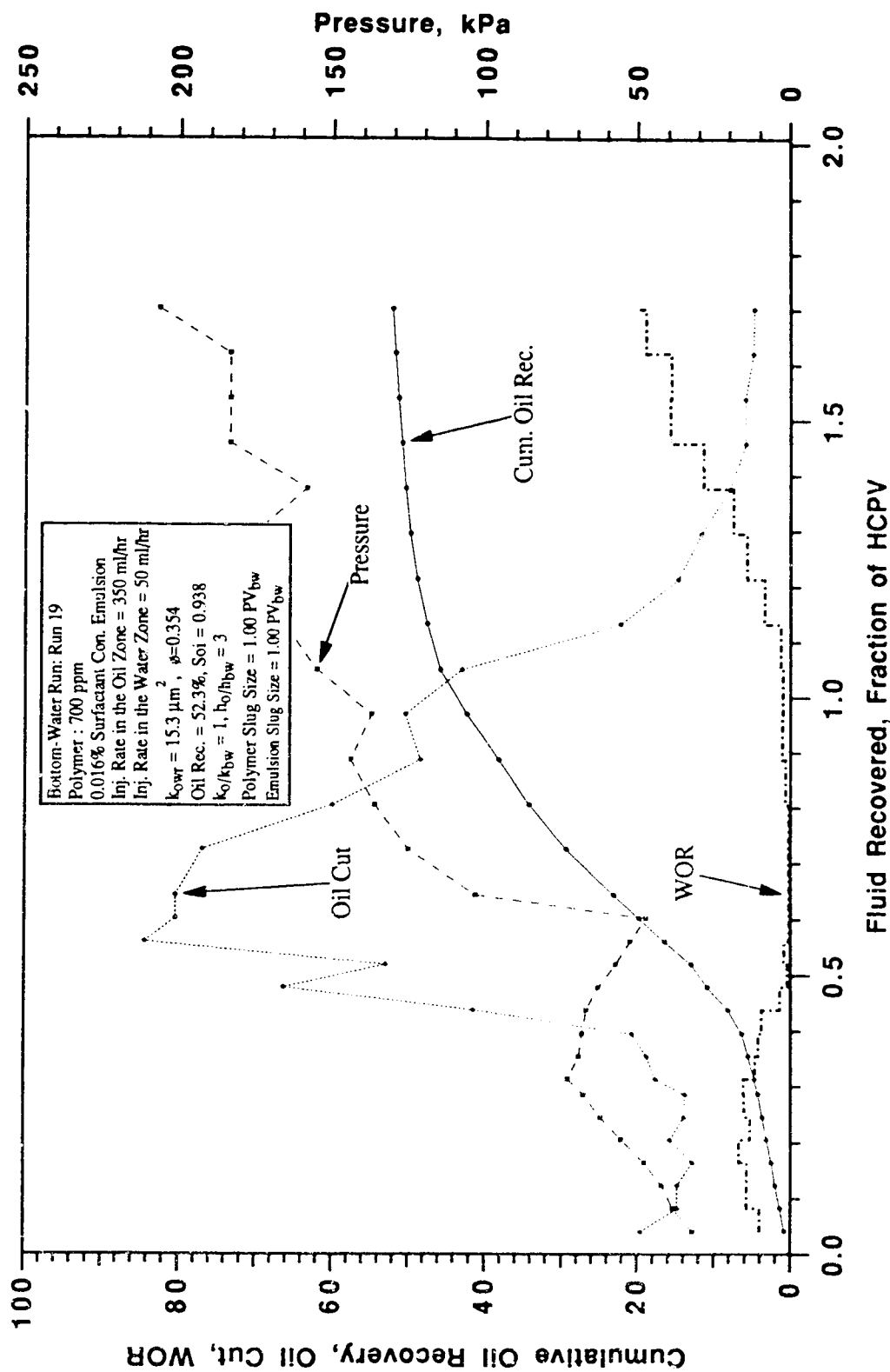
Fig. 7.20: Production History for Run 19. Effect of Polymer Concentration and Rate on Oil Recovery.
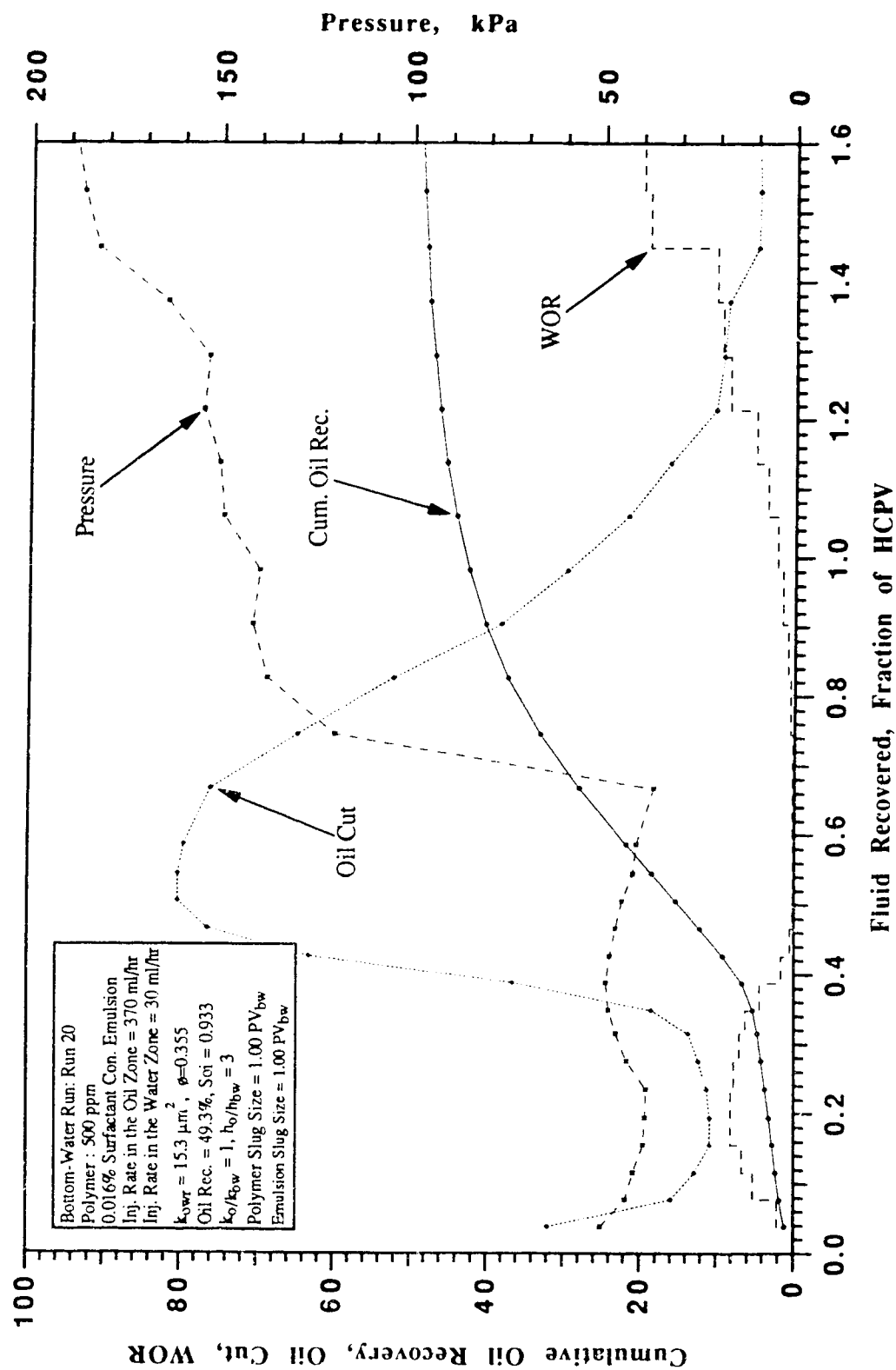
Fig. 7.21: Production History for Run 20.
Effect of Rate on Oil Recovery for Bottom-Water Reservoir.

Run 21: Bottom-Water Run with Polymer and Emulsion Injections, Surfactant Concentration in Emulsion = 0.016%, Polymer : 500 ppm, $h_o/h_w = 3$, $k_o/k_{bw} = 1$, Slug Size = 1.0 PV_{bw}, Rate (oil zone) = 340 ml/hr, Rate (bottom-water zone) = 60 ml/hr.

In this run, the oil zone rate was changed to 340 ml/hr and the rate in the bottom-water zone was changed to 60 ml/hr. Water breakthrough occurred after 0.0377 HCPV of fluid had been produced. The oil cut dropped rapidly to 8% and rose sharply to a maximum of 80%. The ultimate oil recovery was 51% of IOIP. The production history for this experiment is shown in Figure 7.22.

To investigate oil recovery by horizontal wells four horizontal wells were designed. Each well was made up of a quarter inch tubing with a length of 30.48 centimeters. Twenty-one holes were drilled along one side to serve as the injection/production wells. The distance between the holes was 1.3 centimeters. The diameter of the holes was 1 millimeter. Six experiments were conducted using the horizontal wells.

Run 22: Bottom-Water Run, Waterflood using Horizontal Injectors and Vertical Producers, $h_o/h_w = 3$, $k_o/k_{bw} = 1$.

In this run, horizontal injectors and vertical producers were used. The injection of the water was into the oil zone only. This run was conducted as a base run to be compared with the vertical injector/producer run described under Run 4. Water breakthrough occurred after 0.0421 HCPV of fluid had been produced. The instantaneous oil production was constant throughout the test. The oil recovery was 25.6% of IOIP after 2.489 HCPV of fluid had been produced. The production history for this run is shown in Figure 7.23.

Run 23: Bottom-Water Run, Horizontal Injectors and Vertical Producers using Polymer and Emulsion, Surfactant Concentration in Emulsion = 0.016%, Polymer : 500 ppm, $h_o/h_w = 3$, $k_o/k_{bw} = 1$, Slug Size = 1.0 PV_{bw}.

In this run, horizontal injectors and vertical producers were used. Polymer was injected into the oil zone as a mobility control agent and emulsion was injected in the bottom water zone as the blocking agent. Water breakthrough occurred after 0.0310 HCPV of fluid had been produced. The oil cut fell sharply and rose to a maximum of 67%. The oil recovery was 52.6% of IOIP. The production history for this run is shown in Figure 7.24.
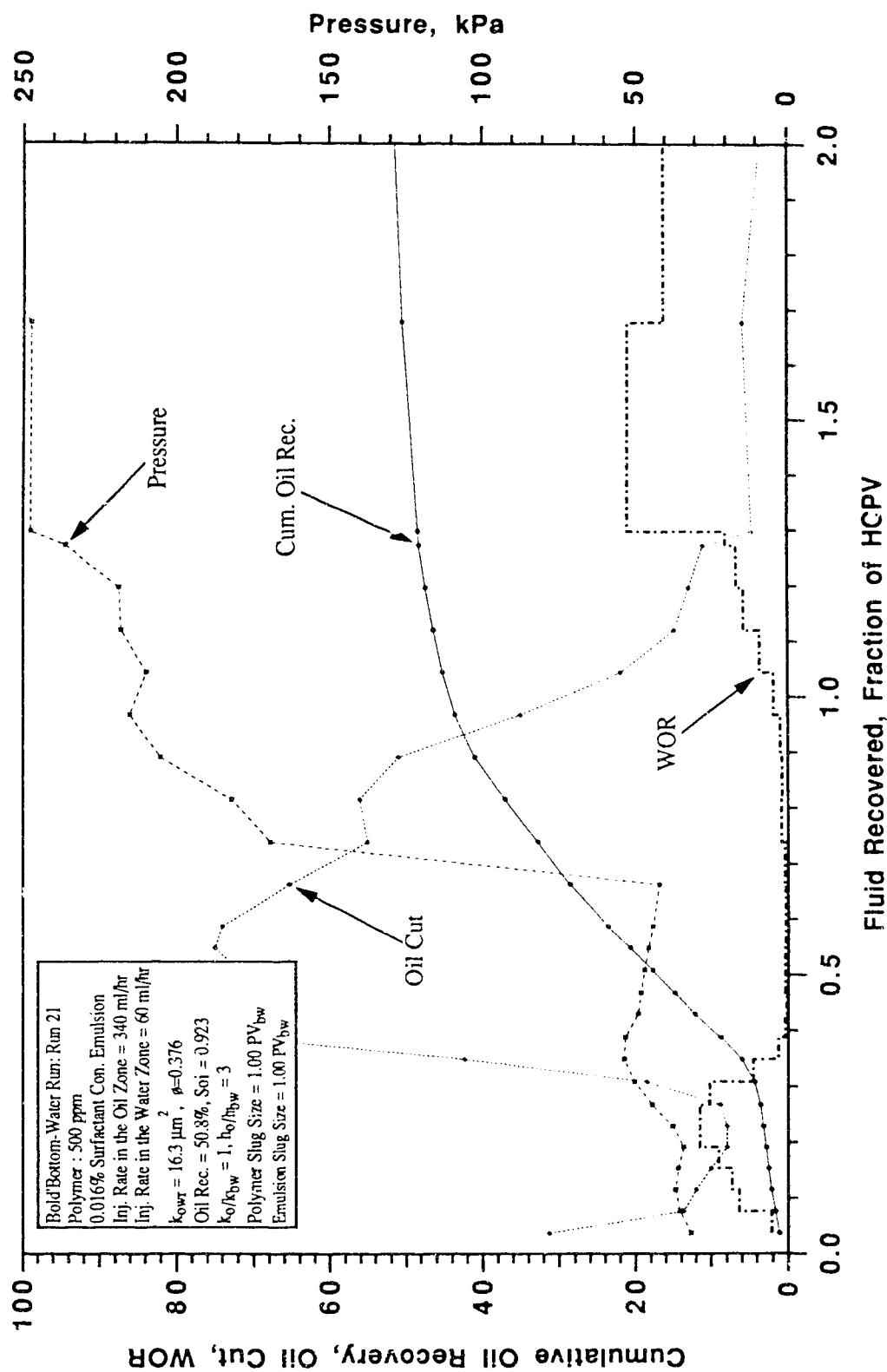
Fig. 7.22: Production History for Run 21.
Effect of Rate on Oil Recovery for Bottom-Water Reservoirs.
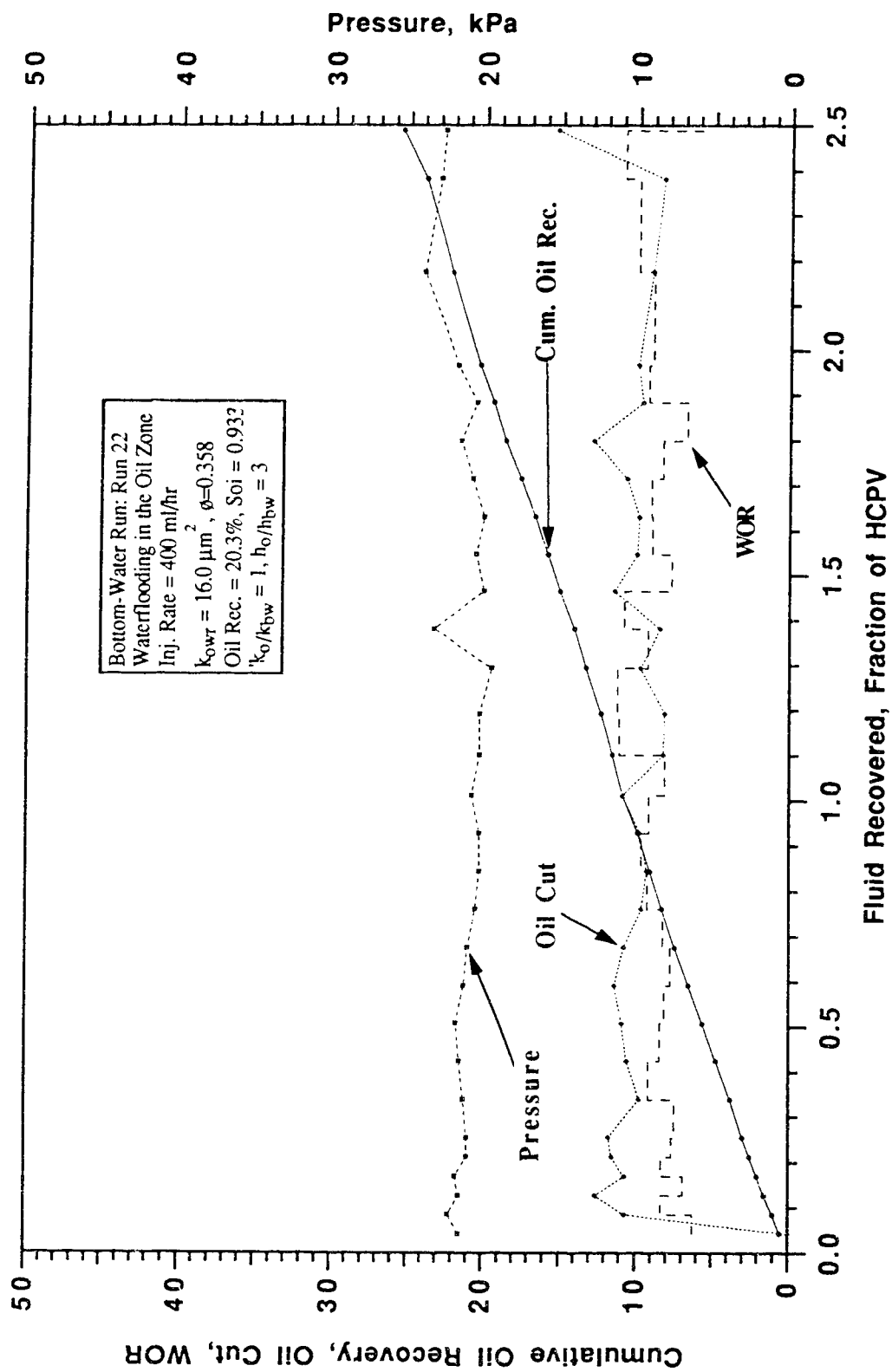
Fig. 7.23: Production History for Run 22.
Effect of Horizontal Injector on Oil Recovery for Continuous Waterflood.
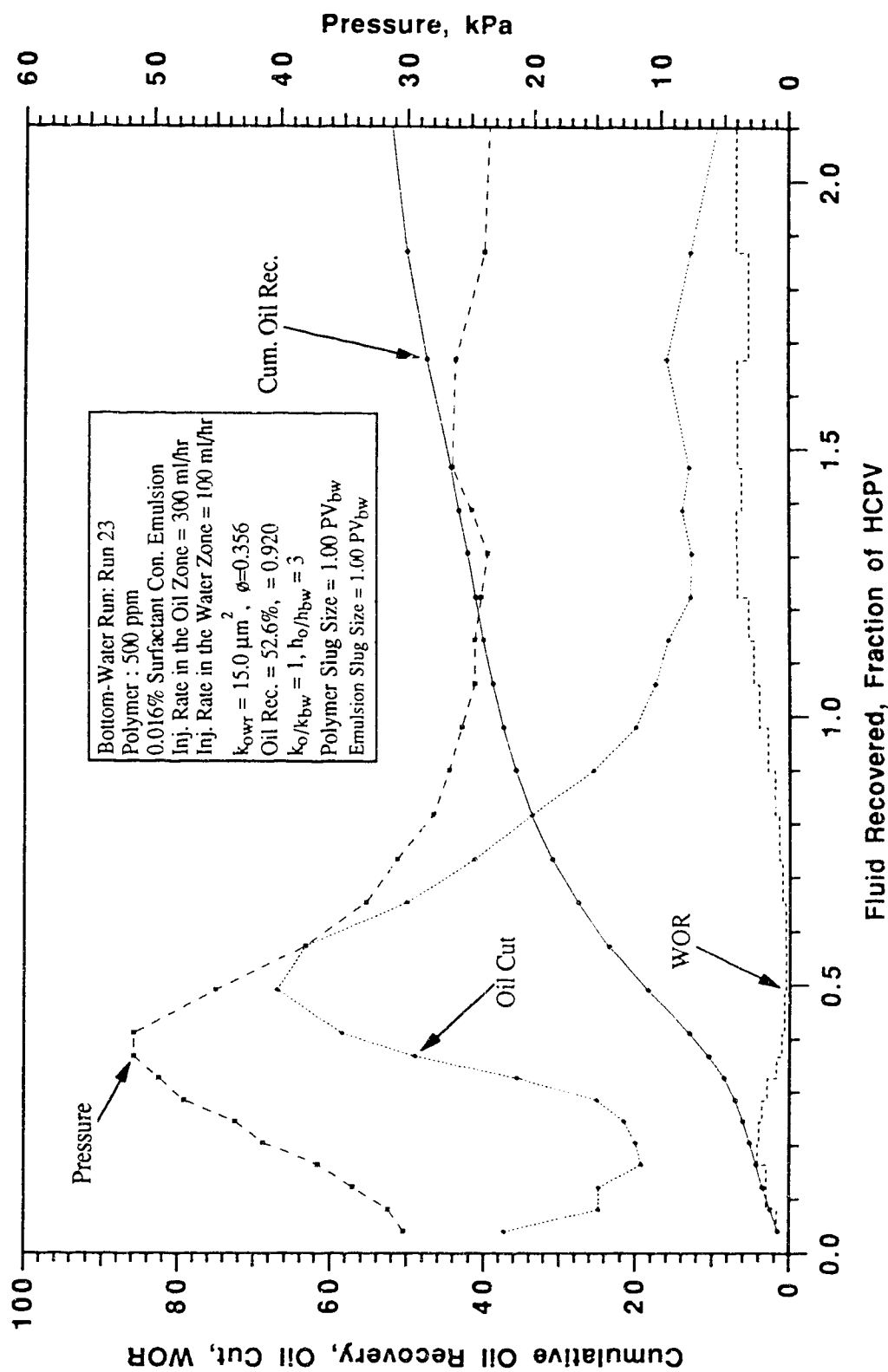
Fig. 7.24: Production History for Run 23.
Effect of Horizontal Injector on Oil Recovery Using Polymer and Emulsion as Injection Fluids.

Run 24: Bottom-Water Run, Waterflood using Horizontal Injectors and Horizontal Producers, $h_o/h_w = 3$, $k_o/k_{bw} = 1$.

In this run, horizontal injectors and producers were used. Water was injected into the oil zone only. Water breakthrough occurred after 0.0396 HCPV of fluid had been produced. The instantaneous oil production dropped sharply from a maximum of 84% to minimum of 7.5 %. The oil recovery was 45.2% of IOIP. The production history for this run is shown in Figure 7.25.

Run 25: Bottom-Water Run, Horizontal Injectors and Horizontal Producers using Polymer and Emulsion, Surfactant Concentration in Emulsion = 0.016%, Polymer : 500 ppm, h_o /h_w = 3, k_o/k_{bw} =1, Slug Size = 1.0 PV_{bw}.

In this run, horizontal injectors and horizontal producers were used. Polymer was injected into the oil zone as a mobility control agent and emulsion was injected into the bottom-water zone as the blocking agent. Water breakthrough occurred after 0.0399 HCPV of fluid had been produced. The instantaneous oil production dropped gradually and rose to a maximum of 62%. The oil recovery was 57.2% of IOIP. The production history for this run is shown in Figure 7.26.

Run 26: Bottom-Water Run, Waterflood using Horizontal and Vertical Injectors and Horizontal and Vertical Producers, $h_o/h_w = 3$, $k_o/k_{bw} = 1$.

In this run, horizontal and vertical injectors and horizontal and vertical producers were used. The horizontal wells were used in the oil zone and the vertical wells were used in the bottom-water zone. Water breakthrough occurred after 0.0398 HCPV of fluid had been produced. The oil cut started at a maximum of 74% and dropped sharply to a minimum value. The oil recovery was 35% of IOIP. The production history of this run is presented in Figure 7.27.
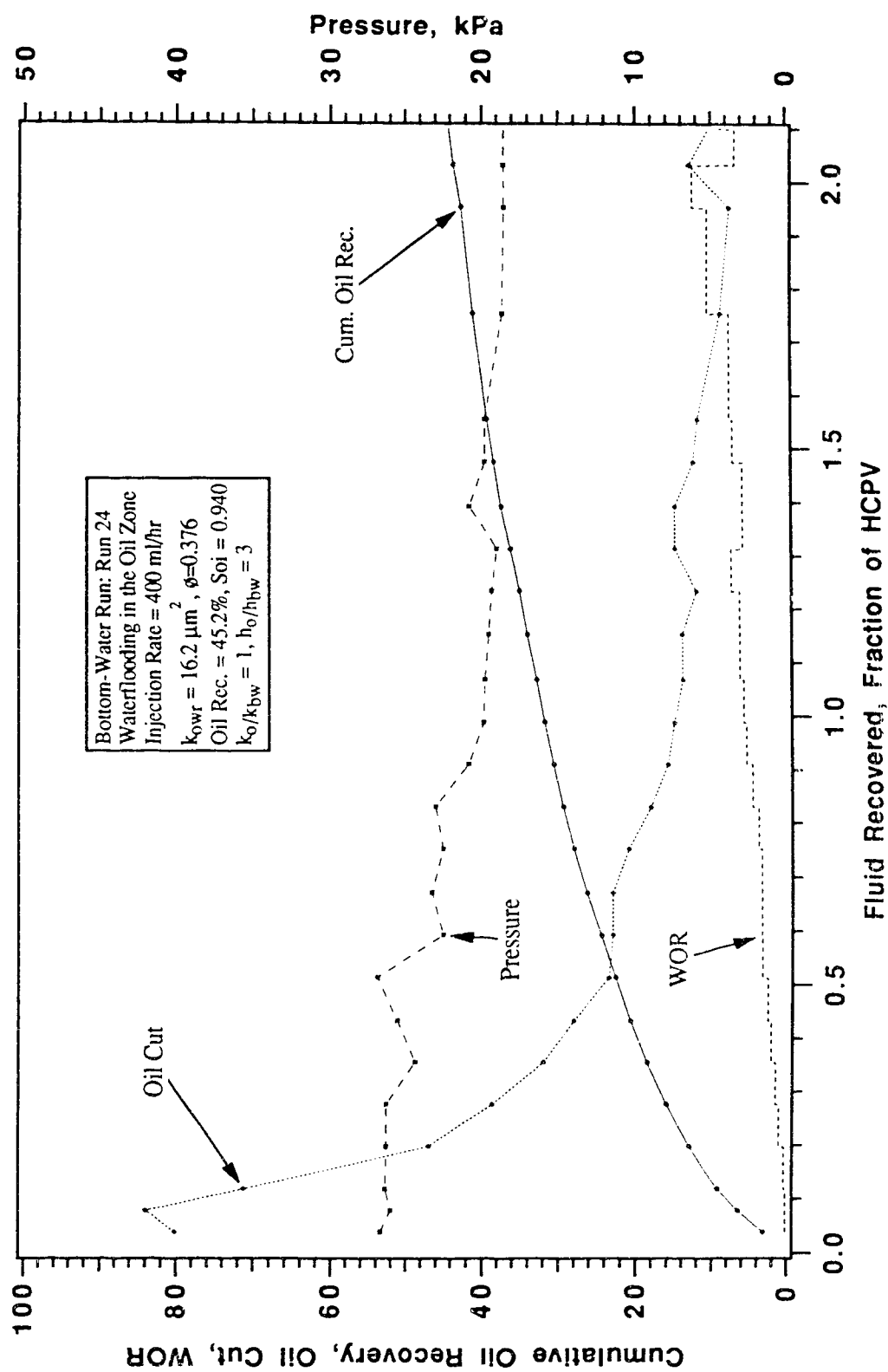
Fig. 7.25: Production History for Run 24.
Effect of Horizontal Injector and Producer on Oil Recovery for Continuous Waterflood.

84
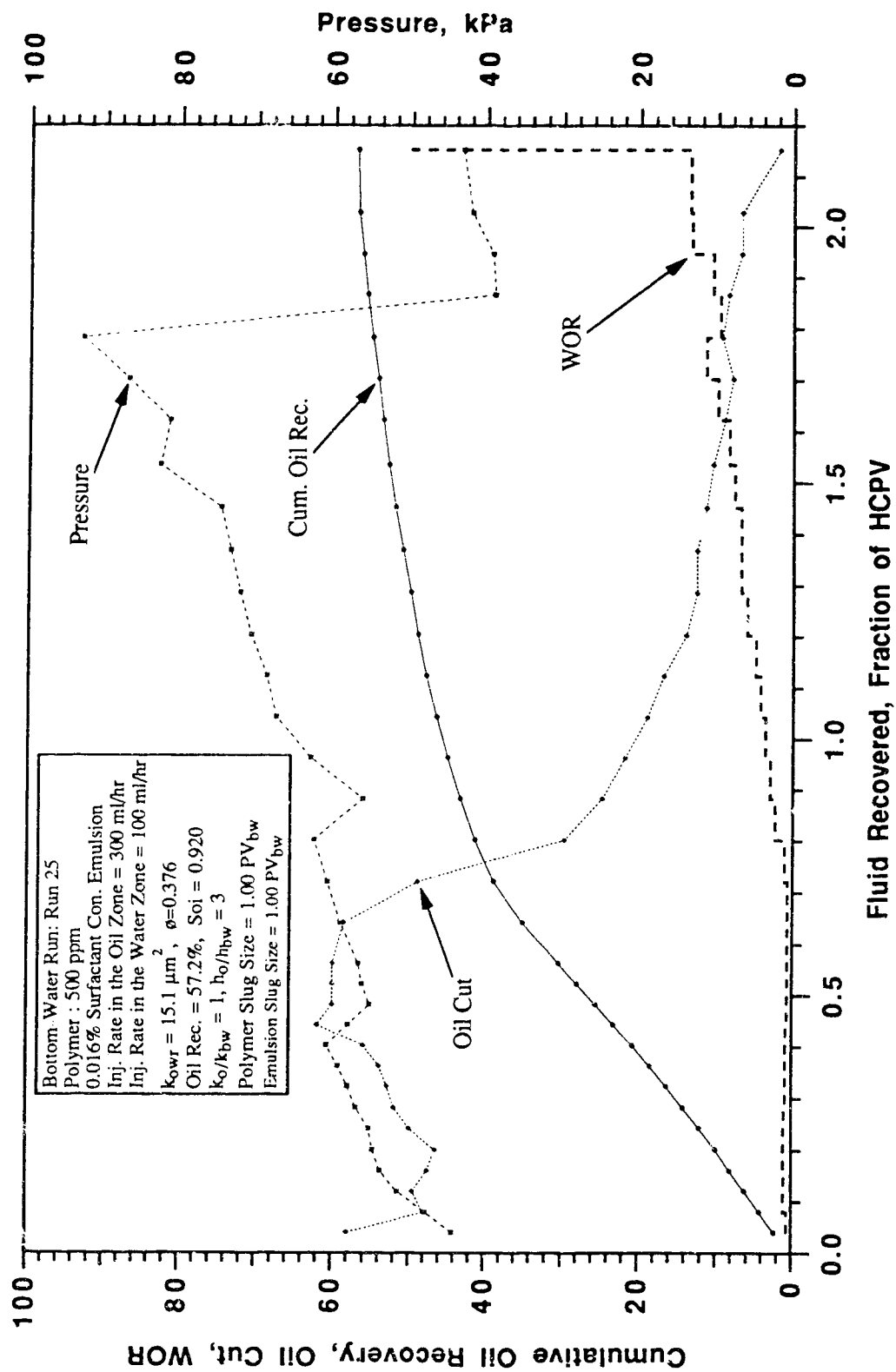
Fig. 7.26: Production History for Run 25.
Effect of Horizontal Injector and Producer on Oil Recovery Using Polymer and Emulsion as Injection Fluids.

Pressure, kPa

80   60   40   20   0

2.0

Cum. Oil Rec.

Bottom-Water Run: Run 26
Waterflooding in the Oil Zone
Injection Rate = 400 ml/hr
$k_{owr} = 15.0 \ \mu m^2$, $\phi = 0.376$
Oil Rec. = 35.4%, Soi = 0.922
$k_o/k_{bw} = 1$, $h_o/h_{bw} = 3$

1.5

Pressure

WOR

1.0

Oil Cut

0.5

Fluid Recovered, Fraction of HCPV

0.0

100   80   60   40   20   0

Cumulative Oil Recovery, Oil Cut, WOR
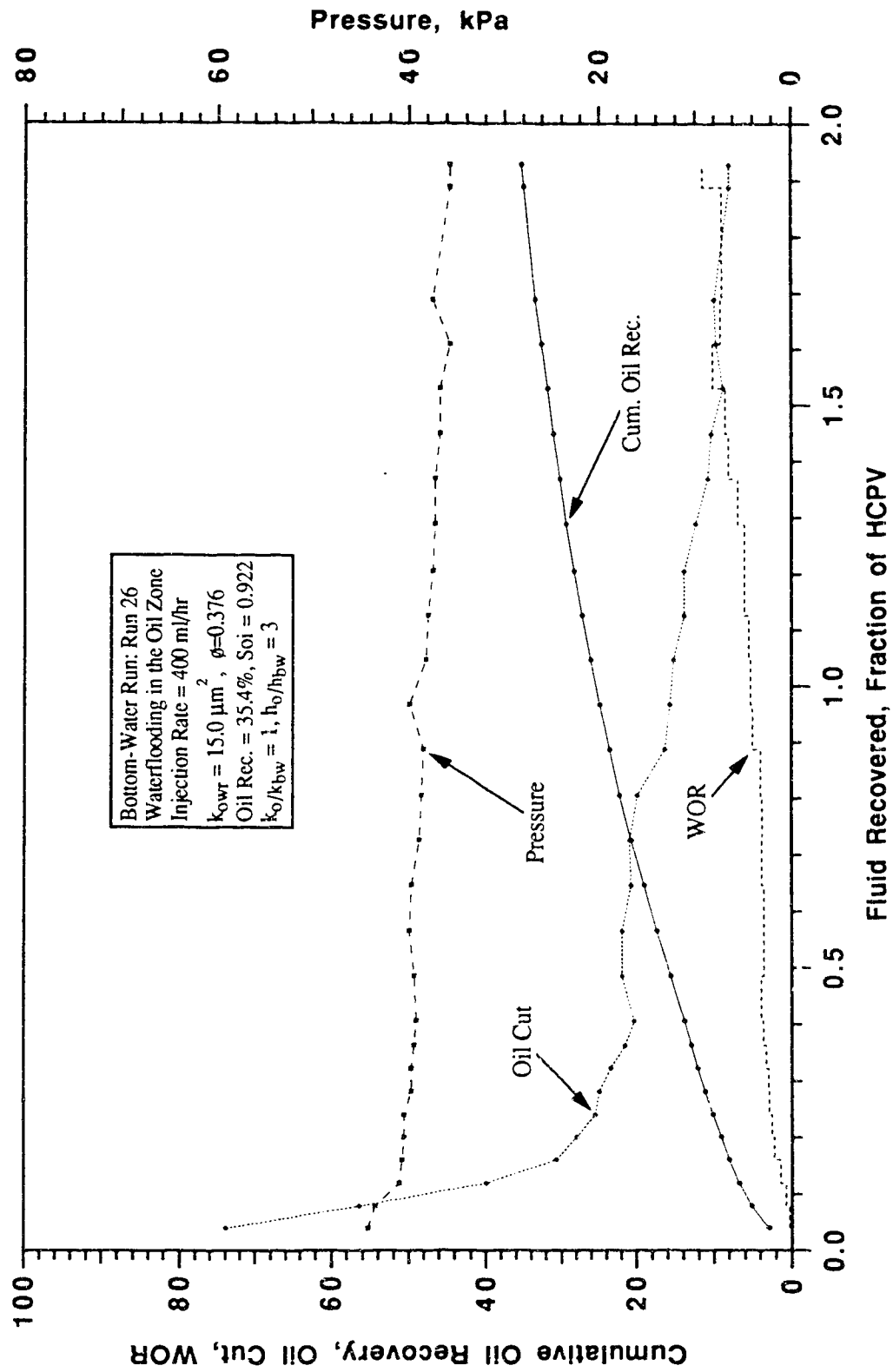
Fig. 7.27: Production History for Run 26.
Effect of Horizontal Well Configuration on Oil Recovery for Continuous Waterflood.

Run 27: Bottom-Water Run, Horizontal and Vertical Injectors and Horizontal and Vertical Producers using Polymer and Emulsion, Surfactant Concentration in Emulsion = 0.016%, Polymer : 500 ppm, h_o/h_w = 3, k_o/k_{bw} =1, Slug Size = 1.0 PV_{bw}.

In this run, horizontal and vertical injectors and horizontal and vertical producers were used. Polymer was injected into the oil zone as a mobility control agent and emulsion was injected into the bottom-water zone as a blocking agent. Water breakthrough occurred after 0.1222 HCPV of fluid had been produced. The instantaneous oil production dropped sharply from 89% to 37% and increased again to a maximum of 57% before decreasing to a smaller value. The oil recovery was 55.2% of IOIP. Figure 7.28 shows the production history of this experiment.

7.2 Experimental Errors and Reproducibility of Experiments
7.2.1 Experimental Errors

The wet-packing method was employed, since a rubber hammer was used to tamp the core-holder, permeability tended to vary from one experiment to the other. The maximum permeability was 23.0 μm^2 and the minimum was 17.0 μm^2, the average being 18.7 μm^2. Another area where errors could be encountered in the experiments was irreducible water saturation estimation. After the model was wet-packed air was passed through it to dry the glass beads. Vacuum was also applied on the core-holder. These attempts were designed to dry the glass beads, but it is possible that the beads did not dry completely. The irreducible water saturation was therefore difficult to calculate, hence estimation was often applied. Another source of error was the calculation of the initial oil-in-place (IOIP). It was calculated using the IOIP of the homogeneous pack multiplied by the ratio of the height of the oil zone thickness to the model thickness. Obtaining the IOIP of the b ‿tom-water layer this way was found to be quite accurate, with less than (3-4 %) error com red to weighing the scraped-off layer to obtain the exact amount of oil removed. Five checks were performed to verify this. Consequently, all the IOIP of the bottom-water experiments were obtained in this manner.
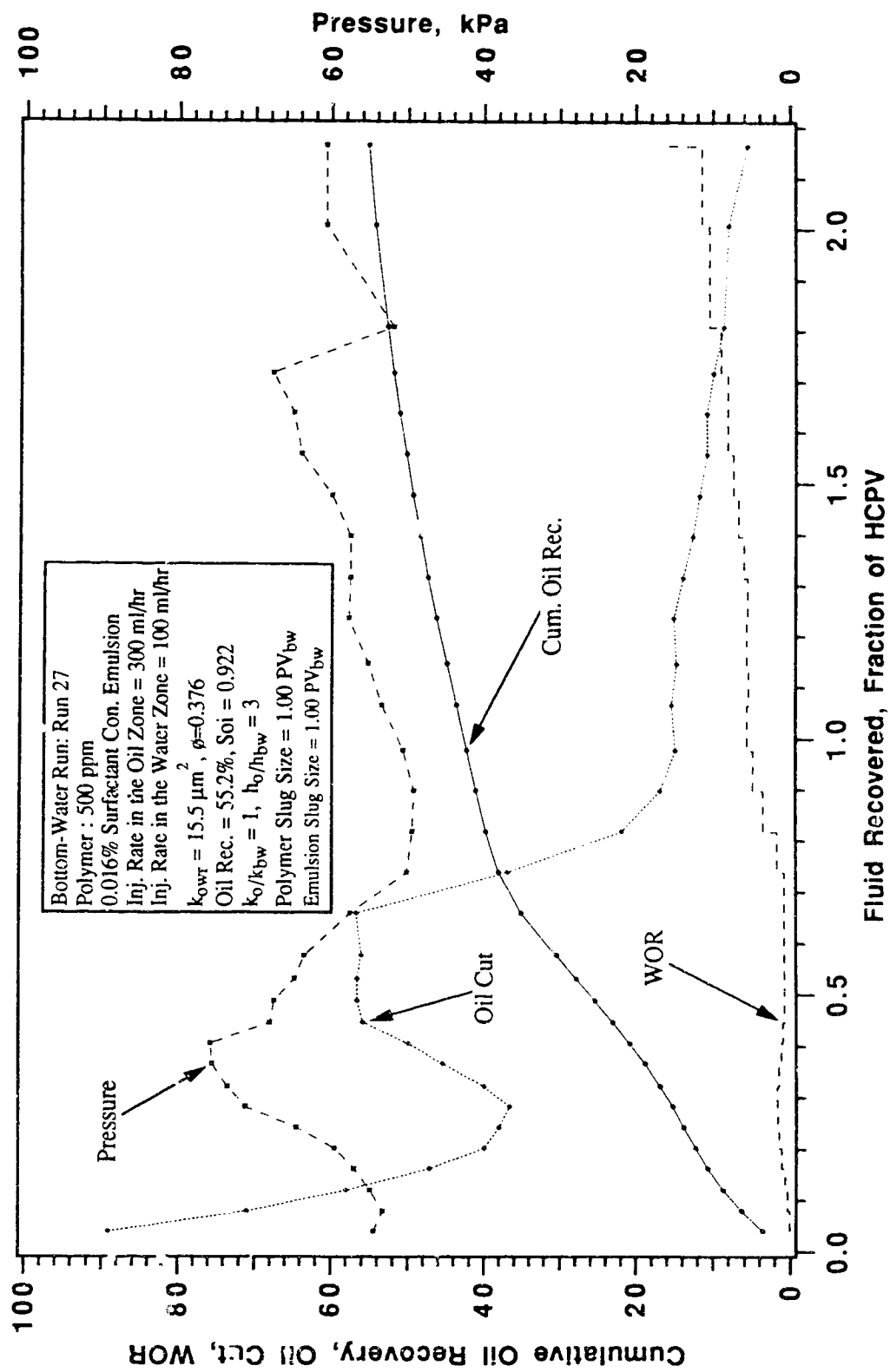
Fig. 7.28: Production History for Run 27.
Effect of Horizontal Well Configuration on Oil Recovery Using Polymer and Emulsion as Injection Fluids.

7.2 Reproducibility of Experiments

Runs 10 and 11 were repeated as Runs 28 and 29 to establish the consistency of the experiments. As mentioned in the experimental procedure, the work involved is labour-intensive hence only two experiments were conducted to verify the repeatability of the experimental results.

Figures 7.29 and 7.30 compare the cumulative oil recovery and oil cut for Runs 28 and 10 and Runs 29 and 11 respectively.The maximum oil cut for Runs 10 and 11 were 75% and 75.3%; for Runs 28 and 29 the maximum oil cuts were 79.5% and 75%. The cumulative oil recovery for Runs 10 and 11 were 69.5% and 61.8% IOIP; the oil recoveries for Runs 28 and 29 were 65.9% and 50.9% IOIP. From the above results it can be concluded that the experiments in this study are reproducible within an error of less than 5% recovery of IOIP.

7.3 Description of the Computer Program Used in the Semi-Analytical Model

The program, given in Appendix B, uses the crossflow equations developed in Section 4. It is made up of a main program and eight subroutines. The main program is called Main and the subprograms are called Dataread, Init., Crossflow_calc., Front_calc.1, Front_calc.2, Performance_calc., Function, and Fileout_result. The Dataread subroutine has the function of reading the input data. The Init. subroutine sets the initial values for all variables. The subroutine called Crossflow_calc. calculates crossflow rates in each section. The Front_calc. 1 and 2 subroutines calculate the front location before breakthrough and after breakthrough, respectively. The Performance_calc. subroutine calculates production of oil and water. The Function subroutine. shows all functions used in the program and finally the Fileout_result outputs all the results to a file.
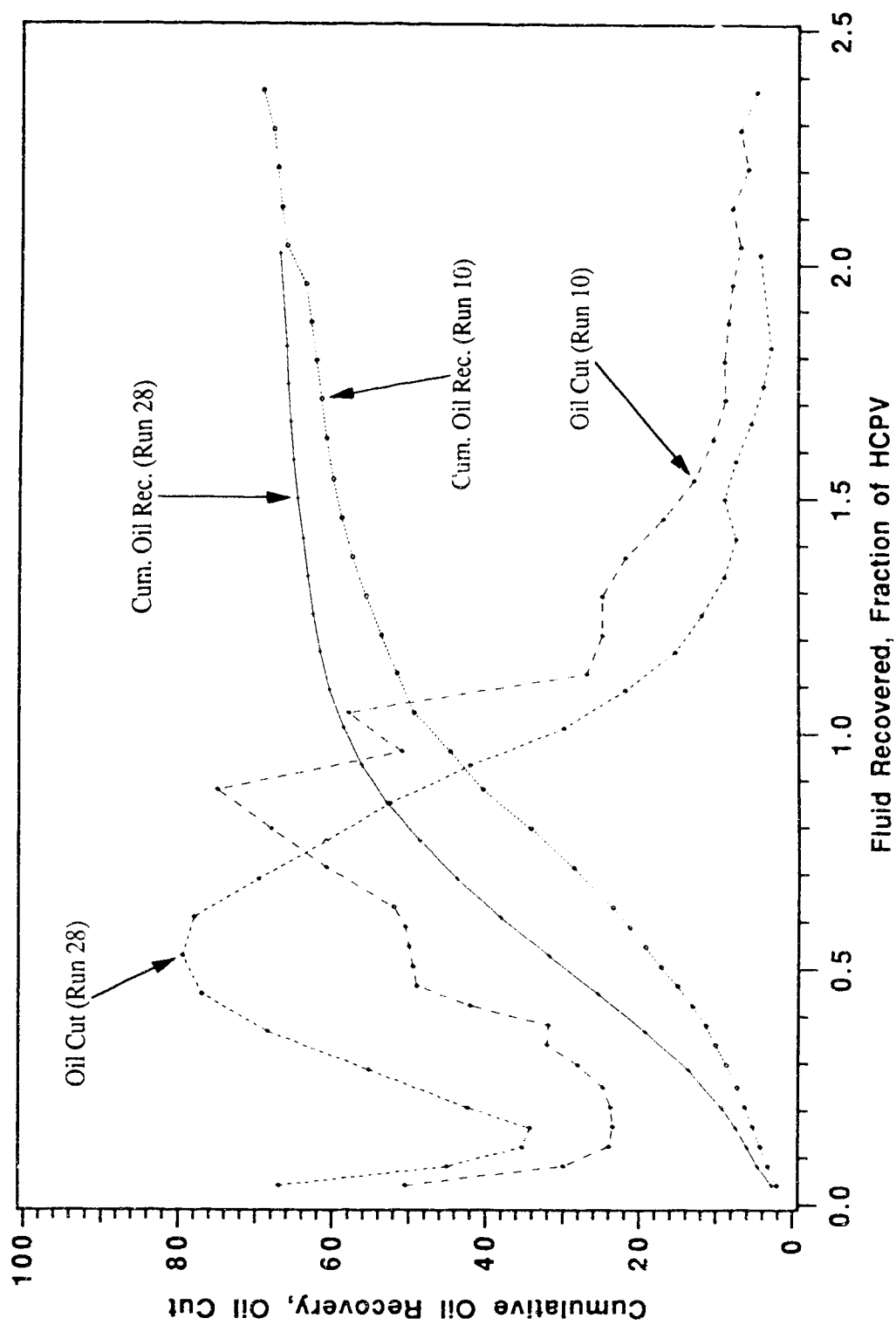
Fig. 7.29: Comparison of Reproducibility of Experiments.
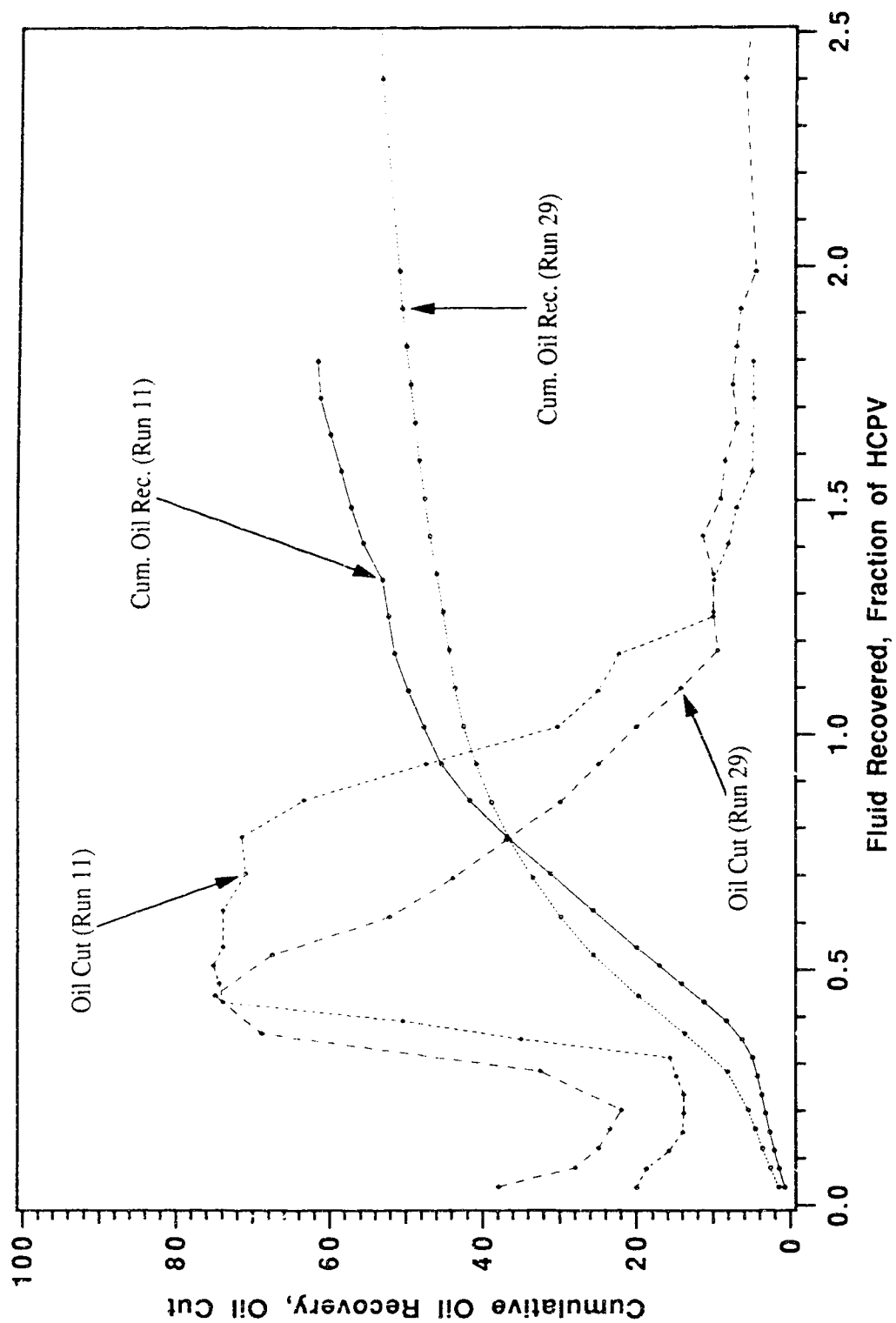
Fig. 7.30: Comparison of Reproducibility of Experiments.

7.4   Calculation Procedure of Oil-Recovery Performance Including Crossflow Effects

[1] Flood conditions and assumptions:

This program calculates oil-recovery performance in the following flood conditions.

(1)   Consider a two-layer porous medium, where the upper layer is the oil zone and the lower layer is the water zone. The oil zone is initially filled with oil at irreducible water saturation, and the water zone is 100% saturated with water. The porous medium is homogeneous and isotropic.

(2)   Water/emulsion/polymer solution is injected into the upper/bottom layer at a constant rate. Crossflow between the upper and lower layer happens simultaneously depending on the flow resistance of each layer. Oil is produced from both layers.

(3)   The outlet pressures in both layers are constant during the flood.

(4)   Gravity and capillarity are neglected.

(5)   Emulsion and polymer solution are assumed to be Newtonian and miscible with water. Water viscosity is a function of polymer and emulsion concentration.

(6)   No residual oil saturation is assumed in the lower layer. Relative permeability curves of both layers are given as mentioned below.

[2]   Calculation procedure of frontal movement with crossflow.

.

(1)   At the beginning of the flood, the fronts of injected fluids, x_{f1} and x_{f2}, appear in both layers as shown below. This figure also shows how each section and zone is defined.
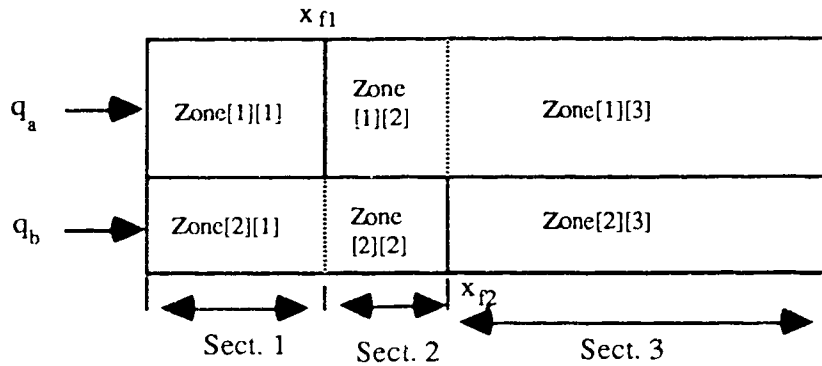
(2)	The crossflow rate was calculated in each section at a certain time step, t. Equations (4 .17) , (4.20) and (4.23) were used to calculate the crossflow rate. The water saturation and polymer/emulsion concentration in each zone were assumed to be constant in each time step. The crossflow rates depended on the mobility ratio between each zone and frontal location of x_{f1} and x_{f2}. These rates were also constant in each time step.

Step (2) is written in the subprograms crossflow_calc0 and crossflow_calc1.

(3)	In the upper layer, the saturation plane from S_{iw} to $1-S_{or}$ was assumed to move at a constant speed. In the lower layer, the saturation plane from $S_w = 0.0$ to 1.0 was assumed to move at a constant speed. By this assumption, the injected and crossflow fluids displace oil in a piston-like fashion (see Appendix C).

(4)	During the time Δt, the lengths of zone [1][1], zone [1][2], zone [2][1], zone [2][2], zone[1][3] and zone [2][3] changed due to the flow of the injected and crossflow fluids. These lengths at time t+1 were calculated using assumption (3). The frontal locations of x_{f1} and x_{f2} at time t+1 were also determined as shown in Appendix C.

(5)   At the time t+1, the location of each zone was updated. The water saturation and polymer/emulsion concentration in each zone were calculated. The water viscosity was a function of polymer and emulsion concentration. The mobility ratios in each section were calculated from the total mobilities in each zone.

Steps (3) to (5) are written in the subprogram front_calc3.

(6)   The oil cut of the production fluids at the upper layer was a function of the water saturation of zone [1][3]. The oil cut of the production fluids at the lower layer was a function of the water saturation of zone [2][3]. The production rate of oil was calculated by summing up the oil production rates in both layers. Oil recovery efficiency and WOR were also calculated the same way.

Step (6) is written in the subprogram performance_calc.

(7)   The steps from (2) to (6) were repeated until either x_{f1} or x_{f2} reached breakthrough.

(8)   After the breakthrough of either front, only one front of injected fluid, x_{f1} or x_{f2}, existed in the upper or lower layer. See diagram above. There are two sections existing in the core.

(9)   The crossflow rate was calculated in each section at a certain time step t, in the same manner as in step (2).

(10)   During the time Δt, the lengths of zone [1][1], zone [1][2], zone [2][1] and zone [2][2] changed due to the flow of the injected and crossflow fluids. These lengths at time t+1 were calculated by using assumptions (3). The frontal location of x_{f1} or x_{f2} at time t+1 was also determined as shown in Appendix C. Each front, x_{f1} or x_{f2} was dependent on L (core length).

(11)   At the time t+1, the location of each zone was updated in the same manner as in step (5).

The steps from (10) to (11) are written in the subprogram front_calc2.

(12)   The oil cut of the production fluids at the upper layer was a function of the water saturation of zone [1][2]. The oil cut of the production fluids at the lower layer was a function of the water saturation of zone [2][2]. The production performance was calculated in the same manner as in step (6).

(13)   The steps from (9) to (12) were repeated until both fronts, x_{f1} and x_{f2}, reached breakthrough.

(14)   After breakthrough of both fronts, only one section existed in the core as shown in Appendix C. In this case, the crossflow rate was calculated at a certain time step t in the same manner as in steps (2) and (9).

(15)   The water saturation and polymer/emulsion concentration in each layer were calculated by material balance.

This step is written in the subprogram front_calc1.

(16)   The oil cut of the produced fluids at each layer was a function of the water saturation of each layer. The production performance was calculated in the same manner as in step (6).

(17)   Steps (14) to (16) were repeated until the end of the flood.

Chapter 8

DISCUSSION OF RESULTS

8.1 Introduction

In this study, two main objectives were pursued: to develop and investigate the effect of crossflow, and to examine strategies using polymer as a mobility control agent and emulsion as a blocking agent to enhance the recovery of light and moderately viscous oil reservoirs with a water-leg. To achieve this, thirty-two (32) displacement tests were conducted with water, mobility control and/or blocking agents.

First, the various aspects of the modified crossflow are discussed and validated using some of the experimental data and data from previous studies. Second, the different injection strategies using polymer and emulsion as mobility control and/or blocking agents are discussed.

8.2 Crossflow

Three experiments were conducted to test the crossflow equations. To establish that the crossflow equations were accurate, data from previous studies were used. The sections that follow discuss the various aspects of the crossflow equation.

8.2.1 The Effect of Injection Strategy on Crossflow

Runs 7, 8, 9, 10 and 11 were designed to study the effect of injection strategy on oil recovery. The injection intervals were located in both the oil and water zones. The volumetric flow rate in the oil and bottom-water zones were proportional to the cross-sectional areas of the respective zones to simulate a vertical-front displacement. The flow rate used in these runs was 400 ml/hr. The objective for the runs was to block the water zone while waterflooding the oil zone. Figure 8.1 shows that the waterflood performances exhibit similar trends, especially the cumulative oil recovery curves. Considering the curves for Runs 7, 8, 9 and 10, they all intersect each other after 0.4 HCPV of fluid had been produced. Afer that the cumulative oil recovery for Run 8 was higher than all the other runs up to 1.05 HC2 hen the injection fluid into the bottom-water zone was changed from polymer to emulsion in Run 10, the oil recovery difference between Runs 10 and 7 at 1.5 HCPV was 9% IOIP.In Runs 7, 8 and 9 the fluid injected into the water zone was water. The only difference among them was the mode of injection. At 1.0 HCPV, 15% oil recovery was obtained in Run 8 more than in Runs 7 and 13% oil recovery more than in Run 9. After 1.0 HCPV of fluid had been produced, there was more oil recovery in Runs 10 and 11 than the
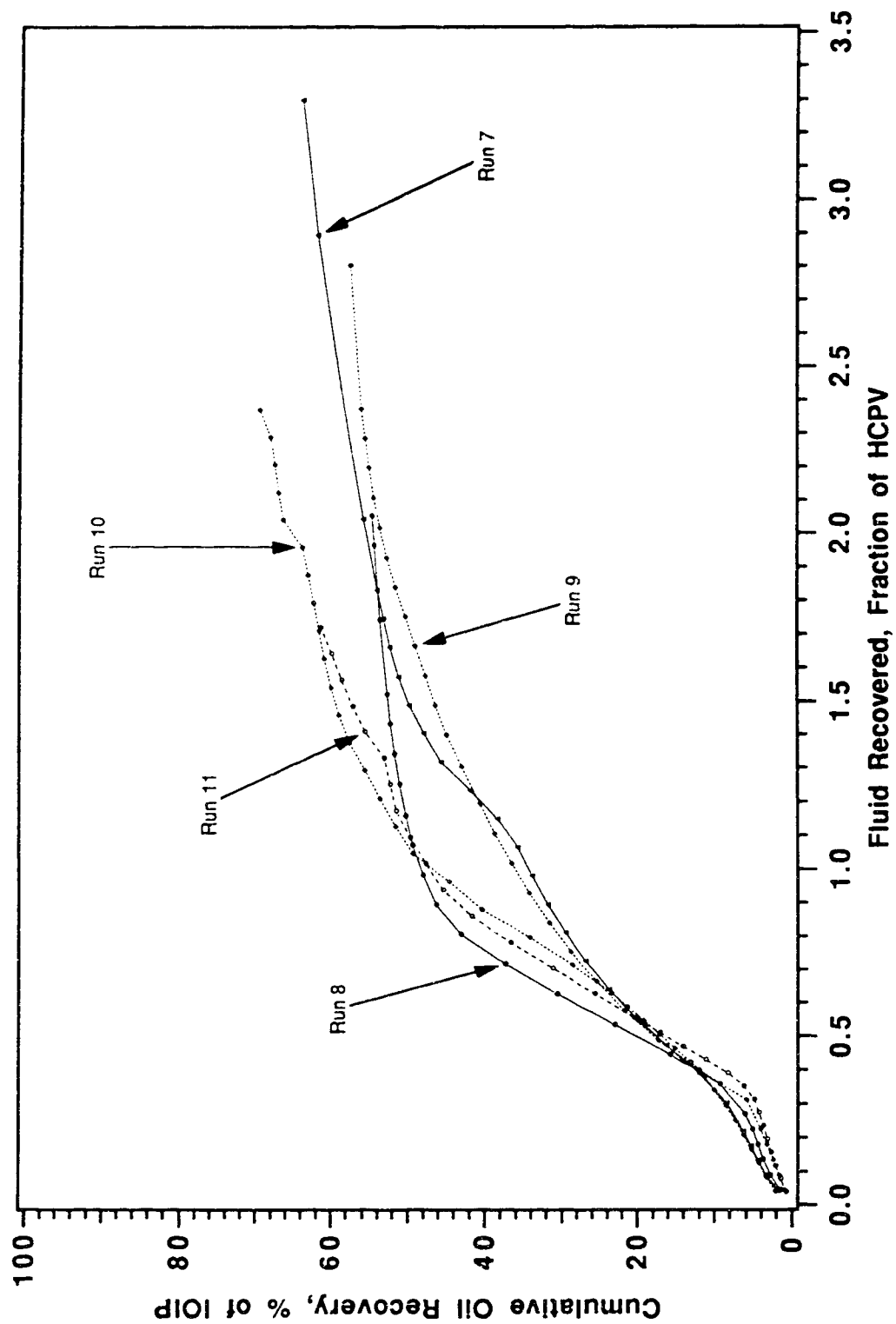
Fig. 8.1: Effect of Injection Strategy on Oil Recovery.

other three runs. This is attributed to the injection strategy adopted. Root and Skiba[16] pointed out that oil recovery could not be improved by blocking access to a highly permeable zone in the injection well. These five runs do not support this premise, because an improvement in oil recovery from 61.8% IOIP in Run 11 to 69.5% IOIP in Run 10 was observed.

Data from three of the five experiments discussed above were simulated using the semi-analytical model developed in this study. Figure 8.2 depicts graphically the simulated results. The cumulative oil recovery trends were similar to the experimental data; however, it was observed that Runs 7a and 11a showed earlier recovery as compared to what was observed experimentally. One of the probable causes for this depature from the experimental result is the fact that the polymer solution in the semi-analytical model was considered to be a Newtonian fluid. Another reason for the deviation can be attributed to the lack of understanding of the blocking mechanism of emulsion in the semi-analytical model. The ultimate oil recovery values are very comparable, viz. 60.6% IOIP for Run 7a, as against 56.0% IOIP for Run 7; 61.1% IOIP for 10a as against 69.5% for Run 10 and 47.9% IOIP for Run 11a, as against 61.8% IOIP for Run 11.

8.2.2   The Possible Directions of Crossflow

On the basis of the crossflow equations derived, four possible directions of crossflow have been identified. Detailed explanations and illustrations have been given in section 6.2. In this section, simulated results using experimental data will be used to shed further light on the crossflow directions and an attempt will be made to show how the direction of crossflow improves or lowers oil recovery as pointed out by Lambeth and Dawe[12].

The crossflow occurring in the middle section, q_{c2}, controls the formation of the oil bank as well as the direction of flow. Figure 8.3a shows pore volumes of fluid injected as a function of the flood-front position. In Run 7 water was injected into the oil zone and polymer was injected into the water zone. The flood-front in the oil zone x_{f1} was initially ahead of the flood-front in the water zone, x_{f2}. After the fronts had traversed about 10% of the model length, x_{f1} overtook x_{f2}. The crossflow as a function of flood-front position is depicted in Figure 8.3b. The positive slope of the crossflow indicated that, the crossflow was from the oil zone to the water zone. After the flood-front has moved about 10% of the model length, the direction of the crossflow in Zone c reversed direction. Just at the beginning of the flood, crossflow was assumed to be as shown below:
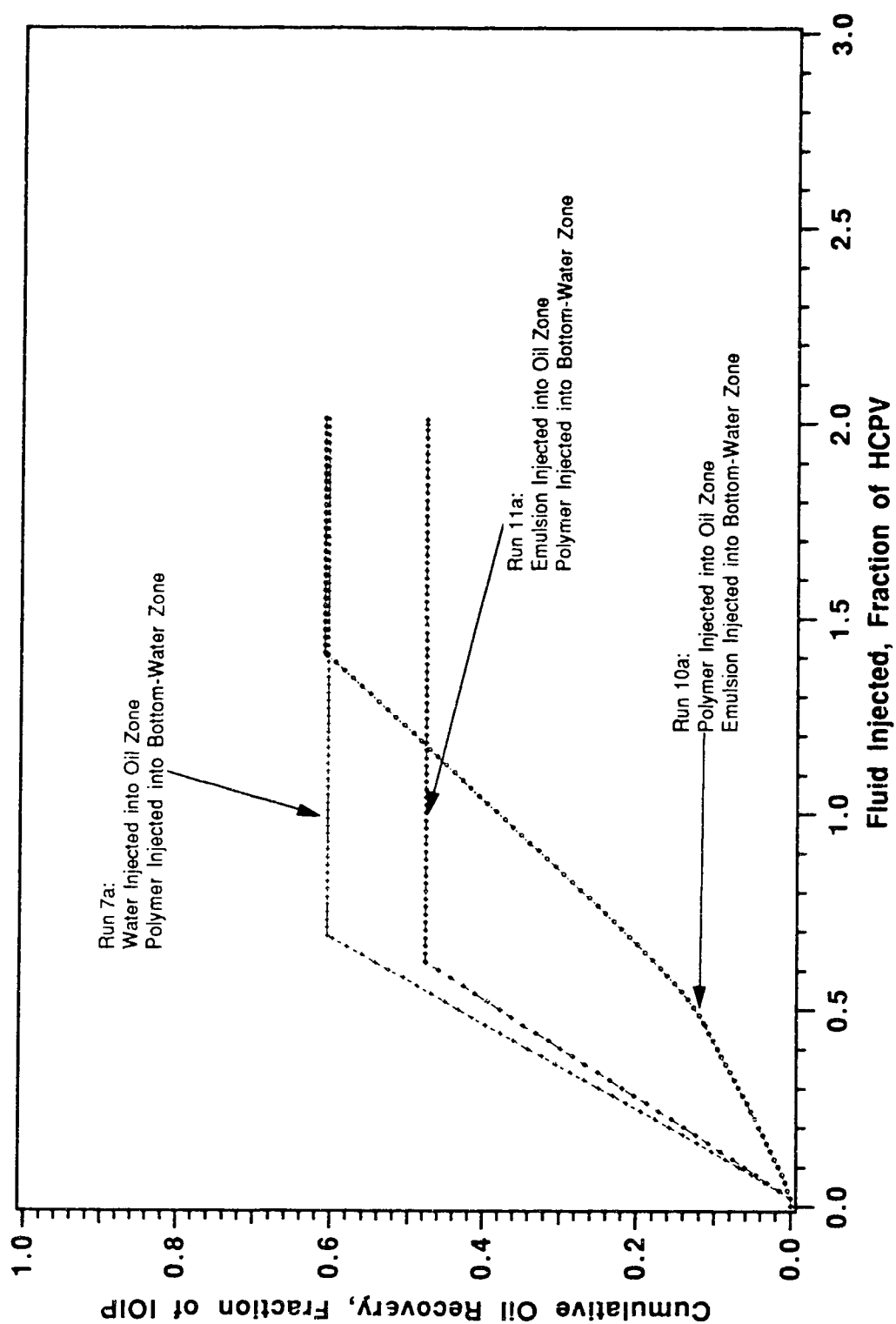
Fig. 8.2: Effect of Injection Strategy on Oil Recovery.
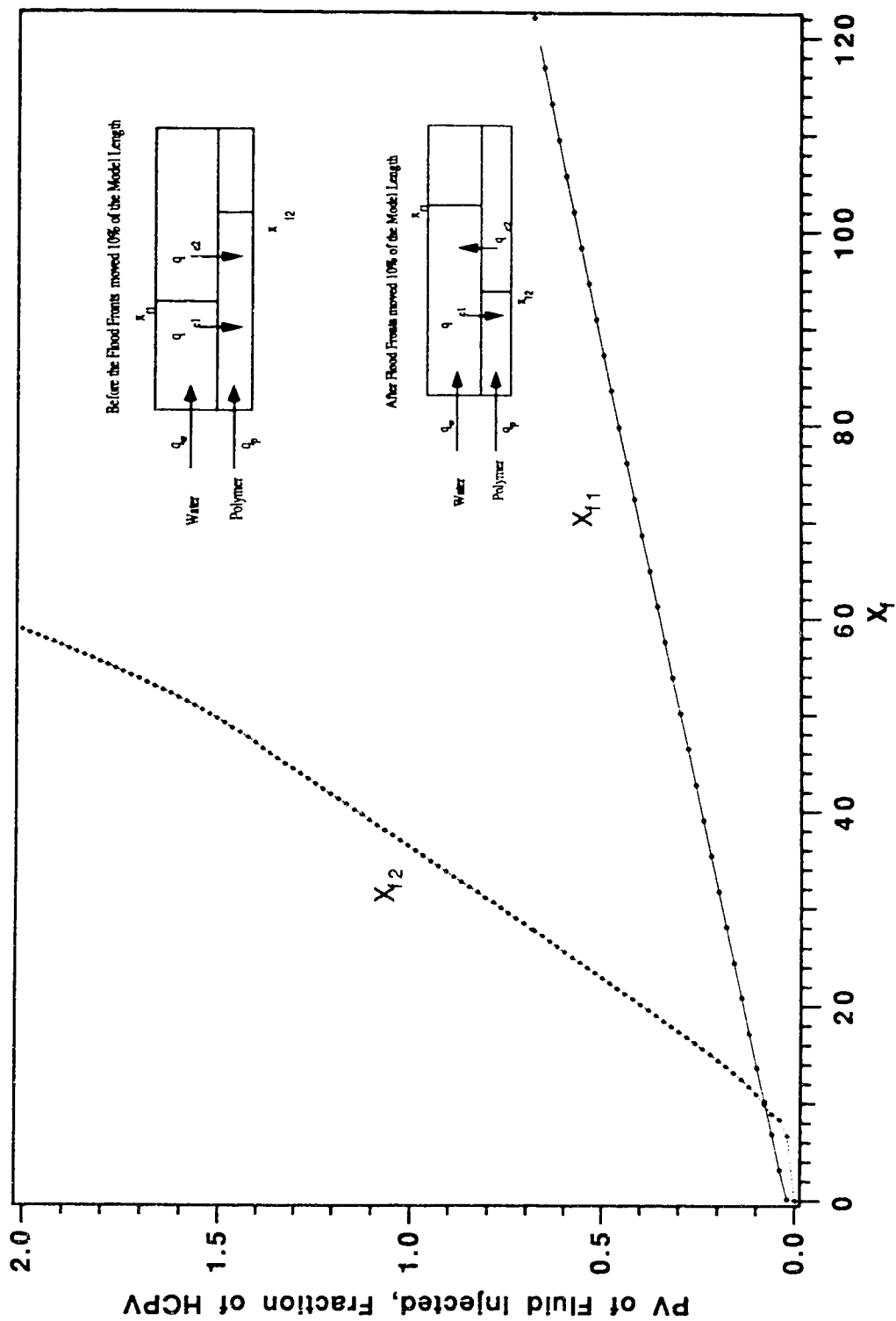
Fig. 8.3a: Pore Volumes of Fluid Injected as a Function of Flood Front Position when Water is Injected into the Oil Zone and Polymer is Injected into the Water Zone.
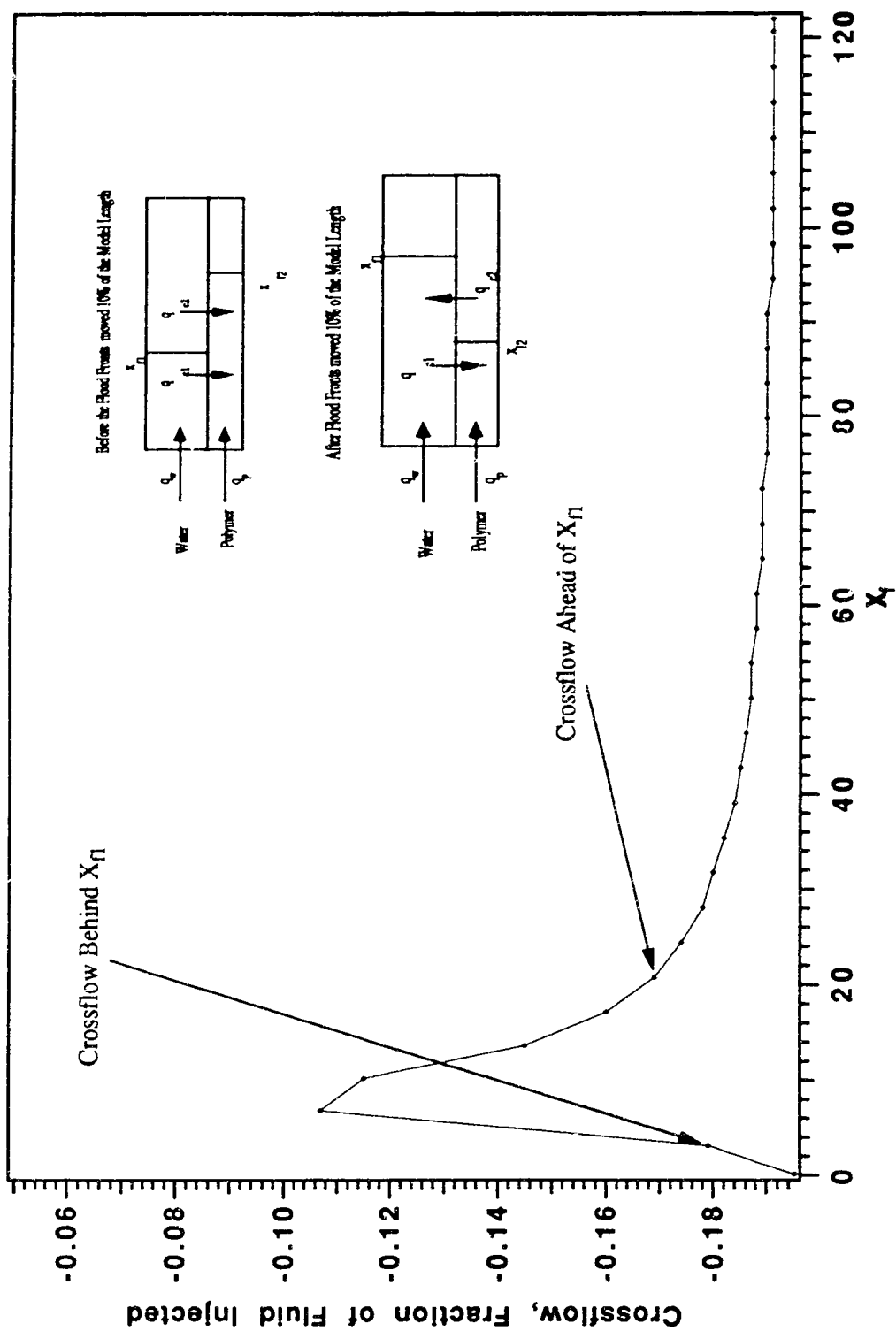
Fig. 8.3b: Crossflow as a Function of Flood Front Position when Water is Injected into the Oil Zone and Polymer is Injected into the Water Zone.
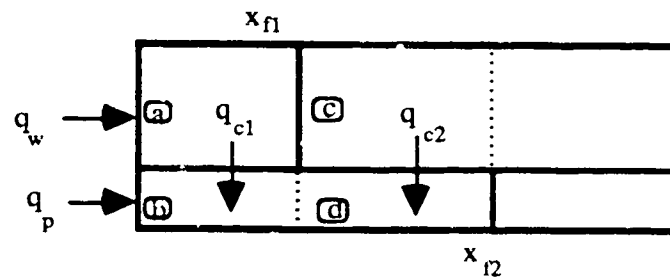
After the flood-front moved about 10% of the model length, crossflow reversed direction due to the injection of polymer into the water zone. The water zone thus became a high resistance region, and the velocity of the flood-front was reduced considerably. The velocity of the flood-front in the oil zone, however, increased due to the crossflow into the oil zone.

The diagram below illustrates this:
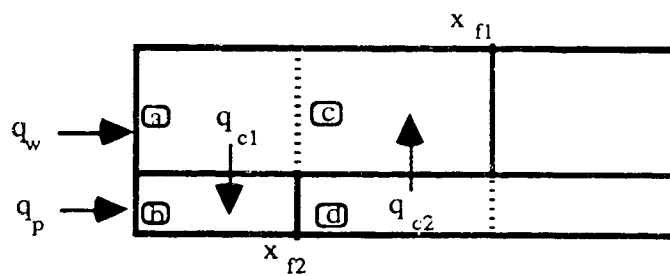
This explains why the earlier part of the cumulative oil recovery in Run 7a (Fig. 8.2) is higher than in Runs 10b and 11c. When polymer was injected into the oil zone and emulsion was injected into the water zone, the flood fronts maintained their positions (that is, x_{f2} was ahead of x_{f1}) until the end of the run. Figure 8.3c shows the positions graphically. Figures 8.3d and e show the crossflow as functions of the flood-front positions using Equations (4.17), (4.20) and (4.23). In Figure 8.3d the crossflow declined to about 25% after the injection fluid was changed from polymer to water in the oil zone. The change, however, was not sensed by flood-front x_{f2}; hence, Figure 8.3e demonstrated no change in the crossflow pattern. It is worthwhile to note that depending on the fluids being used as injection fluids and the strategy being adopted crossflow could increase or decrease oil recovery.

8.2.3   Previous Studies of Reservoirs with Bottom-Water

In this section the semi-analytical method developed in this research was used to evaluate some of the experimental data of Yeung[55], Islam[42] and Hodaie and Bagci[44].

Yeung's data for Run 16[55] was used for the simulation. The run was a bottom-water run. The oil zone was three times thicker than the bottom-water zone. The permeabilities in the oil and the water zone were the same. The process of displacement was a dynamic-displacement procedure, DBP[55]. The two fluids, water and emulsion, were injected into the oil zone and the bottom-water zone simultaneously. The total rate Q of fluid injection was 400 ml/hr. The injection rate into the oil zone was 300 ml/hr and that into the bottom-water zone was 100 ml/hr. After 1 PV_{bw} of emulsion was injected into the bottom-water zone, the emulsion injection was discontinued, and 400 ml/hr of water was injected into the oil zone. The input parameters for the simulation were: width of the model, w = 5.08 cm; depth of the model: oil zone thickness, ho = 5.7150 cm, bottom-water zone thickness, h_{bw} = 1.9050 cm; length of the model, L = 122.0 cm; absolute permeability, k_o = 18.9 μm^2; porosity, ϕ = 0.357; oil viscosity, μ_0 = 63.0 mPa.s; water viscosity, μ_w = 1.0 mP.s; rate: injection rate into the oil zone, q = 300 ml/hr, injection rate into the bottom-water zone, q = 100 ml/hr; irreducible water saturation, S_{iw} = 0.06, residual oil saturation, Sor = 0.4 and surfactant concentration in emulsion was 0.016% (volume). The simulated result is shown in Figure 8.4.

Islam's data for Run 5[42] was used for the simulation. The run was a bottom-water run with the oil zone five times thicker than the bottom-water zone. The permeabilities in the oil and the water zone were the same. The displacement started with a waterflood at a rate of 400 ml/hr in the oil zone. After 1 PV_{bw} of water had been injected, the fluid was changed to a 500 ppm polymer solution of which a slug size of 0.15 PV_{bw} was injected into the oil zone
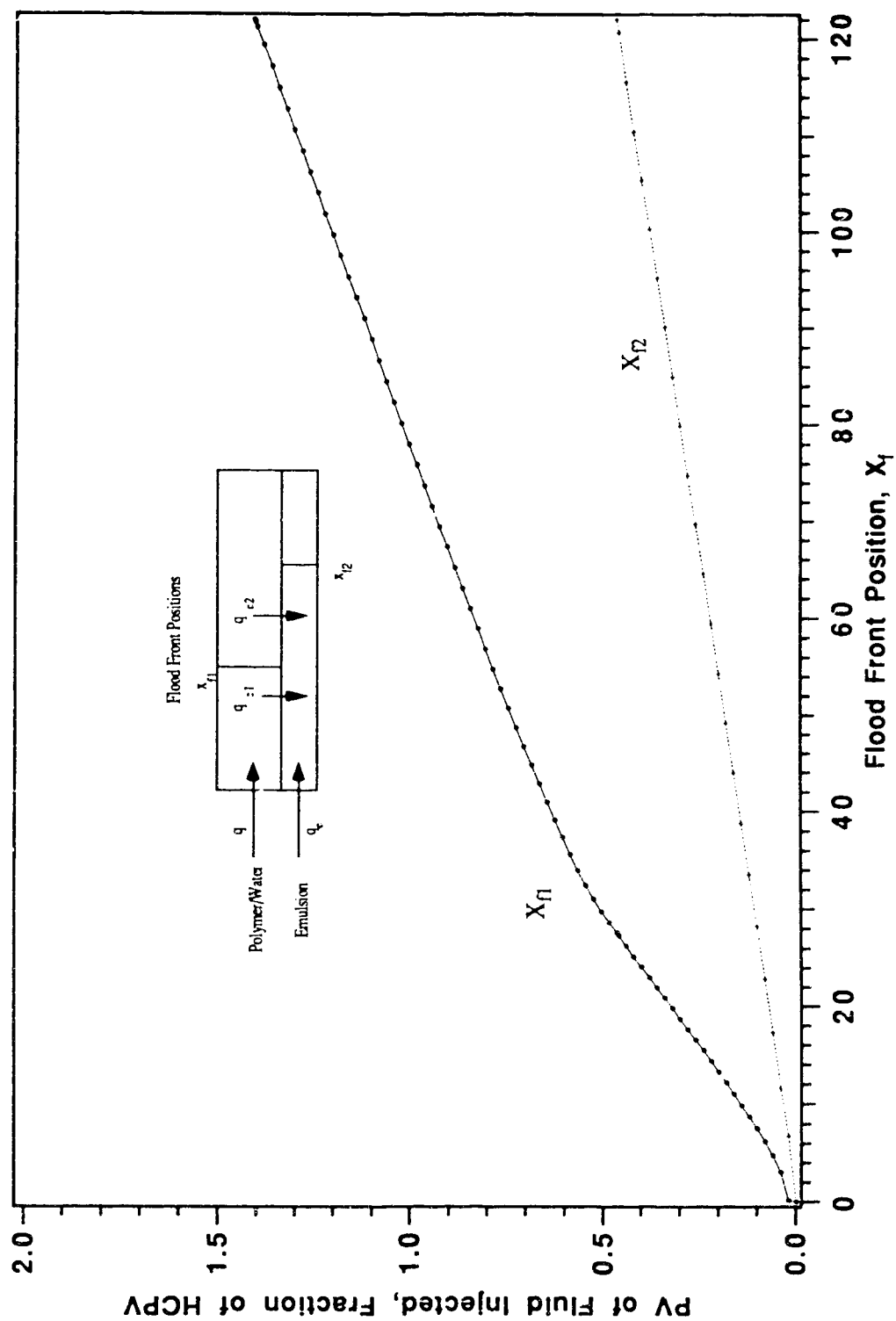
Fig. 8.3c: Pore Volume of Fluid Injected as a Function of Flood Front Position when Polymer is Injected into the Oil Zone and Emulsion is Injected into the Water Zone.
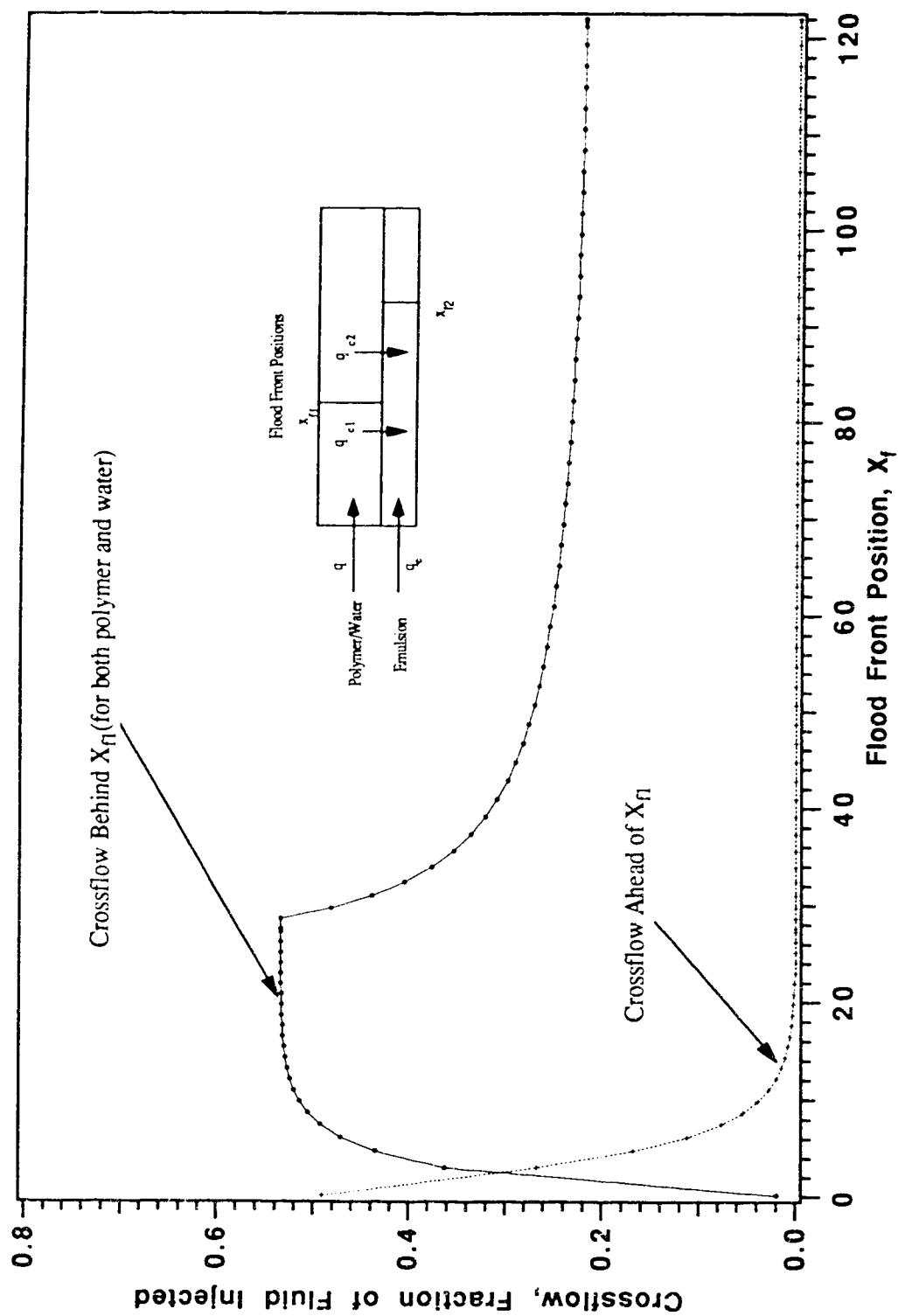
Fig. 8.3d: Crossflow as a Function of Flood Front Position when Polymer is Injected into the Oil Zone and Emulsion is Injected into the Water Zone.
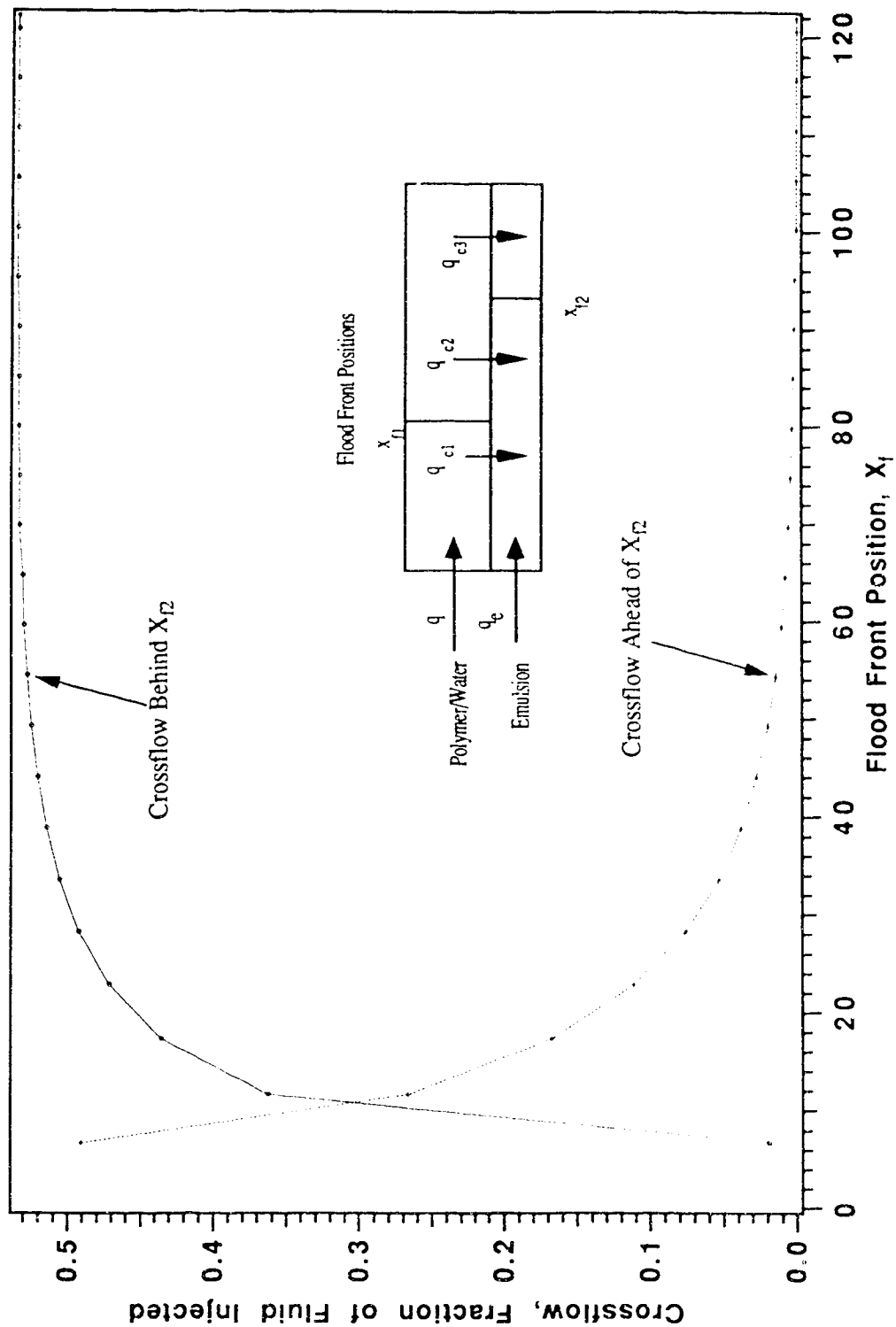
Fig. 8.3e: Crossflow as a Function of Flood Front Position when Polymer is Injected into the Oil Zone and Emulsion is Injected into the Water Zone.
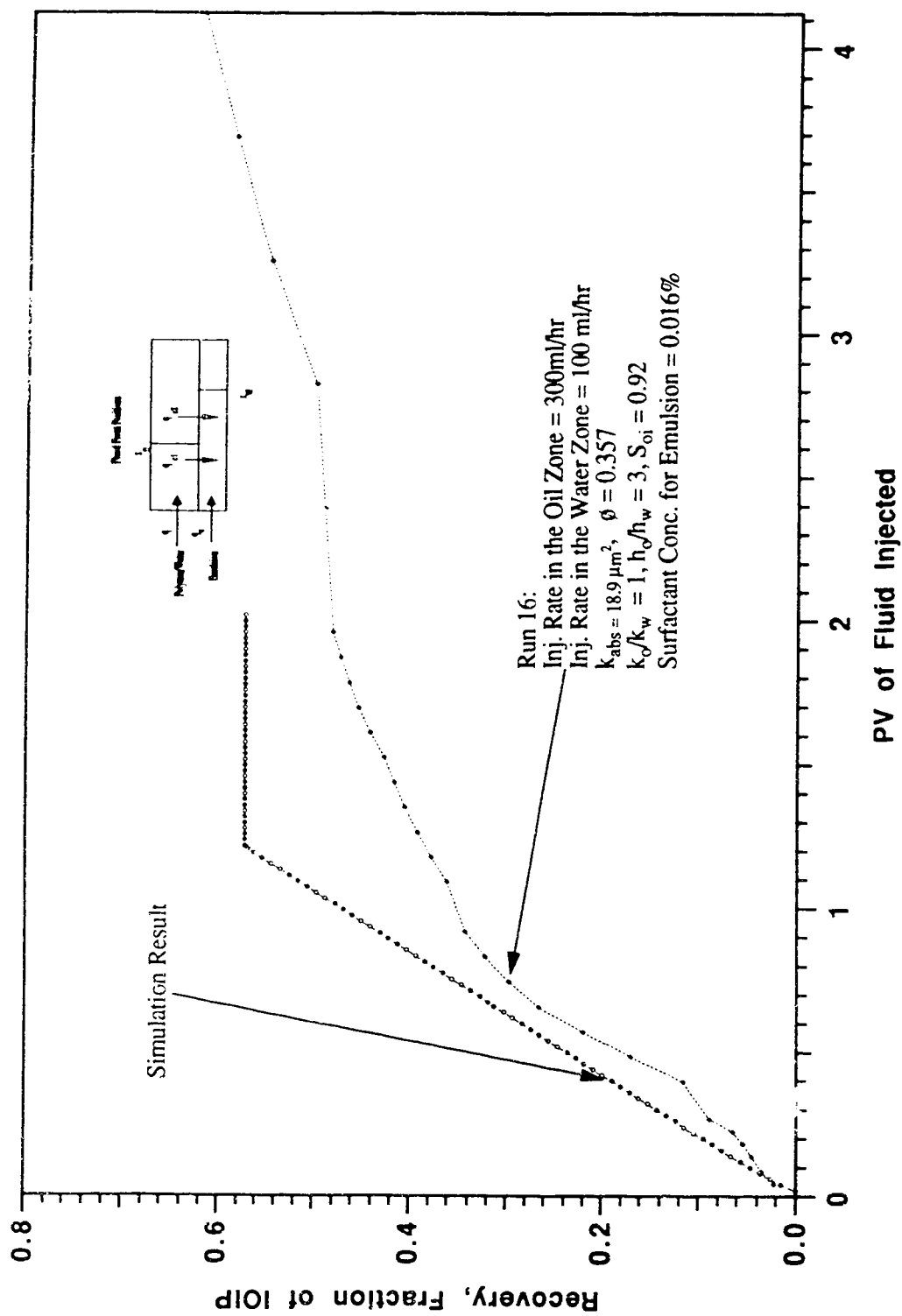
Fig. 8.4 : Simulated Results Compared with Experimental Results of Cumulative Oil
Recovery versus Fluid Injected from Yeung[55].

and this was followed again with a waterflood. The input parameters for the simulation were: width of the model, w = 5.08 cm; depth of the model: oil zone thickness, h_o = 6.35 cm, bottom-water zone thickness, h_{bw} = 1.27 cm; length of the model, L = 122 cm; absolute permeability, k_o = 15.8 μm^2; porosity, ϕ = 0.360; oil viscosity, μ_o = 50.0 mPa.s; water viscosity, μ_w = 1.0 mP.s; rate, q = 400 ml/hr; irreducible water saturation, S_{iw} = 0.06, residual oil saturation, Sor = 0.4 and polymer concentration was 500 ppm. The simulated result is shown in Figure 8.5.

Hodaie and Bagci's data for Run DPF11[44] was used for the simulation. The run was a bottom-water run with the oil zone three times thicker than the bottom-water zone. The permeabilities in the oil and the water zone were the same. Polymer solution was injected at a rate of 400 ml/hr into the oil zone. After 0.6 PV_{bw} of polymer was injected, the fluid was changed water. The input parameters for the simulation were: width of the model, w = 5.0 cm; depth of the model: oil zone thickness, ho = 8.0 cm, bottom-water zone thickness, h_{bw} = 2.0 cm; length of the model, L = 75 cm; absolute permeability, k_o = 12.0 μm^2; porosity, ϕ =0.37 oil viscosity, μ_o = 14.5 mPa.s; water viscosity, μ_w = 1.0 mP.s; rate, q = 400 ml/hr; irreducible water saturation, S_{iw} = 0.20, residual oil saturation, Sor = 0.4 and the polymer was 0.5% by weight concentration. The simulated result is shown in Figure 8.6.

The trend of the simulated results is similar to the trend of the experimental results and the ultimate recovery matches quite well. The semi-analytical model predicts oil recovery for bottom-water models with a maximum error of about 8%.

8.3 Base Runs

The Base Runs refer to waterfloods in homogeneous and bottom-water models using one injection fluid at a time and injecting into the oil zone only.

8.3.1 Homogeneous Pack

Runs 1, 2, and 3 were conducted in a single-layer sand pack. The volumetric injection rate was taken from previous work done by Islam[42] and Yeung[55]. The effective permeability to water, k_{wor}, at residual oil saturation was computed using Run 1. Figure 8.7 illustrates graphically the cumulative recovery of the various runs for a homogeneous pack. The porosities and absolute permeabilities of the sand packs in the three experiments were 37.6%, 37.0% and 36.9% and 17 μm^2, 18 μm^2 and 17.6 μm^2, respectively. Water breakthrough occurred faster in the waterflood experiment as compared to the polymer and emulsion floods, viz. breakthrough occurred after 0.3069 HCPV of fluid had been produced. The water-oil-ratio (WOR), however, increased more rapidly during the polymer flood than in the
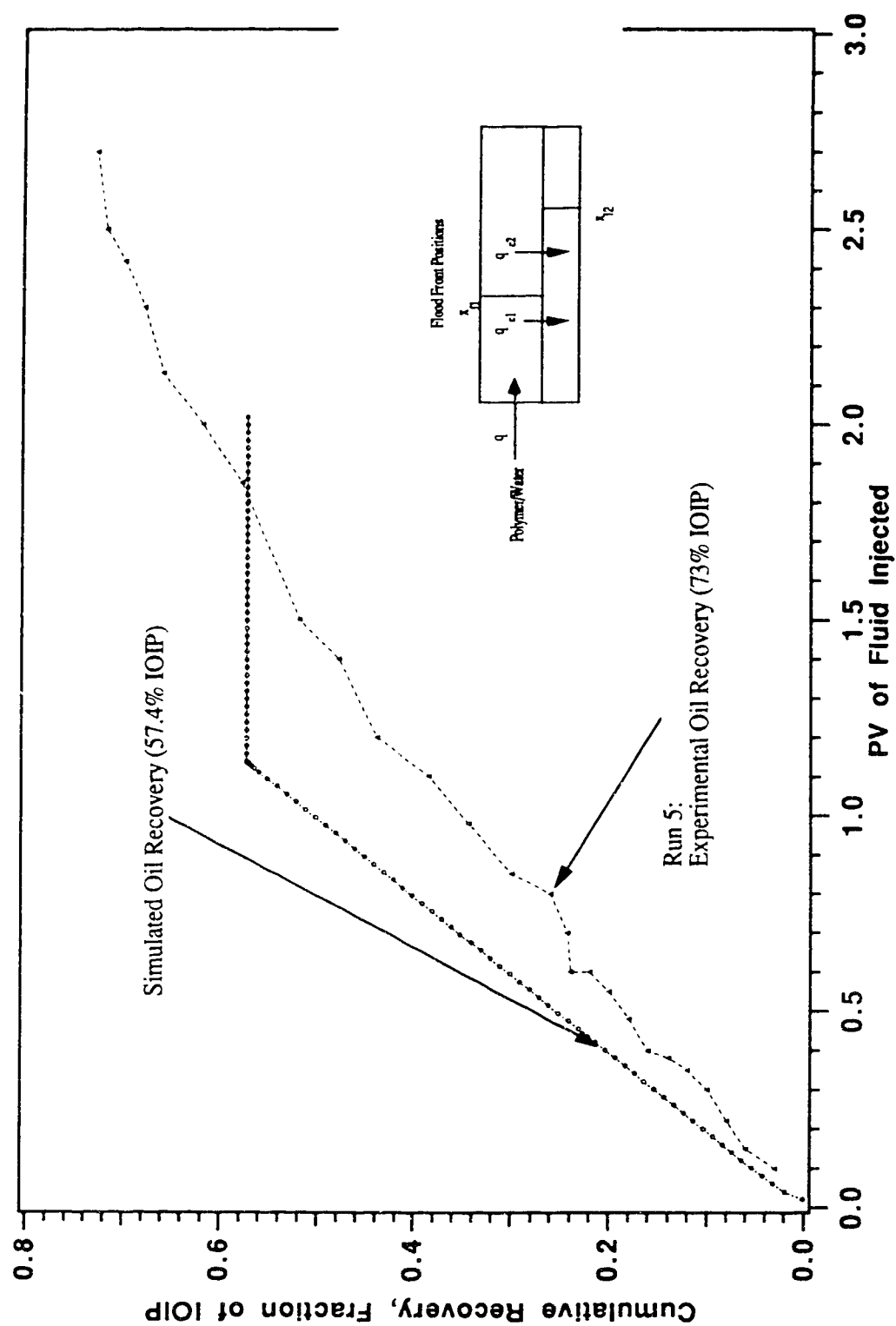
Fig. 8.5 : Simulated Results Compared with Experimental Results of Cumulative Oil Recovery versus Fluid Injected from Islam[42].
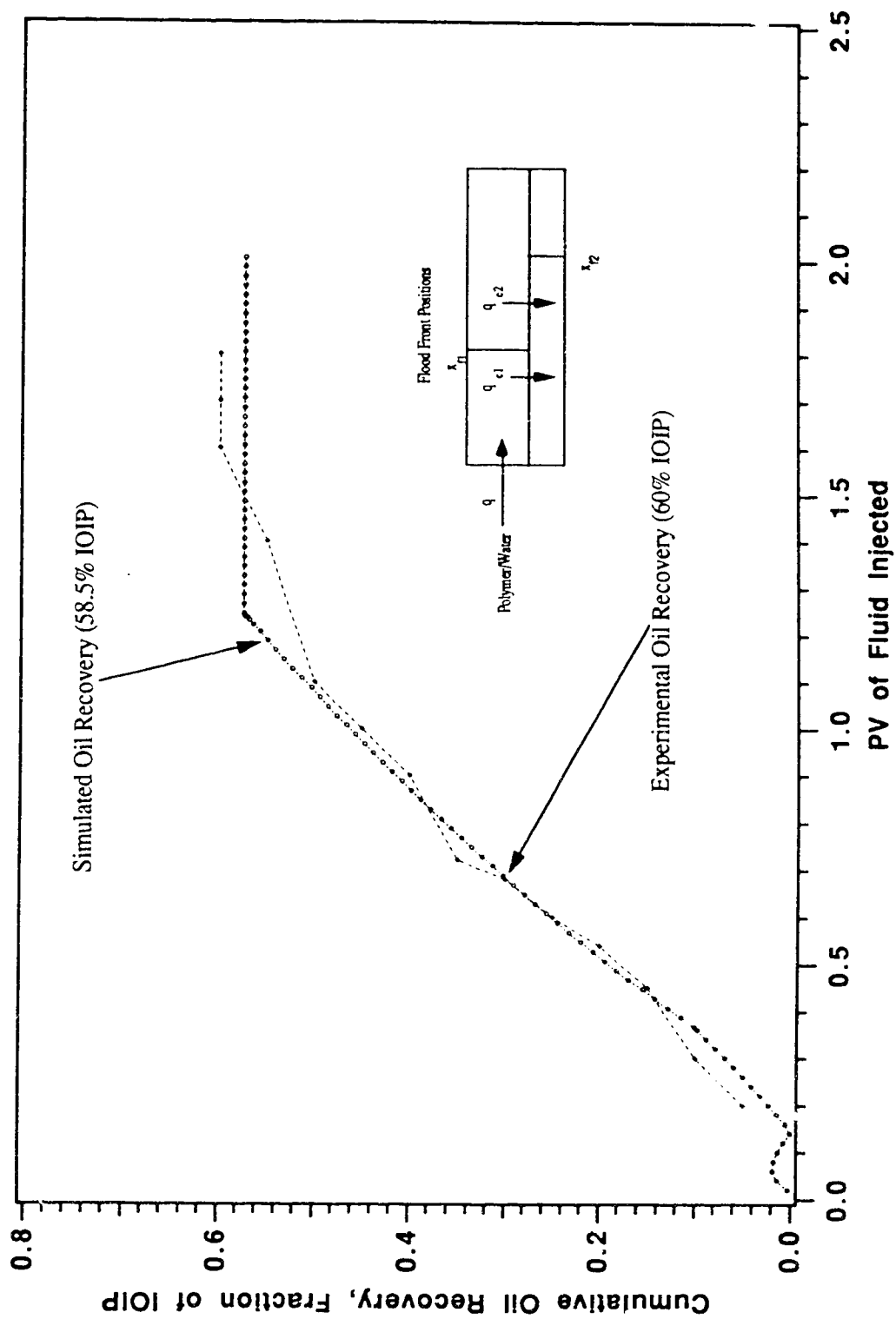
Fig. 8.6: Simulated Results Compared with Experimental Results of Cumualtive Oil Recovery versus Fluid Injected from Hodaie and Bagci[44].
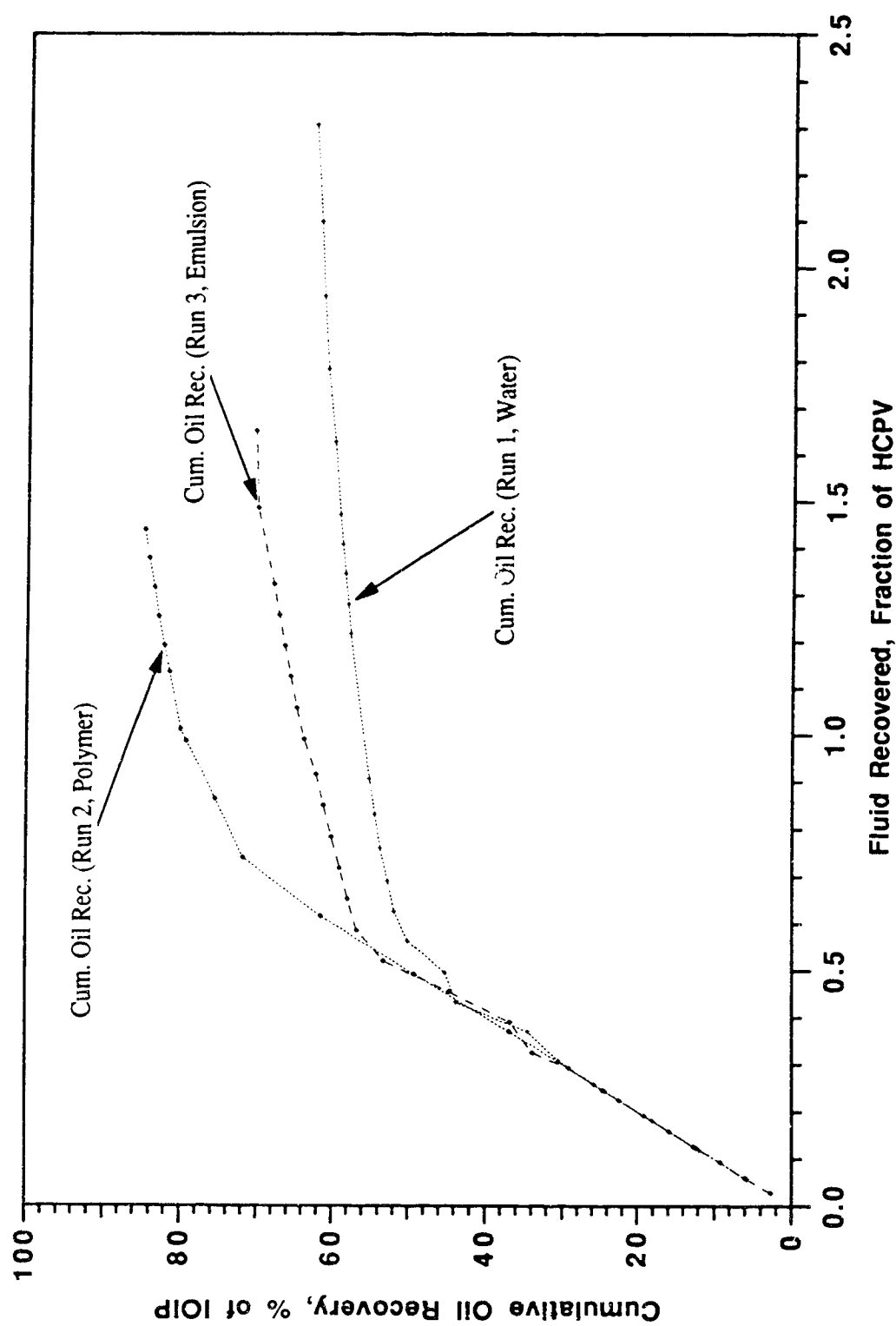
Fig. 8.7: Comparison of Homogeneous Runs.

other two. The cumulative recovery for the waterflood was the lowest among the three experiments (viz. 62.7% of IOIP), after 2.308 HCPV of fluid had been produced. The cumulative recoveries for polymer and emulsion floods were 85.0% and 70.5%, respectively.

8.3.2 Bottom-Water Pack

Three experiments were conducted by injecting water, polymer and emulsion into a model with bottom-water. In each of the experiments, the oil-to-water zone thickness was 3 to 1 (that is, $h_o/h_w = 3$). The permeabilities in the oil and bottom-water zones were equal, thus, $k_o/k_w = 1$. The injection and production wells were situated 50% into the oil zone. In Run 4, water was the injection fluid. The water-oil-ratio (WOR) at the onset of the test was 0.96 and this increased to 5.38 after 0.288 HCPV of fluid had been produced. The oil cut decreased from 51% to 15.7% before increasing to a maximum of 52% and then dropping again. An examination of the pressure graph (Fig. 7.5) shows that the injected water channeled into the bottom-water layer right at the beginning of the experiment and that explains why the oil cut dropped. The cumulative recovery in this test was 57.0% of the IOIP. A comparison of Runs 4 and 5 shows that more water was produced at the beginning of the experiment in the latter than in the former (viz. 2.33 as against 0.96). In Run 5, the WOR increased to a maximum of 6.43 and declined to a minimum of 0.282 before increasing again. At the minimum water-oil-ratio of 0.282, the oil cut was 78%. The oil cut was higher in Run 5 than Run 4 (viz. 78% as against 52%). The cumulative oil recovery was also higher in Run 5 than Run 4 (viz. 55.3% as against 57.0%). Run 6 was an emulsion flood. The injection was in the oil zone. All parameters were the same as in Runs 4 and 5. The water breakthrough occurred after 0.0414 of HCPV had been produced. The WOR was the highest among the three bottom-water experiments (viz. 2.92). The oil cut began at 25.5% and dropped to 11.5%, which was the lowest , before increasing to 41.1%. The cumulative oil recovery was 35.5% after 2.27 HCPV of fluid had been produced. This indicates that for a bottom-water layer pack, polymer is a better displacing fluid, followed by water and then emulsion. Figure 8.8 shows the production history of the bottom-water layer pack, for the three cases.
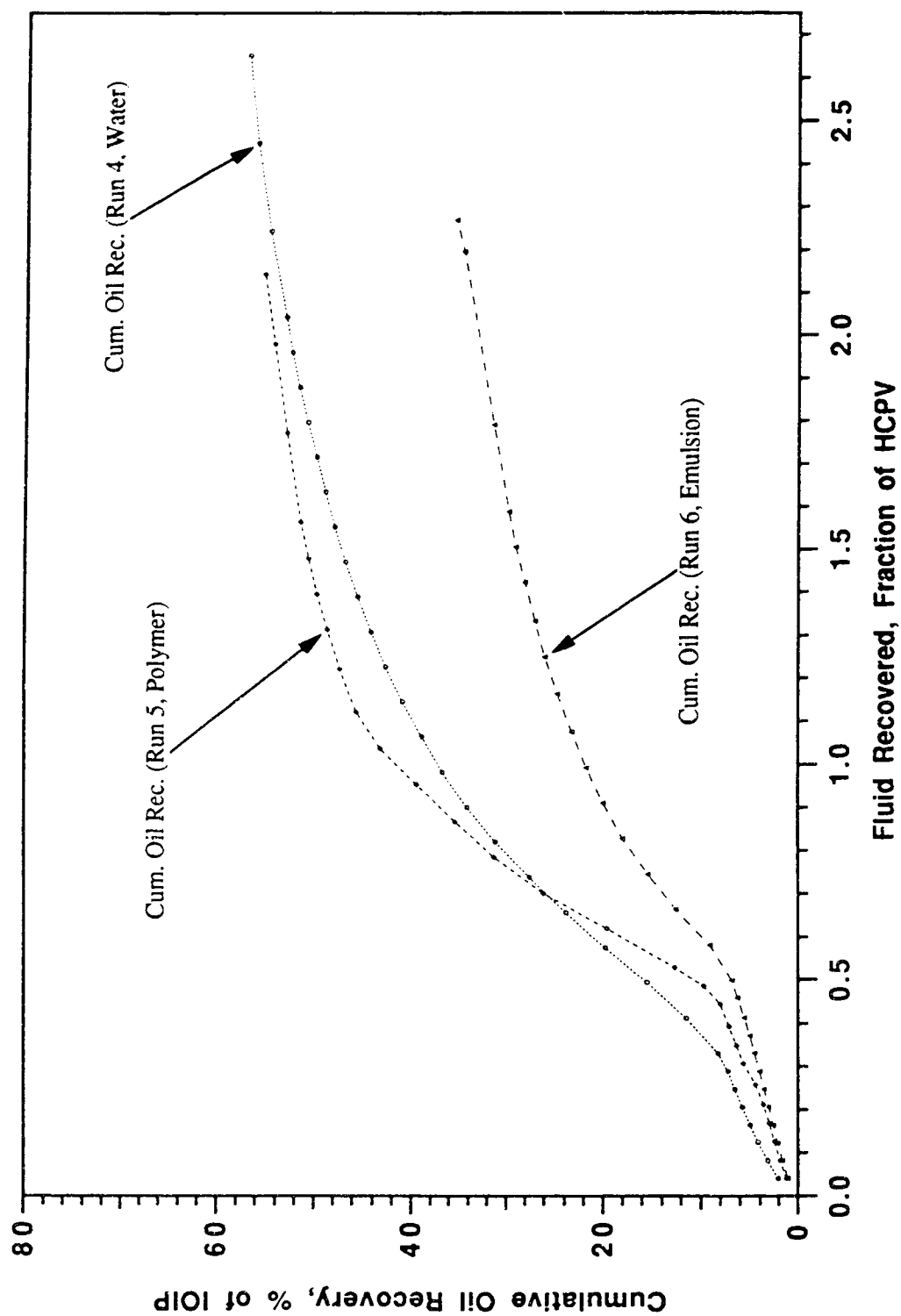
Fig. 8.8: Comparison of Cumulative Oil Recovery for Different Fluids Injected.

8.4. Polymer/Emulsion Flooding Under Bottom-Water Conditions

As mentioned earlier, different strategies were adopted to investigate recovery according to the sub-topics listed below. In the experiments that will be discussed, polymer was injected in the oil zone followed by water, and emulsion was injected in the bottom-water zone.

8.4.1 Effect of Surfactant Concentration on Recovery

The effect of surfactant concentration was investigated in Runs 10 and 12. In these runs, the polymer concentration was 500 ppm. The oil-in-water emulsion was 10% by volume. The permeabilities in the oil and water zones were equal; thus, $k_o/k_w = 1$. The oil-zone thickness was 3 times that of the bottom-water layer (that is, $h_o/h_w = 3$). The pressure increased gradually in Run 10 compared to the rapid increase in Run 12. The pressure climbed to 53.6 kPa (Fig. 7.13) before declining. This came about as a result of the increase in the surfactant concentration from 0.016% by volume in Run 10 to 0.04% by volume in Run 12. The increased pressure however, did not result in increased oil cut nor cumulative oil recovery. In fact it decreased the oil cut from 75.0% (maximum peak) in Run 10 to 66% in Run 12. The water breakthrough occurred earlier in Run 12 than in Run 10 (viz. after 0.042 HCPV of fluid has been produced as compared to 0.392 HCPV). Figure 8.9 illustrates these comparisons.

8.4.2 Effect of Polymer Concentration on Recovery

The effect of polymer concentration was examined in Runs 15 and 19. In these runs, the emulsion had a surfactant concentration of 0.016%. The oil-in-water emulsion was 10% by volume. The permeabilities in the oil and bottom-water zones were equal; thus, $k_o/k_w = 1$. The polymer concentration for Run 15 was 500 ppm and that for Run 19 was 700 ppm. The magnitude of the pressure profile in Run 19 (Fig. 7.20) after 1.4 HCPV of fluid had been produced was 1.8 times that of Run 15. This can be attributed to the increase of polymer concentration from 500 ppm by weight in Run 15 to 700 ppm by weight in Run 19. The increased pressure showed an increase in oil cut from 76% in Run 15 to 84% in Run 19. However, this was not reflected in the cumulative oil recovery. It actually decreased the oil recovery from 57.8% of IOIP in Run 15 to 52.3% of IOIP in Run 19. Figure 8.10 shows these comparisons.
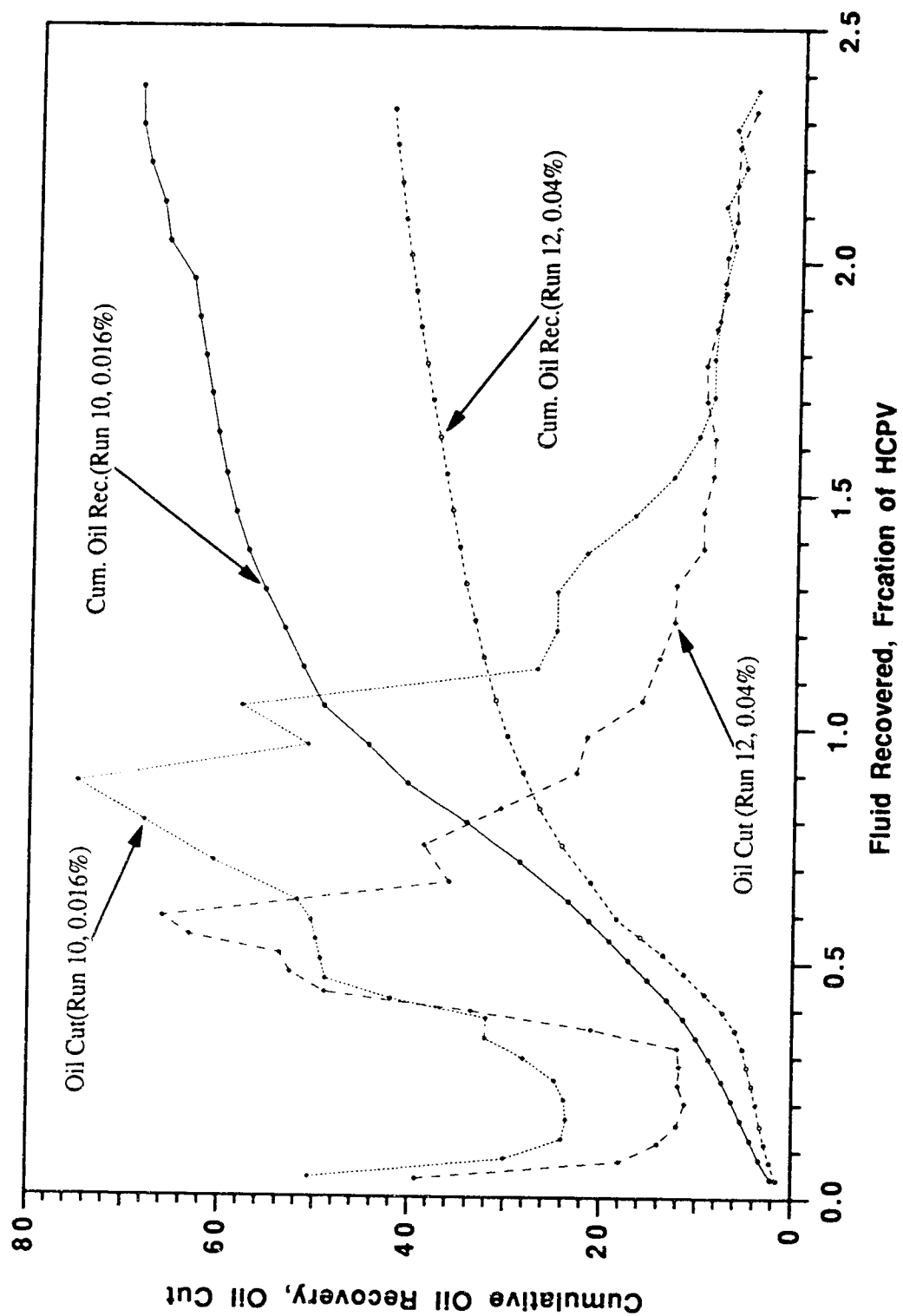
Fig. 8.9: Effect of Surfactant Concentration on Oil Recovery and Oil Cut.
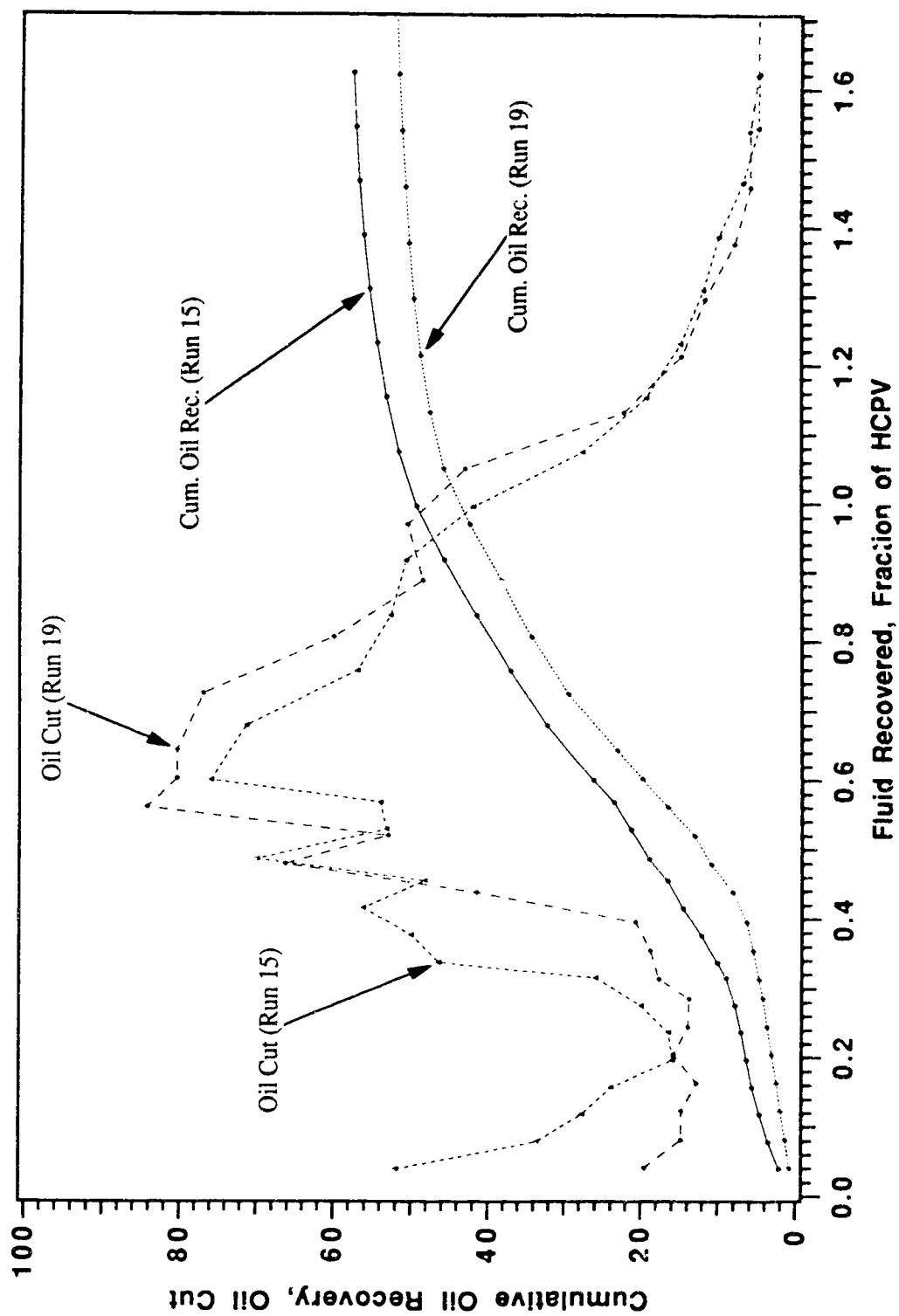
Fig. 8.10: Effect of Polymer Concentration on Oil Recovery and Oil Cut.

8.4.3 Effect of Slug Size on Recovery

Runs 10 and 13 were compared to examine the effect of slug size on recovery. The polymer concentration was 500 ppm and the emulsion had a surfactant concentration of 0.016%. The oil-in-water emulsion was 10% by volume. The permeabilities in the oil and bottom-water zones were equal; thus, $k_o/k_w = 1$. In Run 10, the emulsion and polymer slugs were equal, (that is, 1.0 PV_{bw}), while in Run 13 the slug sizes for emulsion and polymer were 0.75 PV_{bw}. The shape and magnitude of the pressure profile in Run 13 (Fig. 7.14) was very different from that of Run 10 (Fig. 7.11). The experimntal results of Runs 10 and 13 show that slug size has an effect on oil recovery. Figure 8.11 shows a comparison of the oil cut and cumulative oil recovery in Run 10 with that of Run 13. In Run 10, the oil cut starts at 50.5%, declines to a minimum of 24% and peaks at 75.0% before decreasing again. Unlike Run 10, the oil cut in Run 13 starts at low value of 24.1% and decreases further to 16.8% before increasing to a maximum of 63.7%. The blocking action of the 1.0 PVbw slug size in Run 10 is more pronounced. As a result a higher instantaneous oil production is observed. The cumulative oil recovery after 1.8 HCPV of fluid had been produced was 62.5% of the IOIP in Run 10 as compared to 51.8% of the IOIP in Run 13.

8.4.4 Effect of Layer Thickness on Recovery

The effect of oil-water zone thickness was investigated in Runs 10 and 14. In these experiments, the polymer concentration was 500 ppm and the emulsion had a surfactant concentration of 0.016%. The oil-in-water emulsion was 10% by volume. The permeabilities in the oil and bottom-water zones were equal, thus, $k_o/k_w = 1$. In Figure 8.12 a comparison is made of the recovery curves for Run 10 and Run 14. The oil-zone thickness was 3 times that of the bottom-water layer (that is, $h_o/h_w = 3$) in the former and in latter the oil-zone thickness was equal to the water zone(viz. $h_o/h_w = 1$). The effect of the oil-water zone thickness ratio is apparent in this figure. The WOR in Run 14 increased faster initially and then decreased after 1.07 HCPV of fluid had been produced. The oil bank formation in the bottom-water zone was delayed until 1.45 HCPV of fluid had been produced. At this point, the pressure started increasing rapidly (Fig. 7.15) which indicated that channeling of the displacing fluid was reduced appreciably; thus, the oil was being displaced from the oil zone. The ultimate oil recovery for Run 14 was 51.6% IOIP after 3.05 HCPV of fluid had been produced. The increase of the WOR in Run 10 was gradual and this declined after 0.46 HCPV of fluid had been produced. The oil bank formation took place after 0.5 HCPV of fluid had been produced. The ultimate oil recovery for Run 10 was 69.5% of IOIP. About 17.9% of the IOIP was not recovered due to the increase in the water zone thickness.
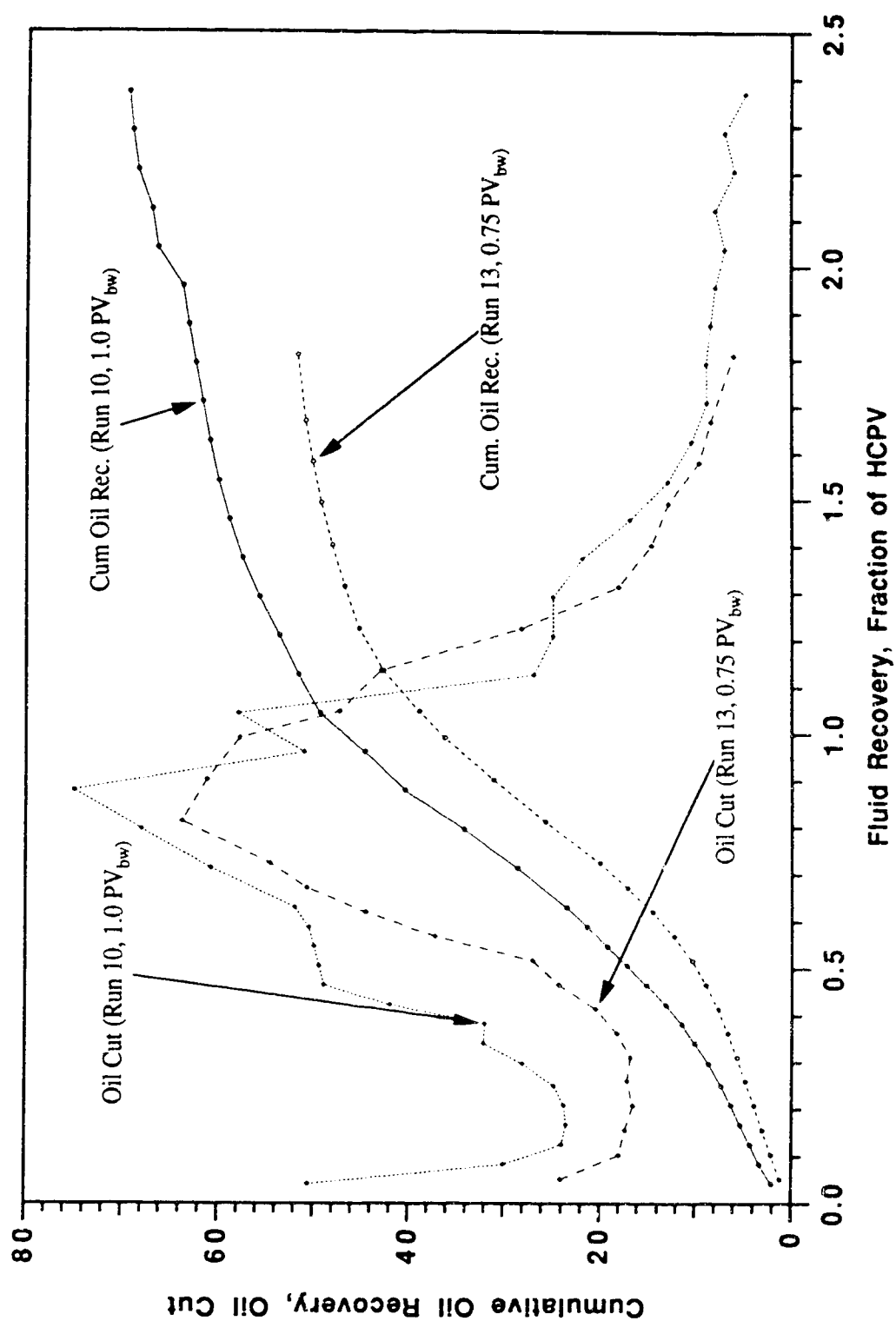
Fig. 3.11: Effect of Slug Size on Oil Recovery and Oil Cut.

118
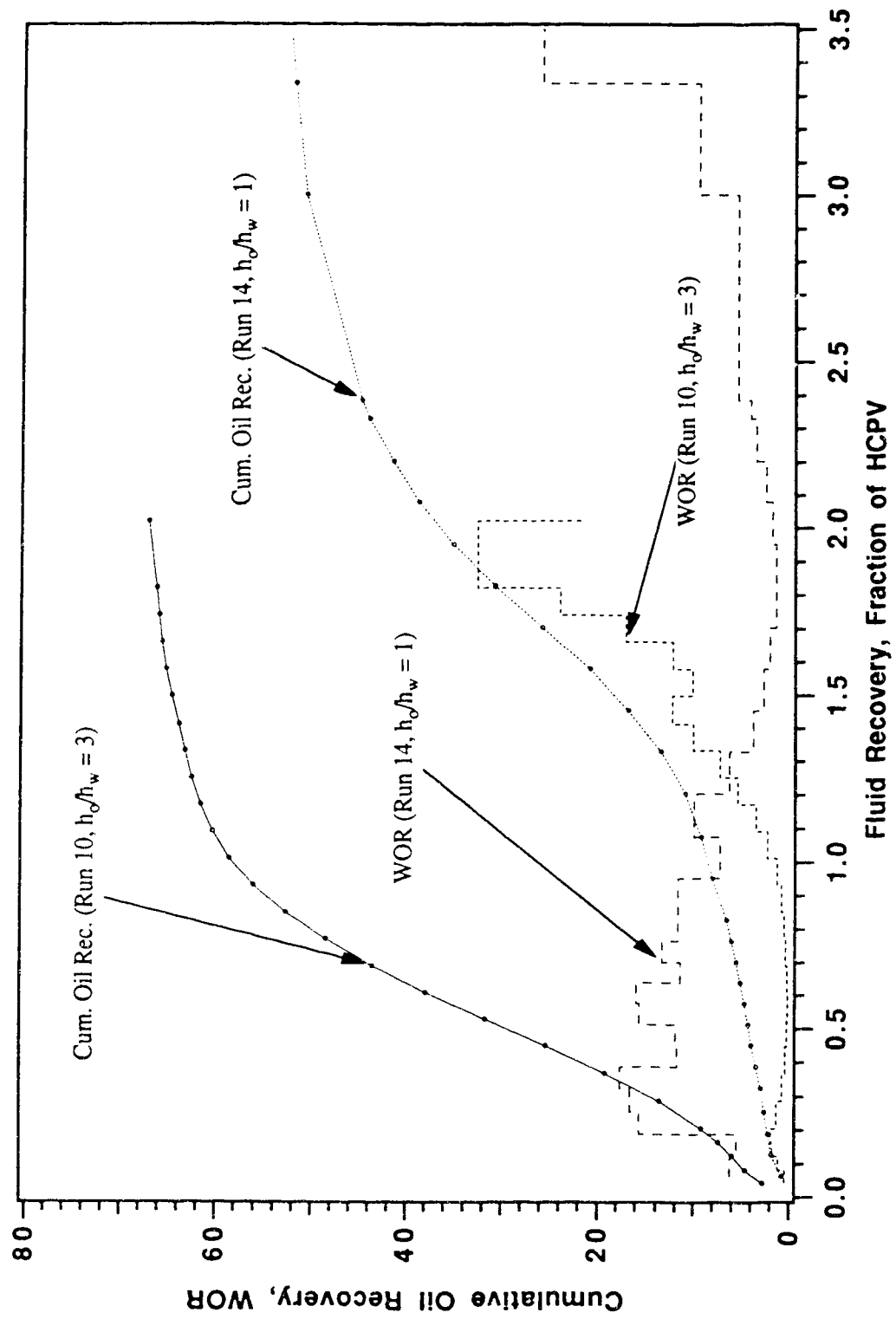
Fig. 8.12: Effect of Layer Thickness on Oil Recovery for Bottom-Water Reservoirs.

8.4.5 Effect of Rate on the Degree of Crossflow and Oil Recovery

Figure 8.13 shows the effect of injection rate on oil recovery. To investigate this effect, the injection rates in the oil and water zone were varied to see whether there was an optimum rate combination that would yield a higher oil recovery and minimize crossflow as well. For the seven experiments conducted, the rate ratio, $q_o/q_w = 3$, corresponding to an injection rate of 300 ml/hr of fluid into the oil zone, and an injection rate of 100ml/hr of fluid into the water zone, yielded the highest ultimate oil recovery. The experimental results indicated that as the rate-ratio became smaller, the ultimate oil recovery also became lower. It was also observed that as the rate-ratio increased the oil recovery attained a maximum value and declined. To confirm this finding, the experimental results were simulated using the semi-analytical model developed. The simulated results confirmed that as the rate-ratio decreased, the oil recovery decreased as well. The simulated results also showed the maximum oil recovery at $q_o/q_w = 3$. It, however, did not show that as the rate-ratio increased the oil recovery decreased; rather it showed that the oil recovery asymptotically approached a limiting case.

8.5 Horizontal Well Flooding under Bottom-Water Conditions

Horizontal injectors and producers were designed and six experiments were conducted to investigate their effect on oil recovery.

8.5.1 Horizontal Injector versus Vertical Injector

This experiment was conducted to investigate the effect of horizontal injectors on oil recovery, as well as comparing the results with the vertical injection experiments. The permeabilities in the oil and water zones were equal; thus, $k_o/k_w = 1$. The oil-zone thickness was 3 times that of the bottom-water layer (that is, $h_o/h_w = 3$). Figure 8.14 compares the recovery performance from a continuous waterflood using a horizontal injector and vertical producer, with the recovery performance from a continuous waterflood using a vertical injector and vertical producer. The oil cut stayed fairly constant at 11.0% in the case of the horizontal injector as compared to the varying oil cut in the vertical injector. The pressure and the water-oil ratio (WOR) were constant as well in the horizontal injector, as compared to varying pressure and WOR in the vertical injector. The ultimate oil recovery for the horizontal injector was 24% of IOIP after 2.4 HCPV of fluid had been produced and that for the vertical injector was 56% of IOIP after 2.4 HCPV of fluid had been produced. The oil bank was eliminated when a continuous waterflood was carried out using a horizontal injector; this, however, did not show any improvement over a vertical injector.

120
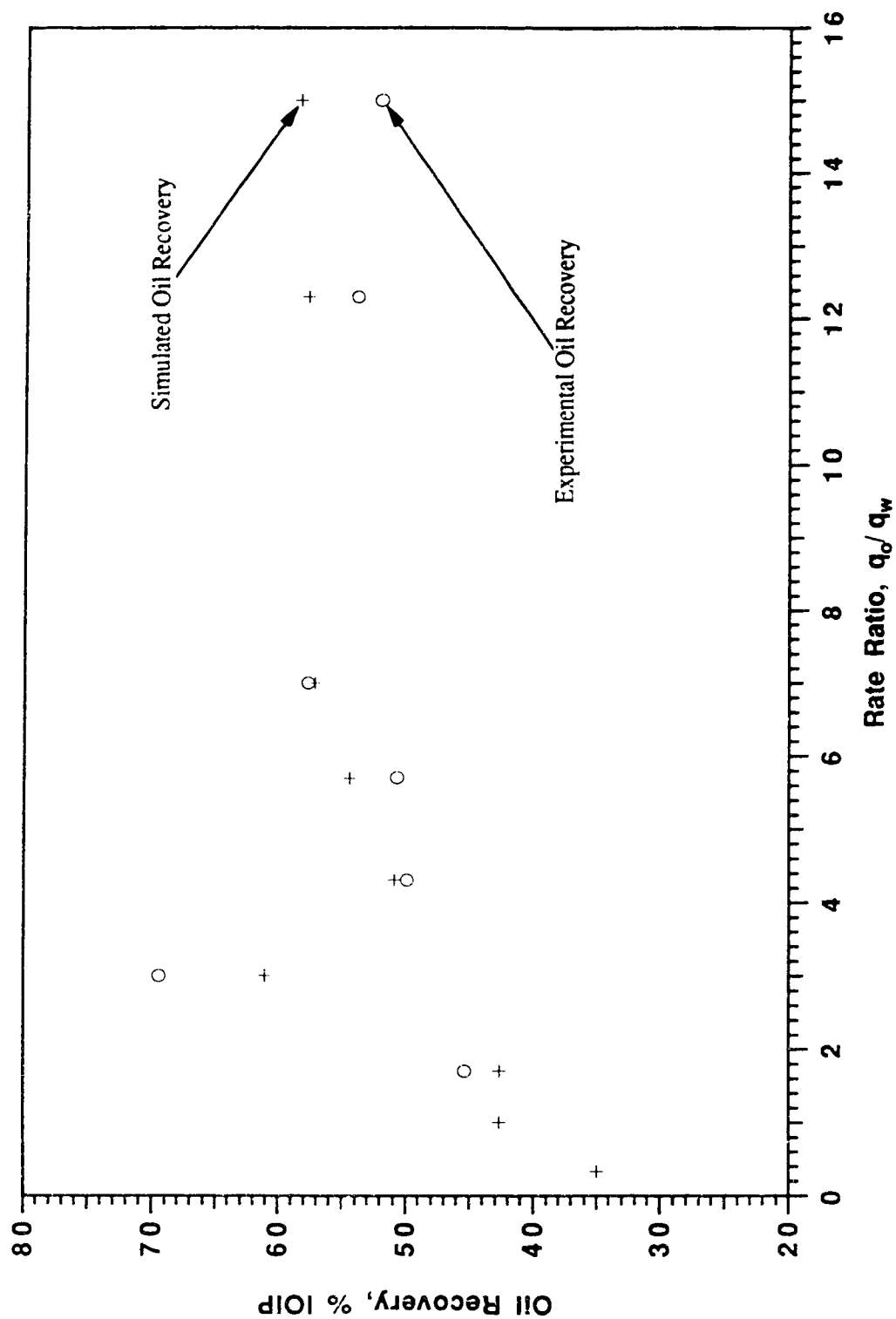
Fig. 8.13: Effect of Rate on Oil Recovery when Crossflow is a Problem
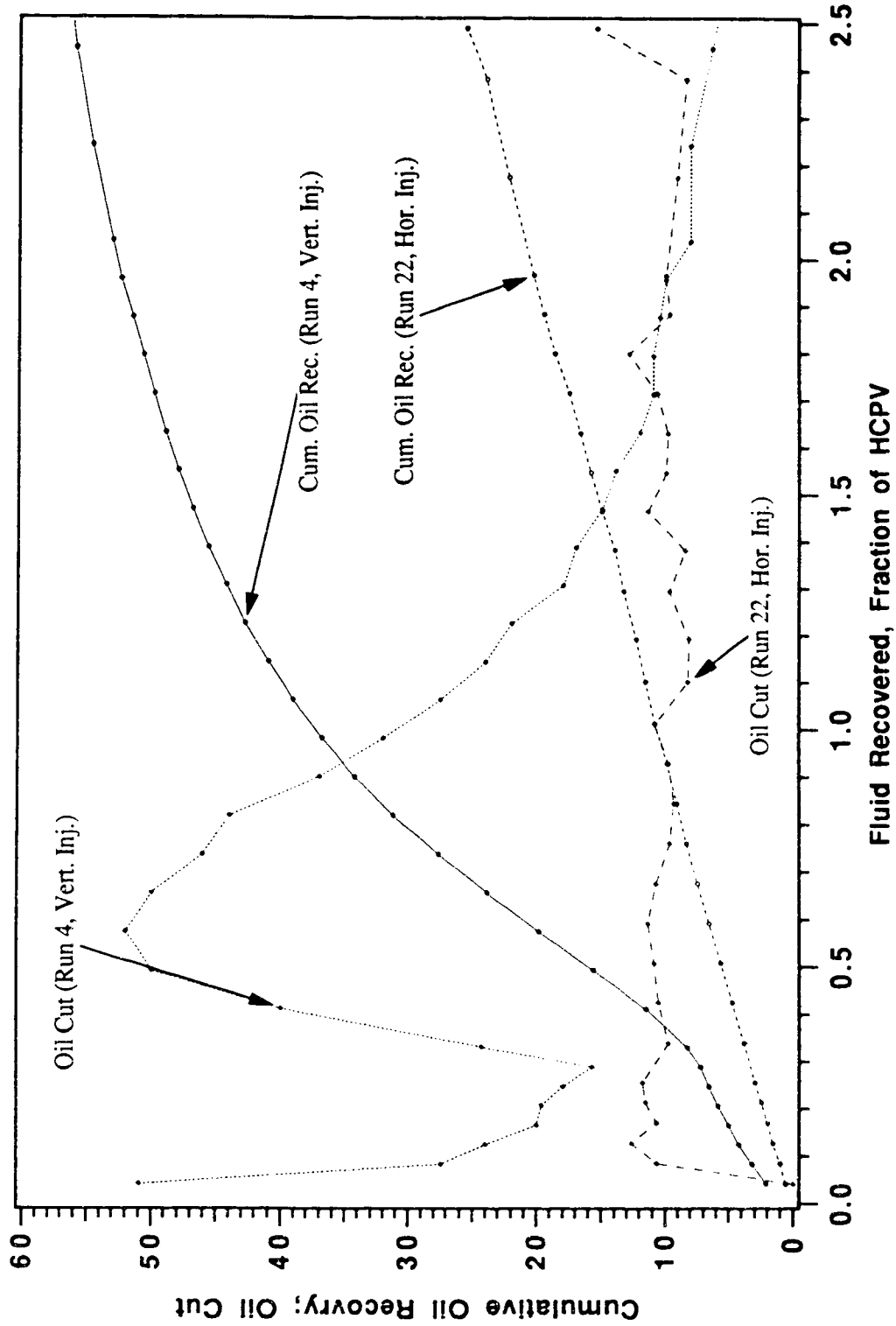
Fig. 8.14: Horizontal Injector versus Vertical Injector.

Polymer and emulsion were also used in conducting experiments for the same well configuration discussed above. The polymer concentration was 500 ppm and the emulsion had a surfactant concentration of 0.016%. Figure 8.15 shows a comparison of the recovery performance of the horizontal injector with the vertical injector, using polymer as a mobility control agent in the oil zone and emulsion as a blocking agent in the bottom-water layer. The oil-zone thickness was 3 times that of the bottom-water layer (that is, $h_o/h_w = 3$), and the permeabilities in the oil and water zones were equal; thus, $k_o/k_w = 1$. The oil cut for the horizontal injector and vertical producer started at 37.5% and peaked at 67% after 0.49 HCPV of fluid had been produced. The oil cut for the vertical injector and vertical producer started at 50.5% and reached a maximum of 75.0% after 0.88 HCPV of fluid had been produced. This indicates that the maximum oil cut for the vertical injector/producer was attained after twice the HCPV of the horizontal injector and vertical producer had been produced. On the basis of oil cut only, the horizontal injector and vertical producer appear to perform better than the vertical injector. This stems from the fact that, after 0.49 HCPV had been produced in each case, the oil production rate for the horizontal injector was 67% as compared to 49.3% for the vertical injector. The ultimate oil recovery for the horizontal injector and vertical producer was 52.6% of IOIP as compared to 69.5% of IOIP for the vertical injector/producer. An oil bank was observed in the horizontal injector and vertical producer experiment. In other words, the application of horizontal injectors and vertical producers did not eliminate the formation of an oil bank, when polymer and emulsion were used in the flooding process.

123
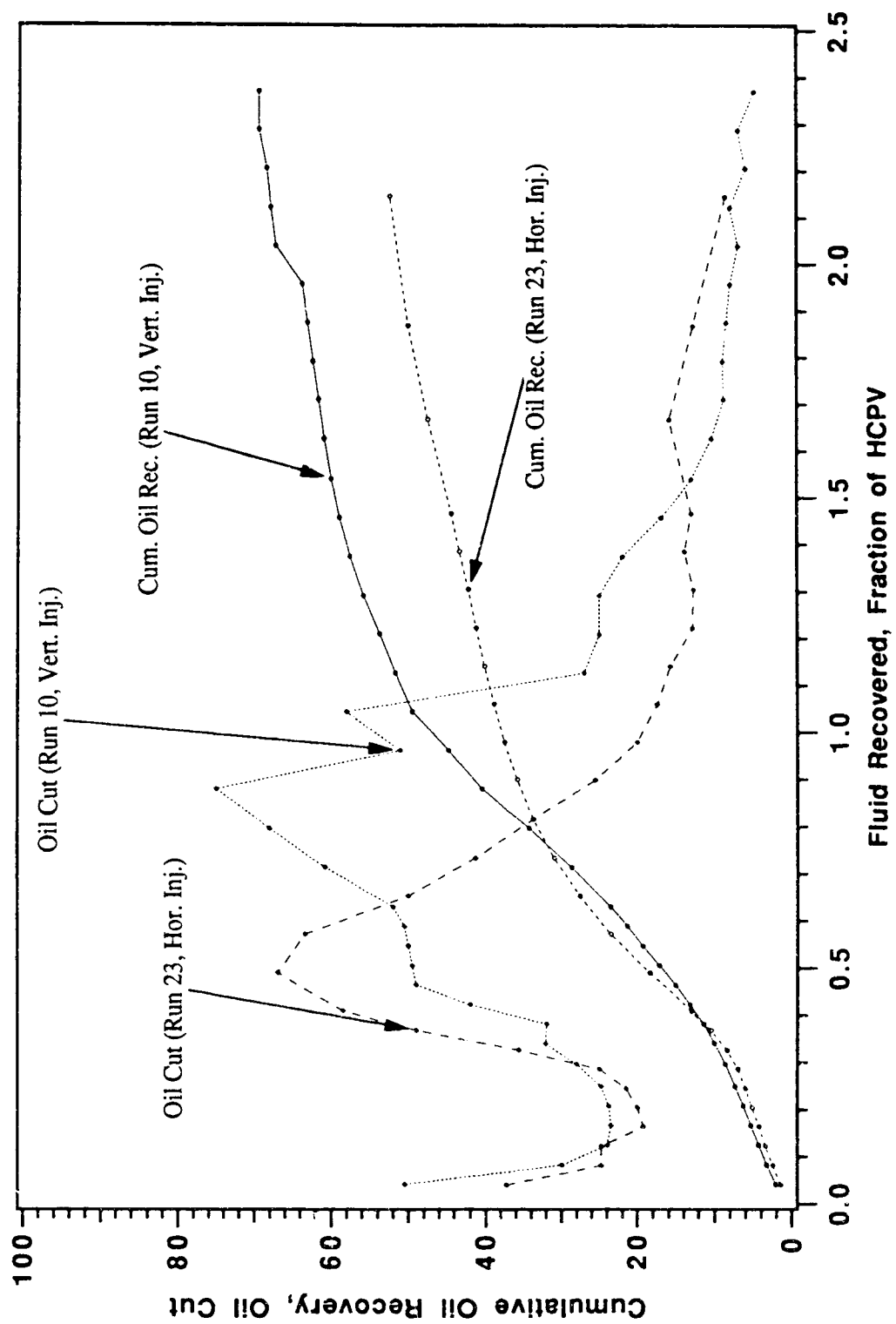
Fig. 8.15 Horizontal Injector versus Vertical Injector Using Polymer and Emulsion as Injection Fluids.

8.5.2 Horizontal Producer versus Vertical Producer

Figure 8.16 compares experiments conducted using a horizontal injector and producer with that conducted using a vertical injector and producer, for both a continuous waterflood and using polymer and emulsion. For the continuous waterflood using horizontal injectors in both the oil and bottom-water layer, the oil cut started at 84% and dropped to a minimum value. When vertical injectors and producers were utilized, the oil cut started at 51%, peaked at 52% and dropped to a minimum value. The oil bank disappeared when horizontal injectors and producers were used, but existed when vertical injectors and producers were used. The water-oil ratio (WOR) increased gradually and the pressure remained virtually constant while using the horizontal injectors and producers. For the vertical injectors and producers the WOR increased gradually also and the pressure increased to a maximum and then declined. For the horizontal injectors and producers the ultimate oil recovery was 45.2% of the IOIP, while that for the vertical injectors and producers, the ultimate oil recovery was 57% of the IOIP.

In Figure 8.17 recovery performance, for the horizontal injector and producer using polymer and emulsion, is compared with that for a vertical injector and producer. In the horizontal injector and producer, the oil cut starts at 58% and is maintained until 0.72 HCPV of fluid is produced before declining. The oil cut for the vertical injector and producer starts at 50.5%, declines to 23.5% and then peaks at 75% after 0.88 HCPV of fluid has been produced. The average WOR in this range (after 0.88 HCPV of fluid has been produced) is 1.071 for the horizontal injector and producer, as compared to 1.70 for the vertical injector and producer. This indicates that there is better blocking of the bottom-water zone for the horizontal injector and producer than for the vertical injector and producer. The ultimate oil recovery for the horizontal injector and producer is 57.2% of the IOIP that is 12.3 percentile lower than that of the vertical injector and producer. Hodaie and Bagci[44] had a similar result in their polymer augmented waterflood.
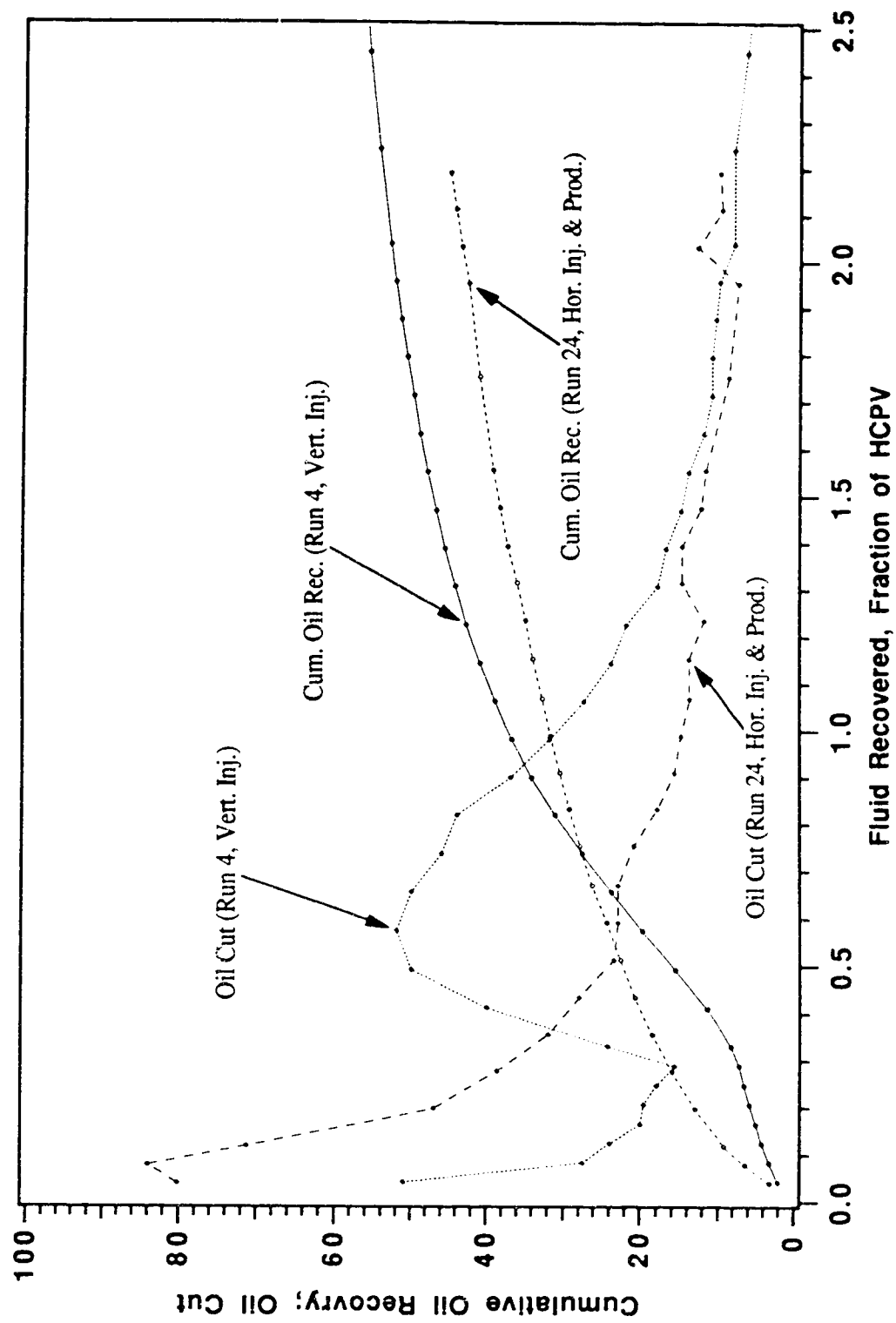
Fig. 8.16: Horizontal Injector and Producer versus Vertical Injector and Producer.
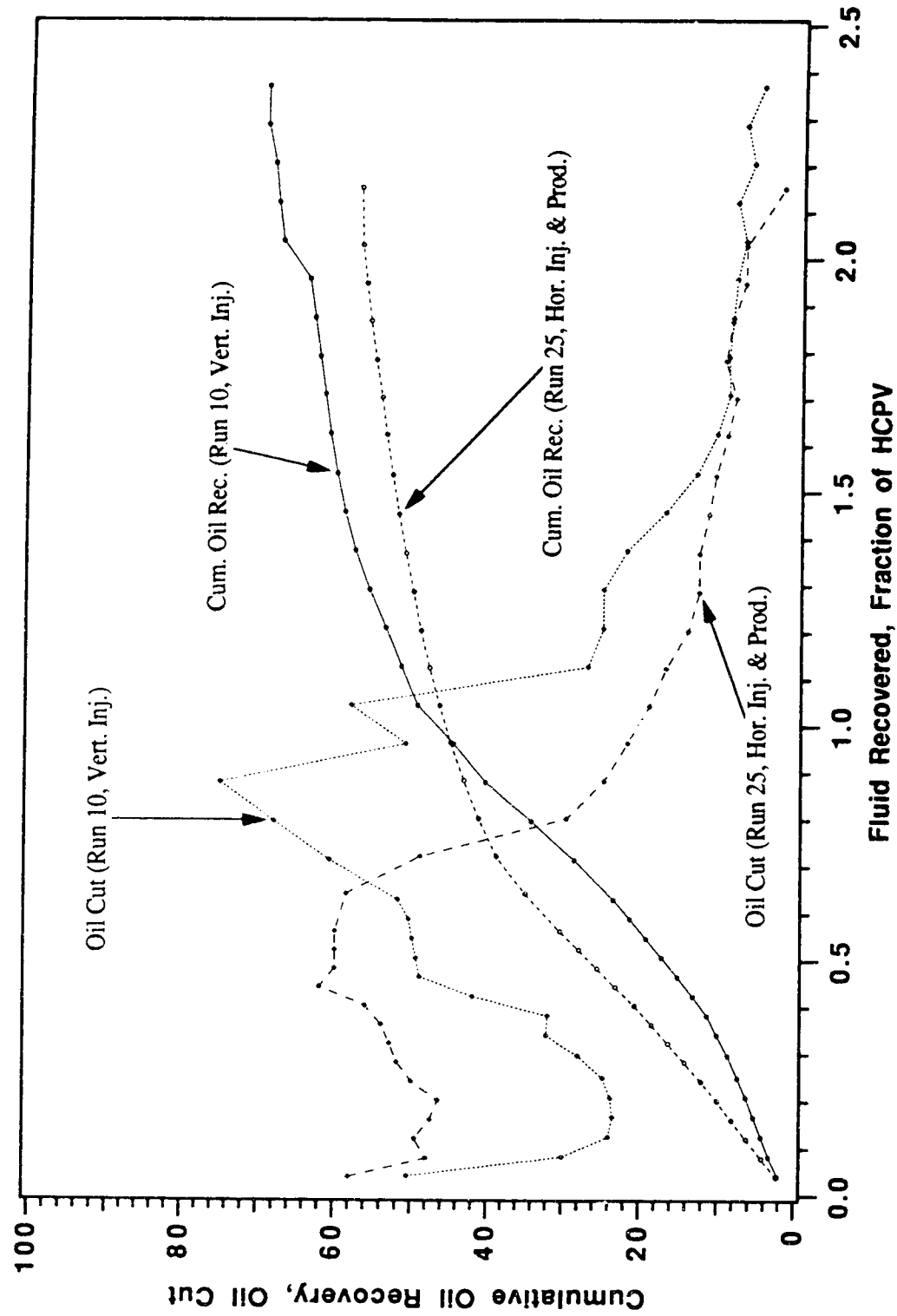
Fig. 8.17: Horizontal Injector and Producer versus Vertical Injector and Producer Using Polymer and Emulsion as Injection Fluids.

8.5.3 Horizontal Well Configuration

This section discusses the various horizontal well configurations. For continuous waterflood, the performance of the horizontal injector and vertical producer, the horizontal injector and horizontal producer and the horizontal and vertical injector and horizontal and vertical producer are compared in Figure 8.18. The WOR for the horizontal injector and vertical producer was constant at 7.40 and so was the oil cut, at 11.0%. For the horizontal injector and producer, the WOR increased more gradually than did that for the horizontal and vertical injector and horizontal and vertical producer. The oil cut started at 84% for the horizontal injector and producer and declined gradually as compared to an oil cut of 74% for the horizontal and vertical injector and horizontal and vertical producer, which declined at a faster rate. The cumulative oil recovery for the horizontal injector and producer was 45% of IOIP, and this was 1.8 times that for the horizontal injector and vertical producer, and 9.8 percentage points higher than that for the horizontal and vertical injector and horizontal and vertical producer. There was no oil bank observed in any of these three experiments. This goes to establish that, for a continuous waterflood, horizontal injectors can enhance the oil rate.

Using the same well configurations as mentioned above, polymer and emulsions were used as injection fluids in the experiments. Figure 8.19 shows the recovery performance for the various horizontal well configurations. In all three experiments, when polymer was used as a control agent and emulsion was used as a blocking agent, oil bank formation was observed. The horizontal injector and producer well configuration gave the highest recovery, viz. 57.2% of IOIP. The horizontal and vertical injectors in the oil zone and water zones, respectively, and horizontal and vertical producers in the oil and water zones, respectively, yielded an oil recovery of 55.2% of IOIP. The horizontal injector and vertical producer yielded an oil recovery of 52.6% of IOIP. From these ultimate oil recovery values it can be concluded that the horizontal injector and producer well configuration in conjuction with the application of polymer and emulsion will be the best well configutation for bottom-water reservoirs. This well configuration does not eliminate oil bank formation in the water zone when polymer and emulsion are used as mobility control and blocking agents, and the oil recovery results compare very well with the oil recovery results from the vertical injector and producer well configuration. For bottom-water reservoirs, vertical injectors and producers can give 12.3 percentage points higher oil recovery than horizontal injectors and producers, therefore, horizontal wells should be used with caution.
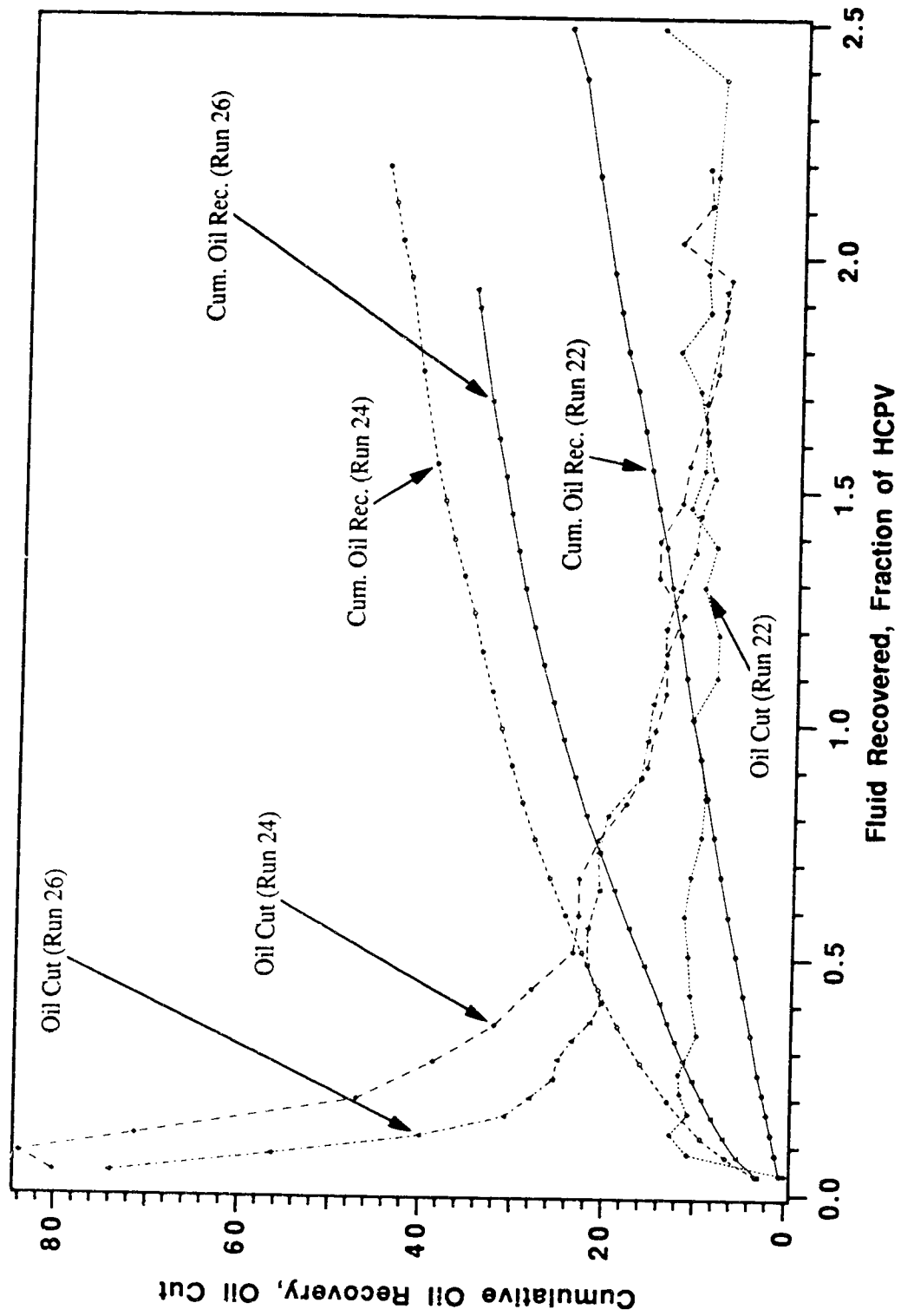
Fig. 8.18: Horizontal Well Configuration on Oil Recovery.
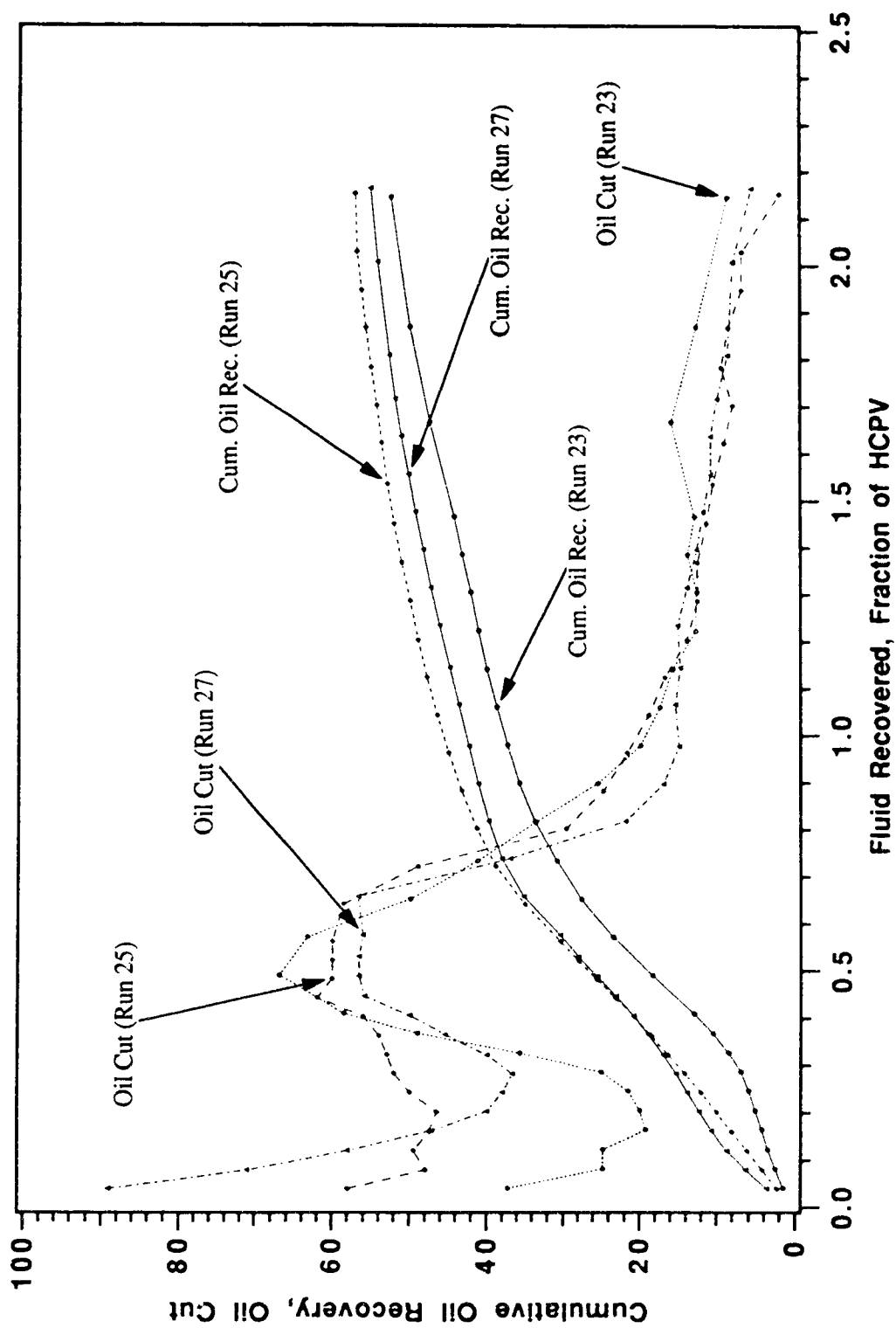
Fig. 8.19: Horizontal Well Configuration Using Polymer and Emulsion on Oil Recvery.

Chapter 9

CONCLUSIONS AND RECOMMENDATIONS

9.1 Conclusions

This research examined waterflooding reservoirs with a communicating bottom-water zone. A generalized mathematical model was developed to estimate crossflow of fluids into or out of the oil zone. A semi-analytical model was developed to predict oil recovery performance for bottom-water reservoirs. The effect of different injection strategies for polymer and emulsion slug was studied. From the semi-analytical model, the mathematical model and the results of the experiments, the following conclusions can be made:

(1)   For bottom-water reservoirs, the amount of fluid channeling into the bottom-water zone can be estimated using Equations (4.17), (4.20) and (4.23).

(2)   Utilizing the semi-analytical model the frontal movements of x_{f1} and x_{f2} can be calculated during a flooding process and the effect of the frontal locations on crossflow can be investigated.

(3)   Recovery predictions can be made with very little error using the semi-analytical model developed in this research.

(4)   In a bottom-water reservoir, the greatest crossflow takes place near the injection well.

(5)   In a bottom-water reservoir, crossflow reverses direction depending on the fluid being injected in the oil and water zones.

(6)   Under bottom-water conditions, the use of a 500 ppm polymer solution as a mobility control agent and a 0.016% surfactant concentration in emulsion as a blocking agent is more effective in enhancing sweep efficiency than other combinations. The apparent viscosity of the emulsion used was about 2.0 mPa.s.

(7)   Under bottom-water conditions, oil recovery is dependent on the rate of fluid injection, the injection strategy adopted and the fluid being injected.

(8)   The blocking action of 1.0 PV_{bw} of slug size is more pronounced than 0.75 PV_{bw} of slug size under bottom-water conditions.

(9)   For bottom-water reservoirs, the use of horizontal injector and producer in waterflooding prevents the formation of an oil bank in the water zone.

(10)   A horizontal injector and vertical producer combination is no better than a vertical injector and vertical producer. In a few cases, the recovery is 50% IOIP.

9.2 Recommendations for Future Research

On the basis of the results of this study, the following recommendations are offered for further work.

(1) To obtain results that will match the experimental data from the derived crossflow equation, a full numerical study should be made;

(2) In the development of the numerical model, the non-Newtonian aspect of the fluids used should be incorporated in the model;

(3) For further displacement work, polymer should be used as the blocking agent while waterflooding the oil zone; and

(4) Application of horizontal wells should be explored further, especially the effect of horizontal well length on oil recovery.

Chapter 10

REFERENCES

1. Stiles, W. E.: "Use of Permeability Distribution in Waterflood Calculation," Trans. AIME, 186, 1949, pp. 9-13.

2. Dykstra, H. and Parsons, R. L.: "The Prediction of Oil Recovery By Waterflood," Secondary Recovery of Oil in the United States, 1950,160-174.

3. Jordan, J. K.: "Reliable Integration of Waterflood Prediction Data," paper presented at the Annual Fall Meeting of the Southern California Petroleum Section in Los Angeles, California October 17-18, 1957.

4. Jordan, J. K., McCardell, W. M. and Hocoott, C. R. : *Oil and Gas Journal*, (May 13 1957) 98-130.

5. Henley, D. H., Owens, W. W. and Craig, F. F. Jr.: "A Scale-Model Study of Bottom Water Drives," *JPT* (January 1961) 90-98.

6. Robertson, J. O. Jr. and Oelefein, F. H.: "Plugging Thief Zones in Water Injection Wells," *JPT* (August 1967) 999-1004.

7. Fitch, R. A. and Griffith, J. D.: "Experimental and Calculated Performance of Miscible Floods in Stratified Reservoirs," *JPT* (November 1964) 1289-1298.

8. Khan, A. R.: "A Scaled Model Study of Water Coning," *JPT* (June 1970) 771-776.

9. Mungan, N.: "Laboratory Study of Water Coning in a Layered Model," *JCPT* 1979, 19 (3) , 66-70.

10. Katz, M. L. and Tek, M. R.: "A Theoretical Study of Pressure Distribution and Fluid Flux in Bounded Stratified Porous Systems with Cross flow," *SPEJ* (March 1962) 68-82.

11. Russell, D. G. and Prats, M. R.: "Performance of Layered Reservoirs with Cross flow Single Compressible Fluid Case," *SPEJ* (March 1962) 53-67.

12. Lambeth, N. and Dawe, R. A.: "Viscous Effects for Miscible Displacements in Regular Heterogeneous Porous Media," *Chem. Eng. Res. Des.* (January 1987) Vol. 65, 52-62.

13. Wright, R. J., Wheat, M. R. and Dawe, R. A.: "Slug Size and Mobility Requirements for Chemically Enhanced Oil Recovery within Heterogeneous Reservoirs," *SPEJ* (February 1987) 92-102.

14. Wright, R. J. and Dawe, R. A.: " Fluid Displacement Efficiency in Layered Porous Media Mobility Ratio Influence," Revue de l'Institut Francais du Petrole, (July-August 1983), Vol. 38, No. 4, 454-474.

15. Warren, J. E. and Cosgrove, J. J.: "Prediction of Waterflood Behavior in a Stratified System," *SPEJ* (June 1964) 149-157.

16. Root, P. J. and Skiba, F. F.: "Cross Flow Effects During an Idealized Displacement Process in a Stratified Reservoir," *SPEJ* (September 1965) .

17. Goddin, C. S. Jr., Craig, F. F. Jr., Wilkes, J. O. and Teck, M. R.: "A Numerical Study of Waterflood Performance In a Stratified System With Crossflow," *JPT* (June 1966) 765-771.

18. Barnes, A. I.: "The Use of Viscous Slug To Improve Waterflood Efficiency In a Reservoir Partially Invaded By Bottom Water," *JPT* (October 1962) 1142-1153.

19. Silva, L. F. and Farouq Ali, S. M: "Waterflood Performance in the Presence of Communicating Strata and Formation Plugging," *LJS,* Vol. 3 (1973) 41-63.

20. El-Khatib, N.: "The Effect of Crossflow on Waterflooding of Stratified Reservoirs," *SPEJ* (April 1985) 291-302.

21. Wright, R. J., Dawe, R. A. and Wall, C. G.: "Surfactant Slug Displacement Efficiency in Reservoirs Tracer Studies in 2-D Layered Models," Proc. 1987 European Symp. on EOR, Bournemouth, U. K. 161-178.

22. Ahmed, G., Castanier, L. M. and Brigham, W. E.: "An Experimental Study of Waterflood From a Two-Dimensional Layered Sand Model," *SPEJ* (February 1987) 92-102.

23. Sheppard, D. A. and Robertson, D. L.: "Performance and Recovery Optimization in a Shallow Bottom Water Oil Reservoir," *JCPT* (May-June 1988) 24-32.

24. Pye, D. J.: "Improved Secondary Recovery by Control of Water Mobility," *JPT* (August 1964) 911-916.

25. Sandiford, B. B.: "Laboratory and Field Studies of Waterfloods Using Polymer Solutions to Increase Oil Recoveries," *JPT* (August 1964) 917-922.

26. Mungan, N., Smith, F. W. and Thompson, J. L.: "Some Aspects of Polymer Floods," *JPT* (September 1966) 1143-1150.

27. Dauben, D. L. and Menzie, D. E.: "Flow Of Polymer Solutions Through Porous Media," *JPT* (August 1967) 1065-1072.

28. Sherborne, J. E., Sarem, A.M. and Sandiford, B. B.: "Flooding Oil Containing Formations with Solutions of Polymer in Water," Seventh World Petroleum Congress, Mexico City, Mexico, 1967.

29. Sarem, A.M.: "On the Theory of Polymer Solution Flooding Process," paper SPE 3002 presented at the 45th Annual Fall Meeting of the Society Of Petroleum Engineers of AIME, held in Houston, Texas (October 4-7, 1970).

30. Zaidel, Ya. M.: "Polymer Flooding of Oil Formations with Bottom Water," Izv. Akad. Nauk SSSR, Mekh. Zhidk. Gaza, No. 3 (May -June 1986) 84-90.

31. Bansbach, P. L.: "The How and Why of Emulsions," *Oil and Gas Journal* (September 1970) 87-93.

32. McAuliffe, C. D.: "Crude Oil-in-Water Emulsions to Improve Fluid Flow in an Oil Reservoir," *JPT* (June 1973) 721-726.

33. Burcik, E. J.: "Pseudo-Dilatant Flow of Polyacrylamide Solutions in Porous Media," *Producers Monthly*, 1967, 32 (2) 27-31.

34. Smith, F. W.: "The Behavior of Partially Hydrolyzed Polyacrylamide Solutions in Porous Media ," *JPT* (February 1970) 148-156.

35. Szabo, M. T.: "Some Aspects of Polymer Retention in Porous Media Using a C^{14} -Tagged Hydrolyzed Polyacrylamide," *SPEJ* (August 1975) 323-337.

36. Szabo, M. T.: "Laboratory Investigations of Factors Influencing Polymer Flood Performance," *SPEJ* (August 1975) 338-346.

37. Duda, J. L. , Klaus, E. E. and Fan, S. K.: "Influence of Polymer-Molecule/Wall Interactions on Mobility Control," *SPEJ* 1981, 21, 613-622.

38. Baijal, S. K. and Dey, N. C.: "Mechanism of Oil Displacement By Polymer Solutions in Unconsolidated Sandpacks," *IJT*, (April 1981) Vol. 19, 139-144.

39. Omar, A. E.: "Effect of Polymer Adsorption on the Mobility Ratio," paper SPE 11503 presented at the SPE Middle East Oil Technical Conference in Manama, Bahrain, (March 14-17, 1983) 509-512.

40. Dietzel, H. J.: "Laboratory Investigations of the Dynamic Stability of Polymer Slugs," *SPEJ* (February 1985) 9-13.

41. Needham, R. B. and Doe, P. H.: "Polymer Flooding Review," *JPT* (December 1987) 1503-1507.

42. Islam, A. R.: "Mobility Control in Reservoirs with a Bottom Water Zone," Ph.D. Thesis, Department of Mining, Metallurgical and Petroleum Engineering, University of Alberta, Edmonton, Alberta (1987).

43. Islam, A. R. and Farouq Ali, S. M.: "Waterflooding Oil Reservoirs with a Bottom Water Zone, " *JCPT* (May-June 1989) 59-66.

44. Hodaie, H. and Bagci, A. S.: "Polymer-Augmented Waterflood in a Reservoir With a Bottom water Zone" paper SPE 25633 presented at the SPE Middle East Oil Technical Conference and Exhibition held in Manama, Bahrain (April 3-6, 1993) 329-338.

45. Masuda, Y., Tang, Ke-Chin, Miyazawa, M. and Tanaka, S.: "1D Simulation of Polymer Flooding Including the Viscoelastic Effect of Polymer Solution," *SPERE* (May 1992) 247-252.

46. Uzoigwe, A. C. and Marsden, S. S.: "Emulsion Rheology and Flow Through Unconsolidated Synthetic Porous Media," paper SPE 3004 presented at the 45th Annual Fall Meeting of the Society of AIME, Houston, Texas (Oct. 4-7, 1970).

47. McAuliffe, C. D.: "Oil-in-Water Emulsions and Their Flow Properties in Porous Media," *JPT* (June 1973) 727-732.

48. Cooke, C. E., Williams, R. E. and Kolodzie, P. A.: "Oil Recovery by Alkaline Waterflooding," *JPT* (December 1974) 1365-1374.

49. Johnson, Jr.: "Status of Caustic and Emulsion Methods," *SPEJ* (January. 1976) 85-92.

50. Soo, H. and Radke, C. J.: "The Flow Mechanism of Dilute, Stable Emulsions in Porous Media," *IECF* (1984) 342-347.

51. Schimdt, D. P., Soo, H. and Radke, C. J.: "Linear Oil Displacement by the Emulsion Entrapment Process," *SPEJ* (June 1984) 351-360.

52. French, T. R., Broz, J. S., Lorenz, P. B. and Bertus, K. M.: "Use of Emulsions for Mobility Control During Steamflooding," Paper presented at the 56th California Regional Meeting of the SPE, Oakland, CA (April 2-4 1986).

53. Islam, M. R. and Farouq Ali, S. M.: "The Use of Oil/Water Emulsions as a Blocking and Diverting Agent," Paper 5, Session 1, presented at the Advances in Petroleum Recovery and Upgrading Technology Conference, Edmonton, Alberta (June 2-3, 1987).

54. Farouq Ali, S. M., Thomas, S. and Khambharatana, F.: Flow of Emulsions in Porous Media, AOSTRA Contract 493, Final Report (1988).

55. Yeung, K.: Mobility Control Under Bottom-Water Conditions, M. Sc. Thesis, Department of Mining, Metallurgical, and Petroleum Engineering, University of Alberta, Edmonton (1991).

56. Yeung, K. and Farouq Ali, S. M.: " Waterflooding Bottom Water Formations Using the Dynamic Blocking Method," Petroleum Society of CIM/AOSTRA Technical Conference, Banff, Alberta (April 21-24, 1991).

57. Mendoza, H., Thomas, S. and Farouq Ali, S. M.: "Effect of Injection Rate on Emulsion Flooding for a Canadian and a Venezuelan Crude Oil," Petroleum Society of CIM/AOSTRA Technical Conference, Banff, Alberta (April 21-24, 1991).

58. Fiori, M. and Farouq Ali, S. M.: "Optimal Emulsion Design for the Recovery of a Saskatchewan Crude," *JCPT* (March-April 1991) 123-132.

59. Devereux, O. F.: "Emulsion Flow in Porous Solids-I. A Flow Model," *CEJ* (1974) 121-128.

60. Alvarado, K. A. and Marsden, Jr., S. S.: "Flow of Oil-in-Water Emulsions Through Tubes and Porous Media," *SPEJ* (December 1979) 369-377.

61. Soo, H. and Radke, C. J.: "A Filtration Model for the Flow of Dilute, Stable Emulsions in Porous Media-I. Theory, " *CES* (1986) 263-272.

62. Abou-Kassem, J. H. and Farouq Ali, S. M. : "Evaluation of Emulsion Flow in Porous Media," submitted for publication to *SPERE* (1991).

63. Abou-Kassem, J. H. and Farouq Ali, S. M.: "Mathematical Representation of Single-Phase Emulsion Flow in Porous Media," submitted for publication to *SPERE* (1991).

64. Khambharatana, F.: Flow of Emulsion in Porous Media, Ph. D. Thesis, Department of Mining, Metallurgical, and Petroleum Engineering, University of Alberta, Edmonton, (1993).

65. Doan, The Quang.: Scaled Experiments of Flow Near, and Inside, a Horizontal Well in Steamflooding, M. Sc. Thesis, Department of Mining, Metallurgical and Petroleum Engineering, University of Alberta, Edmonton, Alberta (1991).

66. Borisov, Ju. P.: "Oil Field Production Using Horizontal and Multiple-Deviation Wells," Moskva, Nedra, 1964. Translated into French by Institute Francais du Petrole, August 1980. Translated into English by J. Strauss, Phillips Petroleum Company.

67. Giger, F. M.: "Horizontal Wells Production Techniques in Heterogeneous Reservoirs," paper SPE 13710, presented at the SPE 1985 Middle East Oil Technical Conference and Exhibition, Manama, Bahrain, (March 11-14, 1985).

68. Joshi, S. D.: "Augmentation of Well Productivity Using Slant and Horizontal Wells," JPT (June 1988) 729-739.

69. Ozkan, E. and Raghavan, R.: "Performance of Horizontal Wells Subject to Bottom Water Drive," paper SPE 18545, presented at the SPE Symposium on Energy, Finance and Taxation Policies, Washington, DC., (September 19-20, 1988).

70. Dikken, B. J.: "Pressure Drop in Horizontal Wells and Its Effect on Their Production Perfomance," JPT (November 1990) 1426-1433.

71. Taber, J. J. and Seright, R. S.: "Horizontal Injection and Production Wells for EOR or Waterflooding," paper SPE 23952, presented at the 1992 SPE Permian Basin Oil and Gas Recovery Conference, Midland, Texas, (March 18-20, 1992), 227-239.

72. Chaperon, I.: "Theoretical Study of Coning Toward Horizontal and Vertical wells in Anisotropic Formations: Subcritical and Critical Rates," paper SPE 15377, presented at the 61st Annual technical Conference and Exhibition of the Society of Petroleum Engineers, New Orleans, LA, (October 5-8, 1986).

73. Muskat, M.: Flow of Homogeneous Fluids Through Porous Media , McGraw-Hill Book Company, Inc. 1937.

74. Papatzacos, P. Herring, T. R., Martinsen, R. and Skjaeveland, S. M.: "Cone Breakthrough Time for Horizontal Wells," paper SPE 19822, presented at the 64th Annual Conference and Exhibition of the Society of Petroleum Engineers, San Antonio, Texas, (October 8-11, 1989).

75. Personal Communication with Dr. Yoshihiro Masuda, Department of Geosystem Engineering, Faculty of Engineering, University of Tokyo, Japan.

11. APPENDIX A: Table of Experimental Resuls.

APPENDIX B: Computer Program for the Semi-Analytical Model.

APPENDIX C: Flow Chart For Computer Program.

APPENDIX D: Figure for Oil Recovery Performance.

APPENDIX A: Tables of Experimental Results

Table A.1

PRODUCTION HISTORY FOR RUN 1

Porosity, ø = 37.6%
kabs = 19.8 µm2
kwor = 3.30 µm2
kowr = 16.3 µm2
IOIP = 1616 ml
Soi = 0.923

Sample No.	Sample, Vol. (ml)	Oil Vol. (ml)	Inj. Press. kPa	Cum. Oil Rec. % IOIP	Oil Cut %	WOR	Fluid Prod. HCPV
1	93	93	135.25	5.75	100.0	0.0	0.058
2	100	100	118.5	11.94	100.0	0.0	0.119
3	100	100	100	18.13	100.0	0.0	0.181
4	101	101	81.5	24.38	100.0	0.0	0.244
5	102	99	60.5	30.51	97.1	0.0	0.307
6	101	34	51.5	32.61	33.7	2.0	0.369
7	101	21	47.75	33.91	20.8	3.8	0.432
8	101	19	44.5	35.08	18.8	4.3	0.494
9	111	14	45	35.95	12.6	6.9	0.563
10	101	14	43.75	52.00	13.9	6.2	0.626
11	105	14	42	52.87	13.3	6.5	0.691
12	113	15	41.5	53.87	13.3	6.5	0.761
13	115	12	40.5	54.54	10.4	8.6	0.832
14	121	11	40.25	55.22	9.1	10.0	0.907
15	501	41	38.75	57.75	8.2	11.2	1.217
16	102	6	38	58.13	5.9	16.0	1.280
17	105	7	37.5	58.56	6.7	14.0	1.345
18	102	6	37.5	58.93	5.9	16.0	1.408
19	102	6	37.25	59.30	5.9	16.0	1.471
20	252	12	37.75	60.04	4.8	20.0	1.627
21	252	14	38.5	60.91	5.6	17.0	1.783
22	252	10	38.5	61.53	4.0	24.2	1.939
23	258	6	37.75	61.90	2.3	42.0	2.098
24	338	13	37.75	62.70	3.8	25.0	2.308

Table A.2

PRODUCTION HISTORY FOR RUN 2

Porosity, ø = 37.6%
kabs = 18.5 µm2
kwor = 3.08 µm2
kowr = 16.5 µm2
IOIP = 406 ml
Soi = 0.967

Sample No.	Sample Vol. (ml)	Oil Vol. (ml)	Inj.Press.(kPa)	Cum. Oil Rec. % IOIP	Oil Cut %	WOR	Fluid Prod. HCPV
1	50	50	112.40	12.32	100.0	0.0	0.123
2	50	50	100.60	24.63	100.0	0.0	0.246
3	50	50	90.80	36.95	100.0	0.0	0.369
4	50	50	80.80	49.26	100.0	0.0	0.493
5	50	50	70.20	61.58	100.0	0.0	0.616
6	51	42	69.40	71.92	97.0	3.1	0.741
7	50	15	48.80	75.62	87.5	14.3	0.865
8	50	15	45.00	79.31	80.3	24.5	0.988
9	10	3	44.60	80.05	79.1	26.5	1.012
10	50	6	40.40	81.53	71.8	39.3	1.135
11	23	3	39.20	82.27	69.0	44.9	1.192
12	25	3	31.40	83.00	66.2	51.0	1.254
13	25	2.5	29.00	83.62	63.6	57.3	1.315
14	25	3	29.60	84.36	61.3	63.2	1.377
15	25	2.5	28.60	84.98	59.1	69.3	1.438

Table A.3

PRODUCTION HISTORY FOR RUN 3

Porosity, ø = 37.6%
kabs = 18.7 µm2
kowr = 16.5 µm2
IOIP = 1527 ml
Soi = 0.323

Sample No.	Sample Vol. (ml)	Oil Vol. (ml)	Inj. Press. kPa	Cum. Oil Rec. % IOIP	Oil Cut %	WOR	Fluid Prod. HCPV
1	42	42	137.50	6.02	100.0	0.0	0.028
2	50	50	134.75	9.30	100.0	0.0	0.060
3	50	50	129.00	12.64	100.0	0.0	0.093
4	51	51	121.50	15.91	100.0	0.0	0.126
5	50	50	109.75	19.19	100.0	0.0	0.159
6	50	50	104.25	22.50	100.0	0.0	0.192
7	50.5	50.5	96.00	25.80	100.0	0.0	0.225
8	50.5	50.5	87.75	29.21	100.0	0.0	0.258
9	52	52	81.50	33.96	100.0	0.0	0.292
10	50	42	73.25	36.84	84.0	0.2	0.325
11	99	44	69.25	44.77	44.4	1.3	0.390
12	100	32	65.50	53.34	32.0	2.1	0.455
13	100	24	62.75	56.71	24.0	3.2	0.521
14	100	21	63.00	57.99	21.0	3.8	0.586
15	101	19.5	62.25	59.14	19.3	4.2	0.652
16	101	17.5	62.25	60.22	17.3	4.8	0.718
17	100	16.5	61.25	61.26	16.5	5.1	0.784
18	102	16	59.50	62.28	15.7	5.4	0.851
19	100	15.5	57.50	63.85	15.5	5.5	0.916
20	115	24	55.50	64.83	20.9	3.8	0.991
21	102	15	58.25	65.72	14.7	5.8	1.058
22	102.5	13.5	56.25	66.44	13.2	6.6	1.125
23	100	11	56.25	67.22	11.0	8.1	1.191
24	100	12	58.00	67.94	12.0	7.3	1.256
25	101	11	58.00	70.17	10.9	8.2	1.323
26	250	34	59.75	70.51	13.6	6.4	1.486
27	250	5	57.75	70.51	2.0	49.0	1.650

Table A.4

PRODUCTION HISTORY FOR RUN 4

Porosity, ∅ = 36.2%
kabs = 19.3 μm2
kowr = 16.1 μm2
IOIP = 1229 ml
Soi = 0.936

Sample No.	Sample Vol. (ml)	Oil Vol. (ml)	Inj. Press. kPa	Cum. Oil Rec. %IOIP	Oil Cut %	WOR	Fluid Prod. HCPV
1	51	26	17.20	2.12	50.98	0.96	0.041
2	51	14	14.60	3.25	27.45	2.64	0.083
3	50	12	15.20	4.23	24.00	3.17	0.124
4	50	10	15.00	5.04	20.00	4.00	0.164
5	51	10	16.40	5.86	19.61	4.10	0.206
6	50	9	19.00	6.59	18.00	4.56	0.247
7	51	8	21.60	7.24	15.69	5.38	0.288
8	51.5	12.5	22.40	8.26	24.27	3.12	0.330
9	100	40	21.40	11.51	40.00	1.50	0.411
10	100	50	20.00	15.58	50.00	1.00	0.493
11	100	52	18.00	19.81	52.00	0.92	0.574
12	100	50	16.00	23.88	50.00	1.00	0.655
13	100	46	14.40	27.62	46.00	1.17	0.737
14	100	44	12.80	31.20	44.00	1.27	0.818
15	100	37	10.80	34.21	37.00	1.70	0.900
16	100	32	9.80	36.82	32.00	2.13	0.981
17	100	27.5	9.00	39.06	27.50	2.64	1.062
18	100	24	8.00	41.01	24.00	3.17	1.144
19	100	22	6.60	42.80	22.00	3.55	1.225
20	100	18	6.60	44.26	18.00	4.56	1.306
21	100	17	6.20	45.65	17.00	4.88	1.388
22	100	15	5.80	46.87	15.00	5.67	1.469
23	100	14	5.40	48.01	14.00	6.14	1.550
24	100	12	5.40	48.98	12.00	7.33	1.632
25	100	11	5.00	49.88	11.00	8.09	1.713
26	100	11	4.60	50.77	11.00	8.09	1.795
27	100	10.5	4.60	51.63	10.50	8.52	1.876
28	100	10	4.40	52.44	10.00	9.00	1.957
29	100	8	4.40	53.09	8.00	11.50	2.039
30	250	20	4.40	54.72	8.00	11.50	2.242
31	252	16	4.40	56.02	6.35	14.75	2.447
32	250	12	4.40	57.00	4.90	19.83	2.651

Table A.5

PRODUCTION HISTORY FOR RUN 5

Porosity, ø = 36.0%
kabs = 18.5 µm2
kowr = 15.9 µm2
IOIP = 1212ml
Soi = 0.925

Sample No.	Sample Vol. (ml)	Oil Vol. (ml)	Inj. Press. kPa	Cum. Oil Rec. % IOIP	Oil Cut %	WOR	Fluid Prod. HCPV
1	50	15	70.25	1.24	30.00	2.33	0.041
2	51	7.5	68.75	1.86	14.71	5.80	0.083
3	52	8	70.25	2.52	15.38	5.50	0.126
4	52	7	72.75	3.09	13.46	6.43	0.169
5	52	7	76.25	3.67	13.46	6.43	0.212
6	56	10	81.50	4.50	17.86	4.60	0.258
7	60	15	86.25	5.73	25.00	3.00	0.308
8	50	8	89.00	6.39	16.00	5.25	0.349
9	53	9	92.75	7.14	16.98	4.89	0.393
10	62	11	97.00	8.04	17.74	4.64	0.444
11	50	21	103.00	9.78	42.00	1.38	0.485
12	51	35	102.75	12.67	68.63	0.46	0.527
13	110	85	99.50	19.68	77.27	0.29	0.618
14	100	78	85.50	26.11	78.00	0.28	0.700
15	100	63	80.00	31.31	63.00	0.59	0.783
16	100	50	77.00	35.44	50.00	1.00	0.866
17	105	50	72.75	39.56	47.62	1.10	0.952
18	100	45.5	70.00	43.32	45.50	1.20	1.035
19	104	29	67.25	45.71	27.88	2.59	1.120
20	121	21	66.50	47.44	17.36	4.78	1.220
21	110	16	64.00	48.76	14.55	5.88	1.311
22	100	13	63.25	49.83	13.00	6.69	1.394
23	101	10	62.00	50.65	9.90	9.10	1.477
24	104	10	60.75	51.49	9.62	9.40	1.563
25	250	18	60.75	52.97	7.20	12.89	1.769
26	252	16	59.75	54.29	6.35	14.75	1.977
27	198	12	52.50	55.28	6.06	15.50	2.140

Table A.6

PRODUCTION HISTORY FOR RUN 6

Porosity, φ = 36.0%
kabs = 18.5 μm2
kowr = 15.7 μm2
IOIP = 1233ml
Soi = 0.928

Sample No.	Sample Vol. (ml)	Oil Vol. (ml)	Inj. Press. kPa	Cum. Oil Rec. % IOIP	Oil Cut %	WOR	Fluid Prod. HCPV
1	51	13	52.25	1.05	25.49	2.92	0.041
2	51.5	7.5	50.25	1.66	14.56	5.87	0.083
3	50	6	50.00	2.15	12.00	7.33	0.124
4	50	6	53.50	2.64	12.00	7.33	0.164
5	51	6	58.25	3.12	11.76	7.50	0.206
6	51	6	58.25	3.61	11.76	7.50	0.247
7	52	6	58.50	4.10	11.54	7.67	0.289
8	51	6	59.50	4.58	11.76	7.50	0.330
9	50.5	6	60.50	5.07	11.88	7.42	0.371
10	51	7	63.00	5.64	13.73	6.29	0.413
11	55	8	63.00	6.29	14.55	5.88	0.457
12	50	7	65.25	6.85	14.00	6.14	0.498
13	101	28	70.00	9.12	27.72	2.61	0.580
14	102	42	65.00	12.53	41.18	1.43	0.663
15	101	36	61.75	15.45	35.64	1.81	0.745
16	101	32	60.00	18.05	31.68	2.16	0.826
17	102	25	60.25	20.07	24.51	3.08	0.909
18	101	21	60.75	21.78	20.79	3.81	0.991
19	102	19	59.50	23.32	18.63	4.37	1.074
20	110	18	59.00	24.78	16.36	5.11	1.163
21	106	15	58.00	25.99	14.15	6.07	1.249
22	103	13	56.25	27.05	12.62	6.92	1.333
23	110	13	55.50	28.10	11.82	7.46	1.422
24	102	12	55.00	29.08	11.76	7.50	1.504
25	102	9	55.00	29.81	8.82	10.33	1.587
26	250	20	58.00	31.43	8.00	11.50	1.790
27	500	40	58.00	34.67	8.00	11.50	2.195
28	90	10	56.00	35.48	11.11	8.00	2.268

Table A.7

PRODUCTION HISTORY FOR RUN 7

Porosity, ø = 35.0%
kabs = 19.3 µm2
kowr = 17.2 µm2
IOIP = 1185 ml
Soi = 0.933

Sample No.	Sample Vol. (ml)	Oil Vol. (ml)	Inj. Press. kPa	Cum. Oil Rec. % IOIP	Oil Cut %	WOR	Fluid Prod. HCPV
1	51	21	20.69	1.77	41.18	1.43	0.043
2	54	19	19.65	3.38	35.19	1.84	0.089
3	51	13	19.31	4.47	25.49	2.92	0.132
4	51	11	19.31	5.40	21.57	3.64	0.175
5	51	12	18.62	6.41	23.53	3.25	0.218
6	100.5	24.5	19.31	8.48	24.38	3.10	0.303
7	102	42	20.00	12.03	41.18	1.43	0.389
8	100	50	19.65	16.24	50.00	1.00	0.473
9	98	48	18.27	20.30	48.98	1.04	0.556
10	100.5	42.5	18.27	23.88	42.29	1.36	0.641
11	101	36	18.62	26.92	35.64	1.81	0.726
12	100	31.5	17.93	29.58	31.50	2.17	0.81
13	100	27.5	16.89	31.90	27.50	2.64	0.895
14	100.5	24	15.86	33.92	23.88	3.19	0.979
15	100	23	15.51	35.86	23.00	3.35	1.064
16	100.5	30.5	16.20	38.44	30.35	2.30	1.149
17	99.5	42	16.55	41.98	42.21	1.37	1.232
18	100	44.5	15.17	45.74	44.50	1.25	1.317
19	101	28	13.45	48.10	27.72	2.61	1.402
20	101	22	12.41	49.96	21.78	3.59	1.487
21	100	16	11.72	51.31	16.00	5.25	1.572
22	105	13	11.38	52.41	12.38	7.08	1.66
23	101.5	10	10.34	53.25	9.85	9.15	1.746
24	100	10.5	9.65	54.14	10.50	8.52	1.83
25	250	22	9.31	55.99	8.80	10.36	2.641
26	1010	70	7.93	61.90	6.93	13.43	2.894
27	480	25	7.93	64.01	5.21	18.20	3.299

Polymer Slug Size = 1.00 PVbw

Table A.8

PRODUCTION HISTORY FOR RUN 8

Porosity, ø = 35.2%
kabs = 18.8 μm2
kowr = 15.8 μm2
IOIP = 1133 ml
Soi = 0.935

Sample No.	Sample Vol. (ml)	Oil Vol. (ml)	Inj. Press. kPa	Cum. Oil Rec. % IOIP	Oil Cut %	WOR	Fluid Prod. HCPV
1	50.5	17.5	15.86	1.54	34.65	1.89	0.045
2	50	14	23.10	2.78	28.00	2.57	0.089
3	52.5	11.5	30.68	3.80	21.90	3.57	0.135
4	50	8	37.23	4.50	16.00	5.25	0.179
5	51	8	41.37	5.21	15.69	5.38	0.224
6	51	11	43.09	6.18	21.57	3.64	0.269
7	100	35.5	44.82	9.31	35.50	1.82	0.357
8	100	73	40.68	15.75	73.00	0.37	0.446
9	100.5	83	35.51	23.08	82.59	0.21	0.534
10	103	86	28.61	30.67	83.50	0.20	0.625
11	104	76.5	22.41	37.42	73.56	0.36	0.717
12	100	65	18.62	43.16	65.00	0.54	0.805
13	100	36.5	14.13	46.38	36.50	1.74	0.894
14	100	20	12.41	48.15	20.00	4.00	0.982
15	100	15	11.03	49.47	15.00	5.67	1.070
16	100	10	13.45	50.35	10.00	9.00	1.158
17	105	9	13.10	51.15	8.57	10.67	1.251
18	102	7.5	8.62	51.81	7.35	12.60	1.341
19	102	6	8.27	52.34	5.88	16.00	1.431
20	101	5	7.93	52.78	4.95	19.20	1.520
21	251	11	7.93	53.75	4.38	21.82	1.742
22	250	9	7.24	54.55	3.60	26.78	1.962
23	100.5	3	6.55	54.81	2.99	32.50	2.051

Polymer Slug Size = 1.00 PVDW

Table A.9

PRODUCTION HISTORY FOR RUN 9

Porosity, φ = 36.2%
kabs = 18.5 μm2
kowr = 16.0 μm2
IOIP = 1136 ml
Soi = 0.940

Sample No.	Sample Vol. (ml)	Oil Vol. (ml)	Inj. Press. kPa	Cum. Oil Rec. % IOIP	Oil Cut %	WOR	Fluid Prod. HCPV
1	51	11	11.38	0.97	21.57	3.64	0.045
2	50.5	7.5	13.79	1.63	14.85	5.73	0.089
3	51	9	16.89	2.42	17.65	4.67	0.134
4	51	10	17.58	3.30	19.61	4.10	0.179
5	51	9	19.65	4.09	17.65	4.67	0.224
6	100	21	26.20	5.94	21.00	3.76	0.312
7	100	69.5	25.86	12.06	69.50	0.44	0.400
8	100	55	22.06	17.34	60.00	0.67	0.488
9	100	51	18.62	21.83	51.00	0.96	0.576
10	100	41.5	17.58	25.48	41.50	1.41	0.664
11	100	38.5	15.17	28.87	38.50	1.60	0.752
12	100	32	14.48	31.69	32.00	2.13	0.840
13	100.5	29.5	14.82	34.29	29.35	2.41	0.929
14	100	27	14.82	36.66	27.00	2.70	1.017
15	100.5	24	14.13	38.78	23.88	3.19	1.105
16	100	22	14.13	40.71	22.00	3.55	1.193
17	124.5	27.5	12.76	43.13	22.09	3.53	1.303
18	109	21.5	12.41	45.03	19.72	4.07	1.399
19	100	17	11.03	46.52	17.00	4.88	1.487
20	100.5	15.5	9.31	47.89	15.42	5.48	1.575
21	100	15	10.69	49.21	15.00	5.67	1.663
22	100	14	9.65	50.44	14.00	6.14	1.751
23	100	14	8.27	51.67	14.00	6.14	1.839
24	100	13	7.93	52.82	13.00	6.69	1.927
25	100.5	10.5	6.55	53.74	10.45	8.57	2.016
26	103	10	6.21	54.62	9.71	9.30	2.107
27	101.5	7	6.21	55.24	6.90	13.50	2.198
28	100	6	6.21	55.77	6.00	15.67	2.284
29	100.5	5.5	6.21	56.25	5.47	17.27	2.372
30	490	15	6.21	57.57	3.05	31.57	2.804

Polymer Slug Size = 100 PVbw

Table A.10

PRODUCTION HISTORY FOR RUN 10

Porosity, φ = 34.8%
k_{abs} = 19.3 μm2
k_{oew} = 17.1 μm2
IOIP = 1212 ml
S_{oi} = 0.923

Sample No	Sample Vol (ml)	Oil Vol (ml)	Inj Press kPa	Cum Oil Rec % IOIP	Oil Cut %	WCR	Fluid Prod HCPV
1	50.5	25.5	17.40	2.10	50.50	0.98	0.042
2	50	15	17.40	3.34	30.00	2.33	0.083
3	50	12	18.60	4.33	24.00	3.17	0.124
4	51	12	21.00	5.32	23.51	3.25	0.166
5	50.5	12	20.00	6.31	23.76	3.21	0.208
6	50.5	12.5	20.00	7.34	24.75	3.04	0.250
7	57	16	21.60	8.66	28.07	2.56	0.297
8	53	17	22.00	10.07	32.08	2.12	0.340
9	50	16	26.00	11.39	32.00	2.13	0.382
10	50	21	25.80	13.12	42.00	1.38	0.423
11	50	24.5	25.00	15.14	49.00	1.04	0.464
12	50.5	25	24.40	17.20	49.50	1.02	0.506
13	50	25	24.40	19.27	50.00	1.00	0.547
14	50.5	25.5	24.60	21.37	50.50	0.98	0.589
15	50	26	26.20	23.51	52.00	0.92	0.630
16	102	62	20.20	28.63	60.78	0.65	0.714
17	100	68	21.00	34.24	68.00	0.47	0.797
18	100	75	16.80	40.43	75.00	0.33	0.879
19	100	51	12.60	44.64	51.00	0.96	0.962
20	100	58	9.20	49.42	58.00	0.72	1.044
21	100	27	8.80	51.65	27.00	2.70	1.127
22	100	28	8.80	53.71	28.00	3.00	1.209
23	100	28	8.14	55.78	28.00	3.00	1.292
24	100	25	6.52	57.59	25.00	3.55	1.374
25	100	20	4.70	58.99	20.00	4.88	1.457
26	100	16	4.40	60.07	16.00	6.69	1.539
27	105	14	4.14	60.97	14.00	8.55	1.626
28	101	12	7.72	61.72	12.00	10.22	1.709
29	100	12	7.04	62.46	12.00	10.11	1.792
30	100	11.5	7.96	63.16	11.50	10.76	1.874
31	100	11	9.60	63.82	11.00	11.50	1.957
32	100	7	9.80	66.40	7.00	13.29	2.039
33	100	8	10.64	67.06	8.00	11.50	2.122
34	101	6	12.20	67.55	5.94	15.83	2.205
35	100	7	12.94	68.13	7.00	13.29	2.288
36	100	4.8	13.98	69.53	4.80	19.83	2.370

Polymer Slug Size = 1.00 PVbw
Emulsion Slug Size = 1.00 PVbw

Table A.11

PRODUCTION HISTORY FOR RUN 11

Porosity, ø = 36.9%
kabs = 23.0 µm2
kowr = 18.3 µm2
IOIP = 1286 ml
Soi = 0.914

Sample No.	Sample Vol. (ml)	Oil Vol. (ml)	Inj. Press. kPa	Cum. Oil Rec. % IOIP	Oil Cut %	WOR	Fluid Prod. HCPV
1	50	10	9.20	0.78	20.00	4.00	0.039
2	50.5	9.5	13.40	1.52	18.81	4.32	0.078
3	50.5	8	20.00	2.14	15.84	5.31	0.117
4	50	7	25.80	2.68	14.00	6.14	0.156
5	50.5	7	31.40	3.23	13.86	6.21	0.196
6	50.5	7	36.20	3.77	13.86	6.21	0.235
7	50.5	7.5	41.40	4.35	14.85	5.73	0.274
8	51	8	45.40	4.98	15.69	5.38	0.314
9	50	17.5	42.00	6.34	35.00	1.86	0.353
10	50.5	25.5	42.40	8.32	50.50	0.98	0.392
11	50	37	41.40	11.20	74.00	0.35	0.431
12	51	38	39.40	14.15	74.51	0.34	0.470
13	50.5	38	37.20	17.11	75.25	0.33	0.510
14	50	37	35.20	19.98	74.00	0.35	0.549
15	100	74	31.20	25.74	74.00	0.35	0.628
16	100	71	27.80	31.26	71.00	0.41	0.704
17	100	71.5	25.00	36.82	71.50	0.40	0.782
18	100	63.5	20.20	41.76	63.50	0.57	0.860
19	100	47.5	14.20	45.45	47.50	1.11	0.937
20	100.5	30.5	13.00	47.82	30.35	2.30	1.016
21	100	25	10.60	49.77	25.00	3.00	1.093
22	103	23	8.60	51.56	22.33	3.48	1.173
23	100	10	8.20	52.33	10.00	9.00	1.251
24	100.5	10	8.40	53.11	9.95	9.05	1.329
25	100	26	8.80	55.73	26.00	2.85	1.407
26	100	19	10.20	57.28	19.00	4.26	1.485
27	100	17	11.00	58.67	17.00	4.90	1.563
28	101	18	12.60	60.05	17.80	4.60	1.641
29	100.5	17	14.20	61.42	16.90	4.56	1.719
30	100	4	15.60	61.79	4.00	24.00	1.797

Emulsion Slug Size = 1.00 PVbw
Polymer Slug Size = 1.00 PVbw

Table A 12

PRODUCTION HISTORY FOR RUN 12

Porosity, Ø = 36.9%
kabs = 18.0 µm2
kowr = 16.0 µm2
IOIP = 1300 ml
Soi = 0.925

Sample No	Sample Vol (ml)	Oil Vol (ml)	Inj Press kPa	Cum Oil Rec % IOIP	Oil Cut %	WOR	Fluid Prod HCPV
1	51	20	34.40	1.54	39.22	1.55	0.039
2	50	9	34.40	2.23	18.00	4.56	0.078
3	50	7	37.10	2.77	14.00	6.14	0.116
4	50	6	39.12	3.23	12.00	7.33	0.155
5	62.5	7	44.80	3.77	11.20	7.93	0.203
6	50.5	6	45.60	4.23	11.88	7.42	0.242
7	51	6	48.40	4.69	11.76	7.50	0.281
8	50	6	51.20	5.15	12.00	7.33	0.319
9	50	10.5	52.60	5.96	21.00	3.76	0.358
10	50.5	17	52.80	7.27	33.66	1.97	0.397
11	51	25	53.60	9.19	49.02	1.04	0.436
12	55	29	51.20	11.42	52.73	0.90	0.478
13	52	28	49.20	13.58	53.85	0.86	0.518
14	49	31	22.80	15.96	63.27	0.58	0.556
15	50	33	23.60	18.50	66.00	0.52	0.594
16	100	36	25.60	21.27	36.00	1.78	0.671
17	101	39	25.60	24.27	38.61	1.59	0.749
18	101	31	25.60	26.65	30.69	2.26	0.827
19	101	23	20.08	28.42	22.77	3.39	0.904
20	101	22	20.46	30.12	21.78	3.59	0.982
21	100	16	22.40	31.35	16.00	5.25	1.059
22	119	17	25.06	32.65	14.29	6.00	1.150
23	102	13	26.14	33.65	12.75	6.85	1.229
24	103	13	24.58	34.65	12.62	6.92	1.308
25	102	10	27.00	35.42	9.80	9.20	1.387
26	101	10	27.26	36.19	9.90	9.10	1.464
27	101	9	28.04	36.88	8.91	10.22	1.542
28	102	9	28.22	37.58	8.82	10.33	1.620
29	103	10	27.16	38.35	9.71	9.30	1.700
30	102	10	29.10	39.12	9.80	9.20	1.778
31	102	9	29.88	39.81	8.82	10.33	1.857
32	101	8	30.84	40.42	7.92	11.63	1.934
33	102	8	31.66	41.04	7.84	11.75	2.013
34	101	7	30.82	41.58	6.93	13.43	2.090
35	101	7	31.64	42.12	6.93	13.43	2.168
36	104	7	32.50	42.65	6.73	13.86	2.248
37	100	5	33.20	43.04	5.00	19.00	2.325

Polymer Slug Size = 1.00 PVbw
Emulsion slug size = 1.00 PVbw

Table A.13

PRODUCTION HISTORY FOR RUN 13

Porosity, ø = 36.2%
kabs = 17.0 μm2
kowr = 15.8 μm2
IOIP = 1334 ml
Soi = 0.960

Sample No.	Sample. Vol. (ml)	Oil Vol. (ml)	Inj. Press. kPa	Cum. Oil Rec. %IOIP	Oil Cut %	WOR	Fluid Prod. HCPV
1	68.46	16.5	216.25	1.24	24.10	3.15	0.051
2	69.46	12.5	216.25	2.17	18.00	4.56	0.103
3	68.96	12	218.50	3.07	17.40	4.75	0.155
4	69.46	11.5	221.75	3.94	16.56	5.04	0.207
5	69.96	12	222.50	4.84	17.15	4.83	0.260
6	68.48	11.5	222.75	5.70	16.80	4.95	0.311
7	68.46	12.5	224.00	6.63	18.26	4.48	0.362
8	68.46	14	116.25	7.68	20.45	3.89	0.414
9	69.96	17	92.75	8.96	24.30	3.12	0.466
10	68.46	18.5	118.00	10.35	27.02	2.70	0.517
11	68.46	25.5	144.25	12.26	37.25	1.68	0.569
12	68.46	30.5	166.00	14.54	44.55	1.24	0.620
13	68.96	35	198.00	17.17	50.75	0.97	0.672
14	70.46	38.5	225.00	20.05	54.64	0.83	0.724
15	118.46	75.5	258.25	25.71	63.73	0.57	0.813
16	118.46	72.5	289.00	31.15	61.20	0.63	0.902
17	118.46	68.5	302.25	36.28	57.83	0.73	0.991
18	75.96	36	308.75	38.98	47.39	1.11	1.048
19	117.46	50.5	321.25	42.77	42.99	1.33	1.136
20	118.46	33.5	321.25	45.28	28.28	2.54	1.225
21	118.46	21.5	324.00	46.89	18.15	4.51	1.314
22	118.46	17.5	325.25	48.20	14.77	5.77	1.402
23	119.46	15.5	320.75	49.36	12.98	6.71	1.492
24	118.46	11.5	317.75	50.23	9.71	9.30	1.581
25	117.46	10	316.25	50.98	8.51	10.75	1.669
26	188.46	11.5	316.25	51.84	6.10	15.39	1.810

Polymer Slug Size = 0.75 PVbw
Emulsion Slug Size = 0.75 PVbw

Table A.14

PRODUCTION HISTORY FOR RUN 14

Porosity, φ = 36.0%
kabs = 17.0 μm2
kowr = 15.0 μm2
IOIP = 804 ml
Soi = 0.920

Sample No.	Sample Vol. (ml)	Oil Vol. (ml)	Inj. Press. kPa	Cum. Oil Rec. % IOIP	Oil Cut %	WOR	Fluid Prod. HCPV
1	49.9	6.9	13.50	0.86	13.83	6.23	0.062
2	52	8	16.50	1.85	15.38	5.50	0.127
3	50	3	18.25	2.23	6.00	15.67	0.189
4	53	3	16.50	2.60	5.66	16.67	0.255
5	56	3	15.50	2.97	5.36	17.67	0.324
6	49.9	3.9	15.25	3.46	7.82	11.79	0.387
7	52	4	15.50	3.95	7.69	12.00	0.451
8	50	3	15.25	4.33	6.00	15.67	0.513
9	51	3	15.75	4.70	5.88	16.00	0.577
10	50	4	16.50	5.20	8.00	11.50	0.639
11	50.5	3.5	18.20	5.63	6.93	13.43	0.702
12	51	4	18.50	6.13	7.84	11.75	0.765
13	51	4	18.23	6.63	7.84	11.75	0.829
14	100	12	21.05	8.12	12.00	7.33	0.953
15	99	9	23.75	9.24	9.09	10.00	1.076
16	103	14	25.83	10.98	13.59	6.36	1.204
17	101	21	28.90	13.59	20.79	3.81	1.330
18	100	27	30.73	16.95	27.00	2.70	1.454
19	100	32	32.08	20.93	32.00	2.13	1.579
20	100	40	18.15	25.90	40.00	1.50	1.703
21	100	40	15.28	30.88	40.00	1.50	1.827
22	100	35	220.00	35.23	35.00	1.86	1.952
23	102	29	237.50	38.84	28.43	2.52	2.078
24	100	22	232.90	41.57	22.00	3.55	2.203
25	102	20	270.00	44.06	19.61	4.10	2.330
26	45	7	279.50	44.93	15.56	5.43	2.386
27	497	47	279.50	50.78	9.46	9.57	3.004
28	270	10	279.50	52.02	3.70	26.00	3.340
29	218	8	279.50	53.02	3.67	26.25	3.611
30	100	4.8	279.50	53.61	4.80	19.83	3.735

Polymer Slug Size = 1.00 PVbw
Emulsion Slug Size = 1.00 PVbw

Table A.15

PRODUCTION HISTORY FOR RUN 15

Porosity, ø = 36.0%
kabs = 22.6 µm2
kowr = 17.4 µm2
IOIP = 1196 ml
Soi = 0.911

Sample No.	Sample. Vol. (ml)	Oil Vol. (ml)	Inj. Press. kPa	Cum. Oil Rec. % IOIP	Oil Cut %	WOR	Fluid Prod. HCPV
1	50	26	11.40	2.17	52.00	0.92	0.039
2	50.5	17	13.40	3.59	33.66	1.97	0.079
3	50.5	14	15.00	4.76	27.72	2.61	0.118
4	50	12	15.24	5.77	24.00	3.17	0.157
5	50	8	18.00	6.44	16.00	5.25	0.197
6	51.5	8.5	19.92	7.15	16.50	5.06	0.237
7	50	10	22.80	7.98	20.00	4.00	0.276
8	50	13	24.42	9.07	26.00	2.85	0.315
9	28	13	2.72	10.16	46.43	1.15	0.337
10	50	25	28.12	12.25	50.00	1.00	0.376
11	50.2	28.2	31.00	14.60	56.18	0.78	0.416
12	50.2	24.2	30.92	16.63	48.21	1.07	0.455
13	40	28	30.34	18.97	70.00	0.43	0.486
14	54.5	29	29.12	21.39	53.21	0.88	0.529
15	50	27	27.60	23.65	54.00	0.85	0.568
16	41.5	31.5	26.78	26.28	75.90	0.32	0.600
17	101	72	86.00	32.30	71.29	0.40	0.680
18	100	57	90.20	37.07	57.00	0.75	0.758
19	101.5	53.5	92.60	41.54	52.71	0.90	0.837
20	101.5	51.5	91.20	45.84	50.74	0.97	0.917
21	100	42	88.00	49.35	42.00	1.38	0.995
22	101	28	97.00	51.69	27.72	2.61	1.074
23	100.5	19.5	94.00	53.32	19.40	4.15	1.153
24	100	15	94.00	54.58	15.00	5.67	1.231
25	100	12	91.80	55.58	12.00	7.33	1.309
26	100	10	100.00	56.42	10.00	9.00	1.388
27	100	7	103.40	57.00	7.00	13.29	1.466
28	100	5	102.00	57.42	5.00	19.00	1.544
29	100	4.8	103.40	57.82	4.80	13.83	1.623

Polymer Slug Size = 1.00 PVbw
Emulsion Slug Size = 1.00 PVbw

Table A.16

PRODUCTION HISTORY FOR RUN 16

Porosity, φ = 36.0%
kabs = 18.1 μm2
kowr = 15.1 μm2
IOIP = 1296 ml
Soi = 0.915

Sample No.	Sample Vol. (ml)	Oil Vol. (ml)	Inj. Press. kPa	Cum. Oil Rec. % IOIP	Oil Cut %	WOR	Fluid Prod. HCPV
1	51	14.5	25.40	1.12	28.43	2.52	0.039
2	51	9	27.40	1.81	17.65	4.67	0.079
3	52	9	30.60	2.51	17.31	4.78	0.119
4	50.5	9	32.20	3.20	17.82	4.61	0.158
5	50	8	36.98	3.82	16.00	5.25	0.196
6	50.2	6.2	40.60	4.30	12.35	7.10	0.235
7	50.5	6.5	43.40	4.80	12.87	6.77	0.274
8	50.5	7	48.20	5.34	13.86	6.21	0.313
9	50.2	7.2	50.60	5.90	14.34	5.97	0.352
10	50	9	53.40	6.59	18.00	4.56	0.390
11	50	14	21.00	7.67	28.00	2.57	0.429
12	29	15	20.20	8.83	51.72	0.93	0.451
13	50	18	51.80	10.22	36.00	1.78	0.490
14	50	23	50.20	11.99	46.00	1.17	0.528
15	50.2	27.2	47.80	14.09	54.18	0.85	0.567
16	27	15	46.20	15.25	55.56	0.80	0.588
17	101	65	70.80	20.26	64.36	0.55	0.666
18	101	62	92.00	25.05	61.39	0.63	0.744
19	101	59	100.40	29.60	58.42	0.71	0.822
20	101	55	81.60	33.84	54.46	0.84	0.900
21	101	41	102.40	37.01	40.59	1.46	0.978
22	101	28	106.00	39.17	27.72	2.61	1.056
23	101	24	108.40	41.02	23.76	3.21	1.134
24	101	18	110.40	42.41	17.82	4.61	1.211
25	101	14	83.00	43.49	13.86	6.21	1.289
26	101	7	94.40	44.03	6.93	13.43	1.367
27	102	7	108.00	44.57	6.86	13.57	1.446
28	102	6	91.60	45.03	5.88	16.00	1.525
29	100	4.8	106.80	45.40	4.80	19.83	1.602

Polymer Slug Size = 1.00 PVbw
Emulsion Slug Size = 1.00 PVbw

Table A.17

PRODUCTION HISTORY FOR RUN 17

Porosity, ø = 36.0%
kabs = 18.0 μm2
kowr = 15.0 μm2
IOIP = 1220 ml
Soi = 0.938

Sample No.	Sample Vol. (ml)	Oil Vol. (ml)	Inj. Press. kPa	Cum. Oil Rec. % IOIP	Oil Cut %	WOR	Fluid Prod. HCPV
1	54	10	13.00	0.82	18.52	4.40	0.044
2	50	8.5	17.80	1.52	17.00	4.88	0.085
3	50	8	18.20	2.17	16.00	5.25	0.126
4	50.5	7.5	21.60	2.79	14.85	5.73	0.168
5	50	7	28.00	3.36	14.00	6.14	0.209
6	50	7	37.20	3.93	14.00	6.14	0.250
7	50.5	6.7	39.60	4.48	13.27	6.54	0.291
8	50.5	7.5	43.40	5.10	14.85	5.73	0.332
9	50	10	8.20	5.92	20.00	4.00	0.373
10	50.5	17	46.40	7.31	33.66	1.97	0.415
11	50	26	45.80	9.44	52.00	0.92	0.456
12	50	26	43.20	11.57	52.00	0.92	0.497
13	50	26.5	40.60	13.74	53.00	0.89	0.538
14	50.5	27.5	38.60	16.00	54.46	0.84	0.579
15	50	28	35.80	18.29	56.00	0.79	0.620
16	11	8.4	12.20	18.98	76.36	0.31	0.629
17	100	73	65.00	24.96	73.00	0.37	0.711
18	100	63.5	83.00	30.17	63.50	0.57	0.793
19	100	54	97.20	34.59	54.00	0.85	0.875
20	100	45	101.80	38.28	45.00	1.22	0.957
21	100	28	106.20	40.57	28.00	2.57	1.039
22	100	20	106.40	42.21	20.00	4.00	1.121
23	100	14	114.20	43.36	14.00	6.14	1.203
24	100	10.5	116.80	44.22	10.50	8.52	1.285
25	100	9	118.40	44.96	9.00	10.11	1.367
26	73	3	118.60	45.20	4.11	23.33	1.426
27	100	7	116.00	45.78	7.00	13.29	1.508
28	100	5	118.00	46.19	5.00	19.00	1.590
29	100	4.8	118.40	46.58	4.80	19.83	1.672

Polymer Slug Size = 1.00 PVbw
Emulsion Slug Size = 1.00 PVbw

Table A.18

PRODUCTION HISTORY FOR RUN 18

Porosity, φ = 34.7%
kabs = 18.0 μm2
kower = 15.7 μm2
IOIP = 1209 ml
Soi = 0.938

Sample No.	Sample Vol. (ml)	Oil Vol. (ml)	Inj. Press. kPa	Cum. Oil Rec. % IOIP	Oil Cut %	WOR	Fluid Prod. HCPV
1	50	17	25.60	1.41	34.00	1.94	0.041
2	50.5	12.5	25.60	2.44	24.75	3.04	0.083
3	50.5	11	27.40	3.35	21.78	3.59	0.125
4	50	10	30.40	4.18	20.00	4.00	0.166
5	57	12	35.20	5.17	21.05	3.75	0.213
6	41	10.5	2.80	6.04	25.61	2.90	0.247
7	50.5	19	41.80	7.61	37.62	1.66	0.289
8	50	14	42.20	8.77	28.00	2.57	0.330
9	50.5	25	43.40	10.84	49.50	1.02	0.372
10	53	36	43.00	13.81	67.92	0.47	0.416
11	50	36.5	40.80	16.83	73.00	0.37	0.457
12	50	16	38.80	18.16	32.00	2.13	0.499
13	13	9	36.00	18.90	69.23	0.44	0.510
14	100	70	42.80	24.69	70.00	0.43	0.592
15	100.2	63	45.80	29.90	62.87	0.59	0.675
16	100	58	51.00	34.70	58.00	0.72	0.758
17	102	48	49.60	38.67	47.06	1.13	0.842
18	100	31	55.40	41.23	31.00	2.23	0.925
19	99	24	61.00	43.22	24.24	3.13	1.007
20	101	23	64.60	45.12	22.77	3.39	1.090
21	100.2	18.2	68.40	46.63	18.16	4.51	1.173
22	100	17	66.60	48.03	17.00	4.88	1.256
23	100	11	78.00	48.94	11.00	8.09	1.339
24	100	9	79.40	49.69	9.00	10.11	1.421
25	100	8	85.60	50.35	8.00	11.50	1.504
26	100	10	66.20	51.17	10.00	9.00	1.587
27	72	3	72.20	51.42	4.17	23.00	1.646
28	100	5	76.40	51.84	5.00	19.00	1.729
29	100	4.8	80.20	52.23	4.80	19.83	1.812

Polymer Slug Size = 1.00 PVbw
Emulsion Slug Size = 1.00 PVbw

Table A.19

PRODUCTION HISTORY FOR RUN 19

Porosity, ø = 36.0%
kabs = 17.3 μm2
kowr = 15.4 μm2
IOIP = 1235 ml
Soi = 0.954

Sample No.	Sample Vol. (ml)	Oil Vol. (ml)	Inj. Press. kPa	Cum. Oil Rec. % IOIP	Oil Cut %	WOR	Fluid Prod. HCPV
1	51	10	32.20	0.81	19.61	4.10	0.041
2	50.5	7.5	38.60	1.42	14.85	5.73	0.082
3	50.5	7.5	42.00	2.02	14.85	5.73	0.123
4	50.5	6.5	47.80	2.55	12.87	6.77	0.164
5	50.5	8	55.40	3.20	15.94	5.31	0.205
6	50	7	62.20	3.76	14.00	6.14	0.245
7	50.5	7	67.80	4.33	13.86	6.21	0.286
8	34	6	73.00	4.82	17.65	4.67	0.314
9	50.5	9.5	69.40	5.59	18.81	4.32	0.355
10	50.5	10.5	68.40	6.44	20.79	3.81	0.395
11	53	22	67.00	8.22	41.51	1.41	0.438
12	50.5	33.5	63.00	10.93	66.34	0.51	0.479
13	50	26.5	57.40	13.07	53.00	0.89	0.520
14	51	43	52.60	16.56	84.31	0.19	0.561
15	51	41	47.40	19.87	80.39	0.24	0.602
16	51	41	103.20	23.19	80.39	0.24	0.644
17	100	77	125.20	29.43	77.00	0.30	0.725
18	100	60	136.20	34.28	60.00	0.67	0.806
19	101	49	144.00	38.25	48.51	1.06	0.887
20	101	51	137.20	42.38	50.50	0.98	0.969
21	100	43	155.20	45.86	43.00	1.33	1.050
22	100.5	22.5	166.20	47.68	22.39	3.47	1.131
23	101	15	168.40	48.90	14.85	5.73	1.213
24	102	12	175.80	49.87	11.76	7.50	1.296
25	100	8	158.60	50.52	8.00	11.50	1.377
26	101	6	183.80	51.00	5.94	15.83	1.458
27	100	6	183.80	51.49	6.00	15.67	1.539
28	100	5	183.80	51.89	5.00	19.00	1.620
29	100	4.8	206.60	52.28	4.80	19.83	1.701

Polymer Slug Size = 1.00 PVbw
Emulsion Slug Size = 1.00 PVbw

Table A.20

PRODUCTION HISTORY FOR RUN 20

Porosity, φ = 35.5%
kabs = 17.3 μm2
kowr = 15.3 μm2
IOIP = 1295 ml
Soi = 0.933

Sample No.	Sample Vol. (ml)	Oil Vol. (ml)	Inj. Press. kPa	Cum. Oil Rec. % IOIP	Oil Cut %	WOR	Fluid Prod. HCPV
1	50	16	50.25	1.24	32.00	2.13	0.039
2	50	8	43.75	1.85	16.00	5.25	0.077
3	50.5	6.5	41.75	2.36	12.87	6.77	0.116
4	50.5	5.5	39.25	2.78	10.89	8.18	0.155
5	50.5	5.5	38.75	3.21	10.89	8.18	0.194
6	53	6	38.50	3.67	11.32	7.83	0.235
7	52.5	6.5	43.50	4.17	12.38	7.06	0.276
8	51	7	46.25	4.71	13.73	6.29	0.315
9	43	8	48.25	5.33	18.60	4.38	0.348
10	50.5	18.5	49.00	6.76	36.63	1.73	0.387
11	50.5	32	48.00	9.23	63.37	0.58	0.426
12	51	39	46.50	12.24	76.47	0.31	0.466
13	51	41	44.75	15.41	80.39	0.24	0.505
14	51	41	42.00	18.58	80.39	0.24	0.545
15	54	43	41.25	21.90	79.63	0.26	0.586
16	105	80	36.75	28.08	76.19	0.31	0.667
17	100	65	120.25	33.10	65.00	0.54	0.745
18	105	55	138.00	37.35	52.38	0.91	0.826
19	100.5	38.5	141.75	40.32	38.31	1.61	0.903
20	101	30	140.00	42.64	29.70	2.37	0.981
21	101	22	149.50	44.34	21.78	3.59	1.059
22	100.5	16.5	150.75	45.62	16.42	5.09	1.137
23	100.5	10.5	154.75	46.43	10.45	8.57	1.215
24	130.5	9.5	153.50	47.16	9.45	9.58	1.292
25	102	9	164.50	47.86	8.82	10.33	1.371
26	101	5	182.50	48.24	4.95	19.20	1.449
27	105	5	186.50	48.63	4.76	20.00	1.530
28	100	5	189.00	49.02	5.00	19.00	1.608
29	122	4	206.00	49.32	3.28	29.50	1.702

Polymer Slug Size = 1.00 PVbw
Emulsion Slug Size = 1.00 PVbw

Table A.21

PRODUCTION HISTORY FOR RUN 21

Porosity, ø = 37.6%
kabs = 18.5 µm2
kowr = 16.3 µm2
IOIP = 1313 ml
Soi = 0.923

Sample No.	Sample Vol. (ml)	Oil Vol. (ml)	Inj. Press. kPa	Cum. Oil Rec. % IOIP	Oil Cut %	WOR	Fluid Prod. HCPV
1	49.5	15.5	31.75	1.18	31.31	2.19	0.038
2	51	7	35.50	1.71	13.73	6.29	0.077
3	50	6	37.00	2.17	12.00	7.33	0.115
4	50	5	36.00	2.55	10.00	9.00	0.153
5	50	4	34.25	2.86	8.00	11.50	0.191
6	50	4	37.75	3.16	8.00	11.50	0.229
7	50.5	4.5	44.50	3.50	8.91	10.22	0.267
8	54	10	50.50	4.27	18.52	4.40	0.309
9	52	22	53.75	5.94	42.31	1.36	0.348
10	52	37	53.50	8.76	71.15	0.41	0.388
11	55	44	49.25	12.11	80.00	0.25	0.430
12	50	36	48.25	14.86	72.00	0.39	0.468
13	53	38	47.00	17.75	71.70	0.39	0.508
14	52	39	45.75	20.72	75.00	0.33	0.548
15	50	37	44.25	23.54	74.00	0.35	0.586
16	101	66	42.00	28.57	65.35	0.53	0.663
17	100	55	169.50	32.76	55.00	0.82	0.739
18	100	56	182.00	37.03	56.00	0.79	0.815
19	100	51	205.25	40.91	51.00	0.96	0.891
20	100	35	215.25	43.58	35.00	1.86	0.968
21	100	22	209.75	45.26	22.00	3.55	1.044
22	99.9	14.9	218.25	46.39	14.91	5.70	1.120
23	100	13	219.00	47.38	13.00	6.69	1.196
24	100	11	236.25	48.22	11.00	8.09	1.272
25	33	1.5	247.50	48.34	4.55	21.00	1.297
26	499	29	247.50	50.54	5.81	16.21	1.678
27	490	15	302.50	51.69	3.06	31.67	2.051

Polymer Slug Size = 1.00 PVbw
Emulsion Slug Size = 1.00 PVbw

Table A.22

PRODUCTION HISTORY FOR RUN 22

Porosity, φ = 34.8%
kabs = 18.0 μm2
kowr = 15.0 μm2
IOIP = 1212 ml
Soi = 0.933

Sample No.	Sample Vol. (ml)	Oil Vol. (ml)	Inj. Press. kPa	Cum. Oil Rec. %IOIP	Oil Cut %	WOR	Fluid Prod. HCPV
1	51	7	21.50	0.58	13.73	6.29	0.042
2	51.5	5.5	22.25	1.03	10.68	8.36	0.085
3	51.5	6.5	21.50	1.57	12.62	6.92	0.127
4	51.5	5.5	21.75	2.02	10.68	8.36	0.170
5	52	6	21.00	2.52	11.54	7.67	0.212
6	51	6	21.00	3.01	11.76	7.50	0.255
7	102	10	21.25	3.84	9.80	9.20	0.339
8	104	11	21.50	4.74	10.58	8.45	0.425
9	101	11	21.75	5.65	10.89	8.18	0.508
10	101	11.5	21.25	6.60	11.39	7.78	0.591
11	102	11	21.00	7.51	10.78	8.27	0.675
12	103	10	20.50	8.33	9.71	9.30	0.760
13	101.5	9.5	20.25	9.12	9.36	9.68	0.844
14	102	10	20.25	9.94	9.80	9.20	0.928
15	101	11	20.75	10.85	10.89	8.18	1.012
16	109	9	20.25	11.59	8.26	11.11	1.101
17	110	9	20.25	12.33	8.18	11.22	1.192
18	123	12	19.50	13.33	9.76	9.25	1.294
19	108	9	23.25	14.07	8.49	10.78	1.381
20	100.5	11.5	20.00	15.02	11.44	7.74	1.464
21	100	10	20.50	15.84	10.00	9.00	1.547
22	101	10	20.00	16.67	9.90	9.10	1.630
23	103	11	20.75	17.57	10.68	8.36	1.715
24	101	13	21.50	18.65	12.87	6.77	1.798
25	103	10	20.50	19.47	9.71	9.30	1.883
26	100	10	21.75	20.30	10.00	9.00	1.966
27	253	23	24.00	22.19	9.09	10.00	2.175
28	251	21	23.00	23.93	8.37	10.95	2.382
29	130	20	22.75	25.58	15.38	5.50	2.489

Table A.23

PRODUCTION HISTORY FOR RUN 23

Porosity, φ = 35.6%
kabs = 17.0 μm2
kowr = 15.0 μm2
IOIP = 1242 ml
Soi = 0.910

Sample No.	Sample Vol. (ml)	Oil Vol. (ml)	Inj. Press. kPa	Cum. Oil Rec. % IOIP	Oil Cut %	WOR	Fluid Prod. HCPV
1	51	19	30.25	.53	37.25	1.68	0.041
2	50.5	12.5	31.50	2.53	24.75	3.04	0.082
3	50.5	12.5	34.25	3.54	24.75	3.04	0.122
4	52	10	37.00	4.35	19.23	4.20	0.164
5	50	10	41.25	5.15	20.00	4.00	0.204
6	51	11	43.50	6.04	21.57	3.64	0.245
7	50	12.5	47.50	7.04	25.00	3.00	0.286
8	50.5	18	49.50	8.49	35.64	1.81	0.326
9	51	25	51.50	10.50	49.02	1.04	0.367
10	53	31	51.50	13.00	58.49	0.71	0.410
11	100	67	45.00	18.39	67.00	0.49	0.490
12	101	64	38.00	23.54	63.37	0.58	0.572
13	100	50	33.25	27.56	50.00	1.00	0.652
14	100.5	41.5	30.75	30.90	41.29	1.42	0.733
15	104	35	28.00	33.72	33.65	1.97	0.817
16	102	26	26.75	35.81	25.49	2.92	0.899
17	100	20	25.75	37.42	20.00	4.00	0.979
18	100	17.5	24.75	38.83	17.50	4.71	1.060
19	101	16	24.75	40.11	15.84	5.31	1.141
20	101	13	24.25	41.16	12.87	6.77	1.222
21	102	13	23.75	42.20	12.75	6.85	1.304
22	99.9	13.9	25.00	43.32	13.91	6.19	1.385
23	100	13	26.50	44.37	13.00	6.69	1.465
24	250	40	26.25	47.59	16.00	5.25	1.666
25	250	32	24.00	50.16	12.80	6.81	1.868
26	345	30	23.50	52.58	8.70	10.50	2.145

Polymer Slug Size = 1.00 PVbw
Emulsion Slug Size = 1.00 PVbw

Table A.24

PRODUCTION HISTORY FOR RUN 24

Porosity, ø = 37.6%
kabs = 18.5 µm2
kowr = 16.2 µm2
IOIP = 1275 ml
Soi = 0.960

Sample No.	Sample Vol. (ml)	Oil Vol. (ml)	Inj. Press. kPa	Cum. Oil Rec. % IOIP	Oil Cut %	WOR	Fluid Prod. HCPV
1	50.5	40.5	26.70	3.18	80.20	0.25	0.040
2	50	42	26.03	6.47	84.00	0.19	0.079
3	50.5	36	26.38	9.30	71.29	0.40	0.118
4	100	47	26.33	12.98	47.00	1.13	0.197
5	101	39	26.30	16.04	38.61	1.59	0.276
6	100	32	24.38	18.55	32.00	2.13	0.355
7	100	28	25.58	20.75	28.00	2.57	0.433
8	102	24	26.93	22.63	23.53	3.25	0.513
9	100	23	22.53	24.44	23.00	3.35	0.592
10	100	23	23.30	26.24	23.00	3.35	0.670
11	105	22	22.53	27.97	20.95	3.77	0.752
12	100	18	23.05	29.38	18.00	4.56	0.831
13	101	16	20.85	30.64	15.84	5.31	0.910
14	100	15	19.88	31.81	15.00	5.67	0.989
15	101	14	19.83	32.91	13.86	6.21	1.068
16	108	15	19.58	34.09	13.89	6.20	1.152
17	104	12.5	19.35	35.07	12.02	7.32	1.234
18	101	15	19.00	36.25	14.85	5.73	1.313
19	101	15	20.80	37.42	14.85	5.73	1.393
20	105	13	19.80	38.44	12.38	7.08	1.475
21	102	12	19.80	39.38	11.76	7.50	1.555
22	252	22	18.60	41.11	8.73	10.45	1.753
23	255	19	18.50	42.60	7.45	12.42	1.953
24	101	13	18.55	43.62	12.87	6.77	2.032
25	103	10	18.58	44.41	9.71	9.30	2.113
26	100	10	18.50	45.19	10.00	9.00	2.191

Table A.25

PRODUCTION HISTORY FOR RUN 25

Porosity, φ = 37.6%
kabs = 17.8 μm2
kowr = 15.1 μm2
IOIP = 1252 ml
Sol = 0.912

Sample No	Sample Vol (ml)	Oil Vol (ml)	Inj Press kPa	Cum Oil Rec %IOIP	Oil Cut %	WOR	Fluid Prod HCPV
1	50	29	44.25	2.32	58.00	0.72	0.040
2	50	24	47.75	4.23	48.00	1.08	0.080
3	50.5	25	51.50	6.23	49.50	1.02	0.120
4	50.5	24	53.75	8.14	47.52	1.10	0.160
5	50.5	23.5	54.75	10.02	46.53	1.15	0.201
6	52	26	55.25	12.10	50.00	1.00	0.242
7	50	26	57.00	14.17	52.00	0.92	0.282
8	51	27	58.00	16.33	52.94	0.89	0.323
9	50	27	59.25	18.48	54.00	0.85	0.363
10	50	28	60.75	20.72	56.00	0.79	0.403
11	50	31	58.00	23.19	62.00	0.61	0.443
12	50	30	55.25	25.59	60.00	0.67	0.483
13	50	30	56.25	27.98	60.00	0.67	0.523
14	50	30	56.75	30.38	60.00	0.67	0.562
15	99	58	59.00	35.01	58.59	0.71	0.642
16	100	49	60.75	38.92	49.00	1.04	0.721
17	101	30	62.50	41.32	29.70	2.37	0.802
18	101	25	56.25	43.31	24.75	3.04	0.883
19	101	22	63.00	45.07	21.78	3.59	0.963
20	100	19	67.50	46.59	19.00	4.26	1.043
21	101	17	68.75	47.94	16.83	4.94	1.124
22	100	14	70.75	49.06	14.00	6.14	1.204
23	103	13	72.25	50.10	12.62	6.92	1.286
24	103	13	73.50	51.14	12.62	6.92	1.368
25	105	12	74.75	52.10	11.43	7.75	1.452
26	104	11	82.75	52.97	10.58	8.45	1.535
27	110	10	81.50	53.77	9.09	10.00	1.623
28	100	8	87.00	54.41	8.00	11.50	1.703
29	101	9.5	93.00	55.17	9.41	9.63	1.783
30	105	9	39.00	55.89	8.57	10.67	1.867
31	101	7	39.25	56.45	6.93	13.43	1.948
32	102	7	42.00	57.01	6.86	13.57	2.029
33	155	3	43.25	57.25	1.94	50.67	2.153

Polymer Slug Size = 1.00 PVbw
Emulsion Slug Size = 1.00 PVbw

Table A.26

PRODUCTION HISTORY FOR RUN 26

Porosity, Φ = 37.6%
kabs = 17.0 μm2
kowr = 15.0 μm2
IOIP = 1258 ml
Soi = 0.922

Sample No.	Sample Vol. (ml)	Oil Vol. (ml)	Inj. Press. kPa	Cum. Oil Rec. % IOIP	Oil Cut %	WOR	Fluid Prod. HCPV
1	50	37	44.25	2.94	74.00	0.35	0.040
2	50.5	28.5	43.50	5.21	56.44	0.77	0.080
3	50	20	41.00	6.80	40.00	1.50	0.120
4	52	16	40.75	8.07	30.77	2.25	0.161
5	50	14	40.50	9.18	28.00	2.57	0.201
6	51	13	40.50	10.22	25.49	2.92	0.241
7	52	13	39.75	11.25	25.00	3.00	0.283
8	51	12	39.75	12.20	23.53	3.25	0.323
9	51	11	39.50	13.08	21.57	3.64	0.364
10	54	11	39.25	13.95	20.37	3.91	0.407
11	100	22	39.50	15.70	22.00	3.55	0.486
12	100	22	40.30	17.45	22.00	3.55	0.566
13	101	21	39.75	19.12	20.79	3.81	0.646
14	100	21	39.00	20.79	21.00	3.76	0.726
15	100	20	38.75	22.38	20.00	4.00	0.805
16	103	17	38.50	23.73	16.50	5.06	0.887
17	101	16	40.00	25.00	15.84	5.31	0.967
18	99.8	15.3	38.25	26.22	15.33	5.52	1.047
19	100	14	38.00	27.33	14.00	6.14	1.126
20	100	14	37.50	28.45	14.00	6.14	1.206
21	104	13	37.25	29.48	12.50	7.00	1.288
22	101	11	37.25	30.36	10.89	8.18	1.369
23	100.5	10.5	36.75	31.19	10.45	8.57	1.448
24	101	9	36.75	31.91	8.91	10.22	1.529
25	102	10	35.75	32.70	9.80	9.20	1.610
26	100	10	37.50	33.50	10.00	9.00	1.689
27	250	20	35.75	35.09	8.00	11.50	1.888
28	50	4	35.75	35.40	8.00	11.50	1.928

Table A.27

PRODUCTION HISTORY FOR RUN 27

Porosity, φ = 37.6%
kabs = 17.2 μm2
kowr = 15.5 μm2
IOIP = 1256 ml
Soi = 0.922

Sample No.	Sample Vol. (ml)	Oil Vol. (ml)	Inj. Press. kPa	Cum. Oil Rec. % IOIP	Oil Cut %	WOR	Fluid Prod. HCPV
1	50.5	45	54.5	3.58	89.11	0.122	0.040
2	50	35.5	53.25	6.41	71.00	0.408	0.080
3	50	29	55	8.72	58.00	0.724	0.120
4	53	25	57	10.71	47.17	1.120	0.162
5	50	20	59.5	12.31	40.03	1.500	0.202
6	50	19	64.5	13.82	38.00	1.632	0.242
7	50.5	18.5	71.25	15.29	36.63	1.730	0.282
8	50	20	73.5	16.89	40.00	1.500	0.322
9	55	25	75.5	18.88	45.45	1.200	0.366
10	50	25	75.75	20.87	50.00	1.000	0.405
11	51	28.5	68	23.14	55.88	0.789	0.446
12	53	30	67.5	25.53	56.60	0.767	0.488
13	53	30	64.75	27.92	56.60	0.767	0.530
14	57	32	63.5	30.47	56.14	0.781	0.576
15	104	59	57.5	35.17	56.73	0.763	0.659
16	100	37	50.25	38.11	37.00	1.703	0.738
17	100	22	49.5	39.86	22.00	3.545	0.818
18	100	17	49.25	41.22	17.00	4.882	0.898
19	100	15	50.75	42.41	15.00	5.667	0.977
20	110	17	53.5	43.77	15.45	5.471	1.065
21	101	15	55.25	44.96	14.85	5.733	1.145
22	112	17	57.75	46.32	15.18	5.588	1.235
23	100	14	57.5	47.43	14.00	6.143	1.314
24	102	13	57.5	48.47	12.75	6.846	1.395
25	101	12	60	49.42	11.88	7.417	1.476
26	101	11	64	50.30	10.89	8.182	1.556
27	101	11	65	51.17	10.89	8.182	1.637
28	100	10	67.75	51.97	10.00	9.000	1.716
29	115	10	52	52.77	8.70	10.500	1.808
30	250	20	57.75	54.36	8.00	11.500	2.007
31	197	11	60.75	55.24	5.58	16.909	2.164

Polymer Slug Size = 1.00 PVbw
Emulsion Slug Size = 1.00 PVbw

Table A.28

PRODUCTION HISTORY FOR RUN 28

Porosity, ø = 35.7%
kabs = 18.5 μm2
kowr = 16.1 μm2
IOIP = 1245 ml
Soi = 0.948

Sample No.	Sample. Vol. (ml)	Oil Vol. (ml)	Inj. Press. kPa	Cum. Oil Rec. % IOIP	Oil Cut %	WOR	Fluid Prod. HCPV
1	51.5	34.5	26.89	2.77	66.99	0.49	0.041
2	50	22.5	28.27	4.56	45.00	1.22	0.082
3	51	18	31.37	6.02	35.29	1.83	0.122
4	51	17.5	33.44	7.43	34.31	1.91	0.163
5	52	22	38.27	9.20	42.31	1.36	0.205
6	100.5	55.5	33.44	13.65	55.22	0.81	0.286
7	101.5	69.5	31.37	19.24	68.47	0.46	0.367
8	100	77	27.58	25.42	77.00	0.30	0.448
9	100	79.5	24.13	31.81	79.50	0.26	0.528
10	100	78	22.41	38.07	78.00	0.28	0.608
11	100.5	70	18.96	43.69	69.65	0.44	0.689
12	101	61.5	16.20	48.63	60.89	0.64	0.770
13	100	52.5	13.79	52.85	52.50	0.90	0.851
14	101	42.5	12.07	56.27	42.08	1.38	0.932
15	100	30	9.65	58.67	30.00	2.33	1.012
16	100	22	9.65	60.44	22.00	3.55	1.092
17	100	15.5	9.31	61.69	15.50	5.45	1.173
18	100	12	9.31	62.65	12.00	7.33	1.253
19	100	9	8.96	63.37	9.00	10.11	1.333
20	100.5	7.5	8.62	63.98	7.46	12.40	1.414
21	106	9.5	8.96	64.74	8.96	10.16	1.499
22	100	7.5	8.96	65.34	7.50	12.33	1.580
23	100	5.5	9.31	65.78	5.50	17.18	1.660
24	100	4	10.00	66.10	4.00	24.00	1.740
25	101	3	10.69	66.35	2.97	32.67	1.821
26	250	11	7.58	67.23	4.40	21.73	2.022

Polymer Slug Size = 1.00 PVbw
Emulsion Slug Size = 1.00 PVbw

Table A.29

PRODUCTION HISTORY FOR RUN 29

Porosity, φ = 35.5%
kabs = 18.6 μm2
kowr = 16.4 μm2
IOIP = 1238 ml
Soi = 0.943

Sample No.	Sample Vol. (ml)	Oil Vol. (ml)	Inj. Press. kPa	Cum. Oil Rec. % IOIP	Oil Cut %	WOR	Fluid Prod. HCPV
1	50	19	33.79	1.53	38.00	1.63	0.040
2	50	14	38.96	2.67	28.00	2.57	0.081
3	50	12.5	43.44	3.68	25.00	3.00	0.121
4	51	12	45.16	4.64	23.53	3.25	0.162
5	50	11	47.23	5.53	22.00	3.55	0.203
6	100	32.5	46.89	8.16	32.50	2.08	0.284
7	100	69	43.44	13.73	69.00	0.45	0.364
8	100	75	37.58	19.79	75.00	0.33	0.445
9	108	73	31.72	25.69	67.59	0.48	0.532
10	100.5	52.5	27.92	29.93	52.24	0.91	0.613
11	100	44	25.17	33.48	44.00	1.27	0.694
12	100	37	22.75	36.47	37.00	1.70	0.775
13	100	30	20.69	38.89	30.00	2.33	0.856
14	100	25	20.00	40.91	25.00	3.00	0.937
15	100	20	18.96	42.53	20.00	4.00	1.017
16	102	14.5	18.27	43.70	14.22	6.03	1.100
17	100.5	9.5	17.58	44.47	9.45	9.58	1.181
18	100	10	17.24	45.27	10.00	9.00	1.262
19	100	10	16.89	46.08	10.00	9.00	1.342
20	101	11.5	14.13	47.01	11.39	7.73	1.424
21	100	9	14.13	47.74	9.00	10.11	1.505
22	100.5	8.5	13.45	48.42	8.46	10.82	1.586
23	100	7	13.10	48.99	7.00	13.29	1.667
24	100.5	7.5	13.10	49.60	7.46	12.40	1.748
25	100	7	12.41	50.16	7.00	13.29	1.829
26	100.5	6.5	11.38	50.69	6.47	14.46	1.910
27	100	4.5	11.03	51.05	4.50	21.22	1.991
28	510	30	9.65	53.47	5.88	16.00	2.403
29	1000	17	9.65	54.85	1.70	57.82	3.210

Emulsion Slug Size = 1.00 PVbw
Polymer Slug Size = 1.00 PVbw

APPENDIX B: Computer Program for the Semi-Analytical Model

PROGRAM FOR CROSSFLOW CALCULATIONS AND OIL RECOVERY PREDICTIONS

```c
#include "define.h"
dataread(direcname)
char *direcname;
{
  FILE *f5;
  int  i, k;
  char  infile[80];

  strcpy(infile,direcname); strcat(infile,"/");
  strcat(infile,"input.dat");
  if ((f5 = fopen(infile,"rt")) != NULL) {
    fscanf(f5,"%lf %lf\n",&del_Qical, &Qi_end);
    fscanf(f5,"%lf %lf %lf %lf\n",&corelength, &corewidth, &h[1], &h[2]);
    fscanf(f5,"%lf %lf %lf %lf\n",&kd, &porosity, &swi_top, &swi_bottom);
    fscanf(f5,"%lf %lf %lf %lf %lf %lf", &siw, &sor, &krw_end, &np,
          &kro_end, &mp);
    fscanf(f5,"%lf %lf %lf\n", &visco_water, &visco_emul, &visco_oil);
    fscanf(f5,"%d\n", &sequence_no);
      for (k=1;k<=sequence_no;k++) {
      fscanf(f5,"%d %lf ", &slug_spec[k], &slug_size[k]);
        for (i=1;i<=2;i++) fscanf(f5,"%lf ", &pol_conc[i][k]);
        for (i=1;i<=2;i++) fscanf(f5,"%lf ", &emul_conc[i][k]);
        for (i=1;i<=2;i++) fscanf(f5,"%lf ", &inj_rate[i][k]);
      fscanf(f5,"\n");
    }
    fscanf(f5,"%lf %lf %lf %lf\n", &k1, &k2, &k3, &k4);
  } else {
    printf("Datafile [ %s ] is not found!!\n",infile);
    exit(1);
  }
  fclose(f5);
}
```

DATA INITIALIZATION

```
#include "define.h"

void data_initialize(section_no, bt_flag, direcname)
int   *section_no, bt_flag[];
char *direcname;
{
    int  i,j,k ;
    char  ss[80], outfile[80];
    FILE *f6;

    /* Setting of output files */

    strcpy(ss,direcname); strcat(ss,"/");
    strcpy(outfile,ss); strcat(outfile,"summary.res");
    f6 = fopen(outfile,"w");
    close(f6);
    strcpy(outfile,ss); strcat(outfile,"total_prod.res");
    f6 = fopen(outfile,"w");
    close(f6);
    strcpy(outfile,ss); strcat(outfile,"layer1_prod.res");
    f6 = fopen(outfile,"w");
    close(f6);
    strcpy(outfile,ss); strcat(outfile,"layer2_prod.res");
    f6 = fopen(outfile,"w");
    close(f6);
    strcpy(outfile,ss); strcat(outfile,"profile_sw.res");
    f6 = fopen(outfile,"w");
    close(f6);
    strcpy(outfile,ss); strcat(outfile,"profile_qc.res");
    f6 = fopen(outfile,"w");
    close(f6);
    strcpy(outfile,ss); strcat(outfile,"profile_kro.res");
    f6 = fopen(outfile,"w");
    close(f6);
    strcpy(outfile,ss); strcat(outfile,"profile_krw.res");
    f6 = fopen(outfile,"w");
    close(f6);
    strcpy(outfile,ss); strcat(outfile,"profile_visco.res");
    f6 = fopen(outfile,"w");
    close(f6);
    strcpy(outfile,ss); strcat(outfile,"profile_L.res");
    f6 = fopen(outfile,"w");
    close(f6);
    strcpy(outfile,ss); strcat(outfile,"profile_cp.res");
    f6 = fopen(outfile,"w");
    close(f6);
    strcpy(outfile,ss); strcat(outfile,"profile_ce.res");
    f6 = fopen(outfile,"w");
    close(f6);
```

```
/* Setting of constant values to specific variables */

*section_no = 3;
swor = 1.0 - sor;
sw_mobile = 1.0 - sor - siw;
for (i=1;i<=2;i++) A[i] = corewidth*h[i];
IOIP = (1.0 - swi_top)*A[1]*corelength*porosity;
a[1] = A[1]*porosity*sw_mobile;
a[2] = A[2]*porosity;
porevol[1] = A[1]*porosity*corelength;
porevol[2] = a[2]*corelength;

for (i=1;i<=2;i++) {
        for (k=1;k<=sequence_no;k++) inj_rate[i][k] /= 3600.0;
}
for (k=1;k<=sequence_no;k++) {
        slug_vol[k] = slug_size[k]*porevol[2];
        Qi_slug [k] = 10000.0;
}


/* Assignment of initial values */

for (i=1;i<=2;i++) {
        q_inj[i] = inj_rate[i][1];
        cp_i [i] = pol_conc[i][1];
        ce_i [i] = emul_conc[i][1];
}

del_t = del_t0 = del_Qical*IOIP / (q_inj[1] + q_inj[2]);
del_Qical0 = del_Qical;

total_Qi = ttime = 0.0;
prod_fo  = 1.0;
er = wor = cum_wor = 0.0 ;
total_prod_rate = total_oil_rate = total_water_rate = prod_fw = 0.0;
prod_water = prod_oil = prod_total = cum_oil_prod = cum_water_prod = 0.0;
oil_cut[1]  = 1.0;  oil_cut[2]  = 0.0;
water_cut[1] = 0.0;  water_cut[2] = 1.0;

for (i=0;i<= 2;i++) {
   Xf[i] = 0.0;
   del_oil[i] = del_water[i] = oil_rate[i] = water_rate[i]
           = prod_rate[i] = cum_inj [i] = 0.0;
   bt_flag[i] = 0;
   for (j=1;j<=*section_no;j++) {
       L [i][j] = 0.0;
       cp[i][j] = 0.0;
       ce[i][j] = 0.0;
   }
}
for (j=1;j<=*section_no;j++) fw_qc[j] = cp_qc[j] = ce_qc[j] = 0.0;

L [1][3] = L [2][3] = corelength;
```

```
    sw[1][1] = sw[1][2] = sw[1][3] = swi_top;
    sw[2][1] = sw[2][2] = sw[2][3] = swi_bottom;
    cp[1][1] = cp[1][2] = cp_qc[1] = cp_i[1];
    ce[1][1] = ce[1][2] = ce_qc[1] = ce_i[1];
    cp[2][1] = cp[2][2] = cp_i[2];
    ce[2][1] = ce[2][2] = ce_i[2];
}
```

MAIN PROGRAM

```
#include "define.h"
main(argc,argv)
int  argc;
char *argv[];
{
    int   i, k, section_no, seq_no, bt_flag[NL], afbt_flag[NL];
    double cum_slug[NL];
    char   direcname[80];

    if (argc != 2) {
    printf("This program requires one parameter!!\n");
    printf("Ex. of Usage:  crosflow-v2 run_nl\n");
    exit(1);
    }
    strcpy(direcname,argv[1]); strcat(direcname,"/");

    dataread(direcnar
      ata_initialize(&    ion_no, bt_flag, direcname);

    /* Calculation at time_step = 1 */
    for (i=1;i<=z;i++) cum_slug[i] = 0.0;
    seq_no  = 1;
    crossflow_calc0(&section_no);
    fileout_result(direcname);

    /* Calculation at time_step = 2 */
    total_Qi += del_Qical;
    ttime  += del_t;
    front_calc0(&section_no, bt_flag);
    performance_calc(&section_no, bt_flag, afbt_flag);
    crossflow_calc1(&section_no);
    fileout_result(direcname);

    do {
        switch(section_no) {
          case 1:  sw_end[1] = sw[1][1];
                   sw_end[2] = sw[2][1];
               performance_calc(&section_no, bt_flag, afbt_flag);
                 front_calc1();
                   break;
          case 2:  front_calc2(&section_no, bt_flag);
               performance_calc(&section_no, bt_flag, afbt_flag);
                   break;
          case 3:  front_calc3(&section_no, bt_flag);
               performance_calc(&section_no, bt_flag, afbt_flag);
                   break;
          default: printf("Calculation error!\n");
                   printf("section_no = %d\n", section_no);
                   exit();
        }
        printf("Qi= %10.5e q_inj[1]= %10.5e q_inj[2]= %10.5e\n",
```

```
                total_Qi, q_inj[1], q_inj[2]);
    total_Qi += del_Qical;
    ttime    += del_.;
      if ((cum_inj[k=slug_spec[seq_no]] - cum_slug[k]) >= slug_vol[seq_no])
      {
        Qi_slug[seq_no] = total_Qi;
        seq_no++;
        for (i=1;i<=2;i++) {
            cum_slug[i] = cum_inj[i];
          q_inj  [i] = inj_rate [i][seq_no];
          cp_i   [i] = pol_conc [i][seq_no];
          ce_i   [i] = emul_conc[i][seq_no];
      }
      }
    crossflow_calc1(&section_no);
    fileout_result(direcname);
  } while ( total_Qi < Qi_end );
  fileout_summary(direcname, bt_flag);
}
```

CROSSFLOW CALCULATIONS

```
include "define.h"
void crossflow_calc(bt_flag)
int bt_flag[];
{

    int        i, j, k, bbt_flag[NL];
    double    water_viscosity(), o_rperm( ), w_rperm( );

    for (k=1;k <= 2;k++) {
        if (bt_flag[k] == 1) {
            Xf[k] = corelength;
            for (i=1;i<=2;i++) {
                L[i][3] = L[i][2];  L[i][2] = 0.0;
                sw[i][3] = sw[i][2];
                cp[i][3]  = cp[i][2];
            }
        }
    }

/* [STEP 1] Evaluate viscosity of aqueous phase, relative permeability,
    mobility, mobility ratio and alpha in each zone and value of m in
    each section.
*/

    for (j=1;j<=3;j++) {
        for (i=1;i<=2;i++) {
            visco_w[i][j] = water_viscosity(cp[i][j]);
            /* viscosity is temporarily assumed to be a function of polymer concentration */
            krw[i][j] = w_rperm(sw[i][j]);
            kro[i][j]  = o_rperm(sw[i][j]);
            rmob[i][j] = krw[i][j] / visco_w[i][j] + kro[i][j] / visco_oil;
        }
        rmob_ratio[1][j] = rmob[1][j] / rmob[2][j];
        rmob_ratio[2][j] = rmob[2][j] / rmob[1][j];
        alpha[1][j] = 2.0 / (h[1]*h[1] + h[1]*h[2]*rmob_ratio[1][j]);
        alpha[2][j] = 2.0 / (h[2]*h[2] + h[1]*h[2]*rmob_ratio[2][j]);
        m[j] = alpha[1][j] + alpha[2][j];
        root_m[j] = sqrt(m[j]);
    }

/* [STEP 2] Evaluate crossflow rate in each section, water cut and
    polymer concentration of crossflowed fluid.
*/

    c3[1] = (rmob_ratio[1][1]*h[1] / h[2]*Q_i[2] - Q_i[1]) / rmob[1][1]
            / root_m[1] / cosh(corelength*root_m[1]);

    for (j=2;j<=3;j++)   c3[j] = c3[j-1]*sinh(root_m[j-1]*(corelength - Xf[j-1])
                                / sinh(root_m[j]*(corelength - Xf[j-1]));

    for (j=1;j<=3;j++) {
```

```
qc[j] = rmob[1][j]*alpha[1][j]*c3[j] / root_m[j]*(cosh(root_m[j]*
          (corelength - Xf[j])) - cosh(root_m[j]*(corelength - Xf[j-1])));
if (qc[j] > 0)  {
    fw_qc[j] = (sw[1][j] - siw) / sw_mobile;
    cp_qc [j] = cp[1][j];
} else {
    fw_qc[j] = sw[2][j];
    cp_qc [j] = cp[2][j];
}
    }
}
```

FRONT CALCULATION

```
#include "define.h"
void front_calc0(section_no, bt_flag)
int   *section_no, bt_flag[];
{
    int    i, j, k, repeat_flag;
    double  sw_a, sw_b, sw_c, sw_d, sw_e, sw_f, del_l, lcd,
         sw1, sw2, deltaL_qi[NL], del_qc[NS],
         L_temp[NL][NS], deltaL_qc[NL][NS];

/* [STEP1] Calculation of frontal location of each section at time n' */

    for (i=1;i<=2;i++)  deltaL_qi[i] = q_inj[i]*del_t / a[i];
    for (j=1;j<=3;j++)  {
       del_qc[j]  = qc[j]*del_t;
       for (i=1;i<=2;i++)  {
          L_temp  [i][j]  = L[i][j];
          deltaL_qc[i][j]  = del_qc[j]/a[i];
       }
    }


    /* ------------------------------------------------------
          Old definition of each zone
          la = L[1][1], lc = L[1][2], le = L[1][3],
          lb = L[2][1], ld = L[2][2], lf = L[2][3]
       ------------------------------------------------------  */

    L[1][1] += deltaL_qi[1] - deltaL_qc[1][3];
    L[2][1] += deltaL_qi[2] + deltaL_qc[2][3];
    L[1][2] -= deltaL_qc[1][2];
    L[2][2] += deltaL_qc[2][2];
    for (i=1;i<=2;i++)  {
       L[i][3]  = corelength - L[i][1] - L[i][2];
       bt_flag[i] = 0;
    }


/* [STEP 2] Calculation of Sw, cp (polymer concentration), ce (emulsion
          concentration) of each zone at time n' */

    /* zone (1,1),  zone_a */
    sw_a  = sw[1][1];
    sw[1][1] = (swor*deltaL_qi[1]-(sw_mobile*fw_qc[3]+siw)*deltaL_qc[1][3]
          +sw_a*L_temp[1][1]) / L[1][1];
    cp[1][1] = (sw_mobile*(cp_i[1]*deltaL_qi[1] - fw_qc[3]*cp_qc[3]
          *deltaL_qc[1][3]) + (sw_a - siw)*cp[1][1]*L_temp[1][1])
          / (sw[1][1] - siw) / L[1][1];
    ce[1][1] = (sw_mobile*(ce_i[1]*deltaL_qi[1] - fw_qc[3]*ce_qc[3]
          *deltaL_qc[1][3]) + (sw_a - siw)*ce[1][1]*L_temp[1][1])
          / (sw[1][1] - siw) / L[1][1];

    /* zone (2,1),  zone_b */
```

```
sw_b = sw[2][1];
sw[2][1] = (deltaL_qi[2] + fw_qc[3]*deltaL_qc[2][3]+sw_b*L_temp[2][1])
        / L[2][1];
cp[2][1] = (cp_i[2]*deltaL_qi[2] + fw_qc[3]*cp_qc[3]*deltaL_qc[2][3]
        + sw_b*cp[2][1]*L_temp[2][1]) / sw[2][1] / L[2][1];
ce[2][1] = (ce_i[2]*deltaL_qi[2] + fw_qc[3]*ce_qc[3]*deltaL_qc[2][3]
        + sw_b*ce[2][1]*L_temp[2][1]) / sw[2][1] / L[2][1];

/* zone (1,2), zone_c */
sw[1][2] = 0.0;
cp[1][2] = 0.0;
ce[1][2] = 0.0;

/* zone (2,2), zone_d */
sw[2][2] = 0.0;
cp[2][2] = 0.0;
ce[2][2] = 0.0;

/* zone (1,3), zone_e */
sw_end[1] = sw[1][3];

/* zone (2,3), zone_f */
sw_end[2] = sw[2][3];


/* [STEP 3] Update Sw[i][j], cp[i][j], ce[i][j], L[i][j], Xf[i]
        from time n' to n+1
*/

Xf[1] = L[1][1];  Xf[2] = L[2][1];
if (Xf[1]<Xf[2]) {
    L [2][1] = Xf[1];
        L [1][2] = L [2][2] = Xf[2] - Xf[1];
    L [1][3] = L[2][3];
    sw[2][2] = sw[2][1]; cp[2][2] = cp[2][1]; ce[2][2] = ce[2][1];
    sw[1][2] = sw[1][3]; cp[1][2] = cp[1][3]; ce[1][2] = ce[1][3];
} else {
    L [1][1] = Xf[2];
    L [2][3] = corelength - Xf[1];
    L [2][2] = L[1][2] = Xf[1] - Xf[2];
    sw[1][2] = sw[1][1];  cp[1][2] = cp[1][1]; ce[1][2] = ce[1][1];
    sw[2][2] = sw[2][3];  cp[2][2] = cp[2][3]; ce[2][2] = ce[2][3];
}

}
```

PERFORMANCE CALCULATION

```
#include "define.h"
void performance_calc(section_no,bt_flag,afbt_flag)
int *section_no, bt_flag[], afbt_flag[];
{

/* Calculate production performances. */

    int i,j;
    double factor();

    water_cut[1] = (sw_end[1] - siw) / sw_mobile;
    water_cut[2] = sw_end[2];
    for (i=1;i<=2;i++) {
        cum_inj [i] += q_inj[i]*del_t;
            prod_rate[i]  = q_inj[i];
            for (j=1;j<=*section_no;j++)
                prod_rate[i] += factor(i)* qc[j];
    }
    total_oil_rate = total_water_rate = prod_oil = prod_water = 0.0;
    for(i=1;i<=2;i++) {
        oil_cut [i]   = 1.0 - water_cut[i];
        oil_rate[i]   = oil_cut[i]*prod_rate[i];
        water_rate[i] = water_cut[i]*prod_rate[i];
        del_oil ['] = oil_rate[i]*del_t;
        del_water[i]  = water_rate[i]*del_t;
        prod_oil    += del_oil[i];
        prod_water  += del_water[i];
        total_oil_rate  += oil_rate[i];
        total_water_rate += water_rate[i];
    }
    prod_total   = prod_oil + prod_water;
    total_prod_rate = total_oil_rate + total_water_rate;
    prod_fo = total_oil_rate / total_prod_rate;
    prod_fw = total_water_rate / total_prod_rate;
    wor = total_water_rate / total_oi'_rate;
    cum_oil_prod  += prod_oil;
    cum_water_prod += prod_water;
    er    = cum_oil_prod / IOIP;
    cum_wor = cum_water_prod / cum_oil_prod;
    for (i=1;i<=2;i++) {
        if (bt_flag[i] & !afbt_flag[i]) {
            afbt_flag [i] = 1;
            cum_inj_BT[i] = total_Qi + del_Qical;
            Er_BT[i] = er;
            Xf1_BT[i] = Xf[1];
            Xf2_BT[i] = Xf[2];
        }
    }
}
```

FRONT CALCULATION

```c
#include "define.h"
void front_calc1()
{
    int i,j;
    double factor();

    del_Qical = del_Qical0;
    del_t    = del_t0;

    /* zone (1,1), zone_a */
    sw[1][1] += (q_inj[1] - water_rate[1] - qc[1]*fw_qc[1])*del_t / porevol[1];
    cp[1][1] += (cp_i[1]*q_inj[1] - cp[1][1]*water_rate[1]
                - cp_qc[1]*fw_qc[1]*qc[1])*del_t / porevol[1] / sw_mobile;
    ce[1][1] += (ce_i[1]*q_inj[1] - ce[1][1]*water_rate[1]
                - ce_qc[1]*fw_qc[1]*qc[1])*del_t / porevol[1] / sw_mobile;

    /* zone (2,1), zone_b */
    sw[2][1] += (q_inj[2] - water_rate[2] + qc[1]*fw_qc[1])*del_t / porevol[2];
    cp[2][1] += (cp_i[2]*q_inj[2] - cp[2][1]*water_rate[2]
                + cp_qc[1]*fw_qc[1]*qc[1])*del_t / porevol[2];
    ce[2][1] += (ce_i[2]*q_inj[2] - ce[2][1]*water_rate[2]
                + ce_qc[1]*fw_qc[1]*qc[1])*del_t / porevol[2];

}
```

```
#include "define.h"
void front_calc2(section_no, bt_flag)
int  *section_no, bt_flag[];
{
    int    i, j, k, repeat_flag;
    double  sw_a, sw_b, sw_c, sw_d, del_l, sw1, sw2, sw3, dt_min, dt_adj,
            factor(), deltaL_qi[NL], del_qc[NS], L_temp[NL][NS],
            deltaL_qc[NL][NS], min();

/* [STEP1] Calculation of frontal location of each section at time n' */

    del_Qical = del_Qical0;
    del_t    = del_t0 ;
    dt_min   = 1.0e+08;
    do {
        repeat_flag = 0;
        for (i=1;i<=2;i++) deltaL_qi[i] = q_inj[i]*del_t / a[i];
        for (j=1;j<=2;j++) {
            del_qc[j]  = qc[j]*del_t;
            for (i=1;i<=2;i++) {
                L_temp  [i][j] = L[i][j];
                deltaL_qc[i][j] = del_qc[j] / a[i];
            }
        }

        /* -----------------------------------------------------------
                Old definition of each zone
                la = L[1][1], lc = L[1][2], *section_no = 2,
                lb = L[2][1], ld = L[2][2],
           ----------------------------------------------------- */

        L[1][1] += deltaL_qi[1] - deltaL_qc[1][1];
        L[2][1] += deltaL_qi[2] + deltaL_qc[2][1];
        for (i=1;i<=2;i++) {
            L[i][2] = corelength - L[i][1];
            if (fabs(L[i][2]) >= HANTEI1) {
                if (L[i][2] < 0.0) {
                    repeat_flag = 1;
                    dt_adj = a[i]*L_temp[i][2] / (q_inj[i]+factor(i)*qc[1]);
                        del_t = dt_min = min(dt_min,dt_adj);
                        del_Qical = del_Qical0*del_t/del_t0;
                    for (k=1;k<=2;k++) {
                        for (j=1;j<=2;j++) L[k][j] = L_temp[k][j];
                    }
                }
            } else L[i][2] = 0.0;
        }
    } while (repeat_flag);


/* [STEP 2] Calculation of Sw, cp (polymer concentration), ce (emulsion
           concentration) of each zone at time n' */

/* zone (1,1), zone_a */
```

```
sw_a  = sw[1][1];
sw[1][1] = (swor*deltaL_qi[1] - (sw_mobile*fw_qc[1] + siw)*deltaL_qc[1][1]
        +sw_a*L_temp[1][1]) / L[1][1];
if (fabs(sw3 = sw[1][1] - siw) < HANTEI2)
        cp[1][1] = ce[1][1] = 0.0;
    else {
        cp[1][1] = (sw_mobile*(cp_i[1]*deltaL_qi[1] - fw_qc[1]*cp_qc[1]
                *deltaL_qc[1][1]) + (sw_a - siw)*cp[1][1]*L_temp[1][1])
                / sw3 / L[1][1];
        ce[1][1] = (sw_mobile*(ce_i[1]*deltaL_qi[1] - fw_qc[1]*ce_qc[1]
                *deltaL_qc[1][1]) + (sw_a - siw)*ce[1][1]*L_temp[1][1])
                / sw3 / L[1][1];
    }

/* zone (2,1), zone_b */
sw_b = sw[2][1];
sw[2][1] = (deltaL_qi[2] + fw_qc[1]*deltaL_qc[2][1] + sw_b*L_temp[2][1])
        / L[2][1];
if (fabs(sw[2][1]) < HANTEI2)
        cp[2][1] = ce[2][1] = 0.0;
    else {
        cp[2][1] = (cp_i[2]*deltaL_qi[2] + fw_qc[1]*cp_qc[1]*deltaL_qc[2][1]
                + sw_b*cp[2][1]*L_temp[2][1]) / sw[2][1] / L[2][1];
        ce[2][1] = (ce_i[2]*deltaL_qi[2] + fw_qc[1]*ce_qc[1]*deltaL_qc[2][1]
                + sw_b*ce[2][1]*L_temp[2][1]) / sw[2][1] / L[2][1];

    }

/* zone (1,2), zone_c */
sw_c = sw_end[1] = sw[1][2];
if (fabs(L[1][2]) < HANTEI1) {
        sw[1][2] = sw[1][1];
        cp[1][2] = cp[1][1];
        ce[1][2] = ce[1][1];
    } else {
        sw[1][2] += (sw_c - siw - sw_mobile*fw_qc[2])*deltaL_qc[1][2]
                    / L[1][2];
        if (fabs(sw3 = sw[1][2] - siw) < HANTEI2)
            cp[1][2] = ce[1][2] = 0.0;
        else {
            cp[1][2] += (cp[1][2]*(sw_c - siw) + sw_mobile*fw_qc[2]
                    *cp_qc[2])*deltaL_qc[1][2] / L[1][2] / sw3;
            ce[1][2] += (ce[1][2]*(sw_c - siw) + sw_mobile*fw_qc[2]
                    *ce_qc[2])*deltaL_qc[1][2] / L[1][2] / sw3;
        }
    }

/* zone (2,2), zone_d */
sw_d = sw_end[2] = sw[2][2];
if (fabs(L[2][2]) < HANTEI1) {
        sw[2][2] = sw[2][1];
        cp[2][2] = cp[2][1];
        ce[2][2] = ce[2][1];
    } else {
```

```
        sw[2][2] += (fw_qc[2] - sw_d)*deltaL_qc[2][2] / L[2][2];
        cp[2][2] += (fw_qc[2]*cp_qc[2] - cp[2][2]*sw_d)*deltaL_qc[2][2]
                / sw[2][2] / L[2][2];
        ce[2][2] += (fw_qc[2]*ce_qc[2] - ce[2][2]*sw_d)*deltaL_qc[2][2]
                / sw[2][2] / L[2][2];
    }


/* [STEP 3] Update Sw[i][j], cp[i][j], ce[i][j], L[i][j], Xf[i]
        from time n' to n+1
*/


if (bt_flag[2]) {
    Xf[1] = L[1][1];  Xf[2] = corelength;
    if (fabs(Xf[1] - corelength) < HANTEI1) {
        bt_flag[1] = 1;
        *section_no -= 1;
    }
    del_l = L[2][1] - Xf[1];
    if (del_l >= 0) {
        sw1 = del_l*sw[2][1];
        sw2 = L[2][2]*sw[2][2];
        sw[2][2] = (sw3 = sw1 + sw2) / L[1][2];
        if (fabs(sw3) < HANTEI2)
                cp[2][2] = ce[2][2] = 0.0;
            else {
            cp[2][2] = (cp[2][1]*sw1 + cp[2][2]*sw2) / sw3;
            ce[2][2] = (ce[2][1]*sw1 + ce[2][2]*sw2) / sw3;
            }
    } else {
        sw1 = L[2][1]*sw[2][1];
        sw2 = - del_l*sw[2][2];
        sw[2][1] = (sw3 = sw1 + sw2) / Xf[1];
        if (fabs(sw3) < HANTEI2)
                cp[2][1] = ce[2][1] = 0.0;
            else {
            cp[2][1] = (cp[2][1]*sw1 + cp[2][2]*sw2) / sw3;
            ce[2][1] = (ce[2][1]*sw1 + ce[2][2]*sw2) / sw3;
            }
    }
    L[2][1] = L[1][1];  L[2][2] = L[1][2];
} else {
    Xf[2] = L[2][1];  Xf[1] = corelength;
    if (fabs(Xf[2] - corelength) < HANTEI1) {
        bt_flag[2] = 1;
        *section_no -= 1;
    }
    del_l = L[1][1] - Xf[2];
    if (del_l >= 0) {
        sw1 = del_l*(sw[1][1] - siw);
        sw2 = L[1][2]*(sw[1][2] - siw);
        sw[1][2] = (sw3 = sw1 + sw2) / L[2][2] + siw;
        if (fabs(sw3) < HANTEI2)
```

```
                cp[1][2] = ce[1][2] = 0.0;
        else {
                cp[1][2] = (cp[1][1]*sw1 + cp[1][2]*sw2)/sw3;
                ce[1][2] = (ce[1][1]*sw1 + ce[1][2]*sw2)/sw3;
        }
    } else {
        sw1 = L[1][1]*(sw[1][1] - siw);
        sw2 = - del_1*(sw[1][2] - siw);
        sw[1][1] = (sw3 = sw1 + sw2) / Xf[2] + siw;
        if (fabs(sw3) < HANTEI2)
                cp[1][1] = ce[1][1] = 0.0;
        else {
                cp[1][1]  = (cp[1][1]*sw1 + cp[1][2]*sw2)/sw3;
                ce[1][1]  = (ce[1][1]*sw1 + ce[1][2]*sw2)/sw3;
        }
    }
    L[1][1] = L[2][1];  L[1][2] = L[2][2];
  }
}
```

```c
#include "define.h"
void front_calc3(section_no, bt_flag)
int  *section_no, bt_flag[];
{
  int    i, j, k, repeat_flag;
  double  sw_a, sw_b, sw_c, sw_d, sw_e, sw_f, del_l, lcd, dt_min, dt_adj,
          sw1, sw2, sw3, factor(), deltaL_qi[NL], del_qc[NS],
          L_temp[NL][NS], deltaL_qc[NL][NS], min();

/* [STEP1] Calculation of frontal location of each section at time n' */

  del_Qical = del_Qical0;
  del_t    = del_t0;
  dt_min   = 1.0e+08;
  do {
    repeat_flag = 0;
    for (i=1;i<=2;i++)  deltaL_qi[i] = q_inj[i]*del_t / a[i];
    for (j=1;j<=3;j++) {
      del_qc[j]  = qc[j]*del_t;
      for (i=1;i<=2;i++) {
        L_temp  [i][j]  = L[i][j];
        deltaL_qc[i][j]  = del_qc[j]/a[i];
      }
    }


/* -----------------------------------------------------
        Old definition of each zone
        la = L[1][1], lc = L[1][2], le = L[1][3],
        lb = L[2][1], ld = L[2][2], lf = L[2][3]
   ----------------------------------------------------- */

    L[1][1] += deltaL_qi[1] - deltaL_qc[1][1];
    L[2][1] += deltaL_qi[2] + deltaL_qc[2][1];
    L[1][2] -= deltaL_qc[1][2];
    L[2][2] += deltaL_qc[2][2];
    for (i=1;i<=2;i++) {
      L[i][3] = corelength - L[i][1] - L[i][2];
      if (fabs(L[i][3]) >= HANTEI1) {
      if (L[i][3] < 0.0) {
        repeat_flag = 1;
        dt_adj = a[i]*L_temp[i][3]/(q_inj[i]+factor(i)
                    *(qc[1]+qc[2]));
        del_t = dt_min = min(dt_min,dt_adj);
          del_Qical = del_Qical0*del_t/del_t0;
        for (k=1;k<=2;k++) {
          for (j=1;j<=3;j++) L[k][j] = L_temp[k][j];
        }
      }
      } else L[i][3] = 0.0;
    }
  } while (repeat_flag);
```

```
/* [STEP 2] Calculation of Sw, cp (polymer concentration), ce (emulsion
          concentration) of each zone at time n' */

    /* zone (1,1), zone_a */
    sw_a  = sw[1][1];
    sw[1][1] = (swor*deltaL_qi[1]-(sw_mobile*fw_qc[1]+siw)*deltaL_qc[1][1]
          +sw_a*L_temp[1][1]) / L[1][1];
    if (fabs(sw3 = sw[1][1] - siw) < HANTEI2)
        cp[1][1] = ce[1][1] = 0.0;
        else {
            cp[1][1] = (sw_mobile*(cp_i[1]*deltaL_qi[1] - fw_qc[1]*cp_qc[1]
                  *deltaL_qc[i][1]) + (sw_a - siw)*cp[1][1]*L_temp[1][1])
                  / sw3 / L[1][1];
            ce[1][i] = (sw_mobile*(ce_i[1]*deltaL_qi[1] - fw_qc[1]*ce_qc[1]
                  *deltaL_qc[1][1]) + (sw_a - siw)*ce[1][1]*L_temp[1][1])
                  / sw3 / L[1][1];
        }

    /* zone (2,1), zone_b */
    sw_b = sw[2][1];
    sw[2][1] = (deltaL_qi[2] + fw_qc[1]*deltaL_qc[2][1]+sw_b*L_temp[2][1])
          / L[2][1];
    if (fabs(sw[2][1]) < HANTEI2)
        cp[2][1] = ce[2][1] = 0.0;
        else {
            cp[2][1] = (cp_i[2]*deltaL_qi[2] + fw_qc[1]*cp_qc[1]*deltaL_qc[2][1]
                  + sw_b*cp[2][1]*L_temp[2][1]) / sw[2][1] / L[2][1];
            ce[2][1] = (ce_i[2]*deltaL_qi[2] + fw_qc[1]*ce_qc[1]*deltaL_qc[2][1]
                  + sw_b*ce[2][1]*L_temp[2][1]) / sw[2][1] / L[2][1];
        }

    /* zone (1,2), zone_c */
    sw_c = sw[1][2];
    if (fabs(L[1][2]) < HANTEI1) {
        sw[1][2] = sw[1][1];
        cp[1][2] = cp[1][1];
        ce[1][2] = ce[1][1];
        } else {
        sw[1][2] = (-(sw_mobile*fw_qc[2]+siw)*deltaL_qc[1][2]
                      +sw_c*L_temp[1][2]) / L[1][2];
        if (fabs(sw3 = sw[1][2] - siw) < HANTEI2)
                cp[1][2] = ce[1][2] = 0.0;
            else {
            cp[1][2] = (-sw_mobile*fw_qc[2]*cp_qc[2]*deltaL_qc[1][2]
                  + (sw_c-siw)*cp[1][2]*L_temp[1][2]) / sw3 / L[1][2];
            ce[1][2] = (-sw_mobile*fw_qc[2]*ce_qc[2]*deltaL_qc[1][2]
                  + (sw_c-siw)*ce[1][2]*L_temp[1][2]) / sw3 / L[1][2];
            }
    }

    /* zone (2,2), zone_d */
    sw_d = sw[2][2];
    if (fabs(L[2][2]) < HANTEI1) {
        sw[2][2] = sw[2][1];
```

```
            cp[2][2] = cp[2][1];
            ce[2][2] = ce[2][1];
        } else {
            sw[2][2] = (fw_qc[2]*deltaL_qc[2][2] + sw_d*L_temp[2][2]) / L[2][2];
            if (fabs(sw[2][2]) < HANTEI2)
                    cp[2][2] = ce[2][2] = 0.0;
                else {
            cp[2][2] = (fw_qc[2]*cp_qc[2]*deltaL_qc[2][2]+sw_d*cp[2][2]
                        *L_temp[2][2]) / sw[2][2] / L[2][2];
                ce[2][2] = (fw_qc[2]*ce_qc[2]*deltaL_qc[2][2]+sw_d*ce[2][2]
                            ·L_temp[2][2]) / sw[2][2] / L[2][2];
                }
        }


    /* zone (1,3), zone_e */
    sw_e = sw_end[1] = sw[1][3];
    if (fabs(L[1][3]) < HANTEI1) {
        sw[1][3] = sw[1][2];
          cp[1][3] = cp[1][2];
          ce[1][3] = ce[1][2];
        } else {
        sw[1][3] += (sw_e-siw-sw_mobile*fw_qc[3])*deltaL_qc[1][3] / L[1][3];
        if (fabs(sw3 = sw[1][3] - siw) < HANTEI2)
            cp[1][3] = ce[1][3] = 0.0;
            else {
            cp[1][3] += (cp[1][3]*(sw_e - siw) - sw_mobile
                    *fw_qc[3]*cp_qc[3])*deltaL_qc[1][3] / L[1][3] / sw3;
                ce[1][3] += (ce[1][3]*(sw_e - siw) - sw_mobile
                    *fw_qc[3]*ce_qc[3])*deltaL_qc[1][3] / L[1][3] / sw3;
            }
        }


    /* zone (2,3), zone_f */
    sw_f = sw_end[2] = sw[2][3];
    if (fabs(L[2][3]) < HANTEI1) {
        sw[2][3] = sw[2][2];
          cp[2][3] = cp[2][2];
          ce[2][3] = ce[2][2];
        } else {
        sw[2][3] += (fw_qc[3] - sw_f)*deltaL_qc[2][3] / L[2][3];
        if (fabs(sw[2][3]) < HANTEI2)
                cp[2][3] = ce[2][3] = 0.0;
                else {
            cp[2][3] += (fw_qc[3]*cp_qc[3] - cp[2][3]*sw_f)
                        *deltaL_qc[2][3] / sw[2][3] / L[2][3];
                ce[2][3] += (fw_qc[3]*ce_qc[3] - ce[2][3]*sw_f)
                            *deltaL_qc[2][3] / sw[2][3] / L[2][3];
            }
        }


    /* [STEP 3] Update Sw[i][j], cp[i][j], ce[i][j], L[i][j], Xf[i]
            from time n' to n+1
    */
```

```
if (Xf[1]<=Xf[2]) {
   Xf[1] = L[1][1];  Xf[2] = L[2][1] + L[2][2];
   if (fabs(Xf[2] - corelength) < HANTEI1)  {
      bt_flag[2] = 1;
      *section_no -= 1;
   }
   if (Xf[1]<Xf[2]) {

      /* ------ Start of Case(1) in UPDATE ROUTINE ------------- */
      del_l = L[2][1] - Xf[1];  lcd = Xf[2] - Xf[1];
      if (del_l >= 0) {
         sw1 = del_l*sw[2][1];
         sw2 = L[2][2]*sw[2][2];
         sw[2][2] = (sw3 = sw1 + sw2) / lcd;
         if (fabs(sw3) < HANTEI2)
               cp[2][2] = ce[2][2] = 0.0;
            else {
                  cp[2][2] = (cp[2][1]*sw1 + cp[2][2]*sw2) / sw3;
               ce[2][2] = (ce[2][1]*sw1 + ce[2][2]*sw2) / sw3;
               }
      } else {
         sw1 = L[2][1]*sw[2][1];
         sw2 = - del_l*sw[2][2];
         sw[2][1] = (sw3 = sw1 + sw2) / Xf[1];
         if (fabs(sw3) < HANTEI2)
               cp[2][1] = ce[2][1] = 0.0;
               else {
               cp[2][1] = (cp[2][1]*sw1 + cp[2][2]*sw2) / sw3;
               ce[2][1] = (ce[2][1]*sw1 + ce[2][2]*sw2) / sw3;
                  }
      }
      L[2][1] = Xf[1];  L[2][2] = lcd;
      del_l = L[1][2] - lcd;
      if (del_l >= 0) {
         sw1 = del_l*(sw[1][2] - siw);
         sw2 = L[1][3]*(sw[1][3] - siw);
         sw[1][3] = (sw3 = sw1 + sw2) / L[2][3] + siw;
         if (fabs(sw3) < HANTEI2)
               cp[1][3] = ce[1][3] = 0.0;
            else {
               cp[1][3] = (cp[1][2]*sw1 + cp[1][3]*sw2)/sw3;
               ce[1][3] = (ce[1][2]*sw1 + ce[1][3]*sw2)/sw3;
            }
      } else {
         sw1 = L[1][2]*(sw[1][2] - siw);
         sw2 = - del_l*(sw[1][3] - siw);
         sw[1][2] = (sw3 = sw1 + sw2) / lcd + siw;
         if (fabs(sw3) < HANTEI2)
               cp[1][2] = ce[1][2] = 0.0;
            else {
               cp[1][2] = (cp[1][2]*sw1 + cp[1][3]*sw2)/sw3;
               ce[1][2] = (ce[1][2]*sw1 + ce[1][3]*sw2)/sw3;
            }
```

```
            }
        L[1][2] = L[2][2];  L[1][3] = L[2][3];
        /* ------ End of Case(1) --------------------------------- */

    } else {

        /* ------ Start of Case(2) in UPDATE ROUTINE -------------- */
        sw1 = sw[2][1]*L[2][1];
        sw2 = sw[2][2]*L[2][2];
        sw[2][1] = (sw3 = sw1 + sw2) / Xf[2];
        if (fabs(sw3) < HANTEI2)
                cp[2][1] = ce[2][1] = 0.0;
                else {
            cp[2][1] = (cp[2][1]*sw1 + cp[2][2]*sw2) / sw3;
            ce[2][1] = (ce[2][1]*sw1 + ce[2][2]*sw2) / sw3;
        }
        L[1][1] = L[2][1] = Xf[2];
        L[2][3] = corelength - Xf[1];

        sw1 = L[1][2]*(sw[1][2] - siw);
        sw2 = L[1][3]*(sw[1][3] - siw);
        sw[1][3] = (sw3 = sw1 + sw2) / L[2][3] + siw;
        if (fabs(sw3) < HANTEI2)
                cp[1][3] = ce[1][3] = 0.0;
            else {
                cp[1][3] = (cp[1][2]*sw1 + cp[1][3]*sw2)/sw3;
                ce[1][3] = (ce[1][2]*sw1 + ce[1][3]*sw2)/sw3;
            }
        L[1][3] = L[2][3];

        sw[1][2] = sw[1][1];  cp[1][2] = cp[1][1]; ce[1][2] = ce[1][1];
        sw[2][2] = sw[2][3];  cp[2][2] = cp[2][3]; ce[2][2] = ce[2][3];
        L [2][2] = L [1][2] = Xf[1] - Xf[2];
        /* ------ End of Case(2) --------------------------------- */

    }
} else {
    Xf[1] = L[1][1] + L[1][2];  Xf[2] = L[2][1];
    if (fabs(Xf[1] - corelength) < HANTEI1) {
        bt_flag[1] = 1;
        *section_no -= 1;
    }
    if (Xf[1] <= Xf[2]) {

        /* ------ Start of Case(3) in UPDATE ROUTINE -------------- */
        sw1 = (sw[1][1] - siw)*L[1][1];
        sw2 = (sw[1][2] - siw)*L[1][2];
        sw[1][1] = (sw3 = sw1 + sw2) / Xf[1] + siw;
        if (fabs(sw3) < HANTEI2)
                cp[1][1] = ce[1][1] = 0.0;
            else {
                cp[1][1] = (cp[1][1]*sw1 + cp[1][2]*sw2)/sw3;
                ce[1][1] = (ce[1][1]*sw1 + ce[1][2]*sw2)/sw3;
            }
```

```
L[2][1] = L[1][1] = Xf[1];
L[1][3] = corelength - Xf[2];

sw1 = L[2][2]*sw[2][2];
sw2 = L[2][3]*sw[2][3];
sw[2][3] = (sw3 = sw1 + sw2) / L[1][3];
if (fabs(sw3) < HANTEI2)
        cp[2][3] = ce[2][3] = 0.0;
        else {
    cp[2][3] = (cp[2][2]*sw1 + cp[2][3]*sw2) / sw3;
    ce[2][3] = (ce[2][2]*sw1 + ce[2][3]*sw2) / sw3;
    }
L [2][3] = L[1][3];

sw[1][2] = sw[1][3];  cp[1][2] = cp[1][3]; ce[1][2] = ce[1][3];
sw[2][2] = sw[2][1];  cp[2][2] = cp[2][1]; ce[2][2] = ce[2][1];
L [2][2] = L [1][2] = Xf[2] - Xf[1];
/* ------ End of Case(3) --------------------------------- */

} else {

    /* ------ Start of Case(4) in UPDATE ROUTINE ------------- */
    del_l = L[1][1] - Xf[2];  lcd = Xf[1] - Xf[2];
    if (del_l >= 0) {
        sw1 = del_l*(sw[1][1] - siw);
        sw2 = L[1][2]*(sw[1][2] - siw);
        sw[1][2] = (sw3 = sw1 + sw2) / lcd + siw;
        if (fabs(sw3) < HANTEI2)
                cp[1][2] = ce[1][2] = 0.0;
                else {
                    cp[1][2] = (cp[1][1]*sw1 + cp[1][2]*sw2)/sw3;
                    ce[1][2] = (ce[1][1]*sw1 + ce[1][2]*sw2)/sw3;
                }
    } else {
        sw1 = L[1][1]*(sw[1][1] - siw);
        sw2 = - del_l*(sw[1][2] - siw);
        sw[1][1] = (sw3 = sw1 + sw2) / Xf[2] + siw;
        if (fabs(sw3) < HANTEI2)
                cp[1][1] = ce[1][1] = 0.0;
                else {
                    cp[1][1] = (cp[1][1]*sw1 + cp[1][2]*sw2)/sw3;
                    ce[1][1] = (ce[1][1]*sw1 + ce[1][2]*sw2)/sw3;
                }
    }
    L[1][1] = Xf[2];  L[1][2] = lcd;
    del_l = L[2][2] - lcd;
    if (del_l >= 0) {
        sw1 = del_l*sw[2][2];
        sw2 = L[2][3]*sw[2][3];
        sw[2][3] = (sw3 = sw1 + sw2) / L[1][3];
        if (fabs(sw3) < HANTEI2)
                cp[2][3] = ce[2][3] = 0.0;
                else {
```

```
                cp[2][3] = (cp[2][2]*sw1 + cp[2][3]*sw2) / sw3;
                ce[2][3] = (ce[2][2]*sw1 + ce[2][3]*sw2) / sw3;
                }
        } else {
            sw1 = L[2][2]*sw[2][2];
            sw2 = - del_l*sw[2][3];
            sw[2][2] = (sw3 = sw1 + sw2) / lcd;
            if (fabs(sw3) < HANTEI2)
                    cp[2][2] = ce[2][2] = 0.0;
                    else {
                cp[2][2] = (cp[2][2]*sw1 + cp[2][3]*sw2) / sw3;
                ce[2][2] = (ce[2][2]*sw1 + ce[2][3]*sw2) / sw3;
                    }
        }
        L[2][2] = L[1][2];  L[2][3] = L[1][3];
        /* ------ End of Case(4) -------------------------------- */

    }
  }
}
```

APPENDIX C: Flow Chart For The Computer Program

START

Input directory name from the command line.

dataread(direcname)
Read input data for a simluation.

data_initialize(section_no, bt_flag[NL], direcname)
Setting of constant values and initial values in the valuables.
time = 0, total_Qi = 0.

crossflow_calc0 (section_no)
(1) Calculate crossflow rate in each layer.
(2) Calcurate fractional flow of water, emulsion and polymer concentration in the crossflowed fluids.

fileout_result(direcname, section_no)
Save the results at time = 0 to output files.

water_viscosity(ce, cw)
Calculate the aqueous-phase viscosity from emulsion (ce) and polymer concentration (cp).

w_rperm(i, sw)
Calculate the relative permeability to water .

o_rperm(i, sw)
Calculate the relative permeability to oil .

total_Qi = total_Qi + del_Qical
time = time + del_t

front_calc0 (section_no, bt_flag[NL])
(1) Calculate frontal location, water saturation, emulsion and polymer concentration of each zone.
(2) Calculate Xf[1], Xf[2].
(3) Calculate section_no.

performance_calc (section_no)
(1) Calculate water cut, oil cut, oil production rate, water production rate, etc. in each layer.
(2) Calculate water cut, oil cut, wor of total production fluids and oil-recovery efficiency.

crossflow_calc1 (section_no)
(1) Calculate crossflow rate in each section.
(2) Calcurate fractional flow of water, emulsion and polymer concentration in the crossflowed fluids.

fileout_result(direcname, section_no)
Save the calculated results at time = del_t into output files.

1

① 1

1 — **section_no** — 3

2

front_calc1
(section_no, bt_flag[NL])
(1) Xf[1] and Xf[2] are fixed to L(core length) after breakthrough of the both fronts.
(2) Calculate water saturation, emulsion and polymer concentration of zone[1][1] and zone[2][1] by material balance.

front_calc2
(section_no, bt_flag[NL])
(1) Either Xf[1] or Xf[2] already reaches to the end of core. This front is fixed to L(core length).
(2) Calculate frontal location of another front. Calculate water saturation, emulsion and polymer concentration of zone[1][1], zone[1][2], zone[2][1] and zone[2][2].
(3) Calculate section_no.

front_calc3
(section_no, bt_flag[NL])
(1) Both Xf[1] or Xf[2] exist in the core.
(2) Calculate frontal location, water saturation, emulsion and polymer concentration of each zone.
(3) Calculate Xf[1], Xf[2].
(4) Calculate section_no.

performance_calc (section_no)
(1) Calculate water cut, oil cut, oil production rate, water production rate, etc. in each layer.
(2) Calculate water cut, oil cut, wor of total production fluids and oil-recovery efficiency.

total_Qi = total_Qi + del_Qical
time = time + del_t

Change the injection rate into each layer, polymer and emulsion concentration of the injected fluids, if total_Qi reaches to the pre-assigned time.

crossflow_calc1 (section_no)
(1) Calculate crossflow rate in each section.
(2) Calcurate fractional flow of water, emulsion and polymer concentration in the crossflowed fluids.

water_viscosity(ce, cw)
Calculate the aqueous-phase viscosity from emulsion (ce) and polymer concentration (cp).

w_rperm(i, sw)
Calculate the relative permeability to water.

filecut_result(direcname, section_no)
Save the calculated results at each timestep into output files.

o_rperm(i, sw)
Calculate the relative permeability to oil.

YES — **total_Qi < Qi_end ?**

NO

APPENDIX D: Figure for Oil Recovery Performance

Diagram (1):

$X_{fl}^{(t)}$

Zone[1][1] | Zone[1][2] | Zone[1][3]

$1-S_{or}$

oil

q_{fl}

oil

q_{f2}

q_{c1} | q_{c2} | q_{c3}

S_{iw}

$q_{fl} + q_{c1} + q_{c2} + q_{c3}$

$q_{fl} - q_{c1} - q_{c2} - q_{c3}$

Zone[2][1] | Zone[2][2] | Zone[2][3]

$X_{f2}^{(t)}$

(1) Frontal locations and length of each zone at time t. Crossflow rates are calculated in each section.

Diagram (2):

$X_{fl}^{(t+1)}$

Zone[1][1] | Zone[1][2] | Zone[1][3]

$1-S_{or}$

oil

$q_{fl}\Delta t$

$q_{c1}\Delta t$

$q_{c2}\Delta t$ | $q_{c3}\Delta t$

oil

S_w

$q_{f2}\Delta t$

Zone[2][1] | Zone[2][2] | Zone[2][3]

$X_{f2}^{(t+1)}$

(2) Frontal locations and length of each zone at time t+Δt. Zone lengths are calculated by assumption of piston-like displacement.

Diagram (3):

$X_{fl}^{(t+1)}$

Zone[1][1] | Zone[1][2] | Zone[1][3]

$1-S_{or}$

oil

q_{fl}

oil | oil

$q_{fl} + q_{c1} + q_{c2} + q_{c3}$

S_w

q_{f2}

$q_{fl} - q_{c1} - q_{c2} - q_{c3}$

Zone[2][1] | Zone [2][2] | Zone[2][3]

$X_{f2}^{(t+1)}$

(3) Update frontal locations and length of each zone at time t+Δt. Water saturation and polymer/emulsion concentration are calculated by averaging in each zone. In the next time step, the crossflow rates are calculated based on this condition, .

Calculation procedure of frontal movement with crossflow when section number is 3.